



University
of Glasgow

Walker, Roderick G. (2008) *Leishmania CRK3:CYC6 cyclin-dependent kinase as a drug target*.
PhD thesis.

<http://theses.gla.ac.uk/313/>

Copyright and moral rights for this thesis are retained by the author

A copy can be downloaded for personal non-commercial research or study, without prior permission or charge

This thesis cannot be reproduced or quoted extensively from without first obtaining permission in writing from the Author

The content must not be changed in any way or sold commercially in any format or medium without the formal permission of the Author

When referring to this work, full bibliographic details including the author, title, awarding institution and date of the thesis must be given

***Leishmania* CRK3:CYC6 cyclin-dependent kinase
as a drug target.**

A thesis submitted for the degree of Doctor of Philosophy
in the Faculty of Veterinary Medicine,
University of Glasgow.

By

Roderick Graeme Walker (B.Sc. Dundee, 2004)

The Wellcome Centre for Molecular Parasitology
Glasgow Biomedical Research Centre
120 University Place
Glasgow
G12 8TA

February 2008

© Roderick Graeme Walker 2008

Abstract

Leishmania species are protozoan parasites which have a complex life cycle, which is coordinated with its cell cycle. There are 11 cyclin dependent kinases (CDKs) and 11 cyclins present in the *Leishmania* genome reflecting the complexity of cell cycle control in this parasite, perhaps due to the requirement for synchronisation with the life cycle. *Leishmania mexicana* CRK3, a cdc2-related serine/threonine protein kinase of the CDK family, is essential for transition through the G2-M-phase checkpoint of the *Leishmania* cell cycle. The *Trypanosoma brucei* homologue of CRK3, with 78% identity to *L. mexicana* CRK3, has been shown to form an active kinase complex with the CYC6 cyclin. Using this knowledge a putative mitotic cyclin, CYC6, from *Leishmania major* was identified. Monomeric CRK3 does not have protein kinase activity, but was activated *in vitro* with CYC6 to produce a protein kinase complex with histone H1 kinase activity. CRK3_{his} and CYC6_{his} were co-expressed and co-purified from *Escherichia coli* via metal affinity and gel filtration chromatography to obtain a 1:1 ratio of CRK3:CYC6 proteins, which formed a stable protein kinase complex. Using histone H1 as a substrate, active CRK3:CYC6 was used to develop a radiometric assay suitable for low to medium throughput compound screening and then an assay suitable for high throughput screening (HTS) using IMAPTM fluorescence polarization technology. This HTS assay was used to screen a 25,000 compound chemical library to identify hits which significantly reduced CRK3:CYC6 protein kinase activity. Two main pharmacophores with the highest potency towards CRK3:CYC6 protein kinase activity were identified from the high throughput screen. Structure Activity Relationship (SAR) analysis of the hits identified the chemical groups attached to the scaffold structures which are essential for the inhibition of CRK3:CYC6 protein kinase activity. The CRK3:CYC6 hits were subsequently counter-screened against a panel of 11 mammalian kinases including human CDK1:CYCB (the functional orthologue of CRK3:CYC6), human CDK2:CYCA and human CDK4:CYCD1 to determine their selectivity. Compound hits that were selective towards CRK3:CYC6, were tested against *Leishmania in vitro*. Progress towards synthesising potent and selective derivatives of the HTS hits will be discussed, with the view to evaluating their potential for the development of novel therapeutics against leishmaniasis.

Table of contents

Abstract	ii
Table of contents	iii
List of figures	ix
List of tables	xiii
List of abbreviations	xv
Acknowledgements	xvii
Declaration	xviii
Chapter 1	1
Introduction	1
1.1 The trypanosomatids.....	1
1.1.1 Parasitic trypanosomatids:	1
1.1.1.1 <i>Leishmania</i> species.....	1
1.1.1.2 African trypanosomes.....	2
1.1.1.3 American trypanosomes.....	2
1.2 Leishmaniasis.....	3
1.2.1 Cutaneous leishmaniasis (CL).....	3
1.2.1.1 Diffuse cutaneous leishmaniasis (DCL).....	4
1.2.1.2 Localised cutaneous leishmaniasis (LCL).	4
1.2.1.3 Mucocutaneous leishmaniasis (MCL).....	4
1.2.2 Visceral leishmaniasis (VL).	4
1.2.3 Post-kala-azar dermal leishmaniasis (PKDL).	5
1.3 <i>Leishmania</i> life cycle.	5
1.4 Current antileishmanial chemotherapy.	7
1.5 The eukaryotic cell cycle.	11
1.5.1 Cyclin-dependent kinase regulation.....	11
1.5.2 The yeast cell cycle.	14
1.5.3 The mammalian cell cycle.	18

1.5.4 The trypanosomatid cell cycle.	24
1.5.4.1 The <i>Leishmania</i> cell cycle.	24
1.5.4.2 The <i>T. brucei</i> cell cycle.	26
1.5.4.3 The <i>T. cruzi</i> cell cycle.	28
1.6 Protein kinases as drug targets.	29
1.6.1 CDKs as potential drug targets.	29
1.7 Protein kinase inhibitors.	33
1.7.1 CDK inhibitors.	34
1.8 The parasite kinome as a target for anti-parasite drug discovery.	39
1.8.1 Trypanosomatid CDKs as drug targets.	40
1.8.1.1 <i>Leishmania</i> CDKs as drug targets.	40
1.9 Antitrypanosomatid drug discovery:	41
1.9.1 Target assessment for antiparasitic drug discovery.	41
1.9.2 The drug discovery process and criteria.	42
1.9.3 The requirement for new antileishmanial therapeutics.	45
1.10 Project aims.	45
Chapter 2	47
Materials and methods	47
2.1 Buffers and reagents.	47
2.2 Molecular biology methods:	51
2.2.1 Bacterial strains.	51
2.2.2 Bacterial culture.	51
2.2.3 Bacterial stabilate preparation (Glycerol stocks).	51
2.2.4 Preparation of competent cells:	52
2.2.4.1 Rubidium chloride method.	52
2.2.4.2 Calcium chloride method.	52
2.2.5 DNA vectors and plasmid constructs.	53
2.2.6 Polymerase chain reaction (PCR).	54

2.2.7 Plasmid preparation and purification.	54
2.2.8 Restriction enzyme digests.....	55
2.2.9 DNA gel electrophoresis.....	55
2.2.10 DNA purification from agarose gels.....	55
2.2.11 DNA ligations.....	56
2.2.12 Bacterial transformations.....	56
2.3 Mouse methods:.....	56
2.3.1 Macrophage (mΦ) extraction and purification.....	56
2.4 <i>Leishmania major</i> methods:	57
2.4.1 <i>Leishmania</i> cell lines.	57
2.4.2 Tissue culture.	57
2.4.3 DNA transfections:.....	58
2.4.3.1 DNA precipitation and sterilization.....	58
2.4.3.2 Bio-Rad electroporator transfection.....	58
2.4.3.3 Amaxa nucleofector transfection.	59
2.4.4 Protein preparation.....	59
2.4.5 <i>Leishmania</i> stabilate preparation.....	60
2.4.6 Alamar blue absorption assays and drugging.....	60
2.4.7 Macrophage infection assays and drugging.	60
2.5 Biochemical methods:	62
2.5.1 General protein purification.	62
2.5.2 <i>Leishmania</i> CRK3:CYC6 protein complex purification.....	63
2.6 SDS- PAGE.....	64
2.6.1 Coomassie gel staining.	64
2.6.2 Western blotting.	64
2.6.2.1 Antibody detection of proteins.	65
2.6.3 Protein quantification.....	65
2.7 Protein kinase assays:.....	65

2.7.1 γ -32P radiometric assays:.....	65
2.7.1.1 Gel-based assays.....	65
2.7.1.2 Plate-based assays.	66
2.7.2 IMAP TM fluorescence polarization assays.....	66
2.8 HTS robotic technology.	67
Chapter 3	68
<i>Leishmania</i> biology 1: The <i>Leishmania</i> CRK3:CYC6 protein kinase complex and radiometric assay development.	68
3.1 Chapter introduction and objectives.	68
3.1.1 Assay development, validation and performance.....	70
3.2 Cloning: To obtain the <i>Leishmania</i> CRK3 and CYC6 genes:	73
3.2.1 <i>L. mexicana</i> CRK3 cloning.	73
3.2.2 <i>L. major</i> CYC6 cloning.....	73
3.3 Purification of cell cycle proteins:	75
3.3.1 <i>L. mexicana</i> CRK3his.....	75
3.3.2 <i>L. major</i> CYC6his.	75
3.3.3 <i>L. mexicana</i> CRK3 ^{T178E} his.....	76
3.3.4 <i>Saccharomyces cerevisiae</i> GST-Civ1.	76
3.4 Protein kinase assays: gel-based assay:.....	81
3.4.1 Activation of the <i>Leishmania</i> CRK3:CYC6 protein kinase complex.	81
3.5 <i>Leishmania</i> CRK3his:CYC6his protein stoichiometry optimisation.....	81
3.6 <i>Leishmania</i> CRK3:CYC6 protein kinase stability analysis.....	84
3.7 <i>Leishmania mexicana</i> CRK3 ^{T178E} his:CYC6his activity assay.	84
3.8 <i>S. cerevisiae</i> GST-Civ1	85
3.9 Large scale <i>Leishmania</i> CRK3:CYC6 protein purification for radiometric assay development:	90
3.9.1 Co-expression and co-purification of <i>Leishmania</i> CRK3:CYC6.....	90
3.10 Protein kinase assays: Radiometric protein kinase assays:	92
3.10.1 <i>Leishmania</i> CRK3:CYC6 protein kinase activity assay.....	92

3.11 <i>Leishmania</i> CRK3:CYC6 time course assay.	92
3.12 <i>Leishmania</i> CRK3:CYC6 ATP and histone H1 substrate K_m determinations.	95
3.13 Staurosporine and olomoucine IC_{50} determinations for the <i>Leishmania</i> CRK3:CYC6 protein kinase complex.....	95
3.14 Preliminary compound screen against <i>Leishmania</i> CRK3:CYC6.	98
3.15 Chapter discussion	100
Chapter 4	108
High throughput assay development and screening.....	108
4.1 Chapter introduction and objectives.	108
4.2 Optimum substrate identification for <i>Leishmania</i> CRK3:CYC6.....	111
4.3 <i>Leishmania</i> CRK3:CYC6 two-fold enzyme titration.	116
4.4 <i>Leishmania</i> CRK3:CYC6 ATP K_m determination.	116
4.5 Staurosporine and olomoucine IC_{50} determinations for <i>Leishmania</i> CRK3:CYC6.	119
4.6 Preliminary compound screen against <i>Leishmania</i> CRK3:CYC6.	119
4.7 Development of an IMAP TM assay suitable for counter screening against human CDK2:CycA:	121
4.7.1 Human CDK2:CycA two-fold enzyme titration.	121
4.8 High throughput screening of the Cyclacel compound library:.....	121
4.8.1 <i>Leishmania</i> CRK3:CYC6 and human CDK2:CycA IMAP TM fluorescence polarization HTS assays.....	121
4.9 Structural analysis of the high throughput screen hits.	130
4.10 Structure activity relationship of the azapurines towards <i>Leishmania</i> CRK3:CYC6.	130
4.11 Mammalian kinase counter screening of the <i>Leishmania</i> CRK3:CYC6 hits.	137
4.12. Alternative approaches to identify <i>Leishmania</i> CRK3:CYC6 inhibitors... 141	
4.12.1 Screening of Naphthostyryl derivatives against <i>Leishmania</i> CRK3:CYC6.	141

4.12.2 Screening of Indirubin derivatives against <i>Leishmania</i> CRK3:CYC6....	141
4.13 Chapter discussion	148
Chapter 5	160
<i>Leishmania</i> biology 2: The <i>Leishmania</i> CRK3:CYC6 protein kinase complex and <i>in vitro</i> compound analysis.	160
5.1 Chapter introduction and objectives.	160
5.2 Analysis of the biological activity of the Cyclacel library high throughput screen hits against cultured <i>L. major</i> parasites:	161
5.2.1 Against cultured <i>L. major</i> promastigote parasites.....	161
5.2.2 Against amastigote <i>L. major</i> in a macrophage infection.	162
5.3 Analysis of the re-synthesised high throughput screen hits and azapurine derivatives against the <i>Leishmania</i> CRK3:CYC6 protein kinase complex.	166
5.4 Analysis of the biological activity of the azapurines against cultured <i>L. major</i> parasites:.....	171
5.4.1 Against cultured <i>L. major</i> promastigote parasites.....	171
5.4.2 Against amastigote <i>L. major</i> in a macrophage infection.	176
5.5. <i>Leishmania</i> CRK3:CYC6 <i>in vivo</i> protein kinase complex.	181
5.5.1 <i>L. major</i> HA-tagged <i>CYC6</i> episomal constructs:	181
5.5.1.1 N-terminal HA-tagged <i>L. major</i> <i>CYC6</i>	181
5.5.1.2 C-terminal HA-tagged <i>L. major</i> <i>CYC6</i>	182
5.5.2 <i>L. major</i> HA-tagged <i>CYC6</i> ribosomal integration constructs:	184
5.5.2.1 N-terminal HA-tagged <i>L. major</i> <i>CYC6</i>	184
5.5.2.2 C-terminal HA-tagged <i>L. major</i> <i>CYC6</i>	184
5.6 Purification and detection of <i>L. major</i> HA-tagged <i>CYC6</i>	186
5.6.1 CRK3:CYC6 co-immunoprecipitation and pull down assay.	186
5.7 Chapter discussion.	188
Chapter 6	196
Final discussion and conclusions.....	196
References.....	203

List of figures

Figure 1.1	Schematic representation of the <i>Leishmania</i> species life cycle in <i>Lutzomyia longipalpis</i>	6
Figure 1.2	Structures and modes of action of current antileishmanial drugs.....	10
Figure 1.3	Schematic of the eukaryotic cell cycle.....	17
Figure 1.4	Some of the potential applications of CDK inhibitors.....	32
Figure 1.5	The chemical structures of the first cyclin-dependent protein kinase inhibitor identified and commercially available protein kinase inhibitor drugs.....	36
Figure 1.6	The chemical structures of a variety of 2, 6, 9-trisubstituted purine CDK inhibitors.....	37
Figure 1.7	The chemical structures of flavopiridol and staurosporine protein kinase inhibitors.....	37
Figure 1.8	The chemical structures of indirubin and paullone protein kinase inhibitors.....	38
Figure 1.9	Traffic-light definitions for target assessment.....	42
Figure 1.10	Schematic representation of the drug development pathway.....	43
Figure 1.11	The criteria for antiparasitic hits, leads and drug candidates.....	44
Figure 3.1	Vector NTI maps of the <i>L. mexicana</i> CRK3 protein expression construct pGL751a and <i>L. major</i> CYC6 protein expression construct pGL1218.....	74
Figure 3.2	<i>L. mexicana</i> CRK3 protein purification.....	77
Figure 3.3	<i>L. major</i> CYC6 protein expression.....	78
Figure 3.4	<i>L. mexicana</i> CRK3 ^{T178E} protein purification.....	79
Figure 3.5	<i>S. cerevisiae</i> GST-Civ1 protein purification.....	80

Figure 3.6	Activation of the <i>Leishmania</i> CRK3:CYC6 protein kinase complex.....	82
Figure 3.7	Optimisation of the ratio of <i>Leishmania</i> CRK3 and CYC6 proteins...	83
Figure 3.8	Stability of the <i>Leishmania</i> CRK3 and CYC6 proteins.....	86
Figure 3.9	Lack of activation of CRK3 ^{T178E} by <i>L. major</i> CYC6.....	87
Figure 3.10	<i>S. cerevisiae</i> Civ1:histone H1 activity assay.....	88
Figure 3.11	Activation of the <i>Leishmania</i> CRK3:CYC6 protein kinase complex with <i>S. cerevisiae</i> Civ1.....	89
Figure 3.12	Expression and purification of the <i>L. mexicana</i> CRK3 and <i>L. major</i> CYC6 cell cycle proteins.....	91
Figure 3.13	Plate based activity assay of the <i>Leishmania</i> CRK3:CYC6 protein kinase complex.....	93
Figure 3.14	Linearity of the <i>Leishmania</i> CRK3:CYC6 radiometric assay.....	94
Figure 3.15	ATP and substrate K _m determinations for the <i>Leishmania</i> CRK3:CYC6 protein kinase complex.....	96
Figure 3.16	Staurosporine and olomoucine IC ₅₀ determinations for the <i>Leishmania</i> CRK3:CYC6 protein kinase complex.....	97
Figure 3.17	Structures of the compound hits from the <i>Leishmania</i> CRK3:CYC6 preliminary compound screen.....	99
Figure 4.1	IMAP TM fluorescence polarisation assay schematic.....	110
Figure 4.2	IMAP TM substrate finder assay schematic.....	112
Figure 4.3	IMAP TM substrate finder assay analysis using Molecular Devices data analysis software.....	113
Figure 4.4	IMAP TM substrate finder assay to identify the best substrates of CRK3:CYC6 for the HTS assay.....	114

Figure 4.5	IMAP™ substrate finder sequence analysis.....	115
Figure 4.6	CRK3:CYC6 IMAP™ assay development and validation – enzyme titration.....	117
Figure 4.7	ATP K_m determination for CRK3:CYC6 using the IMAP™ HTS assay.....	118
Figure 4.8	Biochemical characteristics of CRK3:CYC6 using the IMAP™ HTS assay.....	120
Figure 4.9	Human CDK2:CycA IMAP™ assay development and validation...	122
Figure 4.10	Main compound core structures identified from the CRK3:CYC6 high throughput screen.....	131
Figure 4.11	Azapurine core structures minus the methoxybenzene ring and the cyclohexylmethyl groups.....	132
Figure 4.12	The chemical structure of Naphthostyryl and derivatives.....	143-144
Figure 4.13	The chemical structure of Indirubin and derivatives.....	145-146
Figure 4.14	Binding motifs of CDK2 and CRK3 with their respective inhibitors.	156
Figure 5.1	Life cycle stages of <i>Leishmania</i> highlighting cellular membranes...	163
Figure 5.2	Azapurine derivatives tested against the <i>Leishmania</i> CRK3:CYC6 protein kinase complex.....	168-169
Figure 5.3	Re-synthesised azapurine HTS hits tested against the <i>Leishmania</i> CRK3:CYC6 protein kinase complex and <i>Leishmania in vitro</i>	170
Figure 5.4	Vector NTI maps of the <i>L. major</i> N and C-terminal HA-tagged CYC6 episomal expression constructs pGL1391 and pGL1390....	183
Figure 5.5	Vector NTI maps of the <i>L. major</i> N and C-terminal HA-tagged CYC6 ribosomal integration constructs pGL1484 and pGL1483....	185

Figure 5.6 Western blot analysis of N and C-terminal HA-tagged CYC6
purified from *L. major*.....**187**

List of tables

Table 1.1	Currently identified mammalian CDKs and their known cyclin binding partners.....	23
Table 1.2	Cdc2-related kinases, cyclins and accessory proteins predicted from the <i>L. major</i> and <i>T. brucei</i> genomes.	27
Table 2.1	Bacterial strains used for plasmid cloning and protein expression...	51
Table 2.2	DNA vectors used for gene cloning and protein expression.....	53
Table 2.3	Plasmid constructs generated and used throughout the project.....	53
Table 3.1	The characterisation of screening assay quality by the value of the Z factor.....	72
Table 4.1	The Cyclacel compound library breakdown.....	123
Table 4.2	CRK3:CYC6 and CDK2:CycA primary and secondary screening summary.....	125-129
Table 4.3	Analysis of the azapurine methoxybenzene ring modifications at the 9 position.....	134
Table 4.4	Analysis of the azapurine cyclohexylmethyl group modifications at the 2 position (1).....	135
Table 4.5	Analysis of the azapurine cyclohexylmethyl group modifications at the 2 position (2).....	136
Table 4.6	Protein kinase counter screening panel.....	138
Table 4.7	Protein kinase counter screening panel summary 1.....	139
Table 4.8	Protein kinase counter screening panel summary 2.....	140
Table 4.9	Indirubins screened against <i>Leishmania</i> CRK3:CYC6, human CDK2:CycA and human CDK1:CycB.....	147

Table 5.1	Cyclacel HTS compound testing against promastigote <i>L. major</i>	164
Table 5.2	Cyclacel HTS compound testing against promastigote <i>L. major</i> infected macrophages.....	165
Table 5.3	Re-synthesised Cyclacel HTS and derivative compounds tested against promastigote <i>L. major</i> (1).....	173
Table 5.4	Re-synthesised Cyclacel HTS and derivative compounds tested against promastigote <i>L. major</i> (2).....	174
Table 5.5	Re-synthesised Cyclacel HTS and derivative compounds tested against promastigote <i>L. major</i> (3).....	175
Table 5.6	Re-synthesised Cyclacel HTS and derivative compound testing against promastigote <i>L. major</i> infected macrophages (1)...	178
Table 5.7	Re-synthesised Cyclacel HTS and derivative compound testing against promastigote <i>L. major</i> infected macrophages (2)...	179
Table 5.8	Summary table of azapurine inhibition.....	180

List of abbreviations

ADB	Assay development buffer
ALPHA	Amplified luminescent proximity homogenous assay
ATP	Adenosine triphosphate
AMP	Ampicillin antibiotic
BSA	Bovine serum albumin
CAM	Chloramphenicol antibiotic
CDK	Cyclin-dependent kinase
CRK	Cdc2-related kinase
CRB	Complete reaction buffer
CYC	Cyclin
DMSO	Dimethyl sulphoxide
DTT	Dithiothreitol
DNA	Deoxyribonucleic acid
DNase-1	Deoxyribonuclease-1
EDB	Enzyme dilution buffer
EDTA	Ethylene diamine tetraacetic acid
EGTA	Ethylene glycol tetraacetic acid
EPB	Electroporation buffer
GST	Glutathione S transferase
HEPES	(4-(2-hydroxyethyl)-1-piperazineethanesulfonic acid
HIFCS	Heat inactivated foetal calf serum
His	Histidine
HOMEM	Modified Eagle's medium
HRP	Horseradish peroxidase
IMAP	Immobilized metal affinity-based fluorescence polarization
IPTG	Isopropyl- β -D-Thiogalactopyranoside
IQ	Intensity quenching
KAN	Kanamycin antibiotic
LB	Luria-Bertani (agar and media)
MOPS	3-(N-morpholino) propanesulfonic acid
MΦ	Macrophage
PBS	Phosphate buffered saline
PBST	Phosphate buffered saline plus Tween-20
PCR	Polymerase chain reaction

RF-1	Rubidium chloride buffer 1
RF-2	Rubidium chloride buffer 2
RPMI	Roswell Park Memorial Institute (modified Eagle's medium)
SDS	Sodium dodecyl sulphate
SDS-PAGE	Sodium dodecyl sulphate polyacrylamide gel electrophoresis
TBE	Tris-Borate-EDTA
TEMED	N,N,N',N'-Tetramethylethylenediamine
Tris	Tris (hydroxymethyl) aminomethane
UV	Ultraviolet

Acknowledgements

I would first like to thank my supervisor Jeremy Mottram for the opportunity to carry out the project and for continuous support, guidance and advice throughout. I would also like to thank my supervisor at Cyclacel, Dundee, Graeme Thomson for taking the project on and supervising me when two of my proposed supervisors before him, left the company to take up other posts. It seemed no one wanted to supervise me!!! I would also like to acknowledge the members of the MRC collaboration: Karen Grant, Malcolm Walkinshaw, Matt Nowicki, Sandra Bruce, Kirk Malone and Nick Turner for their continuous advice and suggestions throughout the collaboration.

A big thanks to the guys in my office; Jim and Lesley especially, (for thesis advice, IT advice and unrivalled scientific expertise!!!), Cathy, Elmarie and Severine for lively discussions and for making the place fun to work (and write up) in. Thanks to Felipe Gomes, my chaperone in the lab when I first started, and all other past and present members of the Mottram lab and levels 5 and 6 of the GBRC that I've not mentioned.

At Cyclacel, I would like to acknowledge Susan Davis and Bob Westwood for reading over reports and presentations regarding intellectual property issues, Wayne Jackson for valuable HTS robotic support and assay advice and everyone else at Cyclacel for their support and plenty of drinks!!!

On a personal note, I would like to acknowledge Ian Fleming and Terry Smith, my old summer placement and honours project supervisors, respectively, who got me into Cyclacel and parasitology research in the first place. Mum and Dad, for their continuous support and encouragement throughout my studies. Hopefully I'll get a job Dad, stop being a student and you can finally retire. Finally I would like to thank my girlfriend Jemma for her continuous support and encouragement, for patiently waiting on me coming back to Glasgow from Cyclacel, and for making all those long trips through to Dundee.

Thanks to everyone again, cheers.

Declaration

I declare that the research presented in this thesis is my own work, carried out in the Wellcome Centre for Molecular Parasitology at the Glasgow Biomedical Research Centre, University of Glasgow and at Cyclacel Limited, Dundee. It is an original piece of work except where otherwise stated.

Roderick G. Walker

February 2008

Chapter 1

Introduction

1.1 The trypanosomatids.

Several species of trypanosomatid protozoa are the etiological agents of parasitic diseases in mammals, including humans. These organisms have been the subject of extensive scientific research because of their involvement in a range of diseases, resulting in both medical and economical issues. Current therapeutics used in the treatment of African trypanosomiasis and leishmaniasis, such as the arsenical-based Melarsoprol (Mel B, ArsobalTM) and the antimonial based Sodium stibogluconate (Pentostam[®], SSG) are unsatisfactory for a number of reasons including toxicity and drug resistance (Croft and Coombs, 2003; Fairlamb, 2003; Croft *et al.*, 2006b). As a result, new targets for anti-parasite chemotherapy are being continuously sought after because of the medical and economical implications involved. There have been recent advances in research into possible anti-parasite therapeutic targets, and one such area is that of cyclin dependent kinases (CDKs) in the parasite life cycle. Several protein kinases play essential roles in the cell cycle, and thus provide an attractive area of study for drug design to treat parasitic diseases.

1.1.1 Parasitic trypanosomatids:

1.1.1.1 *Leishmania* species.

Leishmania parasites are parasitic protozoa belonging to the family Trypanosomatidae. There are over 20 known species and sub species of *Leishmania* prevalent in 88 countries worldwide which are grouped into old world (Africa, Asia and Europe) and new world (the Americas and Australasia) species according to their geographic distribution. (www.who.int/tdr/diseases/leish/diseaseinfo). They are the etiological agents of the leishmaniases, a group of diseases transmitted to mammals by the bite of blood feeding

female sand flies (*Phlebotomus spp.* in the old world and *Lutzomyia spp.* in the new world) (Reithinger *et al.*, 2007).

1.1.1.2 African trypanosomes.

African trypanosomes are parasitic protozoa from the genus *Trypanosoma* of which there are a number of subspecies prevalent in 36 countries in sub-Saharan Africa. They are transmitted by the bite of the blood feeding tsetse fly (*Glossina spp.*) and cause debilitating diseases from a health and economical standpoint. *Trypanosoma brucei brucei* is the etiological agent of N’gana, a muscle wasting disease in cattle and other wild mammals, but cannot infect humans (www.who.int/tdr/diseases/trypan/diseaseinfo). *Trypanosoma brucei gambiense* causes the chronic form of human African trypanosomiasis (HAT), also known as African sleeping sickness, which is distributed throughout central and Western Africa. *Trypanosoma brucei rhodesiense* is the causative agent of the acute form of HAT prevalent mainly in Eastern and Southern Africa. It is estimated that 60 million people are at risk of infection and the World Health Organisation estimate that approximately 0.5 million people carry the infection, of which there are 50 000 deaths per annum (Barrett *et al.*, 2003). Post infection, early symptoms include fever and an enlarged spleen (splenomegaly). This is followed by headaches, anaemia and swollen tissues. The parasites then invade the central nervous system (CNS) where symptoms progress to mental retardation, coma and in all cases results in death (www.who.int/tdr/diseases/trypan/diseaseinfo).

1.1.1.3 American trypanosomes.

Trypanosoma cruzi are American trypanosomes which are parasitic protozoa belonging to the *Trypanosoma* genus. They are transmitted by the bite of the blood feeding triatomine insect (sub-family *Triatominae*), also known as “Assassin bugs”. The faeces of the insect contain the parasites which can enter the human host via the wound left after a blood meal, usually when it is scratched or rubbed. *T. cruzi* is the causative agent of Chagas disease

also known as human American trypanosomiasis and it is estimated that between 8 and 11 million people are infected with the disease (www.cdc.gov/chagas/factsheet.html). The disease is prevalent in 18 countries in two ecological zones: the Southern cone, where the vector insects live inside human homes; and Northern South America, Central America and Mexico where the vector insects live both inside and outside human dwellings. Post infection, symptoms include a small sore where the parasite enters the body and if this has occurred near the eye, the eyelid becomes swollen which is known as Romana's sign. The disease occurs in acute and chronic forms. Swollen lymph nodes and fever can develop within a few days and this initial acute phase can result in illness and death, especially in young children. More commonly, patients are subject to the chronic phase of the disease which shows no visible symptoms and can last several months or years. During this time, the parasites invade most of the organs in the body, causing heart, intestinal and oesophageal damage and progressive weakness. In 32% of those infected, substantial damage to the heart and intestinal tract occurs which is fatal to the patient. (www.who.int/tdr/diseases/chagas/diseaseinfo).

1.2 Leishmaniasis.

Leishmaniasis is a vector-borne disease from which an estimated 350 million people are at risk of infection (Reithinger *et al.*, 2007). An estimated 12 million individuals are infected worldwide. There is an annual incidence of 0.5 million of the visceral form of the disease and 1.5-2 million cases of the cutaneous form of the disease (Croft *et al.*, 2006b). Several clinical forms of the disease occur.

1.2.1 Cutaneous leishmaniasis (CL).

CL can result in the production of a large number of lesions or skin ulcers (sometimes up to 200) which usually form on exposed areas, such as the face, arms and legs. These usually heal within a few months invariably leaving the patient permanently scarred, a stigma which can cause serious social prejudice.

(www.who.int/tdr/diseases/leish/diseaseinfo, www.who.int/topics/leishmaniasis/en/). CL can be classified into three forms.

1.2.1.1 Diffuse cutaneous leishmaniasis (DCL).

DCL is mainly caused by *L. aethiopica*, *L. amazonensis* and *L. mexicana*. The disease results in widely spread and chronic skin lesions (www.who.int/topics/leishmaniasis/en/). Multiple parasite laden non-ulcerative nodules arise from the initial site of infection which may cover an individual's entire body (Reithinger *et al.*, 2007). This form of the disease is difficult to treat and patients do not self cure.

1.2.1.2 Localised cutaneous leishmaniasis (LCL).

LCL is caused by all species of *Leishmania*. A small erythema develops at the bite site which develops into a papule and then a nodule which progressively develops into an ulcerative skin lesion. Lesions typically self heal within 2-6 months of development (Reithinger *et al.*, 2007).

1.2.1.3 Mucocutaneous leishmaniasis (MCL).

MCL is mainly caused by *L. braziliensis* and *L. panamensis*. The disease results in lesions which can partially or totally destroy the mucous membranes of the nose, mouth and throat cavities and surrounding tissues (www.who.int/topics/leishmaniasis/en/). It is difficult to diagnose and treat this form of the disease (Herwaldt, 1999), with secondary bacterial infections common and it can be fatal (Reithinger *et al.*, 2007).

1.2.2 Visceral leishmaniasis (VL).

VL is caused by *L. donovani* and *L. infantum*. Also known as kala-azar, this is the most serious form of the disease. It is characterised by symptoms including high fever, substantial weight loss, enlargement of the liver and spleen and other secondary effects such as anaemia and diarrhoea. If left untreated the disease has a fatality rate of 100% within two years (www.who.int/topics/leishmaniasis/en/).

1.2.3 Post-kala-azar dermal leishmaniasis (PKDL).

PKDL occurs as a complication of visceral leishmaniasis and is characterised by a rash of which the most common form is a nodular rash. This form of the disease has been described in India and Sudan in patients who have recovered from visceral leishmaniasis. The rash originates at the mouth and then spreads to other parts of the body depending on the severity (Zijlstra *et al.*, 2003).

1.3 *Leishmania* life cycle.

Leishmania parasites possess a highly complex biphasic life cycle (Figure 1.1), whereby they survive in their sand fly vector and mammalian host. *Leishmania* parasites exist in five major morphological forms: procyclic promastigotes, nectomonad promastigotes, leptomonad promastigotes, metacyclic promastigotes and amastigotes. Procyclic promastigotes are present in the abdominal midgut of the sand fly. They are a flagellated, weakly motile, replicative form of the parasite. After a few days, the parasites slow their replication and develop into elongate, strongly motile nectomonad promastigotes, where they move towards the anterior midgut until they reach the stomodeal valve, which guards the junction between foregut and midgut (Bates, 2007). Once the parasites reach the stomodeal valve, they transform into leptomonad promastigotes, shorter forms of the parasite which resume replication (Gossage *et al.*, 2003). Some of the nectomonad/leptomonad promastigotes also differentiate into haptomonad promastigotes. The leptomonad promastigotes differentiate into mammalian infective metacyclic promastigotes in the mouthparts of the sand fly (Rogers *et al.*, 2002). After transfer of the metacyclic promastigotes to the mammalian host by the sand fly bite, *Leishmania* invade host macrophage cells where they transform into the non-motile amastigote form and live within the phagosomal compartment of the host macrophage. As the number of amastigotes increases, the macrophage eventually dies releasing the amastigotes, which then go on to infect other macrophages. This process continues until the infected macrophages are taken up in the blood meal of another feeding sand fly. In the gut of the

sand fly, the amastigotes emerge from macrophages and differentiate into procyclic promastigotes and the life cycle then repeats.

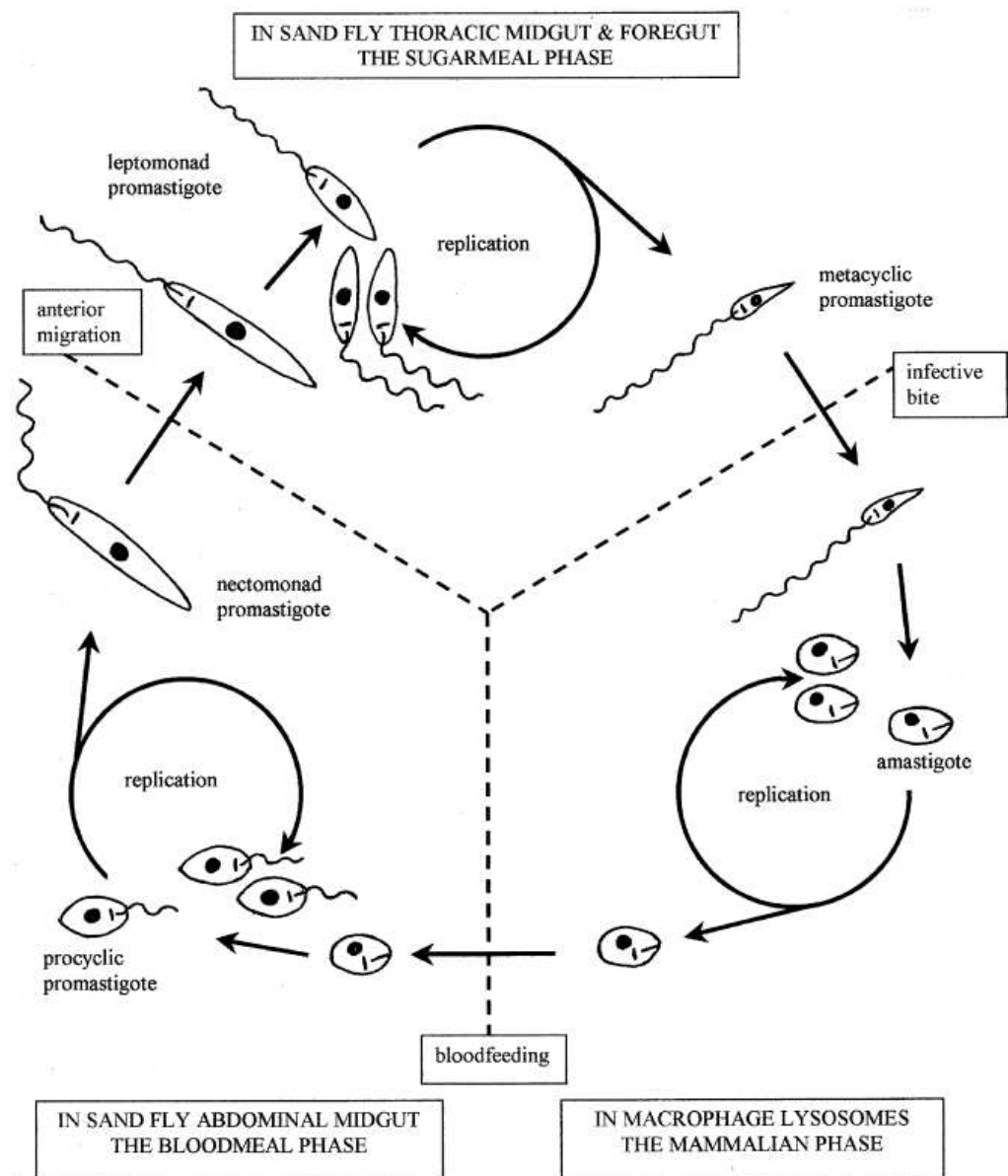


Figure 1.1 – Schematic representation of the *Leishmania* species life cycle in *Lutzomyia longipalpis*. Taken from the International Journal for Parasitology (Gossage *et al.*, 2003).

1.4 Current antileishmanial chemotherapy.

The chemotherapy currently available for leishmaniasis is far from satisfactory. The demand for new antileishmanial drugs has been driven by the parasite acquired resistance to the pentavalent antimonial drugs, the first line chemotherapy against the disease, which are now almost obsolete in India (Croft and Coombs, 2003; Croft *et al.*, 2005). Antimonial based treatments recommended for VL and CL were introduced in 1945 and remain effective treatments for certain forms of leishmaniasis (Croft and Coombs, 2003). However, the requirement for new antileishmanials is paramount.

There are a number of drugs currently recommended for the treatment of leishmaniasis such as the pentavalent antimonials Sodium stibogluconate (Pentostam[®], SSG) and Meglumine antimoniate (Glucantime[®]). Also included are Amphotericin B and its lipid formulation AmBisome[®] and Pentamidine (Croft and Coombs, 2003). Miltefosine (Impavido[®]) and Paromomycin have also been registered to treat leishmaniasis. Those that remain in clinical trials include Imiquimod and Sitamaquine. These drugs exhibit a variety of modes of action and structures (Figure 1.2).

The antimonials, introduced over 60 years ago have been the recommended drugs used to treat CL and VL for over 20 years (Croft and Coombs, 2003; Croft *et al.*, 2005). However, they require parenteral administration for up to 28 days and exhibit varying efficacies against CL and VL. Perhaps the most significant factor limiting the usefulness of these drugs is the emergence of drug resistance. A prime example of this limiting factor, as mentioned, is in India where the pentavalent antimonials are almost no longer used to treat leishmaniasis in this part of the world.

Amphotericin B is a highly effective polyene antibiotic used in the treatment of antimonial resistant *L. donovani* VL and certain cases of MCL (Croft and Coombs, 2003). It has selective activity against fungi as well as *Leishmania* and *Trypanosoma cruzi*. Its efficacy

is due to the higher selectivity towards ergosterol, the main sterol in these organisms over cholesterol, the predominant sterol in mammals (Croft *et al.*, 2006b). However, it is an unpleasant drug due to its acute toxicity and the need for slow infusion parenteral administration over four hours (Croft and Coombs, 2003).

Numerous Amphotericin B lipid formulations developed in the 1980s for the treatment of immunocompromised patients with systemic mycoses have proved effective as anti-leishmanials. These lipid formulations have a reduced toxicity and been shown to have an extended half life, in comparison to the parent drug, for the treatment of fungal infections (Croft and Coombs, 2003). AmBisome[®], the liposomal formulation of Amphotericin B, was first shown to cure a case of VL in 1991 and is currently registered for the treatment of VL as a first line drug by the Food and Drug Administration (Croft and Coombs, 2003; Croft *et al.*, 2005). However, high cost has limited its use as an antileishmanial drug.

The diamidine Pentamidine was introduced in 1952 and has been used to treat those with VL, CL and DCL. It is primarily used as a second line treatment in cases where antimonial resistance occurs and the antimonials are ineffective (Croft and Coombs, 2003; Croft *et al.*, 2006b). The primary mode of action is unclear and Pentamidine is not a widely used drug to treat leishmaniasis (Croft *et al.*, 2006b).

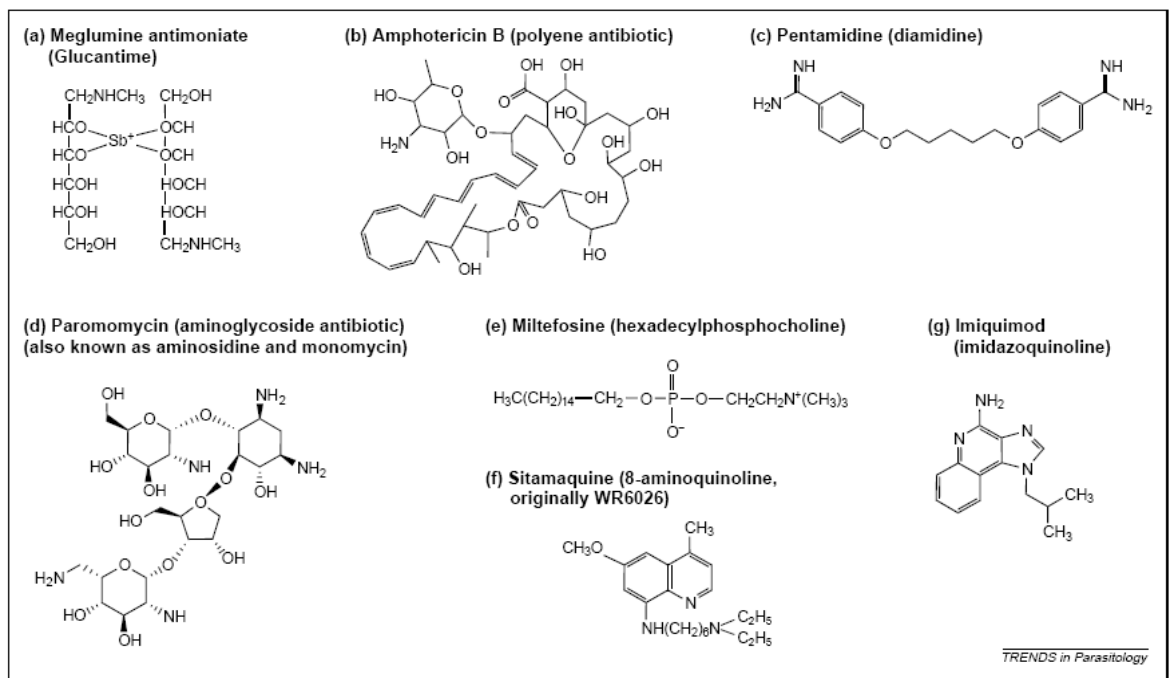
The antileishmanial activity of Miltefosine (Impavido[®]) (hexadecylphosphocholine) was identified at Wellcome, and although originally identified as an anticancer agent, had its antileishmanial activity proven by 1985. It is a lysophospholipid analogue and the first oral treatment produced for VL whilst also being effective against CL (Croft *et al.*, 2005). Miltefosine, registered in India in 2002 and in phase IV clinical trials, is used in cases of antimonial resistance. However, there is a number of limitations regarding Miltefosine. The main limitation being its teratogenicity and therefore women of child bearing age are excluded from its use (Croft and Coombs, 2003). Furthermore, there are concerns

regarding the long half life of the drug which might encourage drug resistance and there is also a narrow therapeutic window with Miltefosine (Croft *et al.*, 2006a).

Imiquimod [1-(2-methylpropyl)-1*H*-imidazo(4,5-*c*)quinolin-4-amine] is an antiviral compound commonly used to treat genital warts caused by the human papillomavirus. It has been shown to have an effect in experimental infections of CL and successfully treat patients with cutaneous lesions, who did not respond to antimonial treatment alone (Croft *et al.*, 2006a).

Paromomycin (Aminosidine) is an aminoglycoside-amino-cyclitol antibiotic originally identified as an antileishmanial in the 1960s (Croft and Coombs, 2003). It is used to treat VL in a parenteral formulation and CL in topical and parenteral formulations (Croft *et al.*, 2005; Croft *et al.*, 2006b). It is currently in phase III clinical trials in Africa and was registered in 2006 to treat Leishmaniasis in India (www.dndi.org).

Sitamaquine is an 8-aminoquinoline derivative (4-methyl-6-methoxy-8-aminoquinoline) whose antileishmanial activity was identified in the 1970's at the Walter Reed Army Institute of Research (WRAIR) (Croft and Coombs, 2003; Croft *et al.*, 2006a). It is currently in development at GlaxoSmithKline (GSK) in phase II clinical trials for the treatment of VL (Croft and Coombs, 2003; Croft *et al.*, 2006b). Sitamaquine toxicity seems to be reasonably mild, causing mild methaemglobinaemia (Croft and Coombs, 2003).



Generic name of drug (chemical type)	Mechanism of action ^a
Pentavalent antimonials: Meglumine antimoniate (Glucantime) Sodium stibogluconate (Pentostam™)	Structure of sodium stibogluconate is still not known despite its use for over 50 years. Activated within the amastigote, but not in the promastigote, by conversion to a lethal trivalent form. Activation mechanism not known. Antileishmanial activity might be due to action on host macrophage.
Amphotericin B (polyene antibiotic)	Complexes with 24-substituted sterols, such as ergosterol in cell membrane, thus causing pores which alter ion balance and result in cell death.
Pentamidine (diamidine)	Accumulated by the parasite; effects include binding to kinetoplast DNA. Primary mode of action uncertain.
Paromomycin (aminoglycoside antibiotic) (also known as aminosidine or monomycin)	In bacteria, paromomycin inhibits protein synthesis by binding to 30S subunit ribosomes, causing misreading and premature termination of mRNA translation. In <i>Leishmania</i> , paromomycin also affects mitochondrion.
Miltefosine (hexadecylphosphocholine)	Primary effect uncertain, possible inhibition of ether remodelling, phosphatidylcholine biosynthesis, signal transduction and calcium homeostasis.
Sitamaquine (8-aminoquinoline, originally WR6026)	Unknown, might affect mitochondrial electron transport chain.
Imiquimod (imidazoquinoline)	Stimulates nitric oxide production from macrophages.

Figure 1.2 – Structures and modes of action of current antileishmanial drugs. Upper panel: Structures of current antileishmanial drugs. Lower panel: modes of action of current antileishmanials. Both were taken from TRENDS in Parasitology (Croft and Coombs, 2003).

1.5 The eukaryotic cell cycle.

The generalised eukaryotic cell cycle is divided into four main stages: G1, S, G2 and M-phase (Figure 1.3). However, there is another cell cycle stage, called gap 0 (G0). G1 is the first gap phase where the cell grows and prepares for S-phase. During G1, the cell makes the decision to continue, pause or exit the cell cycle process. Cells that should cease division enter G0 where they leave the cell cycle and quit dividing, which can be a temporary resting period or more permanent. Cells continuing the division process then enter a restriction point referred to as START, which is where they are committed to completing the cell cycle. This proceeds into S-phase where the cell replicates its genome. The cell then progresses into G2, the second gap phase where it again grows and prepares itself for the onset of M-phase. M-phase or mitosis is the process by which the cell segregates its duplicated chromosomes into two separate nuclei. The final process is cytokinesis where the cell separates into two identical daughter cells which marks the completion of the cell cycle (Johnson and Walker, 1999).

1.5.1 Cyclin-dependent kinase regulation.

Cyclin dependent protein kinases (CDKs) are a class of enzymes shown to be vital for the regulation and progression of the cell cycle (Nurse, 1990; Pines and Hunter, 1990) and are ubiquitously expressed in eukaryotic organisms. CDKs are serine/threonine protein kinases which catalyse a phosphotransfer reaction whereby the γ -phosphate from ATP is transferred onto a serine or threonine residue of a substrate. At least six mechanisms govern and control the activity of CDKs; cyclin subunit binding, CDK phosphorylation, inactivation by CDK inhibitory subunits (CKIs), inactivation by regulatory kinases (Morgan, 1997), CDK cellular localisation and CDK structure.

CDKs are catalytic subunits which are inactive as monomers and require the binding of a regulatory cyclin subunit to become activated, thereby forming an active protein kinase

complex (Moreno *et al.*, 1989; Solomon *et al.*, 1990). Homology among cyclins is usually limited to a relatively well conserved domain of approximately 100 amino acids, termed the “cyclin box”, which is responsible for CDK binding and activation (Kobayashi *et al.*, 1992; Lees and Harlow, 1993) via a PSTAIRE binding motif in the CDK. However, recent analysis of the human genome has identified the cyclin box as being comprised of 150 amino acids (Malumbres and Barbacid, 2005). Cyclin function is primarily controlled by changes in cyclin levels which increase and decrease throughout the cell cycle as required. Their degradation involves ubiquitin-mediated proteolysis, requiring a recognition motif, termed the “destruction box” near the amino terminus end of the cyclin (Glotzer *et al.*, 1991).

In addition to cyclin binding, complete CDK activation requires phosphorylation at a conserved threonine residue, in a region called the T-loop, by a CDK activating kinase (CAK) (Morgan, 1995). CAK was identified and shown to phosphorylate and activate Cdc2 (Ducommun *et al.*, 1991; Solomon *et al.*, 1992). Civ1, a CAK from *Saccharomyces cerevisiae* was shown to tightly bind and phosphorylate CDC28 *in vivo* and to be essential for cell viability (Thuret *et al.*, 1996). Additional work on mammalian CDKs has shown that phosphorylation is vital for CDK1-cyclinB activity, where cyclin binding alone has little effect on activity, or CDK2-cyclinA activity, where high affinity cyclin binding can not occur without phosphorylation (Desai *et al.*, 1995). CDK1 (Cdc2) is phosphorylated on Thr 161 and CDK2 on Thr 160 (Morgan, 1995) which has been shown to be carried out by CDK7-cyclinH-MAT1, the mammalian CAK (Fesquet *et al.*, 1993; Fisher and Morgan, 1994). An interesting point, however, is that activation of some complexes such as CDK5-p35 and CDK7-cyclinH-MAT1 itself do not require phosphorylation (Nigg, 1996; Qi *et al.*, 1995) and CDK8-cyclinC does not contain a phosphorylatable residue at the analogous site in the T-loop (Tassan *et al.*, 1995b).

CDK-cyclin complexes can also be inhibited by phosphorylation as seen with human CDK1 and CDK2 on the Thr 14 and Tyr 15 residues (Morgan, 1995). Phosphorylation of these residues is important in the control of CDK1 activation at mitosis. CDK1-cyclinB complexes are maintained in an inactive state until dephosphorylation of these residues occurs at the end of G2 and CDK1 becomes active (Morgan, 1995). Tyr 15 of CDK1 has been shown to be phosphorylated by the kinase Wee1; however, it does not phosphorylate Thr 14. This is carried out by a dual specificity, membrane-bound kinase encoded by *Myt1* (Borgne and Meijer, 1996). Thr 14 and Tyr 15 are both dephosphorylated by a dual specificity phosphatase termed CDC25 which promotes CDK1 activity (Morgan, 1995).

The fourth mechanism of CDK regulation is the association with a diverse family of proteins, termed cyclin-dependent kinase inhibitors (CKIs) which bind and inactivate CDK-cyclin complexes. A number of CKIs are present in yeast; FAR1 and p40 in *S. cerevisiae* and PHO81 in *S. pombe* (Morgan, 1995). There are currently two families of CKIs identified in mammals, the Cip/Kip and Ink4 families (Laine *et al.*, 2007; Johnson and Walker, 1999). The Cip/Kip family is comprised of p21^{Cip1}, p27^{Kip1} and p57^{Kip2} which can act on most CDK-cyclin complexes (Johnson and Walker, 1999) and are known to inhibit CDK2 and CDK4/6-cyclin complexes involved in G1 and G1-S control (Johnson and Walker, 1999; Morgan, 1995; Morgan, 1997). The Ink4 family is comprised of p15^{INK4b}, p16^{INK4a}, p18^{INK4c} and p19^{INK4d}, which have a relatively narrow specificity for CDK4/6-cyclinD complexes, preventing their association (Morgan, 1997; Johnson and Walker, 1999; Carnero and Hannon, 1998).

The cellular localisation of CDKs can also regulate their function. For example, the function of human CDK1 is partially dependent on it and its cyclin binding partner's location within the cell. CDK1:CycB1 colocalizes with cytoplasmic microtubules during interphase (Porter and Donoghue, 2003; Migone *et al.*, 2006), and then translocates to the nucleus to initiate mitosis. However, the CDK1:CycB2 complex colocalizes with the golgi

apparatus whereas CDK1:CycB3 is permanently located in the nucleus (Porter and Donoghue, 2003).

Finally, the structure of CDKs has a role in their activation. This has been elucidated from detailed studies carried out mainly on CDK2 and one of its binding partners, CycA. For example, when CycA binds CDK2, by comparison with free CDK2, large conformational changes occur in the active site. These changes to the PSTAIRE helix and the T-loop realign active site residues and makes the active site accessible, which in turn, activates CDK2 (Jeffrey *et al.*, 1995).

1.5.2 The yeast cell cycle.

Pioneering work has been carried out in the field of yeast molecular genetics which has heightened our understanding of the eukaryotic cell cycle. The yeast cell cycle is governed by a single CDK. This is Cdc28 in the budding yeast *Saccharomyces cerevisiae* and Cdc2 in the fission yeast *Schizosaccharomyces pombe* (Morgan, 1997). Cdc28 was shown to have a key role in the cell cycle (Hartwell, 1974) where it initiated the first step in the cell cycle, termed START (Hereford and Hartwell, 1974). Cdc28 was necessary to activate two independent pathways, one leading to DNA replication and nuclear division and the other to bud emergence and cytokinesis (Hartwell *et al.*, 1974; Hartwell, 1991). It was shown that the gene product of *Cdc28* had a dual role in two phases of the cell cycle (Piggott *et al.*, 1982) and that that Cdc28 was indeed a protein kinase (Reed *et al.*, 1985). Work on the distantly related yeast *S. pombe* identified the Cdc28 homologue, Cdc2, which was required for entry into the cell cycle and for controlling the onset of mitosis (Nurse and Bissett, 1981). Cdc2 was shown to have 62% identity to Cdc28, and *Cdc2* encoded a 34 kDa gene product (Hindley and Phear, 1984) which was determined to be a protein kinase (Simanis and Nurse, 1986). These protein kinases are involved in all stages of the cell cycle of their respective species of yeast.

The ability to control cell cycle progression is in part due to the association of protein kinases (CDKs) with cyclin proteins which activate the CDKs. Cyclins were discovered due to their oscillating levels in abundance during sea urchin cleavage divisions (Evans *et al.*, 1983; Nasmyth, 1993). Numerous cyclin proteins have been identified since whose biochemical properties help promote the correct timing of CDK activity during the cell cycle (Loog and Morgan, 2005). In *S. cerevisiae*, two families of cyclins (Cln and Clb (B-type)) control the cell cycle; based on sequence, function and timing of expression, they can be grouped into three categories: the G1 cyclins Cln1, Cln2 and Cln3, the S-phase cyclins Clb5 and Clb6, and the mitotic cyclins Clb1, Clb2, Clb3 and Clb4 (Jackson *et al.* 2006). The G1 cyclins, Cln1 Cln2 and Cln3 are essential for START. None of these *Cln* genes are essential for cell division; however, deletion of all three genes is lethal causing cells to arrest in G1 (Richardson *et al.*, 1989). Clb5 and Clb6 trigger the transition from G1 to S-phase (Basco *et al.*, 1995; Epstein and Cross, 1992; Kuhne and Linder, 1993; Schwob and Nasmyth, 1993) and play redundant roles in the initiation of S-phase (Nasmyth, 1993). Either Clb5 or Clb6 can promote entry into S-phase on schedule (Basco *et al.*, 1995; Epstein and Cross, 1992; Schwob and Nasmyth, 1993); however, Clb5 but not Clb6 is required for timely progression through S-phase (Epstein and Cross, 1992; Schwob and Nasmyth, 1993). Mitosis is then governed by Clb1, Clb2, Clb3 and Clb4 where these proteins are necessary for the formation and function of the mitotic apparatus (Fitch *et al.*, 1992; Richardson *et al.*, 1992; Surana *et al.*, 1991), and deletion of *Clb2* alone greatly delays the onset of mitosis (Surana *et al.*, 1991).

In *S. pombe*, four cyclin proteins control the cell cycle, Cig1, Cig2, Cdc13 and Puc1. Cig1 Cig2 and Cdc13 are B-type cyclins, whereas Puc1 is more closely related to *S. cerevisiae* Cln cyclins (Fisher and Nurse, 1996; Stern and Nurse, 1996). The B-type cyclins are essential for entry into S-phase and mitosis (Fisher and Nurse, 1996; Hayles *et al.*, 1994; Martin-Castellanos *et al.*, 1996; Mondesert *et al.*, 1996) and also promote G1 progression past START (Martin-Castellanos *et al.*, 1996; Obara-Ishihara and Okayama, 1994). Cig2

regulates entry into S-phase (Martin-Castellanos *et al.*, 1996; Mondesert *et al.*, 1996; Obara-Ishihara and Okayama, 1994) while Cig1 also contributes to the onset of S-phase (Fisher and Nurse, 1996; Mondesert *et al.*, 1996). Cdc13 controls entry into mitosis (Booher *et al.*, 1989; Moreno *et al.*, 1989) and Puc1 has been shown to play an important regulatory role in the G1 phase of the cell cycle (Martin-Castellanos *et al.*, 2000). As cyclins have an important regulatory role in the cell cycle, it is evident that they are tightly controlled. Two regulatory processes identified in cyclin control have been identified, gene transcription and protein degradation (Morgan, 1997).

However, although only one CDK controls the cell cycle in yeast, it is important to realise that there are other CDKs involved in yeast cellular processes. For example, in *S. cerevisiae*, five CDKs function to regulate transcription; Kin28, Srb10, Ctk1, Sgv1 and Pho85. Three of these CDKs, Kin28 (Valay *et al.*, 1993), Srb10 (Liao *et al.*, 1995) and Ctk1 (Sterner *et al.*, 1995; Lee and Greenleaf, 1991), regulate mRNA synthesis by phosphorylating the carboxyl-terminal domain (CTD) of RNA polymerase II. Sgv1 regulates transcription, possibly also as a CTD kinase, as its mammalian orthologue CDK9, functions as a CTD kinase (Prelich and Winston, 1993). Lastly, Pho85 functions to inhibit gene transcription in response to phosphate levels (Lenburg and Oshea, 1996). However, Pho85 also has a secondary role in cell cycle progression, promoting the G1-S-phase transition in the absence of the G1 cyclins, Cln1 and Cln2 (Espinoza *et al.*, 1994; Measday *et al.*, 1994).

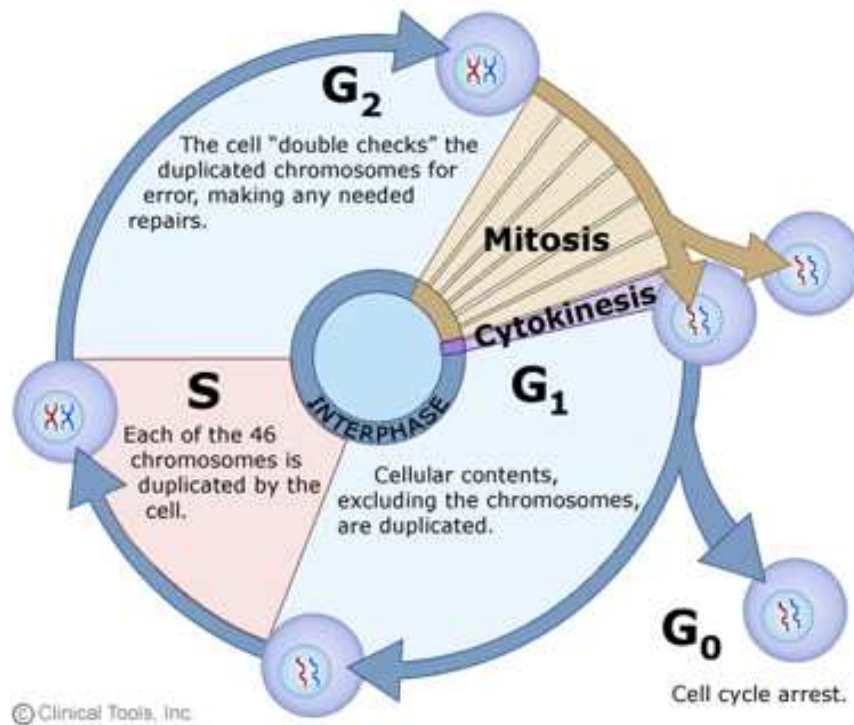


Figure 1.3 – Schematic of the eukaryotic cell cycle. Quiescence: Cells which are not proliferating are said to be quiescent or in "G₀" phase. **G₁ Phase:** Cells grow in size in response to mitogenic signals, which may trigger a commitment to entering the next phase of the cell cycle. During G₁ phase protein kinases become active and thereby send a signal that the cell division process has begun. **The Restriction Point:** Late in G₁, many cell types become committed to entering the next phase of the cell cycle at a time termed the restriction point or START. **S-Phase:** Soon after the restriction point a cell begins to replicate its genetic material. Cells synthesize an exact replica of their DNA genome replicating of all their chromosomes. **G₂ Phase:** At the completion of S-phase, DNA replication ceases and cells enter the G₂ phase of the cell cycle where they grow and prepare for the onset of mitosis. **Mitosis:** Mitosis is the phase of the cell cycle in which cells segregate their duplicated chromosomes into two separate nuclei and physically divide into two separate daughter cells. **Cytokinesis** is the process whereby the cytoplasm of a single cell is divided to spawn two daughter cells. It usually initiates during the late stages of mitosis to complete the cell cycle. The cell cycle schematic was taken from www.images.clinicaltools.com.

1.5.3 The mammalian cell cycle.

The mammalian cell cycle, by comparison with yeast, is controlled by a number of CDKs. At present, 13 CDK proteins have been identified in the human and mouse genomes and around 29 cyclins have been identified in man (Malumbres and Barbacid, 2005). A summary of mammalian CDKs and their cyclin partners is shown in Table 1.1. Mammalian CDK function has been determined from biochemical studies with human tumor cell lines and by their ability to complement yeast CDK mutants. Additional research has been carried out using genetic manipulation of mouse models which is considered the gold standard method of establishing CDK function and essentiality.

Homologues of Cdc2 were identified in human cells by their ability to complement yeast mutants (Draetta *et al.*, 1987; Lee and Nurse, 1987). Human Cdc2 was named CDK1, the first mammalian CDK identified and is functionally homologous to Cdc2/Cdc28 in yeast (Morgan, 1997). CDK1 binds preferentially to A-type (A1 and A2) and B-type (B1, B2 and B3) cyclins which are involved in the G2 and M phases of the cell cycle (Malumbres and Barbacid, 2005). At the end of S-phase, A-type cyclins associate with CDK1 and are involved in cell cycle progression into G2-phase. During G2, the A-type cyclins are degraded by ubiquitin-mediated proteolysis and the B-type cyclins are synthesised (Malumbres and Barbacid, 2005). As a result, CDK1 complexes with the B-type cyclins, preferentially binding to cyclins B1 and B2. The CDK1-cyclinB complexes are thought to regulate several events during both the G2-M transition and progression through mitosis itself (Nigg, 2001) where CDK1-cyclinB is also known as the M-phase promoting factor (MPF) (Morgan, 1997). Finally, the inactivation of CDK1-cyclinB complexes is required for the successful exit from mitosis occurring via ubiquitin-mediated degradation of the B-type cyclins. Genetic manipulation has recently shown that CDK1 can execute all the events that are required to drive cell division in the absence of other CDKs (Santamaria *et al.*, 2007). CDK1 can functionally compensate in the absence of interphase CDKs (CDK2,

CDK3, CDK4 and CDK6), by binding the G1 cyclins (D and E-type cyclins). This shows that CDK1 is the only essential CDK and is sufficient to drive the mammalian cell cycle.

CDK2 was cloned by three independent approaches based on the complementation of *S. cerevisiae* *Cdc28* mutants, differential display or interaction with Cyclin A (Elledge and Spottswood, 1991; Paris *et al.*, 1991; Tsai *et al.*, 1991; Ninomiya-Tsuji *et al.*, 1991). Like CDK1, CDK2 is functionally homologous to Cdc2/Cdc28 in yeast but primarily associates with the A-type (A1 and A2) and E-type (E1 and E2) cyclins (Morgan, 1997) and CDK2-cyclinE is required for the G1-S-phase transition (Tsai *et al.*, 1993). CDK2 interacts with the A and E-type cyclins at the beginning of S-phase to induce the initiation of DNA synthesis, and then binds cyclin A throughout S-phase for DNA synthesis (Morgan, 1997). Genetic approaches to study *CDK2* have been carried out showing that CDK2 is not essential for the mammalian cell cycle, since *CDK2* knockout mice are viable (Berthet *et al.*, 2003).

CDK3 is closely related to Cdc2 and CDK2 and can complement Cdc28 mutants in *S. cerevisiae* (Meyerson *et al.*, 1992). CDK3 interacts with the A and E-type cyclins suggesting it may have a similar role to CDK2 during interphase of the cell cycle. It also complexes with cyclin C during the G0-G1 transition (Ren and Rollins, 2004). Little genetic analysis of *CDK3* has been carried out in mice because most laboratory strains of mice are deficient in CDK3 due to a naturally occurring mutation (Ye *et al.*, 2001).

CDK4 was originally identified as PSK-J3, later renamed CDK4 (Hanks, 1987) and associates exclusively with the D-type cyclins (D1, D2 and D3) (Malumbres and Barbacid, 2005). Along with CDK6, CDK4 is the principle contributor of cell cycle initiation and required for progression through G1 into S-phase (Matsushime *et al.*, 1994). *CDK4* knockout mice have shown that loss of *CDK4* is not detrimental to cell cycle progression

and that cell proliferation continues (Malumbres *et al.*, 2004), although, S-phase entry is delayed (Tsutsui *et al.*, 1999).

CDK5 was originally identified as PSSALRE, later renamed CDK5 (Hellmich *et al.*, 1992) and is primarily involved in neuronal function (Kesavapany *et al.*, 2003). CDK5 is activated by non-cyclin partners p35 and p39, two proteins that are almost uniquely expressed in brain (Cruz and Tsai, 2004; Kesavapany *et al.*, 2004). It has been shown that targeted disruption of the *CDK5* locus in mice results in embryonic lethality (Ohshima *et al.*, 1996) where the embryos show abnormalities in the development and structure of their nervous system. Furthermore, p35:p39 double mutant mice show similar phenotypes to mice lacking CDK5, further validating these proteins as essential CDK5 partners (Ko *et al.*, 2001).

CDK6 was originally identified as PLSTIRE and later renamed CDK6. CDK6, like CDK4 associates with the D-type cyclins (D1, D2 and D3) (Meyerson and Harlow, 1994). CDK6-cyclinD complexes are required for progression through G1-phase of the cell cycle by repressing the retinoblastoma (Rb) protein through phosphorylation (Meyerson and Harlow, 1994). As with CDK2 and CDK4, it has been shown that loss of CDK6 does not greatly affect cell proliferation (Malumbres *et al.*, 2004).

CDK7 was originally identified as p40-MO15 and later renamed CDK7 because it was found to associate with cyclin H (Fisher and Morgan, 1994; Mäkelä *et al.*, 1994). CDK7-cyclinH associates with an assembly factor MAT1 (Tassan *et al.*, 1995a) and has been shown to be a component of the RNA polymerase II transcription factor complex, TFIIF. CDK7-cyclinH-MAT1 is the CAK in mammals which phosphorylates and activates other CDKs involved in the cell cycle (Lolli and Johnson, 2005). Limited genetic analysis of CDK7 or Cyclin H has been carried out in mice; however, the disruption of MAT1 results in an inability to enter S-phase of the cell cycle (Rossi *et al.*, 2001).

CDK8 was identified and shown to be a putative kinase binding partner for cyclin C (Tassan *et al.*, 1995b). CDK8-cyclinC regulates transcription through phosphorylation of the C-terminal domain of the large subunit of RNA polymerase II and is a component of the RNA polymerase holoenzyme. CDK8-cyclinC complexes also phosphorylate cyclin H to inhibit CAK activity (Akoulitchev *et al.*, 2000). It has recently been shown that *CDK8* is essential in mice during the pre-implantation phase of embryonic development (Westerling *et al.*, 2007).

CDK9, originally identified as PITALRE is a Cdc2-related protein kinase that was shown to phosphorylate the Rb protein (Grana *et al.*, 1994b) and renamed CDK9. CDK9 complexes with cyclins K and T to form P-TEFb transcription factors. CDK9-cyclinT complexes also regulate transcription in the same manner as CDK8-cyclinC complexes (Malumbres and Barbacid, 2005).

CDK10, originally identified as PISSLRE is a Cdc2-related protein kinase and was renamed CDK10 (Grana *et al.*, 1994a). No cyclin partner has been identified for CDK10 so far (Kasten and Giordano, 2001). CDK10 was shown to be involved in regulating the G2-M-phase of the cell cycle (Li *et al.*, 1995) and has also been shown to inhibit transactivation of the Ets2 transcription factor, a regulator of CDK1 expression (Kasten and Giordano, 2001).

CDK11, originally identified as PITSLRE (Xiang *et al.*, 1994), binds the L-type cyclins (L1 and L2) and interacts with RNA polymerase II, playing a role in transcript production and regulation of RNA processing (Loyer *et al.*, 2005). As with *CDK8*, *CDK11* has been shown to be required for pre-implantation in mice, with loss of CDK11 resulting in embryonic lethality (Li *et al.*, 2004).

CDK12 was originally named CrkRS and is a Cdc2-related protein kinase. CrkRS was shown to associate with the L-type cyclins (L1 and L2) and was renamed CDK12 (Chen *et al.*, 2006). CDK12-cyclinL complexes regulate alternative splicing.

CDK13 was originally identified as CDC2L5 with strong sequence homology to CDK12. CDC2L5 was shown to interact with the L-type cyclins (L1 and L2) and was renamed CDK13 (Chen *et al.*, 2007). CDK13 also regulates alternative splicing.

CDK	PSTAIRE motif	Main activating cyclin (other cyclins)	Other interacting proteins	Cellular function
CDK1	PSTAIRE	A1, A2, B1, B2 (B3, D1, D2, E)	Cks	Cell cycle (G2-M)
CDK2	PSTAIRE	A1, A2, E1, E2 (D1, D2, B1, B3)	–	Cell cycle (G1-S)
CDK3	PSTAIRE	E1, E2, A1, A2, C	E2F/DP	Cell cycle (G0-G1-S)
CDK4	PISTVRE	D1, D2, D3	MyoD	Cell cycle (G1-S)
CDK5	PSSALRE	p35, p39 (D-, E- and G-type cyclins)	–	Senescence, Postmitotic neurons
CDK6	PLSTIRE	D1, D2, D3	–	Cell cycle (G1-S)
CDK7	NRTALRE	H	MAT1	Cdk-activating kinase, Transcription
CDK8	SMSACRE	C (K?)	–	Transcription
CDK9	PITALRE	T1, T2, K	–	Transcription
CDK10	PISSLRE	Unknown	Ets2	Transcription, Cell cycle (G2-M)
CDK11	SMSACRE	L1, L2 (D)	CK2, RNA pol II, 14-3-3, eIF3	Transcription, Cell cycle (M)
CDK12	PITAIVRE	L1, L2	–	Alternative RNA splicing
CDK13	PITAIVRE	L1, L2	–	Alternative RNA splicing

Table 1.1 – Currently identified mammalian CDKs and their known cyclin binding partners. Included is the PSTAIRE motif involved in cyclin binding, known interacting proteins and a general description of the cellular function of these protein kinases.

1.5.4 The trypanosomatid cell cycle.

Studies on the yeast and mammalian cell cycles have established the key CDKs and cyclins that are involved in cell cycle regulation. This work is relevant to the study of the parasite cell cycle as many of these cell cycle proteins are homologous to those in parasites such as CDK1 in humans and CRK3 in *Leishmania* (Grant *et al.*, 1998). Due to their pivotal role in the cell cycle, these proteins offer an attractive area for drug discovery and development against trypanosomatids.

The CDK family in trypanosomatids is relatively large with 11 in *T. brucei* and *L. major* and 10 in *T. cruzi* (Table 1.2, upper panel). Analysis of the genome of the three trypanosomatids identified 10 putative cyclins, CYC2-11 (Table 1.2, lower panel) (Naula *et al.*, 2005). CYC1 from *T. brucei*, originally identified as a mitotic-like cyclin (Affranchino *et al.*, 1993), was subsequently shown to lack the characteristics of a mitotic-like cyclin (Hammarton *et al.*, 2000). *L. major* has an additional cyclin, CYCA, named so because there is no homologue of this cyclin in *T. brucei*, where *T. brucei* cyclins have been named CYC2, CYC3 etc.

1.5.4.1 The *Leishmania* cell cycle.

Two Cdc2-related protein kinase genes, *CRK1* and *CRK3* have been cloned from *L. mexicana* (Mottram *et al.*, 1993; Grant *et al.*, 1998) and studied in detail. *CRK1* encodes a 34 kDa protein kinase with 56% amino acid identity to human Cdc2 (CDK1). *CRK1* is present in all life cycle stages; however, it has stage regulated histone H1 kinase activity restricted to the insect stages of the parasite, both proliferative promastigotes and non-dividing metacyclic promastigotes (Mottram *et al.*, 1993). Gene disruptions showed *CRK1* is essential in promastigotes (Mottram *et al.*, 1996) where attempts to create null mutants, replacing the alleles with hygromycin (*hyg*) and phleomycin (*ble*), were unsuccessful. Second round transfections with a *ble*-targeting fragment produced two forms of mutants, neither of which was null. First, the transfected fragment formed an episome; second, the

transfectants contained wild-type *CRK1* alleles in addition to *hyg* and *ble* cassettes showing plasticity in chromosome number (Mottram *et al.*, 1996). This is accepted as an indication of retaining an essential gene as it is not possible to obtain a null mutant (Barrett *et al.*, 1999; Cruz *et al.*, 1993; Mottram *et al.*, 1993; Mottram *et al.*, 1996). *T. brucei* *CRK1* encodes a protein which shares 72% identity with *L. mexicana* *CRK1* (Mottram and Smith, 1995) and was shown to complement *L. mexicana* *CRK1* function (Mottram *et al.*, 1996). Although, the precise function of *L. mexicana* *CRK1* is yet to be determined, *T. brucei* *CRK1* function has been indicated by ribonucleic acid interference (RNAi) experiments indicating a redundant function for these proteins in the two parasites (Section 1.5.4.2).

CRK3 is predicted to encode a 35.6 kDa protein with 54% identity to human Cdc2 and 78% identity to *T. brucei* *CRK3*. It is a single copy gene whose product has protein kinase activity towards histone H1 (Grant *et al.*, 1998). Sequence analysis showed the *Leishmania* *CRK3* contains the domains and residues characteristic of a serine/threonine protein kinase. Furthermore, *CRK3* contains residues and domains conserved in other organisms; Thr-14 and Tyr-15 which are required for ATP binding, and Thr-161 which is predicted to be phosphorylated by a CDK activating kinase (Grant *et al.*, 1998). X-ray crystallography showed the PSTAIRE box in CDKs is the region, which binds the cyclin partner (Jeffrey *et al.*, 1995). This is a highly conserved region and consists of 16 amino acids EGV PSTAIREISLLKE. The equivalent domain found in *Leishmania* *CRK3* is EGIPQTALREVSILQE and has six substitutions by comparison (Grant *et al.*, 1998) and is identical to that found in *T. brucei* *CRK3* (Mottram and Smith, 1995). The presence of this domain in *CRK3* suggests that specific cyclin binding plays an important role in *CRK* regulation (Grant *et al.*, 1998).

Gene disruption was carried out to establish whether *CRK3* was essential for the cell cycle progression of *L. mexicana* (Hassan *et al.*, 2001). Attempts were carried out to replace both *CRK3* alleles with *hyg* and *ble* resistance cassettes. Southern blot analysis indicated that mutants heterozygous for *CRK3* had been successfully disrupted by *hyg* and *ble* constructs. Double resistant clones were found to contain *hyg* and *ble* resistance cassettes indicating the two alleles had been successfully replaced. However, the wild type *CRK3* gene remained and as seen with *CRK1*, ploidy changes had occurred to retain the *CRK3* gene (Hassan *et al.*, 2001). This confirmed that *CRK3* is essential for cell cycle progression in *L. mexicana* as a *CRK3* null mutant could not be generated.

L. major CRK3 was shown to complement a temperature sensitive *S. pombe cdc2* null mutant (Wang *et al.*, 1998). *L. major CRK3* shares 99% identity with *L. mexicana CRK3* suggesting these two proteins are functional homologues of *cdc2* and therefore mammalian CDK1. Indeed as discussed in 1.8.1.1, *L. mexicana CRK3* inhibition causes a G2-M cell cycle block further indicating its role as a functional homologue of mammalian CDK1.

1.5.4.2 The *T. brucei* cell cycle.

There is a large family of putative CDKs and cyclins in *T. brucei* (Table 1.2) but few have been characterised in detail. Gene functions in *T. brucei* can be analysed by RNAi, which has been carried out on *CRK1*, 2, 3, 4 and 6 (Tu and Wang, 2004; Tu and Wang, 2005). Downregulation of *CRK1* in both procyclic and bloodstream form trypanosomes resulted in a reduced growth rate and an accumulation of cells in the G1-phase of the cell cycle. This indicated a role in the G1-S transition in both forms of *T. brucei* (Tu and Wang, 2004; Tu and Wang, 2005). Simultaneous downregulation of *CRK1* and either *CRK2*, 4 and 6 enhanced the phenotype seen with *CRK1* downregulation only, suggesting a supplementary role for these three *CRKs*.

Cdc2-related kinases predicted from the genome of *Leishmania major* and *Trypanosoma brucei*

<i>L. major</i>	Name	Size kDa	T ¹⁴ , Y ^{15*}	T ^{160*}	Cyclin binding	<i>T. brucei</i> orthologue	CMGC family
LmjF21.1080	CRK1	34.4	T, Y	T	PCTAIRE	Tb10.70.7040	CDK
LmjF05.0550	CRK2	36.4	S, Y	T	SVSSIRE	Tb07.30D13.430	CDK
LmjF36.0550	CRK3	35.6	T, Y	T	PQTALRE	Tb10.70.2210	CDK
LmjF16.0990	CRK4	51.7	T, Y	S	PGAAIRE	Tb08.5H5.130	CDK
LmjF35.5010	CRK5	44.2	T, F	T	QVNRLRE	Tb09.211.0960	RCK-MOK
LmjF27.0560	CRK6	37.3	T, Y	T	PATTIRE	Tb11.47.0031	CDK
LmjF26.0040	CRK7	32.4	Q, F	S	PHPVARE	Tb07.43M14.340	CDK
LmjF11.0110	CRK8	44.4	T, F	T	HRCTFRE	Tb11.02.5010	CDK
LmjF27.1940	CRK9	101.8	A, S	T	QREEARP	Tb927.2.4510	CDK
LmjF29.2150	CRK10	48.4	C, G	V	RKGAFDA	Tb03.48K5.160	CDK
LmjF30.1780	CRK11	66.3	G, Y	P	SATVLRE	Tb06.5F5.880	CDK
LmjF09.0310	CRK12	54.4	T, Y	T	PQTSLRE	Tb11.01.4130	CDK

Cyclins and protein kinase accessory proteins predicted from the genome of *Leishmania major* and *Trypanosoma brucei*

<i>L. major</i>	Name	Size kDa	<i>T. brucei</i> orthologue	Name	Alternative name	Products
LmjF25.1470	CYCA	34.2	none	–	–	Mitotic-like cyclin
LmjF32.0820	CYC2	18.8	Tb11.01.5660	CYC2	CycE1	CYC2 cyclin
LmjF30.0080	CYC3	46.9	Tb06.3A7.1310	CYC3	CycB1	Mitotic-like cyclin
LmjF05.0710	CYC4	149	Tb07.21H1 5.170	CYC4	CycE3	CYC2-like cyclin
LmjF33.0770	CYC5	93.6	Tb10.26.0510	CYC5	CycE4	CYC2-like cyclin
LmjF32.3320	CYC6	35.2	Tb11.01.8460	CYC6	CycB2	Mitotic cyclin
LmjF30.3630	CYC7	27.6	Tb06.30P15.430	CYC7	CycE2	CYC2-like cyclin
LmjF26.0330	CYC8	50.6	Tb07.27M11.950	CYC8	CycB3	Mitotic-like cyclin
LmjF32.0760	CYC9	32.9	Tb11.01.5600	CYC9	–	Cyclin C-like
LmjF24.1890	CYC10	68.7	Tb08.11J15.340	CYC10	–	CYC2-like cyclin
LmjF24.1880	CYC11	101.6	Tb08.11J15.300	CYC11	–	CYC2-like cyclin
LmjF06.0960	MOB1	–	Tb07.10C21.430	MOB1A	–	MOB1
LmjF32.3790	CKS1	–	Tb07.10C21.440	MOB1B	–	MOB1
			Tb11.01.8085	CKS1	–	CKS1

Table 1.2 – Cdc2-related kinases, cyclins and accessory proteins predicted from the *L. major* and *T. brucei* genomes. Taken from *Biochimica et Biophysica Acta* (Naula *et al.*, 2005).

Downregulation of CRK3 in both procyclic and bloodstream form trypanosomes resulted in a mitotic block and growth arrest. CRK3 was found to associate with two cyclins; CYC2 and a mitotic cyclin homologue CYC6 (Van Hellemond *et al.*, 2000; Hammarton *et al.*, 2003a; Li and Wang, 2003; Hammarton *et al.*, 2004), and downregulation of these two cyclins correlated with CRK3 downregulation. CYC2 downregulation by RNAi caused an irreversible growth arrest in procyclic and bloodstream form trypanosomes (Hammarton *et al.*, 2004; Li and Wang, 2003) and CRK3:CYC2 was shown to be the protein kinase complex required for progression through the G1-S phase transition in both forms of trypanosomes. CYC6 downregulation resulted in a mitotic block in both procyclic and bloodstream form trypanosomes. Therefore, the CRK3:CYC6 protein kinase complex has the properties of a G2-M phase kinase required for the transition into mitosis showing CRK3 is a functional homologue of mammalian CDK1.

1.5.4.3 The *T. cruzi* cell cycle.

As with *L. mexicana*, two CDKs, CRK1 and CRK3, have been studied in *T. cruzi* (Gomez *et al.*, 1998; Gomez *et al.*, 2001; Santori *et al.*, 2002; da Cunha *et al.*, 2005). CRK1 was active throughout G1 and S-phases of the cell cycle whereas CRK3 is a possible CDK1 homologue as its activity peaked at the G2-M boundary (Santori *et al.*, 2002). Both CRKs are cyclin-dependent kinases as they were able to interact with mammalian cyclins. However, interestingly, CRK1 was active as a recombinant protein, highlighting that cyclin binding may not be as vital for its activity (Gomez *et al.*, 1998). CRK3 and to a lesser extent CRK1 was capable of phosphorylating histone H1 where the activity peaked at the G1-S and G2-M phase transitions. It is known that histone H1 phosphorylation varies during the life cycle of *T. cruzi* (da Cunha *et al.*, 2005) but the relevance of histone H1 phosphorylation by CRK3 has not been identified.

1.6 Protein kinases as drug targets.

A number of diseases are attributed to defects in protein kinase-controlled cell signalling pathways. Protein kinases therefore represent an attractive area for therapeutics by way of inhibitor design. There are 518 protein kinases encoded in the human genome (termed the kinome), representing approximately 2% of all genes (Manning *et al.*, 2002) which are grouped by class. Tyrosine kinases transfer a phosphate group from ATP onto a tyrosine residue of a protein. Two classes of tyrosine kinase are present in the human genome, non-receptor tyrosine kinases such as SRC and receptor tyrosine kinases such as vascular endothelial growth factor receptor (VEGFR) and endothelial growth factor receptor (EGFR). An example of targeting a receptor tyrosine kinase is with the commercially available drug Gefitinib (Iressa[®]) (www.iressa.com) (Figure 1.5, lower left). It is a small molecule inhibitor that binds to the EGFR receptor kinase domain and is registered for the treatment of metastatic non-small cell lung cancer (NSCLC) (Barker *et al.*, 2001). Other protein kinases such as GSK-3 are inhibited in healthy patients as part of the signalling pathway triggered by insulin when it binds to its receptor. However, in patients with adult onset or Type 2 Diabetes, GSK-3 is not inhibited due to a defective insulin receptor. Therefore, GSK-3 phosphorylates and inactivates glycogen synthase, thereby inhibiting glycogen synthesis, resulting in high blood glucose levels. As a result, GSK-3 is the focus of inhibitor design for diabetes (Engler *et al.*, 2004) (www.cyclacel.com). CDKs, which are serine/threonine protein kinases will be discussed in greater detail as potential drug targets in section 1.6.1.

1.6.1 CDKs as potential drug targets.

The search for chemical inhibitors of CDKs was initiated due to their potential as anti-tumour agents (Meijer, 1995). The involvement of CDKs in a number of cellular events and disorders has resulted in CDKs being the focus of research as potential drug targets in a number of other disease areas (Figure 1.4).

The effects of CDK inhibitors on the cell cycle and their potential value for the treatment of cancer have been extensively studied (Sielecki *et al.*, 2000; Malumbres and Barbacid, 2001). Many CDKs are over expressed in cancer, and it is known that inhibition of CDKs arrest cells in G1 (Soni *et al.*, 2001) or G2-M (Damiens *et al.*, 2001) and also triggers apoptosis (Edamatsu *et al.*, 2000). To date, CDK1, 2, 4 and 6 have been the most explored targets; however, CDK7, 8 and 9 are also appealing targets.

A number of neurodegenerative disorders such as Alzheimer's disease (AD) and amyotrophic lateral sclerosis (ALS) are associated with abnormal regulation of CDK5, which is highly expressed in the nervous system (Fischer *et al.*, 2003). A characteristic of AD is the aggregation of the microtubule protein tau, which is phosphorylated by a number of kinases including CDK5 (Tsai *et al.*, 2004). ALS leads to the loss of motor neurones, resulting in paralysis and death (Bajaj, 2000) and CDK5 has been implicated in ALS pathogenesis (Nguyen *et al.*, 2001). The increasing evidence that neuronal cell death is associated with increased CDK activity suggests that CDK5 inhibition may influence the outcome of some of these diseases (Knockaert *et al.*, 2002; Fischer *et al.*, 2003).

In recent years, pharmacological inhibitors of CDKs have been reported to prevent viral replication *in vitro* (Schang, 2001). Viral replication is known to be frequently coordinated with the cell cycle and a number of viruses require CDKs for their replication and in some cases they express their own cyclins (Knockaert *et al.*, 2002; Fischer *et al.*, 2003). Therefore, targeting cellular kinases may be effective as a way of establishing anti-viral therapeutics.

Glomerulonephritis is a disease of the renal system where inflammation of glomeruli and small blood vessels occurs in the kidney. IgA nephropathy, the leading cause of glomerulonephritis worldwide, is characterised by abnormal, but non-tumoral mesangial cell proliferation (D'amico, 1987; Donadio and Grande, 2002). Glomerular diseases

constitute potential targets for treatment with pharmacological inhibitors of CDKs, as illustrated in HIV-associated nephropathy (Nelson *et al.*, 2001).

CDKs may also be targeted when treating cardiovascular diseases. The proliferation of smooth muscle cells is a common feature of atherosclerosis and restenosis. Atherosclerosis is an inflammatory response in the walls of arteries, commonly referred to as “hardening” or “furring”, and is the leading cause of coronary heart disease (Lusis, 2000). Restenosis is a common consequence of balloon angioplasty, the main intervention for symptomatic atherosclerotic lesions (Dangas and Kuepper, 2002). These proliferative cardiac disorders are potential areas for therapeutic treatment with cell cycle inhibitors (Sriram and Patterson, 2001).

The involvement of CDKs in reproductive biology has been evaluated for the *in vitro* production of animal embryos. The use of CDK inhibitors to arrest nuclear oocyte maturation (meiotic divisions), while allowing oocyte cytoplasmic maturation *in vitro* (final growth and developmental) is under investigation (Fischer *et al.*, 2003). After the reversible inhibition of nuclear maturation by the CDK inhibitors and *in vitro* fertilisation, the embryos can be obtained with no loss of developmental ability (Ponderato *et al.*, 2001).

CDK inhibition in inflammatory diseases such as rheumatoid arthritis (RA) is being investigated as a possible treatment. A characteristic of RA is the overgrowth of synovial fibroblast cells, highlighting an increase in cell cycle activity. Treatment of animal models with collagen-induced arthritis with flavopiridol proved successful, where joint destruction due to RA was suppressed (Sekine *et al.*, 2008).

A promising area of investigating CDKs as drug targets is in unicellular parasites. As this is of particular relevance to this project, it will be focused on and discussed in section 1.8.

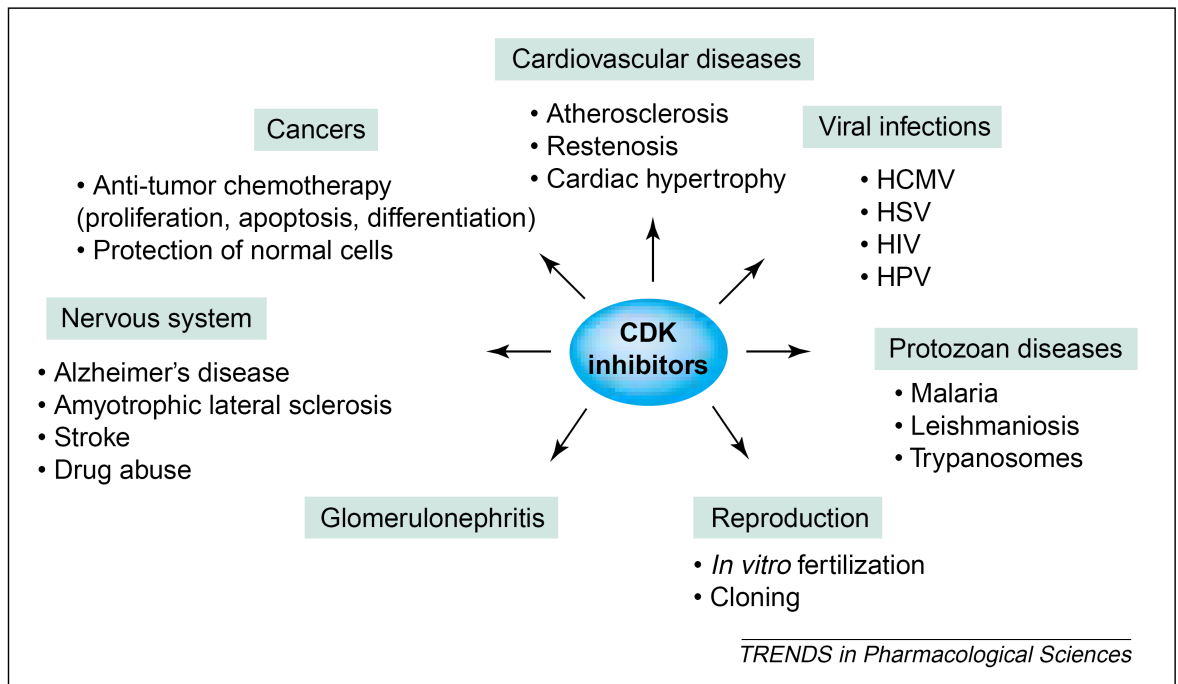


Figure 1.4 – Some of the potential applications of CDK inhibitors. As CDKs are involved in cell proliferation, apoptosis, neuronal function, and transcription, pharmacological inhibitors of CDKs are of serious interest in tackling diseases and disorders related to these cellular functions. Taken from *TRENDS in pharmaceutical Sciences* (Knockaert *et al.*, 2002).

1.7 Protein kinase inhibitors.

Protein kinase inhibitors fall into four main groups: substrate-specific inhibitors, ATP-competitive inhibitors, activation inhibitors and irreversible inhibitors where the ideal protein kinase inhibitor prevents activation rather than competing with ATP or the substrate. The first protein kinase inhibitors were developed over 20 years ago (Cohen, 2002), and formation of derivatives of these compounds have found widespread application, which has formed the basis for much of what is currently known about the physiological roles of their targets (Knight and Shokat, 2005). There is a vast number of protein kinase inhibitors currently in various stages of development which have been extensively reviewed, a number of which have been patented (Fischer and Gianella-Borradori, 2005; Pevarello and Villa, 2005; Rosania and Chang, 2000). This highlights the interest and financial commitment in this area of drug development put in by academia, biotechnology and pharmaceutical industries to develop protein kinase inhibitors to treat a number of diseases.

The discovery of staurosporine (Figure 1.7, right), an antifungal agent produced by bacteria of the genus *Streptomyces*, which was a nanomolar inhibitor of protein kinase C (PKC), resulted in the pharmaceutical industry taking interest in this area of pharmacological inhibitors (Cohen, 2002). As a result, a number of kinase inhibitors have been developed and approved for clinical use for a variety of disorders. Most notably is Imatinib (Gleevec®) (Figure 1.5, upper right), a tyrosine kinase inhibitor used to treat Chronic Myeloid Leukaemia (CML). It was the first important drug which targeted a protein kinase specifically, the Abl tyrosine kinase (Abl) (Cohen *et al.*, 2002a; Cohen *et al.*, 2002b) (www.gleevec.com). However, it has been shown to be equipotent towards two other tyrosine kinase receptors, platelet derived growth factor receptor (PDGFR) and c-Kit (Knight and Shokat, 2005). A further example of a small molecule protein kinase inhibitor is HA1077 (Fasudil®) (Figure 1.5, lower right), which is not used in the

treatment of cancer. It was approved for the treatment of cerebral vasospasm after surgery for subarachnoid haemorrhage, and associated cerebral ischaemic symptoms. At micromolar concentrations, it inhibits several protein kinases, such as the RHO-dependent protein kinase ROCK (Cohen, 2002). These examples highlight that protein kinase inhibitors which target single or multiple protein kinases in the cell, can be fully developed to become commercially available drugs to treat a variety of diseases.

1.7.1 CDK inhibitors.

The majority of the known pharmacological CDK inhibitors are ATP-antagonistic inhibitors of multiple CDK functions (Fischer, 2004). The first reported CDK inhibitor was 6-dimethylaminopurine (6-DMAP) (Figure 1.5, upper left), discovered as a puromycin analogue. It is a purine based compound which inhibited CDK1 with an IC_{50} value of $120\mu M$ (Rosania and Chang, 2000). 2, 6, 9-trisubstituted purines are the CDK inhibitors most structurally similar to ATP, whose binding they antagonise (Fischer, 2003). Screening a series of purine inhibitors, lead to the discovery of olomoucine and roscovitine (Figure 1.6, left) which both inhibited CDK1 with IC_{50} values of $7\mu M$ and $460nM$, respectively (Rosania and Chang, 2000). Olomoucine is also an inhibitor of CDK2:CycA, CDK2:CycE and CDK5, whose discovery has lead to the synthesis of many purines to identify more active and specific CDK inhibitors. One of these, roscovitine, is a close analogue of olomoucine and inhibits cyclin complexes of CDKs 1, 2, 5, 7 and 9 with low micromolar (μM) to high nanomolar (nM) IC_{50} values, but shows a lesser potency towards CDKs 4 and 6 (Fischer, 2003). CYC-202 (Seliciclib), a defined form of R-roscovitine, developed at Cyclacel Ltd, Dundee, inhibits cyclin complexes of CDKs 2, 7 and 9 with similar potency; CDKs 1 and 4 are also targeted but to a lesser extent (Fischer, 2004). CYC-202 induces apoptotic cancer cell death and is currently undergoing Phase IIb clinical trials for the treatment of NSCLC (www.cyclacel.com).

The co-crystal structures of CDK2 with olomoucine and roscovitine contributed to the discovery of purvalanols (Figure 1.6, right), which exhibit a similar selectivity profile and are among the most potent CDK2 inhibitors reported (Fischer, 2003). Purvalanols were reported as some of the best CDK inhibitors at the turn of the century (Rosania and Chang, 2000). Purvalanol B inhibits CDKs 1 and 2 with IC_{50} values $<10nM$ but it has no effect on cell proliferation unlike purvalanol A, due to the lack of cellular uptake (Fischer, 2003). In summary, it was seen that 2, 6, 9-trisubstituted purines were selective towards some cellular CDKs, essentially inhibiting CDK1, CDK2, CDK5, CDK7 and CDK9, but not CDK4 and CDK6 (Meijer and Raymond, 2003). They inhibit cellular proliferation leading to cell cycle arrest in G1 and G2 and can induce apoptosis in mitotic cells.

There are a number of other classes of CDK inhibitors that have been the subject of interest. These include indirubins (Hoessel *et al.*, 1999) (Figure 1.8, left), specifically indirubin-3-monoxime and indirubin-5-sulfonate which are selective towards CDK1 and CDK2 (Marko *et al.*, 2001). These have been investigated further showing that the indirubin derivatives also target glycogen synthase kinase 3 (GSK-3) (Polychronopoulos *et al.*, 2004). Another class of inhibitors, paullones (Figure 1.8, right), were found to be potent CDK inhibitors; kenpaullone is a selective inhibitor of CDKs 1, 2 and 5 with nM activity with the most potent in the series named alsterpaullone (Schultz *et al.*, 1999).

However, perhaps the greatest success with CDK inhibitors to date is alvocidib (Flavopiridol®) (Figure 1.7, left), the first CDK inhibitor to reach clinical trials (Senderowicz, 1999). Developed by the National Cancer Institute (NCI), Flavopiridol is a non-purine CDK inhibitor, most potent against CDKs 1 (IC_{50} for CDK1 = 400nM (Rosania and Chang, 2000)), 4, 6 and 9 and can inhibit CDKs 2 and 7 as well as a number of other protein kinases (Fischer, 2004; Fischer and Gianella-Borradori, 2005). It can induce cell cycle arrest at both the G1-S and G2-M boundaries (Rosania and Chang, 2000) and tumor growth inhibition in a number of solid tumor cell lines (Shapiro, 2004). It has undergone

several phase II and phase III trials, but without living up to the initial expectations of a CDK inhibitor. It has, however, recently showed activity in patients suffering from refractory chronic lymphocytic leukaemia (Byrd *et al.*, 2007).

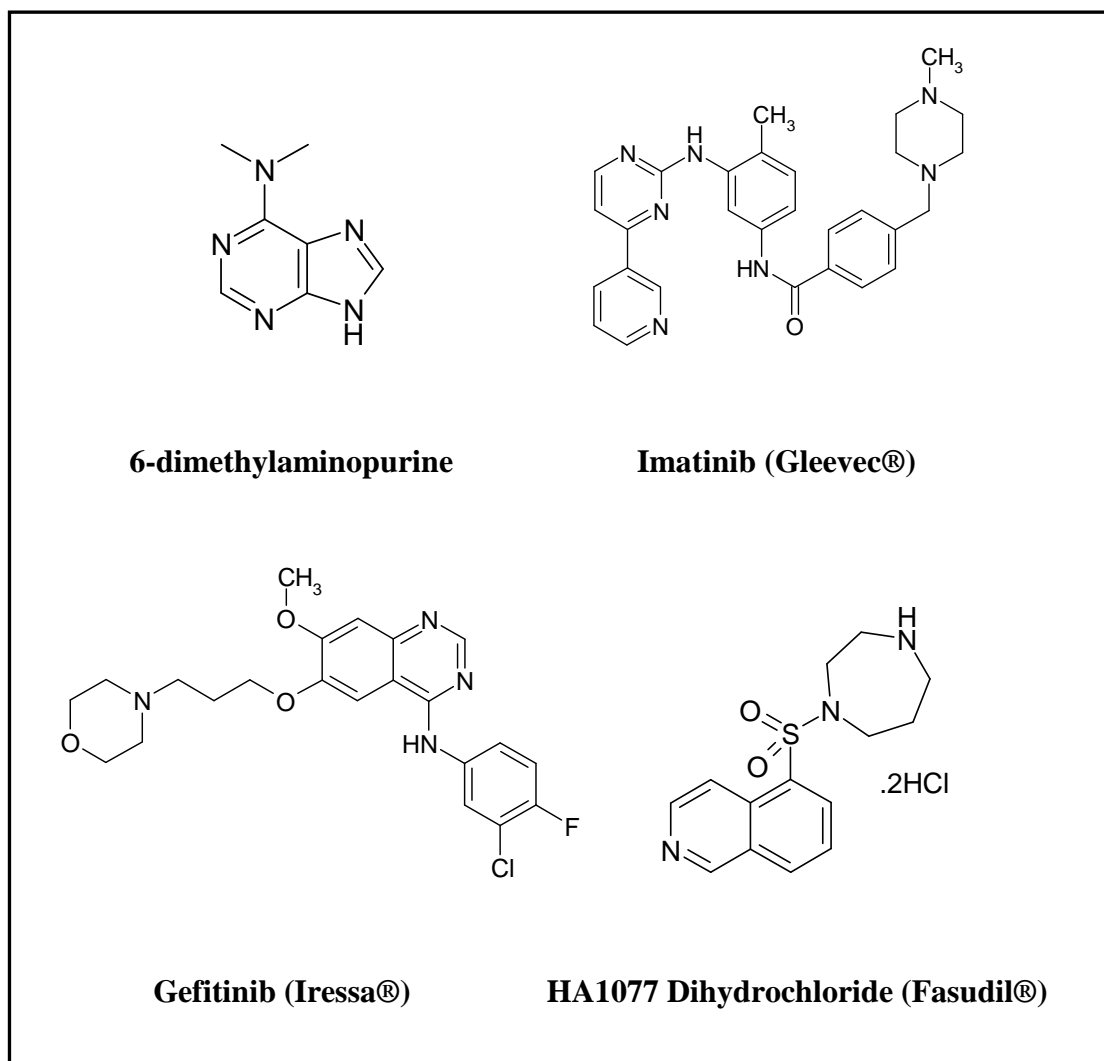


Figure 1.5 – The chemical structures of the first cyclin-dependent protein kinase inhibitor identified and commercially available protein kinase inhibitor drugs.

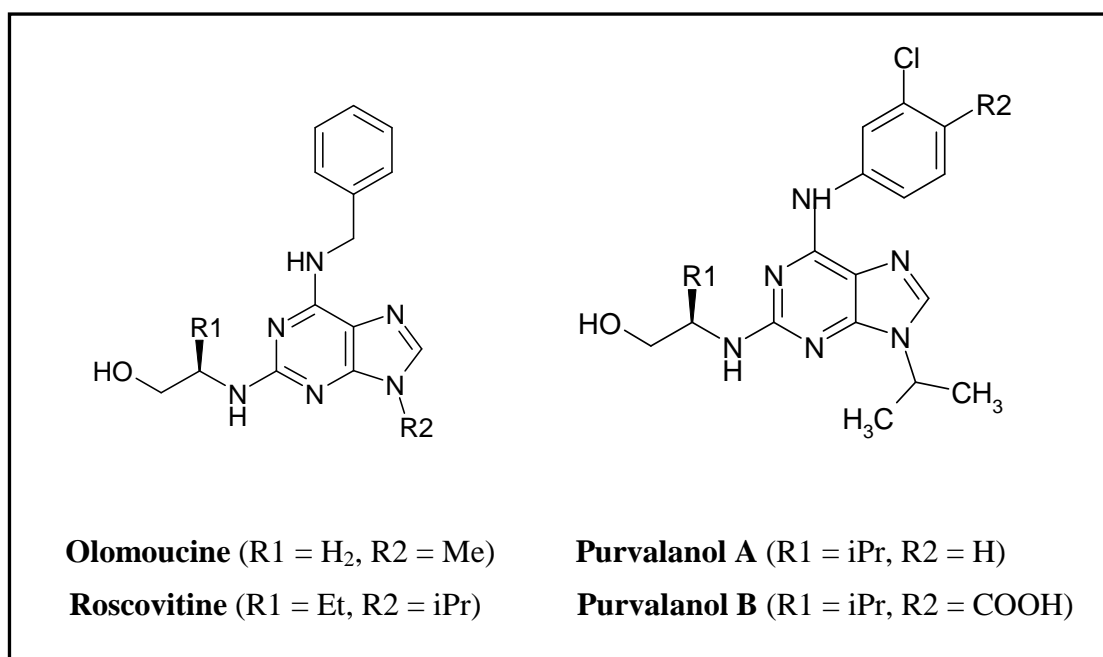


Figure 1.6 – The chemical structures of a variety of 2, 6, 9-trisubstituted purine CDK inhibitors.

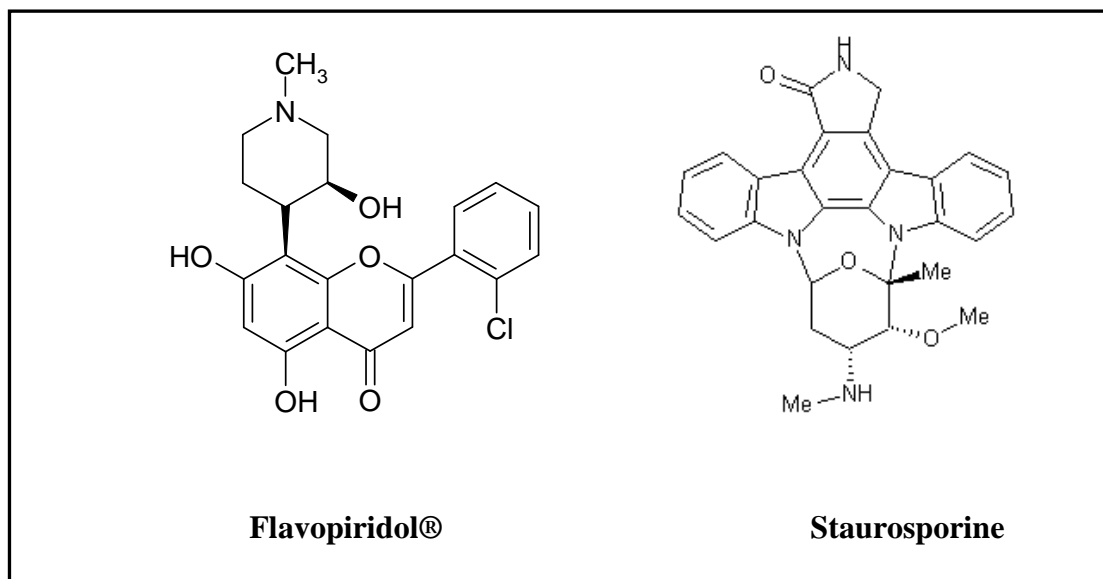


Figure 1.7 – The chemical structures of Flavopiridol® and staurosporine protein kinase inhibitors.

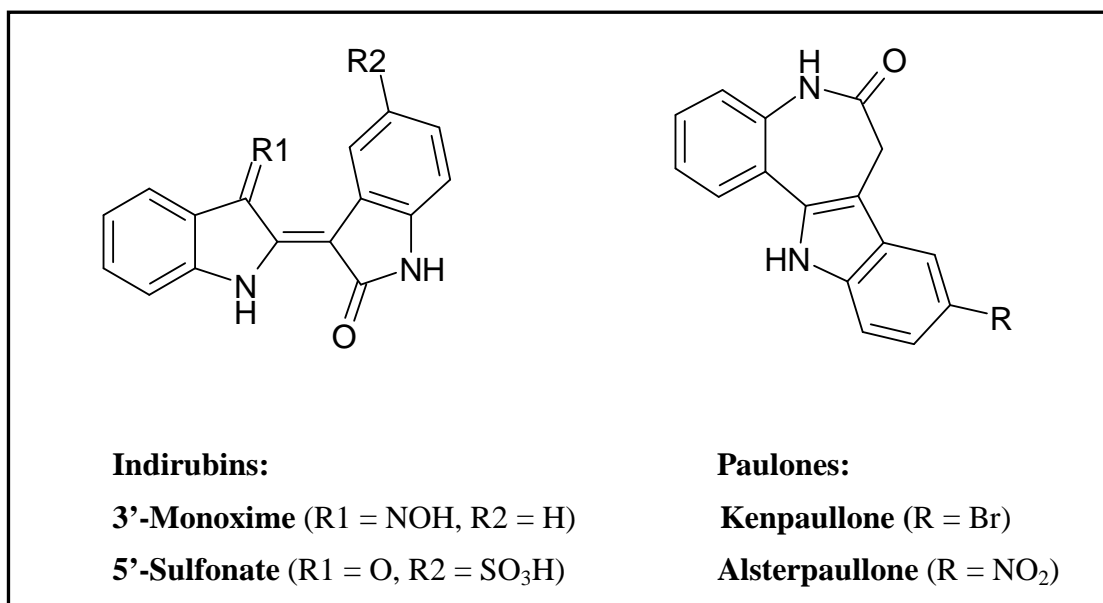


Figure 1.8 – The chemical structures of indirubin and paullone protein kinase inhibitors.

1.8 The parasite kinome as a target for anti-parasite drug discovery.

Protein kinases are attractive drug targets due to the success of drugs such as imatinib (Gleevec®) and other kinase inhibitors, as previously discussed. However, before these drugs were developed against cellular kinases, it was viewed in the pharmaceutical industry that protein kinases were not viable targets (Renslo and McKerrow, 2006). This was largely due to the belief that it would prove difficult to produce selective kinase inhibitors due to the vast number of kinases present in the genome (the kinome). Identifying kinase targets and screening compound libraries against kinases has now become a promising area of drug discovery research in a variety of scientific fields, including parasitology. Furthermore, the discovery and use of anti-parasitic kinase inhibitors may prove to be influential in establishing and dissecting signalling pathways within parasitic organisms (Naula *et al.*, 2005).

The recent availability of the *T. brucei*, *T. cruzi* and *L. major* (TriTryp) genome sequences has facilitated the search for novel drug targets and has established the number of protein kinases encoded by these parasites. The TriTryp kinomes are closely related and encode 179, 156 and 167 distinct eukaryotic protein kinases (ePKs) in *L. major* (Ivens *et al.*, 2005), *T. brucei* (Berriman *et al.*, 2005) and *T. cruzi* (El Sayed *et al.*, 2005), respectively, as well as 17, 20 and 19 atypical protein kinases (aPKs), respectively (El Sayed *et al.*, 2005; Parsons *et al.*, 2005). This is approximately 30% of the number present in the human host, double that of the malaria parasite, *Plasmodium falciparum*, and one third larger than in *S. cerevisiae* (El Sayed *et al.*, 2005; Parsons *et al.*, 2005; Ward *et al.*, 2004). Trypanosomatid protein kinases represent approximately 2% of each genome suggesting a key role for phosphorylation in parasite biology. The knowledge from the genome projects and that there is complex regulation of cell division in unicellular parasites provides a wide variety of potential targets for novel anti-parasitic agents.

1.8.1 Trypanosomatid CDKs as drug targets

Trypanosomatid CDKs belong to the CMGC (CDKs, MAP kinase, Glycogen synthase kinase and CDK-like) group of kinases which is highly represented (e.g., 45 in *L. major* as compared to 61 in humans) (Parsons *et al.*, 2005). Despite 40-60% identity with human CDKs, protozoan protein kinases diverge significantly from the closest mammalian homologues (Doerig *et al.*, 2002). This highlights a potential therapeutic window where structural differences between the parasite and host CDKs may result in different affinities for inhibitory compounds. Therefore, there is value in investigating analogues of compounds which are active against mammalian CDKs, as they may display different efficacy and/or selectivity towards the parasite CDK. An example of this was with mammalian CDK and Erk-selective purvalanol compounds, which targeted casein kinase 1 in four different species of unicellular parasites (Knockaert *et al.*, 2000). This highlights that parasite CDKs can be targeted by inhibitors, which is a potential avenue for drug development against trypanosomatids.

1.8.1.1 *Leishmania* CDKs as drug targets.

As discussed, most work on parasite CDKs to date has been carried out on CRK1 and CRK3, two *cdc2*-related protein kinases. As mentioned *L. mexicana* CRK1 is an essential gene in promastigotes; however, its role in amastigotes has yet to be defined. For this reason, it therefore remains to be determined whether CRK1 could be a useful drug target (Mottram *et al.*, 1993).

L. mexicana CRK3 was established as an essential gene and additional studies were carried out using known CDK inhibitors to attempt to significantly reduce CRK3 protein kinase activity. Flavopiridol was shown to be a potent inhibitor of *L. mexicana* CRK3his protein kinase activity *in vitro* and inhibited growth of promastigotes in a dose dependent manner, with higher concentrations resulting in cell death. At lower concentrations, Flavopiridol@

arrested *L. mexicana* at the G2-M-phase of the cell cycle (Hassan *et al.*, 2001). This provided chemical validation of CRK3 as a target for rational drug design.

Following CRK3his inhibition by Flavopiridol®, a number of chemical inhibitors were screened against CRK3his for antileishmanial activity (Grant *et al.*, 2004). The chemical library screen identified additional inhibitors which had antileishmanial activity, which disrupted cell cycle progression and had an irreversible catastrophic effect on cell structure and morphology. These inhibitors caused growth arrest and inhibited macrophage infection *in vitro*, which provided further evidence that *L. mexicana* CRK3 was a valid drug target. The inhibitors with antileishmanial activity were grouped into four chemical classes. Group one were 2, 6, 9-trisubstituted purines, including the C-2-alkynylated purines, group two were indirubins, group three were paullones and group four were derivatives of staurosporine, a non-specific protein kinase inhibitor (Grant *et al.*, 2004). Of the four groups, indirubins were found to be the most potent and were studied further with the cellular effects of the drugs observed. It was seen that they exerted a number of effects consistent with that of cell cycle disruption (Grant *et al.*, 2004). This confirmed that CRK3 could be targeted by chemical inhibition, providing evidence that drug development against CRK3 is an attractive avenue to pursue.

1.9 Antitrypanosomatid drug discovery:

1.9.1 Target assessment for antiparasitic drug discovery

The Drug Discovery Unit at the University of Dundee has recently devised molecular-target assessment criteria for assessing and prioritising parasitic drug targets, termed the “traffic-light” system (Figure 1.9) (Frearson *et al.*, 2007). Each of the six criteria has an attributed scoring system in the colours of a traffic light. This enables the scoring of particular targets, highlighting any weaknesses with each, and allowing their prioritisation in terms of which are the most suitable for entering the drug discovery pipeline (Figure 1.10). When considering *Leishmania* CRK3:CYC6 in terms of the traffic light system for

target assessment, it scores favourably. Target validation, druggability, assay feasibility, resistance potential and structural information are all green, with only toxicity in the amber section due to the presence of the human homologue of CRK3, CDK1.

Criterion	Red	Amber	Green
Target validation	No or weak evidence that the target is essential for growth or survival	Either genetic or chemical evidence that target is essential for growth or survival	Genetic and chemical evidence that target is essential for growth or survival
Druggability	No drug-like inhibitors are known and active site of target is not druggable	Drug-like inhibitors are known or active site is druggable potentially	Drug-like inhibitors are known and druggable active site (i.e. clinical precedent within the target family)
Assay feasibility	No <i>in vitro</i> assay developed and/or significant problems with reagents (cost or supply)	<i>In vitro</i> assay exists, development into plate format feasible but not achieved	Assay ready in plate format and protein supply assured within appropriate timelines
Toxicity	Human homologue present and little or no structural or chemical evidence that selective inhibition is possible	Human homologue present but some structural or chemical evidence that selective inhibition is possible	No human homologue present or human homologue known to be non-essential
Resistance potential	Target has multiple gene copies or isoforms within the same species and is subject to escape from inhibition	Target has isoforms within the same species or might be subject to escape from inhibition	Target has no known isoforms within the same species and is not subject to escape from inhibition
Structural information	No structure of target or closely related homologue	Structure without ligand available and/or poor resolution (>2.3 Å) or opportunity to build a good homology model	Ligand-bound structure of target (or ligand in closely related homologue) available at high resolution (<2.3 Å)

Figure 1.9 – Traffic-light definitions for target assessment. Taken from TRENDS in Parasitology (Frearson *et al.*, 2007).

1.9.2 The drug discovery process and criteria.

The discovery of novel therapeutics for neglected diseases is more difficult than other areas for some aspects. This includes factors such as cost of goods, compound/formulation stability and the requirement to dose children and pregnant women. Despite these areas, the progression from “hit to lead” to “drug candidate” (Figure 1.10) for antiparasitic drug discovery follows the same pattern as for other drugs.

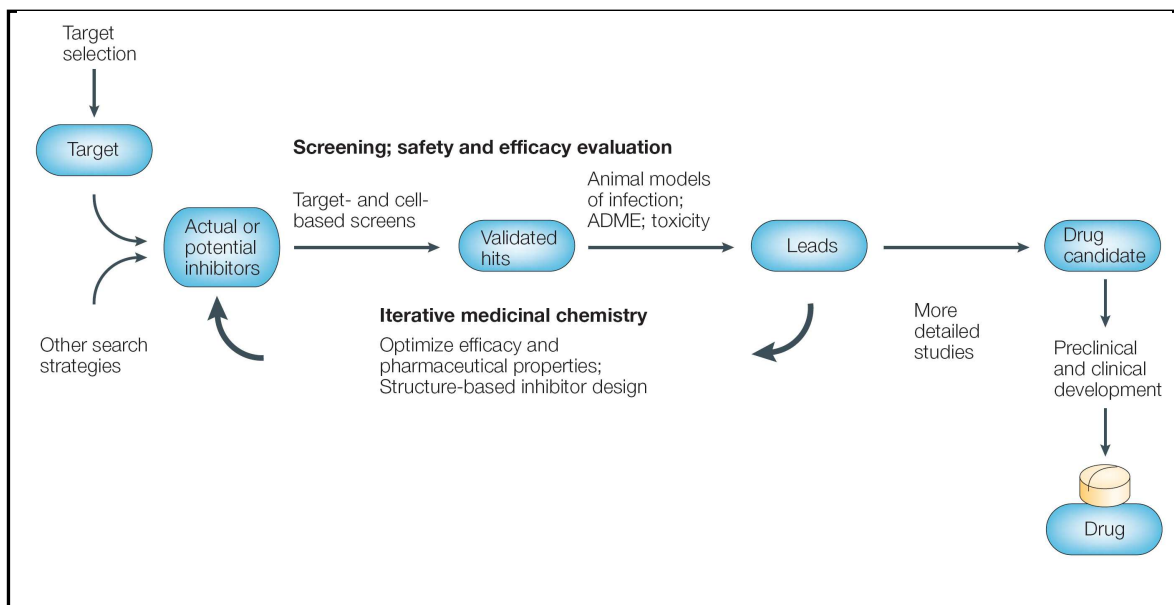


Figure 1.10 – Schematic representation of the drug development pathway. Drug discovery initiates with molecular biology and biochemistry to identify and validate molecular drug targets. Compounds are assayed to establish activity against the target and those that are active are defined as hits, (see figure 1.11) which can be considered for testing in animal models. Pharmacokinetic studies are performed on the hits at this stage in the pipeline. Compounds active in animal models and considered “drug like” or “lead like” are defined as leads, (see figure 1.11) which require further optimisation via iterative chemistry. Compounds which can be considered for human testing are then considered drug candidates (see figure 1.11). From here, a compound then undergoes preclinical and clinical studies before becoming a commercially available drug. Taken from Nature Reviews Drug Discovery (Pink *et al.*, 2005).

Hit

At the start of a screening campaign, compound that is:

- Active *in vitro* against whole protozoa with IC₅₀ of ≤ 1 μg per ml (for protozoa), or inhibiting mobility of helminths *in vitro* to, for example, $\geq 75\%$ at 10 μg per ml.
- Selective (at least tenfold more active against parasite than against a mammalian cell line, such as MRC-5).

Lead

At the start of a screening campaign, compound that is:

- Active *in vivo* against parasites at a dose ≤ 100 mg per kg.
- Not overtly toxic in animals at efficacious dose.
- Active *in vitro* against relevant parasite types (for example, drug-resistant parasites).
- Chemically tractable (analogues can be obtained).

During the campaign, criteria are made more stringent. A candidate for lead optimization should be:

- Active *in vitro* with activity approaching that of standard drugs.
- Active *in vivo* against parasites in the relevant small animal model (for example, chronic or late-stage disease), when delivered by a relevant route (preferably oral) in an acceptable formulation at a reasonable dose ($\ll 100$ mg per kg).
- Show good selectivity when tested against several mammalian cell lines.

Drug development candidate

Compound that has emerged from a lead optimization process and looks likely to fulfill at least the essential criteria in the desired product profile. It should:

- Be active *in vivo* with activity comparable to or exceeding that of standard drugs in the most relevant animal models.
- Be effective against desired range of parasites (for example, drug-resistant parasites and different species).
- Pass early toxicity/mutagenicity criteria.
- Have an acceptable metabolic profile *in vitro* and *in vivo* (preferably with no major species differences).
- Have an acceptable pharmacokinetic profile.
- Be amenable to cost-effective scale-up.
- Preferably have a mode of action that is well understood.

Clinical development candidate

Drug development candidate for which additional criteria have been met in studies of detailed pharmacology, pharmacokinetics/absorption, distribution, metabolism and excretion, mutagenicity and toxicity, formulation, scale-up for production, cost of goods and so on.

Figure 1.11 – The criteria for antiparasitic hits, leads and drug candidates. Taken from Nature Reviews Drug Discovery (Pink *et al.*, 2005).

1.9.3 The requirement for new antileishmanial therapeutics.

There is an urgent need to develop new therapeutic agents against eukaryotic parasites such as *Leishmania* and *Trypanosoma*. Although many of the current drugs are dated, chemotherapy remains the main method for disease control. However, these current therapies are unsatisfactory for a variety of reasons such as acute toxicity, poor efficacy, undesirable route of administration, cost of administration and the emergence of drug resistance. There have, however, been recent advances in areas of research to identify and develop possible antileishmanial therapeutic agents. One such area is that of cyclin dependent kinases (CDKs) in the Trypanosomatid cell cycle. As many protein kinases are essential to the cell cycle and because of the recent successes of imatinib (Gleevec) and other kinase inhibitors, this provides a promising and attractive area of study for drug discovery and development (Renslo and McKerrow, 2006).

1.10 Project aims.

The aim of this study was to identify specific *Leishmania* CRK3 inhibitors in order to contribute to combating leishmaniasis. A variety of approaches were used to identify and develop novel families of CDK inhibitors against CRK3 from *Leishmania* and possibly African Trypanosomes because of CRK3 shared identity. The project looked to shorten the drug discovery process by working in collaboration with Cyclacel Limited in Dundee and adopting a piggy-back approach to drug discovery, exploiting their expertise, technology and compound libraries for the identification and design of CDK inhibitors. Nowadays, some companies see value in supporting tropical disease drug discovery as a way to boost their lead discovery efforts (Nwaka and Hudson, 2006).

The main goal of the drug discovery project was to identify lead compounds against parasite CRK3 that can be developed for clinical trials. These would be small molecules, which significantly reduce and/or abolish the activity of parasite CRK3 *in vivo*. The

running hypothesis was that unique aspects of CRK3 biochemistry can be exploited for the design of specific small molecule inhibitors.

In order to achieve this objective, active recombinant *L. mexicana* CRK3 was produced via bacterial protein expression, for use in low and high throughput assay development and screening. An assay system using IMAPTM fluorescent polarization technology was developed, suitable for high throughput screening, which involved screening a chemical compound library at Cyclacel consisting of approximately 25,000 compounds. Once lead hits were identified and analysed, these were tested against *Leishmania in vitro* to establish their biological activity with the view to carrying out *in vivo* studies and initiating pharmacokinetic studies on the lead compounds.

Chapter 2

Materials and methods

2.1 Buffers and reagents.

Adenosine triphosphate (ATP): Stock solution is 100mM in distilled water. Stored at -20°C. Used at the concentration relevant for the described assays.

Ammonium persulfate: 10% working solution prepared in distilled water. Stored at -20°C.

Ampicillin: Stock solution is 50mg ml⁻¹ in distilled water. Used at 50µg ml⁻¹. Stored at -20°C.

Anion exchange column elution buffer: 50mM Tris, 5mM EDTA pH 7.0 and 1M NaCl.

Assay development buffer (ADB): 20mM MOPS, pH 7.0, 25mM β-glycerophosphate, 5mM EGTA, 1mM NaVO₃, 1mM DTT and 15mM MgCl₂. Freshly prepared.

Blocking solution 1: 5% (w/v) milk powder in PBS-Tween. Freshly prepared.

Blocking solution 2: 3% (w/v) milk powder in PBS-Tween. Freshly prepared.

Chloramphenicol: Stock solution is 34mg ml⁻¹ in ethanol. Used at 34µg ml⁻¹. Stored at -20°C.

Complete reaction buffer (CRB): 10mM Tris-HCl, pH 7.2, 10mM MgCl₂, 0.05% NaN₃, 0.01 % Tween-20 and 1mM DTT. Made up fresh.

Coomassie blue R250: 45% ethanol, 45% distilled water, 10% glacial acetic acid, 0.25% Coomassie blue R250.

Coomassie blue R250 destain: 45% ethanol, 45% distilled water, 10% glacial acetic acid.

Dithiothreitol (DTT): Stock solution is 1M in distilled water. Used at 1mM. Stored at -20°C.

DNA loading buffer (6x): 15% Ficoll, 0.25% bromophenol blue, 0.25% xylene cyanol FF. Stored at 4°C.

DNase-1: Stock solution is 10mg ml⁻¹. Used at 10µg ml⁻¹. Stored at -20°C.

Electroporation buffer (EPB): 21mM HEPES pH 7.5, 137mM NaCl, 5mM KCl, 0.7mM Na₂PO₄ and 5mM glucose. Stored at -20°C.

Enzyme dilution buffer (EDB): 20mM Tris-HCl pH, 0.5mg ml⁻¹ BSA, 2.5% glycerol and 0.006% Brij-35.

Ethidium bromide: Stock solution is 10mg ml⁻¹ in distilled water. Stored at room temperature. Used at 0.2mg ml⁻¹.

Gel filtration buffer/enzyme storage buffer: 20mM HEPES pH 7.4, 50mM NaCl, 2mM EGTA, 2mM DTT and 0.02% Brij-35.

Giemsa's stain: 100% Giemsa's R66 solution. Prepared to a 10% working concentration in distilled water.

Histone H1: Stock solution is 2mg ml⁻¹ in distilled water. Used at 0.4mg ml⁻¹. Stored at -20°C.

IMAPTM progressive binding reagent: Proprietary buffer from Molecular Devices plus tri-valent metal containing nanoparticles. Freshly prepared.

Isopropyl-β-D-Thiogalactopyranoside (IPTG): Stock solution is 1M in distilled water. Used at relevant concentrations for the proteins described. Stored at -20°C.

Kanamycin: Stock solution is 30mg ml⁻¹ in distilled water. Used at 30µg ml⁻¹. Stored at -20°C.

Kinase assay buffer (KAB): 50mM MOPS pH 7.2, 20mM MgCl₂, 10mM EGTA and 2mM DTT.

Leishmania lysis buffer: 50mM MOPS pH 7.2, 100mM NaCl, 10% (v/v) glycerol and 1% (v/v) Triton X-100.

Luria-Bertani (LB) agar: LB-media plus 0.8% (w/v) agar. Autoclaved to sterilise and stored at room temperature.

Luria-Bertani (LB) media: 1% (w/v) bacto tryptone, 0.5% (w/v) yeast extract and 0.5% (w/v) NaCl. Prepared in distilled water and autoclaved for sterilisation. Stored at room temperature.

Lysozyme: Stock solution is 100mg ml⁻¹. Used at 100µg ml⁻¹. Stored at -20°C.

Neomycin (G418): Stock solution is 10mg ml⁻¹. Used at 10µg ml⁻¹. Stored at -20°C.

Ni²⁺ column loading/wash buffer: 50mM Na₂H₂PO₄, 300mM NaCl pH 8.0 and 20-50mM imidazole.

Ni²⁺ column elution buffer: 50mM Na₂H₂PO₄, 300mM NaCl pH 8.0 and 500mM imidazole.

NuPage transfer buffer (20x): 500mM bicine, 500mM Bis-Tris, 20.5mM EDTA and 1mM chlorobutanol. Stored at 4°C.

PBS-Tween (PBST): PBS buffer plus 0.1% Tween-20.

PCR mix (10x): 450mM Tris-HCl, pH 8.8, 110mM ammonium sulphate, 45mM MgCl₂, 67mM β-mercaptoethanol, 44mM EDTA, pH 8.0, 1.13mg ml⁻¹ BSA, 10mM dATP, 10mM dCTP, 10mM dGTP and 10mM dTTP. Stored at -20°C.

Phosphate buffered saline (PBS): 10mM phosphate buffer, 2.7mM KCl, 137mM NaCl, pH 7.4. Stored at room temperature.

Protease inhibitor cocktail (1x): 100µg ml⁻¹ leupeptin, 500µg ml⁻¹ pefabloc, 5µg ml⁻¹ pepstatin, 1mM phenanthroline, 1mM EDTA and 1mM EGTA.

Puromycin: Stock solution is 10mg ml⁻¹ in distilled water. Stored at -20°C. Used at 50µg ml⁻¹.

RF-1: 100mM RbCl, 50mM MnCl₂, 30mM potassium acetate, 10mM CaCl₂ and 15% glycerol, pH 5.8.

RF-2: 10mM MOPS, 10mM RbCl, 75mM CaCl₂ and 15% glycerol, pH 6.8.

Roche EDTA-free, complete protease inhibitors: Proprietary mixture of protease inhibitors inhibiting a broad range of serine and cysteine proteases.

SDS: 10% solution prepared in distilled water and stored at room temperature.

SDS-PAGE running buffer (10x): 25mM Tris, 192mM glycine and 0.1% SDS.

SDS-PAGE sample buffer (4x): 564mM Tris, 2.04mM EDTA, 0.88mM Serva Blue G250, 0.7mM Phenol red, 40% glycerol and 8% LDS, pH 8.5.

SYBR safe: 10,000 x stock solution in DMSO. Used at 0.2 x and stored at room temperature.

TEMED: Stock solution stored at 4°C.

Tris: Working solutions prepared in distilled water and stored at room temperature.

Tris-Borate-EDTA (TBE) (10x): 0.9M Tris-HCl, 0.9M boric acid, 25mM EDTA. Stored at room temperature.

2.2 Molecular biology methods:

2.2.1 Bacterial strains.

The bacterial strains used throughout this project are described in table 2.1.

Bacterial strain	Genotype	Application	Manufacturer
XL1-Blue	<i>recA1 endA1 gyrA96 thi-1 hsdR17 supE44 relA1 lac</i> [F' <i>proAB lac^RZΔM15 Tn10</i> (Tet ^R)]	Cloning of recombinant plasmids	Stratagene
DH5 Alpha	F- ϕ 80dlacZM15 (<i>lacZYA-argF</i>)U169 <i>deoR recA1 endA1 hsdR17(r_K⁻, m_K⁺) phoA supE44 thi-1 gyrA96 relA1 λ-</i>	Cloning of recombinant plasmids	Invitrogen
BL21 (DE3) pLys-S	F' <i>ompT hsdS_B(r_B⁻m_B⁻) gal dcm</i> (DE3) Δ (<i>srl-recA</i>)306:: <i>Tn 10</i> pLysS (Cam ^R , Tet ^R)	High level protein expression	Invitrogen
Origami (DE3) pLys-S	Δ <i>ara-leu7697 ΔlacX74 ΔphoA PvuII phoR araD139 ahpC galE galK rpsL</i> F' [<i>lac⁺ lacI^q pro</i>] (DE3) <i>gor522::Tn 10 trxB</i> pLysS (Cam ^R , Kan ^R , Str ^R , Tet ^R)	Protein expression increasing protein folding	Novagen
Rosetta (DE3) pLys-S	F' <i>ompT hsdS_B(r_B⁻m_B⁻) gal dcm</i> (DE3) pLysSRARE2 ⁶ (Cam ^R)	Protein expression providing rare codon translation	Novagen
Rosetta-Gami (DE3) pLys-S	Δ <i>ara-leu7697 ΔlacX74 ΔphoA PvuII phoR araD139 ahpC galE galK rpsL</i> (DE3) F' [<i>lac⁺ lacI^q pro</i>] <i>gor522::Tn 10 trxB</i> pLysS (Cam ^R , Kan ^R , Str ^R , Tet ^R)	Protein expression providing rare codon translation and increasing protein folding	Novagen

Table 2.1 – Bacterial strains used for plasmid cloning and protein expression.

2.2.2 Bacterial culture.

LB-agar was melted and cooled before the addition of relevant antibiotics, and poured into Petri dishes to set. Transformed bacterial cells were plated on LB-agar plates with a glass spreader sterilised in ethanol, and incubated at 37°C overnight. Using a sterile cocktail stick, a single colony was used to inoculate 5-10ml of LB-medium with the appropriate antibiotics. Bacterial cultures were grown at 37°C in an incubator with agitation for the appropriate time depending on the bacterial strain being prepared.

2.2.3 Bacterial stabulate preparation (Glycerol stocks).

Transformed bacterial cells were plated on LB-agar plates complete with the relevant antibiotics and incubated at 37°C overnight. A single colony was used to inoculate 5-10ml

of LB-media complete with the relevant antibiotics and the bacterial culture grown at 37°C overnight. 0.5ml of the bacterial culture was added to 0.5ml of 2% peptone/40% glycerol and the cells store at -80°C.

2.2.4 Preparation of competent cells:

2.2.4.1 Rubidium chloride method.

A single colony was used to inoculate 5ml of LB-media complete with relevant antibiotics and the culture grown at 37°C overnight. The culture was diluted 1:100 in 50ml of fresh LB-media and grown until an optical density of 0.6 was reached at a wavelength of 600nm (O.D._{600nm}). The culture was incubated on ice for 10 minutes and harvested at 2000 x g for 15 minutes at 4°C. The cell pellet was resuspended in 16ml of pre-chilled RF-1 buffer, mixed by slow vortexing and incubated on ice for 15 minutes. The suspension was harvested at 2000 x g for 15 minutes at 4°C and the cell pellet resuspended in 4ml of pre-chilled RF-2 buffer. The suspension was incubated on ice for 1 hour, aliquoted in 200µl volumes and snap-frozen in ethanol pre-chilled at -20°C. Competent cells were stored at -80°C.

2.2.4.2 Calcium chloride method.

A single colony was used to inoculate 5ml of LB-media complete with relevant antibiotics and the culture grown at 37°C overnight. The culture was diluted 1:100 in 25ml of fresh LB-media and grown until an optical density of 0.4 was reached at a wavelength of 595nm (O.D._{595nm}). The culture was harvested at 2000 x g for 10 minutes at 4°C. The cell pellet was resuspended in 12.5ml of pre-chilled, sterile 50mM CaCl₂ buffer by slow pipetting and incubated on ice for 30 minutes. The suspension was harvested at 2000 x g for 10 minutes at 4°C and the cell pellet resuspended in 2.5ml of pre-chilled, sterile 50mM CaCl₂ buffer. The suspension was aliquoted in 200µl volumes and snap-frozen in dry ice. Glycerol was added to a final concentration of 10% and competent cells stored at -80°C.

2.2.5 DNA vectors and plasmid constructs.

The DNA vectors used throughout this project and plasmids constructed are described in tables 2.2 and 2.3, respectively.

Vector	Protein tag	Description	Manufacturer
PCR-Script	No tag	Gene cloning vector	Stratagene
pGEM-T Easy	No tag	Gene cloning vector	Promega
pET5a	His-tag	His-tagged protein expression construct	Promega
pET-15b	N-terminal His-tag	His-tagged protein expression construct	Novagen
pET-21a	N-terminal His-tag	His-tagged protein expression construct	Novagen
pET-28a	C-terminal His-tag	His-tagged protein expression construct	Novagen
pGEX	GST-tag	GST-tagged protein expression construct	GE Healthcare
pXG	No tag	Episomal protein expression construct	University of Glasgow
pRIB	No tag	Ribosomal integration expression construct	University of Glasgow

Table 2.2 – DNA vectors used for gene cloning and protein expression.

Plasmid	Backbone	Protein tag	Gene of interest	Description
pGL665	pET5a	His-Tag	<i>L. mexicana</i> CRK3 ^{T178E}	<i>L. mexicana</i> CRK3 T-loop mutant
pGL716	pGEX	GST-tag	Yeast CIV1	GST-tagged CIV1 (Yeast CDK activating kinase)
pGL751a	pET28a	C-terminal His-tag	<i>L. mexicana</i> CRK3	His-tagged <i>L. mexicana</i> CRK3
pGL1169	PCR Script	No tag	<i>L. major</i> CYC6	<i>L. major</i> CYC6 gene
pGL1218	pET15b	N-terminal His-tag	<i>L. major</i> CYC6	His-tagged <i>L. major</i> CYC6
pGL1390	pXG	No tag	<i>L. major</i> CYC6	Episomal expression of C-terminally HA-tagged CYC6
pGL1391	pXG	No tag	<i>L. major</i> CYC6	Episomal expression of N-terminally HA-tagged CYC6
pGL1483	pRIB	No tag	<i>L. major</i> CYC6	Ribosomal integration of C-terminally HA-tagged CYC6
pGL1484	pRIB	No tag	<i>L. major</i> CYC6	Ribosomal integration of N-terminally HA-tagged CYC6

Table 2.3 – Plasmid constructs generated and used throughout the project.

2.2.6 Polymerase chain reaction (PCR).

Polymerase chain reactions were used to amplify DNA fragments for subsequent cloning or colony PCR to analyse DNA ligations. Reactions were carried out in a final volume of 20µl comprising 2µl of 10x PCR mix, 10pmol of each oligonucleotide primer (sense and antisense), 1µl of template DNA, 0.5µl of Taq/Deep Vent DNA polymerase (New England BioLabs, NEB) and milli-Q H₂O added to 20µl. For colony PCR, a single colony was picked with a sterile cocktail stick and added directly to the 20µl reaction mixture. This supplied the template DNA for the reaction. Typically, reactions were carried out as follows:

DNA denaturing - 95°C for 5 minutes

DNA denaturing - 92°C for 30 seconds

Primer annealing - 55°C for 2 minutes

Initial DNA extension - 72°C for 90 seconds

25 cycles

Final DNA extension - 72°C for 10 minutes

DNA storage - 4°C overnight

2.2.7 Plasmid preparation and purification.

Molecular biology kits from Qiagen were used to prepare and purify genomic DNA (gDNA) (DNeasy) from *Leishmania*, DNA fragments and plasmids for subsequent sequencing and cloning. Plasmids were sequenced using The Sequencing Service at the University of Dundee, where 200-300ng of double stranded plasmid was provided per sequencing reaction required. QIAquick PCR purification kits (QIAGEN) were used to purify DNA fragments obtained from PCR. QIAprep spin miniprep kits (QIAGEN) were used to obtain high purity plasmid DNA (up to 20µg) with both kits used according to the manufacturer's protocol.

2.2.8 Restriction enzyme digests.

Restriction enzymes (NEB) were used according to the manufacturer's recommendations with the buffers supplied. Plasmid digestions were normally carried out in a final volume of 30µl, digesting plasmid DNA with appropriate enzymes and buffers for 2-3 hours at 37°C. Digest volumes were scaled where appropriate depending on the individual digest. Digests were stopped by the addition of DNA loading buffer to a 1 x final concentration from a 6 x concentrated stock and analysed by DNA gel electrophoresis.

2.2.9 DNA gel electrophoresis.

DNA agarose gels were prepared by adding 0.5 x TBE buffer to powdered agarose and melted. Gels contained 0.8-1.2% agarose (w/v) according to the size of the DNA fragment to be separated. Ethidium bromide (0.2mg ml⁻¹) or SYBR Safe (1 in 5000 dilution) (Invitrogen) was added to the molten gel prior to the gel setting. DNA samples were mixed with 6 x DNA loading buffer to a final concentration of 1 x loading buffer and electrophoresed at 80-120 volts, until the dye front was three quarters of the length of the gel. Gels were viewed under ultra violet illumination in a Bio-Rad gel documentation system and photographed for analysis.

2.2.10 DNA purification from agarose gels.

DNA agarose gels were prepared as described in 2.1.8 and the DNA fragments electrophoresed. The gels were viewed under low intensity ultraviolet light to minimise mutagenesis of the DNA band of interest. The band of interest was excised from the gel with a scalpel blade. The DNA band was processed with a QIAquick gel extraction kit (QIAGEN) to purify the DNA fragment and was performed in accordance with the manufacturer's protocol.

2.2.11 DNA ligations.

Ligation of DNA fragments into pET expression vectors (Novagen) was carried out in a final volume of 10µl comprising the DNA insert, plasmid vector, 200units of T4 DNA ligase, 1x T4 DNA ligase buffer and milli-Q H₂O added to 10µl. The ligation mixture was incubated at room temperature for at least 1 hour and then for 10 minutes at 65°C before being stored on ice until required for bacterial transformations.

2.2.12 Bacterial transformations.

Competent cells were transformed by heat shock. The DNA ligation mixture was added to 50µl of competent cells (see section 2.1.4) and mixed gently with a pipette tip. The transformation was incubated on ice for 15 minutes. The transformation was heat shocked by incubating at 42°C for 45 seconds and placed back on ice for 2 minutes to incorporate the plasmid of interest into the competent cells. Cells were then plated onto LB-agar plates and incubated overnight at 37°C. Correct clones were identified by colony PCR (section 2.2.6).

2.3 Mouse methods:

2.3.1 Macrophage (mΦ) extraction and purification.

Sufficient fresh RPMI 1640 media (PAA cat no. E15-842) supplemented with 10% (v/v) heat inactivated foetal calf serum (HIFCS) and 1% (v/v) Gentamicin antibiotic was prepared for the number of mice to be processed. Institute for Cancer Research (ICR) mice were killed by inhalation of CO₂ gas prior to their necks being broken by forceps. Mice were sprayed with 70% EtOH and laid on their back with legs splayed. Mouse skin was cut at the belly, between the top of the hips, by pulling the skin taught with forceps and removed by pulling off the skin from the abdomen. The inside of the mouse was sprayed with 70% EtOH to sterilise. Using forceps, the membrane at the sternum was pulled taught and a 21G needle inserted with the bevel facing upwards, just underneath the membrane. The cavity was filled with 10ml RPMI supplemented with 10% HIFCS and 1%

Gentamicin. The base of the tail and shoulders were held and the mouse shaken for 30 seconds to release the macrophages. A 26G needle with an empty 10ml syringe was inserted into the mouse's side with the bevel facing into the body. The skin was pulled taught against the needle and the fluid removed. Macrophages were harvested at 1000 x g for 10 minutes at 4°C and the supernatant retained. The cells were resuspended in fresh RPMI supplemented with 10% HIFCS and the cell density counted as described in 2.3.2. Macrophages were diluted to a cell density of 5×10^5 cells ml⁻¹ in RPMI supplemented with 10% HIFCS. 100µl of macrophages were added to each well of a 16-well Lab-tek™ cavity slide (50,000 mφ/well) and incubated at 37°C, 5% CO₂ for subsequent experiments.

2.4 *Leishmania major* methods:

2.4.1 *Leishmania* cell lines.

The cell line used in this project was *L. major* wild type promastigotes (Friedlin strain: WHO designation MHOM/JL/81/Friedlin). All transgenic cell lines developed, originated from this parent cell line.

2.4.2 Tissue culture.

L. major promastigote cells were grown at 25°C in HOMEM medium (Invitrogen cat no. 041-94699111) supplemented with 10% (v/v) HIFCS and 1% (v/v) penicillin/streptomycin antibiotics. Cells were inoculated into fresh medium at approximately 1×10^6 cells ml⁻¹ and were passaged into fresh medium when cultures reached a late log or early stationary phase (approximately $1-2 \times 10^7$ cells ml⁻¹).

Transgenic *L. major* cell lines were maintained with Puromycin antibiotic (Calbiochem) used at a concentration of 50µg ml⁻¹ and Neomycin (G418) antibiotic (Calbiochem) used at a concentration of 10µg ml⁻¹.

L. major promastigote cells were diluted and fixed by adding 50µl of cells to 50µl of 2% (v/v) formaldehyde in PBS. The cell mixture was loaded onto a haemocytometer and counted under microscopy to determine the cell density.

Cells were harvested by centrifugation at 1000 x g for 10 minutes 4°C. The cell pellets were resuspended gently in 10ml of ice-cold, PBS sterilised through a 0.2µm filter, to wash the cells and harvested as before. Cell pellets were used immediately for all subsequent experiments.

2.4.3 DNA transfections:

2.4.3.1 DNA precipitation and sterilization.

Purified DNA for each construct had sodium acetate (NaAc) added to a final concentration of 0.3M. Two volumes worth of 100% ethanol (EtOH) were added and the preparations kept at -20°C for 30 minutes. Samples were centrifuged at 12000 x g for 30 minutes and the supernatant removed under sterile conditions. The pellet was washed twice in 70% EtOH and the excess supernatant removed. The pellet was allowed to dry under sterile conditions before resuspension in 20µl of sterile H₂O, ready for transfection.

2.4.3.2 Bio-Rad electroporator transfection.

Mid-log stage *L. major* cells at a density of 5×10^7 cells ml⁻¹ were harvested at 1000 x g for 10 minutes. Cells were washed in half the original cell volume with electroporation buffer (EPB) before being resuspended at 1×10^8 cells ml⁻¹ in ice-cold EPB and kept on ice. 10 to 50µg of DNA was added to a 2mm gap ice cold cuvette with 400µl of cells and mixed. Cells were electroporated once in a Bio-Rad Gene Pulser II with Capacitance Extender II at 0.45kV and capacitance 500µF with the resulting time constant of 4.8ms (range from 4.6 to 5.1ms). The transfected cells were allowed to recover on ice for 10 minutes before being transferred to 10ml of fresh HOMEM medium with 20% (v/v) HIFCS and incubated at 25°C overnight. The following day, Neomycin (G418) antibiotic

was added to a final concentration of $10\mu\text{g ml}^{-1}$ (v/v) to select for transfected clones and cultures incubated at 25°C .

2.4.3.3 Amaxa nucleofector transfection.

Transfections were carried out using a human T-cell Amaxa nucleofector kit (Amaxa Biosystems) according to the manufacturer's protocol. 5×10^7 mid-log phase *L. major* cells were harvested at $1000 \times g$ for 10 minutes and resuspended in $100\mu\text{l}$ of the Amaxa nucleofector buffer. $1\text{-}5\mu\text{g}$ of DNA was added and mixed. Cells were electroporated using the U-14 Amaxa programme used for high cell viability before being transferred to 10ml of fresh HOMEM medium with 10% (v/v) HIFCS. 10ml cultures were split into two 5ml cultures to select for independent transfection events and incubated at 25°C overnight. The following day, Puromycin antibiotic (Calbiochem) was added to a final concentration of $100\mu\text{g ml}^{-1}$ to select for transfected clones. $100\mu\text{l}$ of cells were plated out in 96-well plates and incubated at 25°C until the control cell lines were dead and the transfected cells grew up.

2.4.4 Protein preparation.

Mid-log phase *L. major* parasites were grown to a cell density of 1×10^7 cells ml^{-1} in 200ml of HOMEM medium supplemented with 10% HIFCS and 1% penicillin/streptomycin antibiotics (Sigma). Cells were harvested at $1000 \times g$ for 10 minutes at 4°C . The cell pellets were resuspended gently in 10ml of ice-cold PBS, sterilised through a $0.2\mu\text{m}$ filter, to wash the cells and the cells harvested as before. Cell pellets were gently resuspended in 3ml of ice-cold, filter sterile *Leishmania* lysis buffer supplemented with a protease inhibitor cocktail. Cells were incubated on ice for 1 hour and harvested in an ultra centrifuge at $100,000 \times g$ for 1 hour at 7°C . The S100 supernatant fraction was analysed by Coomassie R250 gel staining (see section 2.5.1) and Western blotting for protein detection (see section 2.5.2).

2.4.5 *Leishmania stabilate* preparation.

0.5ml of mid-log phase *L. major* promastigote cultures were added to 0.5ml pre-chilled HOMEM medium supplemented with 20% HIFCS and 10% DMSO per cryovial. Cryovials were placed in a cotton wool insulated container, and stored at -80°C overnight. This was to allow gradual temperature reduction ensuring maximum survival of cells during the freezing process. Cryovials were subsequently transferred to liquid nitrogen for long term storage.

2.4.6 Alamar blue absorption assays and drugging.

Compounds to be assayed were made up to double the final screening concentration desired in HOMEM medium supplemented with 10% HIFCS. Five-fold or ten-fold serial dilutions of the compounds were carried out into HOMEM medium supplemented with 10% HIFCS. 100µl of each drug concentration were added to a 96 well plate in duplicate. 100µl of five-fold or ten-fold serial dilutions of 1mM Pentamidine (Sigma) and 100% DMSO solvent were included as positive and negative controls, in duplicate, respectively. *L. major* promastigote cells were diluted to a cell density of 2×10^6 cells ml⁻¹ in HOMEM media supplemented with 10% HIFCS. 100µl of 2×10^6 cells ml⁻¹ *L. major* cells were added to all wells in 96 well plates. Plates were sealed with parafilm and incubated for 5 days at 25°C. After 5 days, 20µl of filter sterile reazurin solution (12.5mg reazurin salt in 100ml PBS) (Sigma) was added to each of the wells and the plate incubated for a further 24 hours at 25°C. Absorption was read using an Envision plate reader (Perkin Elmer) with excitation at 540nm and emission at 590nm to assess the biological effect of the compounds.

2.4.7 Macrophage infection assays and drugging.

Day 1: Peritoneal macrophages (mφ) were harvested by lavage as described in section 2.2.1 and incubated at 37°C, 5% CO₂ for 24 hours. **Day 2:** Macrophage cells were infected

with *L. major* promastigotes: stationary phase promastigote *L. major* cells were counted as described in section 2.3.2 and diluted to a density of 4×10^6 cells ml^{-1} in RPMI 1640 medium supplemented with 10% HIFCS. This allowed for a desired infection ratio of 8 to 1 (*L. major* to macrophages). 100 μl of *L. major* promastigote cells were added to each of the wells and the slides incubated for a further 24 hours at 37°C with 5% CO_2 . **Day 3:** To determine if there was a suitably high infection after 24 hours for the experiment to proceed, one slide was processed by removing the medium with a pasteur pipette and washed 2 x with fresh RPMI 1640 medium supplemented with 10% HIFCS. Cells were fixed with 100% methanol and stained with 10% Giemsa's stain (BDH) for 10 minutes. Infectivity after 24 hours was determined by light microscopy under oil immersion, and where suitably high (where ~80% of macrophages were infected), the experiment proceeded. The remaining slides had their medium removed with a pasteur pipette and were washed 2 x with fresh RPMI 1640 medium supplemented with 10% HIFCS. Compounds to be assayed were set up in five-fold dilution series in RPMI 1640 medium supplemented with 10% HIFCS. 200 μl of compound were added to the wells in serial dilution and slides incubated for 72 hours at 37°C with 5% CO_2 . **Day 6:** The slides had their medium removed and were washed as previously described. Compounds were prepared as described for the first drugging on day 3 and were added to the macrophage cells to ensure the compound concentrations were kept at the desired level for the duration of the experiment. The slides were incubated for a further 48 hours at 37°C with 5% CO_2 . **Day 8:** The experiment was stopped by removing the medium from the slides and washing as previously described. The cells were fixed with 100% methanol and stained with 10% Giemsa's stain for 10 minutes. The percentage of infected macrophages and number of amastigotes per macrophage were determined by light microscopy under oil immersion.

2.5 Biochemical methods:

2.5.1 General protein purification.

Escherichia coli BL21 (DE3) pLys-S strains were transformed with the relevant DNA plasmid and plated onto an LB-agar plate supplemented with the relevant antibiotics. A single colony was used to inoculate 5ml of LB-media with the appropriate antibiotics and grown with agitation overnight at 37°C. Bacterial cultures were bulked up to an appropriate volume and grown at 37°C in LB-media supplemented with the appropriate antibiotics to an optical density of 0.7 at a wavelength of 600nm (O.D._{600nm}). Cultures were shifted to their induction temperature for 30 minutes and protein expression was induced over night using Isopropyl-β-D-Thiogalactopyranoside (IPTG) at the appropriate concentration and induction temperature for the relevant protein. Cells were harvested at 4000 x g for 15 minutes and resuspended in ice-cold PBS, pH 7.4 supplemented with DNase-I (10μg ml⁻¹) and Lysozyme (100μg ml⁻¹) and incubated for 60 minutes on ice. The cell lysate was sonicated 5 x 15 seconds (1sec. on/1sec. off) to break open the cells. The lysate was harvested at 12000 x g for 20 minutes. The proteins were purified via BioCAD chromatography using a metal chelate Ni²⁺ charged column. For *L. major* CYC6 only, Ni²⁺ purification was followed by purification on a strong anion exchange Poros HQ 10 micron 4.6mmD/100mmL column (Applied Biosystems). Proteins were loaded onto the Ni²⁺ column and the flow through collected. The column was washed with Ni²⁺ column loading/wash buffer to remove non-specific proteins bound to the column, and the wash collected. Proteins were eluted using the Ni²⁺ column elution buffer with a gradient of 50-500mM imidazole over 10 column volumes (1 column volume = 1.75ml). The fractions showing peaks of protein were pooled and passed through a PD-10 desalting column (Amersham) before being loaded onto the strong anion exchange column. The flow through from the column was collected and pooled. Proteins were eluted using the anion exchange column elution buffer and the fractions collected. Proteins were analysed as described in section 2.5.

2.5.2 *Leishmania* CRK3:CYC6 protein complex purification.

E. coli BL21 (DE3) pLys-S cells were transformed with plasmid pGL1218 (CYC6his) and plated on an LB-agar plate with the appropriate antibiotics. A single colony was picked and competent cells prepared as described in 2.1.4. CYC6 competent cells were re-transformed with plasmid pGL751a (CRK3his) and plated onto an LB-agar plate supplemented with the relevant antibiotics. A single colony of co-transformed *E. coli* BL21 (DE3) pLys-S cells were used to inoculate 5ml of LB-media with the relevant antibiotics and grown with agitation at 37°C overnight. The 5ml bacterial culture was bulked up to a volume of 1 litre and the culture grown at 37°C to 0.7 O.D.₆₀₀ nm. The 1 litre culture was shifted to an induction temperature of 19°C for 30 minutes and protein expression induced with 1mM IPTG. Cultures were induced at 19°C over night with agitation. After 16 hours cells were harvested at 4000 x g for 15 minutes and resuspended in ice-cold PBS pH 7.4 supplemented with DNase-1 (10µg ml⁻¹) (Invitrogen) and Lysozyme (100µg ml⁻¹) (Sigma) for 60 minutes on ice. The cell lysate was sonicated 4 x 30 sec (30sec. on/30sec. off). The cell lysate was harvested at 12000 x g for 20 minutes and the soluble extract filtered through a 0.2µm filter syringe. The proteins were purified via BioCAD chromatography using a metal chelate Ni²⁺ charged column followed by a Hiload 16/60 Superdex-200 gel filtration column. The protein complex was loaded onto the Ni²⁺ column pre-equilibrated with Ni²⁺ column loading/wash buffer and the flow through collected. The column was washed with the Ni²⁺ column loading/wash buffer to remove non-specific proteins bound to the column and the wash collected. CRK3:CYC6 was eluted at 1ml min⁻¹ with Ni²⁺ column elution buffer with a linear gradient of 50-500mM imidazole over 10 column volumes (1 column volume = 1.75ml). The fractions showing peaks of protein were pooled and loaded onto a Hiload 16/60 Superdex-200 gel filtration column pre-equilibrated with gel filtration buffer/enzyme storage buffer. The complex was eluted at 1ml min⁻¹ with gel filtration buffer/enzyme storage buffer and the fractions collected. The protein samples were analysed as described in section 2.5. The fractions showing CRK3his and CYC6his

proteins were pooled together, had glycerol added to 10% of the final volume along with Roche EDTA-free, complete protease inhibitors, were aliquoted and stored at -80°C.

2.6 SDS- PAGE.

Protein samples were added to 4 x SDS-PAGE sample buffer (Invitrogen) and 10 x sample reducing agent (Invitrogen) to a final concentration of 1 x for each. Samples were boiled at 100°C for 5 minutes to denature the proteins. Protein samples were separated by SDS-PAGE on 12% acrylamide mini-gels (per 15ml: 6ml 30% acrylamide; 3.8ml 1.5M Tris, pH 8.8; 150µl 10% sodium dodecyl sulphate; 150µl 10% ammonium persulfate; 6µl TEMED; 4.9ml H₂O), prepared using a gel casting cassette system (Invitrogen). Proteins were electrophoresed in an XCell *SureLock* Mini-Cell (Invitrogen) with 1 x SDS-PAGE running buffer at 180 volts for approximately 1 hour until the dye front reached the foot of the gel.

2.6.1 Coomassie gel staining.

SDS-PAGE acrylamide gels were incubated with agitation in Coomassie blue R250 stain for approximately 20 minutes and rinsed with milli-Q H₂O. The Coomassie blue R250 stain was removed by incubating gels with agitation in destain solution, changing the solution several times until the gel was free of Coomassie blue R250 and proteins of interest were visible.

2.6.2 Western blotting.

Following SDS-PAGE, separated proteins were transferred to Hybond-C nitrocellulose membrane (Amersham) by electroblotting using a NOVEX XCell II blotting module (Invitrogen). The transfer sandwich was assembled according to the manufacturer's protocol and proteins transferred in 1 x NuPage transfer buffer (Invitrogen) supplemented with 10% methanol (v/v) at 30 volts for 1 hour. The nitrocellulose membrane was transferred to a 50ml Falcon tube and incubated in protein rich Blocking solution 1

overnight at 4°C, to block the remainder of the membrane which was protein free and prevent non-specific binding of antibodies to the membrane.

2.6.2.1 Antibody detection of proteins.

Nitrocellulose membranes were incubated with primary antibodies in Blocking solution 2 for 1 hour at room temperature. Blots were washed 3 x 10 minutes with PBS-Tween (PBST) and incubated with secondary antibodies (anti-mouse IgG or ant-rabbit IgG) conjugated to horseradish peroxidase (HRP) (Promega). Secondary antibodies were generally used at a 1 in 5000 dilution in Blocking solution 2 and incubated for 1 hour at room temperature. Blots were washed in PBST as before. Antibody binding and protein detection was detected by Supersignal West Pico Chemiluminescent substrate reagents (Pierce) according to the manufacturer's protocol. Fluorescence was detected by autoradiography film (Kodak) and developed by a Kodak X-omat automated developer.

2.6.3 Protein quantification.

Purified proteins were quantified using a Micro BCA Protein Assay kit (Pierce) and Coomassie (Bradford) Protein Assay kit (Pierce) both according to the manufacturer's protocols.

2.7 Protein kinase assays:

2.7.1 γ -³²P radiometric assays:

2.7.1.1 Gel-based assays.

Protein kinase assays were performed using CRK3, CYC6 and Civ1 cell cycle proteins in a final volume of 20 μ l. Assays were performed using the kinase assay buffer (KAB) supplemented with 4 μ M ATP, 0.5 μ Ci of γ -³²P ATP and histone H1 as a substrate used at 0.25mg ml⁻¹. Assays were carried out for 30 minutes at 30°C before stopping the reaction by the addition of 7.5 μ l of 4 x SDS-PAGE sample buffer. The samples were incubated at 100°C for 5 minutes and electrophoresed on a 12% SDS-PAGE gel as described in section

2.5. Gels were processed as described in section 2.5.1 and dried before overnight exposure to KODAK autoradiography film, and developed by a Kodak X-omat automated developer. Gels were also analysed by exposure to a Typhoon Phosphor Imager to quantify the band intensities.

2.7.1.2 Plate-based assays.

Leishmania CRK3:CYC6 protein kinase assays were performed in 96-well microtiter plates in a final volume of 25 μ l. Each assay point contained approximately 7.5ng of co-expressed *Leishmania* CRK3:CYC6 protein kinase complex diluted in enzyme dilution buffer (EDB). Assays were performed using the assay development buffer (ADB) supplemented with 100 μ M ATP, 0.5 μ Ci of γ -³²P ATP and histone H1 as a substrate used at 0.4mg ml⁻¹. Two and three-fold titrations were set up to determine the concentration of enzyme to be used per assay point and to determine the concentrations of selected inhibitors required for 50% inhibition of *Leishmania* CRK3:CYC6 protein kinase activity (IC₅₀ values), respectively. For IC₅₀ determinations, assay mixes contained DMSO to a final concentration of 2%, plus or minus the inhibitor. Mammalian protein kinase assays were carried out according to the assay protocols developed at Cyclacel. Assays were carried out for 30 minutes at 30°C before stopping the reaction by the addition of an equal volume (25 μ l) of 75mM phosphoric acid. Samples were spotted onto a p81 cellulose filterplate (Nunc) and a vacuum applied. Wells were washed 3 x 200 μ l with 75mM phosphoric acid and the bottom of the plate sealed. 50 μ l of Microscint 40 (Perkin Elmer) was added per well before incorporation of radioactivity was determined on a Topcount microplate scintillation counter.

2.7.2 IMAP™ fluorescence polarization assays.

Protein kinase assays were performed in 384-well non-treated black plates (Nunc) in a final volume of 20 μ l. Each assay point contained approximately 1.25ng of co-expressed *Leishmania* CRK3:CYC6 protein kinase complex. Assays were performed using enzyme

complex, 100nM fluorescently labelled peptide substrate (5FAM-GGGRSPGRRRRK-OH) (Molecular Devices), 100 μ M ATP and plus or minus an inhibitor. The enzyme complex, peptide and ATP were made up in the IMAPTM complete reaction buffer (CRB). Assays were carried out for 1 hour 20 minutes at room temperature and the reaction stopped by the addition of 50 μ l of the IMAPTM progressive binding reagent. The assay was left to proceed for a further 1 hour 20 minutes at room temperature and the fluorescence polarization read in a Perkin Elmer Fusion microplate reader, with excitation at 485nm and emission at 535nm.

2.8 HTS robotic technology.

HTS assays were carried out using robotic technology at Cyclacel. Assay and compound plates were placed by hand in a Cytomat Plate Hotel (Heraeus). The assay was then fully automated as described. The plates were taken from the Cytomat by a Microlab ML-Swap 1400 robotic arm (Hamilton Robotics) and assembled on the deck of a Microlab ML-4200 MPH96 liquid handling robot (Hamilton Robotics). The assay components were added by a 96-needled liquid dispenser as part of the liquid handling robot. Once the components were added, the assay and compound plates were returned to the Cytomat by the Swap arm. The process was repeated to the assay plates to add the IMAPTM progressive binding reagent. Once the assay was complete, the Swap arm placed the assay plates in a Fusion Alpha-FP plate reader (Packard Bioscience) and the fluorescence polarization was determined.

Chapter 3

***Leishmania* biology 1: The *Leishmania* CRK3:CYC6 protein kinase complex and radiometric assay development.**

3.1 Chapter introduction and objectives.

Cyclin-dependent kinases (CDKs) are serine/threonine protein kinases that are ubiquitous in eukaryotes. They play crucial roles in the regulation of the cell cycle. A number of CDK homologues have been identified in *Leishmania* (Hammarton *et al.*, 2003b; Mottram, 1994) one of which, CRK3, has been studied in detail. The CRK3 homologues from three species of *Leishmania* have been cloned and are almost identical (Grant *et al.*, 1998; Wang *et al.*, 1998; Ali, 2002). There is a single amino acid change out of 311, in a non-conserved region in other CDKs, between *L. mexicana*, *L. major* and *L. donovani* CRK3. This implies that CRK3 plays an important and highly conserved role across the three *Leishmania* species and that CRK3 may therefore be exploited for drug discovery.

The literature supports CRK3 as the functional homologue of mammalian CDK1 where *CRK3* has been shown to be an essential gene in *L. mexicana* (Hassan *et al.*, 2001). In *L. mexicana* promastigotes, CRK3 histone H1 kinase activity peaks at the G2/M phase transition and CRK3 appears to play an essential role in cell cycle control (Hassan *et al.*, 2001).

CRK3 from *Trypanosoma brucei*, showing 78% homology to *Leishmania* CRK3, was shown to interact with the mitotic cyclin TbCYC6 (Hammarton *et al.*, 2003a). This complex is essential for entry into mitosis in both procyclic and bloodstream form trypanosomes (Hammarton *et al.*, 2003a). Using this rationale, we identified a putative mitotic cyclin from *L. major* and have shown this can activate *L. mexicana* CRK3 *in vitro*.

In an attempt to elucidate the function of *L. mexicana* CRK3, targeted gene knockout was performed but was unsuccessful (Hassan *et al.*, 2001). In each case, the parasite underwent changes in its ploidy to ensure it retained at least one copy of the *CRK3* gene, which is considered an indication of gene essentiality (Barrett *et al.*, 1999). These gene knockout experiments suggest that CRK3 is essential (Hassan *et al.*, 2001). In addition, the histone H1 kinase activity of CRK3, purified from leishmanial lysates was inhibited *in vitro* by Flavopiridol®, a known CDK inhibitor, with an IC₅₀ value of 100nM. Incubation of *L. mexicana* with Flavopiridol® caused cell cycle arrest and parasite death, consistent with intracellular inhibition of a CDK (Hassan *et al.*, 2001). This demonstrated that a compound that inhibited parasite enzyme activity *in vitro* could prevent parasite replication, further validating CRK3 as a potential drug target. In *T. brucei*, RNAi knockdown of the cyclin in the CRK3:CYC6 protein kinase complex blocks mitosis causing an irreversible catastrophic cell cycle defect (Hammarton *et al.*, 2003a). We predict that a similar effect would be seen for the *Leishmania* CRK3:CYC6 protein kinase complex.

CDKs do not function as monomers; for kinase activity they require to bind a regulatory subunit protein, a cyclin partner, and to have the correct phosphorylation status (Doerig *et al.*, 2002). A transgenic *Leishmania* cell line expressing a hexa-histidine tagged CRK3 was developed (Grant *et al.*, 1998). This expression and purification system allowed the CRK3 to be expressed in its native state and bind its natural cyclin partner for full activation. CRK3^{his} was used to develop a 96-well microtitre plate-based assay and a small chemical library screened as a result (Knockaert *et al.*, 2002). The most potent inhibitors of CRK3 were investigated further. Twenty seven of the most potent CRK3 inhibitors were tested against *Leishmania* infected macrophages *in vitro*. 60% of the compounds displayed antileishmanial activity with 7% toxic towards the macrophages (Grant *et al.*, 2004). The screen showed proof of principle in the identification of hits that could be developed into lead compounds for drug design to treat the leishmaniases.

The transgenic CRK3 developed could not be produced in sufficient active quantities for further assay development suitable for screening larger compound libraries. Furthermore, there were problems with the variability of protein quantity between purifications. When purifying the transgenic CRK3 it is possible that there could be a mix of CDKs that are purified and not just CRK3, or that CRK3 is bound to different cyclins other than CYC6. As a result, this chapter will focus on the generation of a recombinant *L. mexicana* CRK3 in complex with *L. major* CYC6 expressed in *E. coli*. Initial activity was established through gel-based protein kinase assays with the view to further assay development. The active protein kinase complex was used to develop a radiometric γ -³²P-ATP 96-well filter plate assay, capable of low to medium throughput compound screening. The radiometric assay was used as a reference assay and as a basis for the future development of a high throughput screening (HTS) assay. The HTS assay was used to screen a compound library provided by Cyclacel under license from Lexicon Pharmaceuticals Inc. (formerly Coelacanth Corporation), which was carried out at Cyclacel Limited in Dundee. This was with the intention of identifying hits specific to *L. mexicana* CRK3 which could be developed into lead compounds for drug design to treat the leishmaniasis.

3.1.1 Assay development, validation and performance.

There are factors to take into consideration when planning to develop an assay suitable for compound screening. These include quality control of the assay and assay performance. Once the target enzyme has been chosen (*Leishmania* CRK3:CYC6 in this study), assay development is carried out. Initially, a suitable substrate must be identified and with this, a signal window of activity can then be generated, validating suitable quantities of protein and substrate. This is carried out by determining the K_m for the substrate and then selecting a quantity sufficiently above the K_m to provide sufficient substrate for the enzyme while not saturating the assay. When developing a protein kinase assay, this is also carried out for ATP. In order to establish the quantity of enzyme which will provide a signal

sufficiently above a background signal (no enzyme) and is in the linear phase of the assay, an enzyme titration is carried out. Determining the linearity with a suitable quantity of enzyme identifies when the assay has run to completion and highlights the time points when the assay is in the linear phase and therefore suitable for compound screening. For example, a suitable signal:background window employed at Cyclacel, in the linear phase of the assay, is 10:1. Once these parameters are determined an assay can be validated and its performance monitored.

In order to validate an assay, the Z' score and the coefficient of variation are both determined. The Z' score is a statistical parameter which measures the validity and robustness of an assay using the controls and without the intervention of compounds. Similarly, the Z factor is used to evaluate the performance of an assay in the presence of compounds. In order to calculate the Z' score, three independent assays are carried out, each with a sample and control plate. The sample plate is set up with the kinase, substrate, ATP and the solvent which the compounds are in (DMSO in this study), in each well of the plate. The control plate is set up with the same components minus the enzyme (control). The standard deviation and mean signal for each sample and control plate are determined and the Z' calculation carried out for each of the three determinations (Table 3.1). The criteria used to evaluate a Z factor can be used for the Z' score (Table 3.1). The ideal assay would return a Z' score of 1, however; an assay with a Z' score >0.5 is considered excellent and satisfactory for compound screening. The Z' score is an indication of assay quality which is essential as it is important to have confidence in the assay so that the "hits" identified can be considered real. The coefficient of variation measures plate uniformity highlighting a drift in signal within a plate. In order for an assay to be validated at Cyclacel, a coefficient of variation must be $<10\%$ (a variability in signal within a plate of $<10\%$). This parameter can also be used to evaluate inter-plate variability by comparing values, another statistic to evaluate the performance of the assay.

$$Z = 1 - \frac{3SD \text{ of sample} + 3SD \text{ of control}}{|\text{mean of sample} - \text{mean of control}|} *$$

<i>Z-factor value</i>	<i>Structure of assay</i>	<i>Related to screening</i>
1	SD = 0 (no variation), or the dynamic range $\rightarrow \infty$	An ideal assay
$1 > Z \geq 0.5$	Separation band is large	An excellent assay
$0.5 > Z > 0$	Separation band is small	A double assay
0	No separation band, the sample signal variation and control signal variation bands touch	A "yes/no" type assay
<0	No separation band, the sample signal variation and control signal variation bands overlap	Screening essentially impossible

Table 3.1 – The characterisation of screening assay quality by the value of the Z factor. Included is the Z score calculation. Taken from Journal of Biomolecular Screening (Zhang et al., 1999).

It is vital to monitor the performance of an assay to ensure it is functioning as expected and required. Quality control of an assay is carried out with positive and negative controls on each assay plate. When carrying out compound screening, a no enzyme control with the solvent in which the compounds are stored in, is used. This is used as a negative control, and is the background signal for the assay. As a positive control, the enzyme without any inhibitor or in the case of a kinase assay, a pre-phosphorylated substrate can be used, generating the “maximum signal”. In addition, including an inhibitor with a known IC₅₀ value against the enzyme of choice, (Staurosporine for CRK3:CYC6) also allows the assay performance to be monitored on each plate. If these quality controls regularly return the signal values expected then it can be said with confidence that the assay is performing as expected.

Once an assay is validated and its performance satisfactory, compound screening can be carried out. It is important to validate the hits identified from a screen in addition to having a validated assay. Any hits identified from a high throughput screen for example, can be re-screened using another assay platform such as a radiometric assay format to further confirm their activity against the target enzyme. The structure and purity of compounds

taken into potency assays can be checked using liquid chromatography-mass spectrometry (LCMS). In addition, it is standard practice in drug development to re-synthesise the identified hits. These would be assayed against the target to confirm their activity and validate them as genuine hits.

3.2 Cloning: To obtain the *Leishmania CRK3* and *CYC6* genes:

3.2.1 *L. mexicana CRK3* cloning.

The *CRK3* gene from *L. mexicana* was previously cloned in the Mottram laboratory by Karen Grant (Grant *et al.*, 1998). The *L. mexicana CRK3* gene amplified through a PCR reaction was ligated into a pGEM-T cloning vector and sequenced. Using oligonucleotide 225 (5' GAATTCATATGTCTTCGTTTGGCCGTGTGA 3') and oligonucleotide 894 (5' GGCGAGCAAGGTAGAGCAC 3'), the *CRK3* gene was amplified further in this study to generate *NdeI* and *XhoI* restriction sites, respectively. This was sub-cloned into pET-28a(+) previously digested with *NdeI* and *XhoI*. The pET-28a(+) construct added an N-terminal tag comprising six histidines to aid purification by Ni-NTA affinity chromatography and was named pGL751a (Figure 3.1, upper map). This plasmid was used to express and affinity purify the CRK3his protein via the his-tag.

3.2.2 *L. major CYC6* cloning.

The *CYC6* gene from *L. major*, LmjF32.3320, identified from GeneDB (www.genedb.org) was amplified by PCR. This was performed using Deep Vent DNA polymerase, *L. major* genomic DNA and oligonucleotides 1515 (5' GCATATGTTTCGTGGAACGAGAGCGGCAGG 3') and 1516 (5' GCTCGAGTCACAGCGCCGGCAGCTCGTTAGGC 3'). The PCR product was gel purified and ligated into PCR-Script cloning vector generating pGL1169. The DNA sequence was confirmed by sequencing. The PCR product from pGL1169 was sub-cloned in the expression vector pET-15b(+) using *XhoI* and *NdeI*. This construct added an N-terminal tag comprising six

histidines and was named pGL1218 (Figure 3.1, lower map). This plasmid was used to express and affinity purify the CYC6his protein via the his-tag.

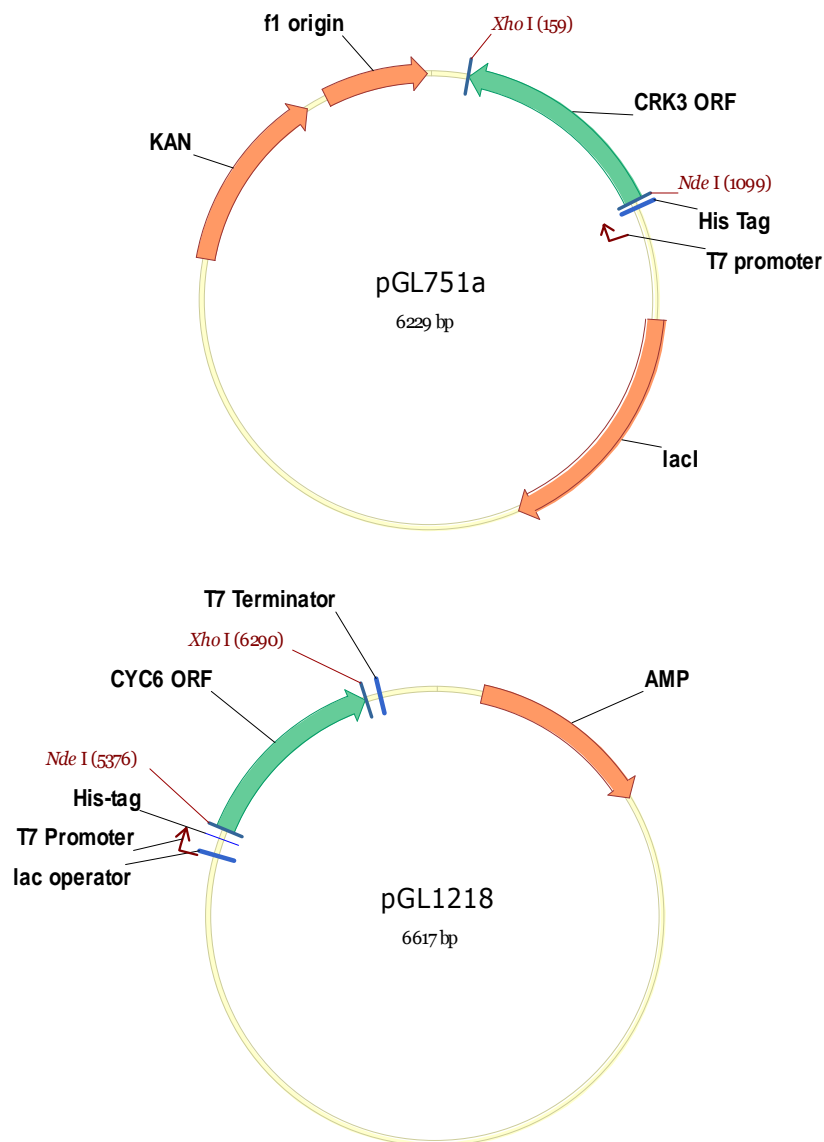


Figure 3.1 – Vector NTI maps of the *L. mexicana* CRK3 protein expression construct pGL751a and *L. major* CYC6 protein expression construct pGL1218. The *CRK3* open reading frame (ORF) sub-cloned into *NdeI* and *XhoI* digested pET-28a(+) with a kanamycin resistance marker (KAN) and an N-terminal hexa-his tag (Upper map). The *CYC6* open reading frame sub-cloned into *NdeI* and *XhoI* digested pET-15b(+) with an ampicillin (AMP) resistance marker and an N-terminal hexa-his tag (Lower map).

3.3 Purification of cell cycle proteins:

3.3.1 *L. mexicana* CRK3his.

Escherichia coli BL21 (DE3) pLys-S cells were transformed with pGL751a to express the CRK3his protein. Protein expression using an induction temperature of 19°C with 300µM IPTG was carried out overnight. *E. coli* BL21 (DE3) pLys-S cells were lysed and CRK3his purified via a Ni-NTA affinity column. Samples were loaded on a 12% acrylamide mini-gel and separated by SDS-PAGE. CRK3his was detected by Coomassie blue R250 gel staining (Figure 3.2, upper panel). These samples were also assessed using Western blot analysis with an anti-tetra-his antibody and the CRK3his protein detected at ~38kDa (Figure 3.2, lower panel). This was the expected size of CRK3his and was purified to give a yield of 1mg litre⁻¹.

3.3.2 *L. major* CYC6his.

E. coli BL21 (DE3) pLys-S cells were transformed with pGL1218 to express the CYC6his protein. Protein expression using an induction temperature of 19°C with 1mM IPTG was carried out overnight. *E. coli* BL21 (DE3) pLys-S cells were lysed and CYC6his purified via Ni-NTA affinity and strong anion exchange columns. Samples were loaded on a 12% acrylamide mini-gel and separated by SDS-PAGE. CYC6his was detected by Coomassie blue R250 gel staining (Figure 3.3). Western blot analysis with an anti-tetra-his antibody was used to detect CYC6his with initial expression and purifications (data not shown). However, due to the continuous successful purification of CYC6, it was deemed unnecessary to perform Western blot analysis on each purification from the anion exchange column. CYC6his was obtained at the expected size of ~35kDa and was purified to 0.5mg litre⁻¹. However, contaminant proteins were observed in the purification, likely to be additional bacterial proteins which bind the Ni-NTA and strong anion exchange columns, and peptides as a result of cleavage by bacterial peptidases.

3.3.3 *L. mexicana* CRK3^{T178E}his.

E. coli BL21 (DE3) pLys-S cells were transformed with pGL665 to express a mutant of the *L. mexicana* CRK3 protein, CRK3^{T178E}his (Nahla Ali, Ph.D thesis, 2002). Protein expression using an induction temperature of 25°C with 50µM IPTG was carried out overnight. *E. coli* BL21 (DE3) pLys-S cells were lysed and CRK3^{T178E}his purified via a Ni-NTA affinity column. Samples were loaded onto a 12% polyacrylamide mini-gel and separated by SDS-PAGE. CRK3^{T178E}his protein detection was via Coomassie blue R250 gel staining (Figure 3.4, upper panel) and via Western blotting with an anti-histidine (tetra-his) antibody (Figure 3.4, lower panel). CRK3^{T178E}his was detected at 38kDa which is the same size as the native CRK3his protein (Figure 3.2) and was purified to give a yield of 3.5mg litre⁻¹.

3.3.4 *Saccharomyces cerevisiae* GST-Civ1.

E. coli BL21 (DE3) pLys-S cells were transformed with pGL716, a pGEX vector obtained from Jane Endicott, University of Oxford, to express the GST-Civ1 protein (Thuret et al., 1996). GST-Civ1 was expressed and purified using established conditions (Brown *et al.*, 1999a). *E. coli* BL21 (DE3) pLys-S cells were lysed and GST-Civ1 purified via a GST affinity column. Samples were loaded on a 12% acrylamide mini-gel and separated by SDS-PAGE. GST-Civ1 protein detection was via Coomassie blue R250 staining (Figure 3.5, upper panel) and Western blotting with an anti-GST antibody (Figure 3.5, lower panel). The GST-Civ1 protein was detected at 75kDa, as expected; however, other contaminant bands were also present in the purification. This has been seen previously when purifying GST-Civ1 with regard to the higher molecular weight protein bands. (Brown *et al.*, 1999a). The lower weight proteins are likely to be a result of cleavage by bacterial peptidases as protease inhibitors were not used in the purification of GST-Civ1. The protein purification was purified to give a yield of 15mg litre⁻¹.

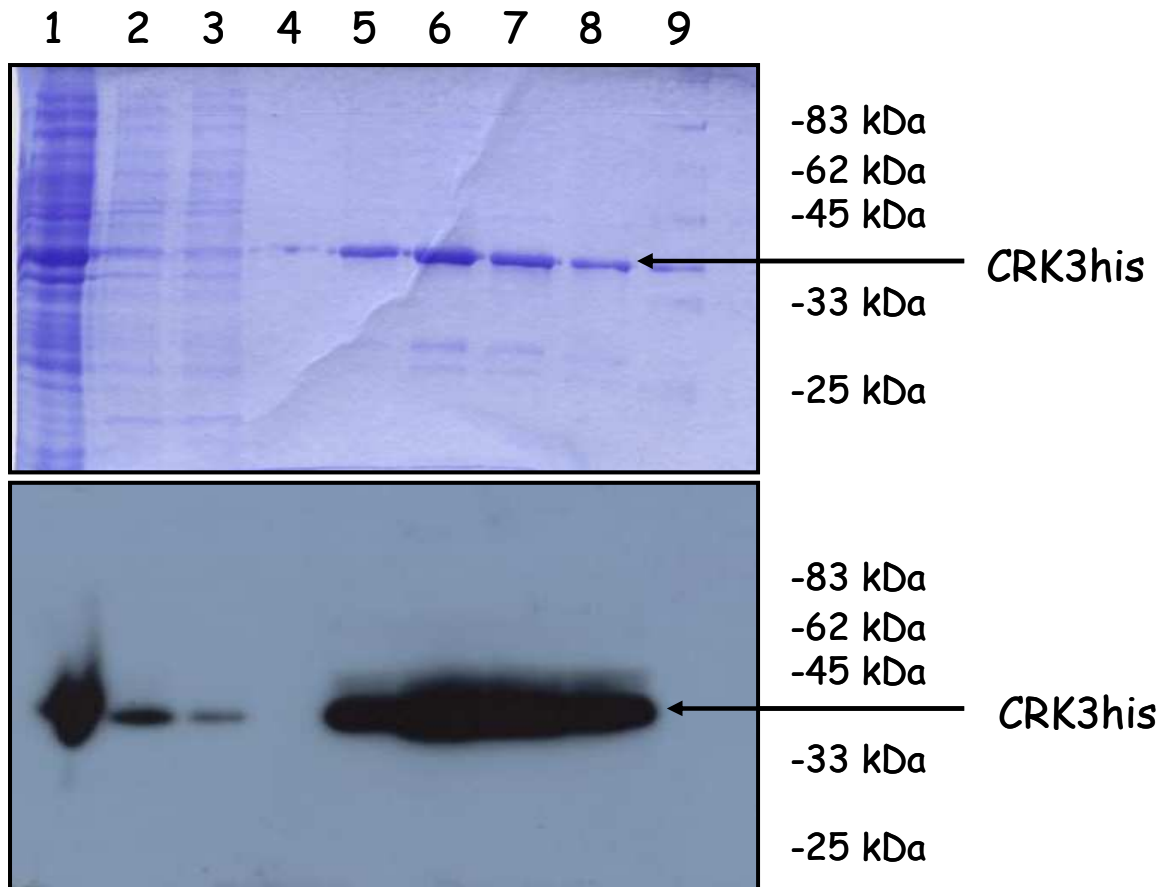


Figure 3.2 – *L. mexicana* CRK3 protein purification. Top panel: CRK3his protein detection via Coomassie blue R250 gel staining. Bottom panel: CRK3his protein detection via Western blotting with an anti-tetra-histidine antibody (Sigma). Lane 1, insoluble protein fraction. Lane 2, soluble protein fraction. Lane 3; unbound protein fraction. Lanes 4-8; protein fractions eluted from the Ni-NTA affinity column. Lane 9, molecular weight protein standards.

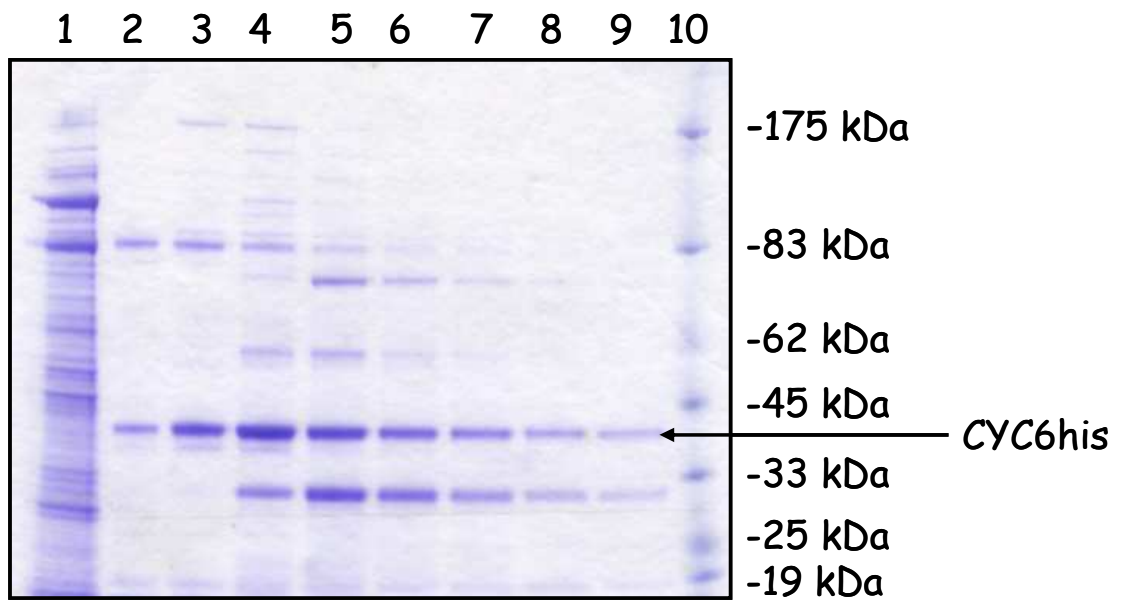


Figure 3.3 – *L. major* CYC6 protein expression. CYC6his protein detection via Coomassie blue R250 gel staining. Lane 1, CYC6his fraction purified from a Ni-NTA column and loaded onto the anion exchange column. Lane 2-9 protein fractions eluted from the anion exchange column. Lane 10, molecular weight protein standards.

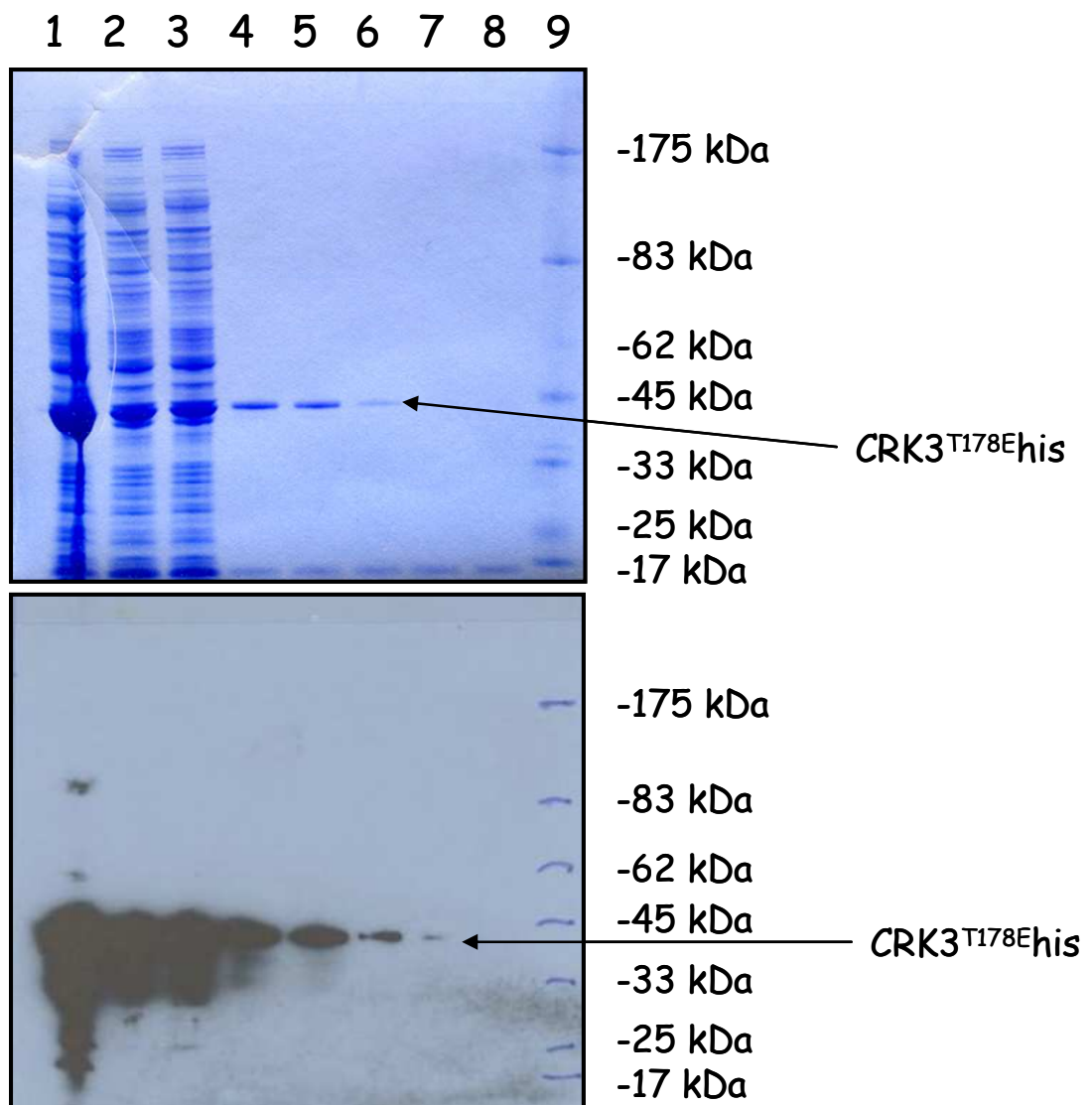


Figure 3.4 – *L. mexicana* CRK3^{T178E} protein purification. Top panel: CRK3^{T178E}his protein detection via Coomassie blue R250 gel staining. Bottom panel: CRK3^{T178E}his protein detection via Western blotting with an anti-tetra-histidine antibody. Lane 1, insoluble protein fraction. Lane 2, soluble protein fraction. Lane 3, unbound protein fraction. Lanes 4-8, protein fractions eluted from the Ni-NTA affinity column. Lane 9, molecular weight protein standards.

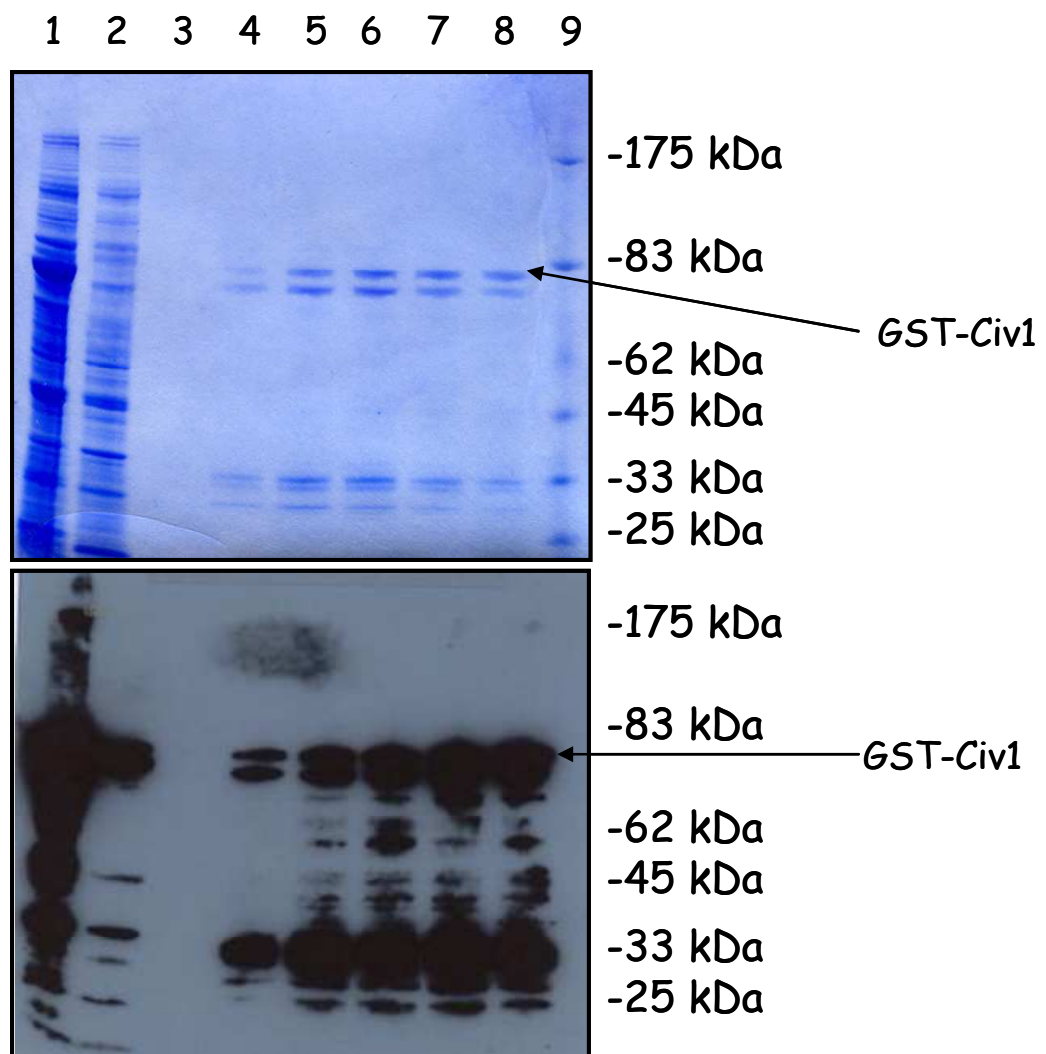


Figure 3.5 – *S. cerevisiae* GST-Civ1 protein purification. Top panel: GST-Civ1 protein detection via Coomassie blue R250 gel staining. Bottom panel: GST-Civ1 protein detection via Western blotting with an anti-GST antibody. Lane 1, insoluble protein fraction. Lane 2, unbound protein fraction. Lanes 3-8, protein fractions eluted from a GST column. Lane 9, molecular weight protein standards.

3.4 Protein kinase assays: gel-based assay:

3.4.1 Activation of the *Leishmania* CRK3:CYC6 protein kinase complex.

Monomeric CRK3 does not have protein kinase activity and requires the binding of cyclin protein to become active. Cyclin binding provides domains important for substrate selection thereby creating a substrate binding pocket. The *L. major* cyclin, CYC6, was used to activate *L. mexicana* CRK3. Following purification and quantification of the CRK3his and CYC6his proteins, a radiometric kinase assay was carried out to assess CRK3 activation by CYC6. A quantity of 1.25µg of CRK3his was used throughout the assay with increasing quantities of CYC6his added to the CRK3his. Histone H1 was used as a CRK3 substrate to analyse CRK3 activity. A background activity of CRK3his was observed which may be a result of a contaminant kinase in the purification of CRK3his phosphorylating histone H1 (Figure 3.6, lane 1). As increasing CYC6his quantities were added to CRK3his, increased activity was observed, validating CYC6 from *L. major* as an active functional cyclin (Figure 3.6).

3.5 *Leishmania* CRK3his:CYC6his protein stoichiometry optimisation.

In order to establish the quantity of CRK3his in relation to CYC6his required for optimum activity, analysis of varying CRK3his and CYC6his ratios was carried out. As the molecular weights of CRK3his and CYC6his are almost identical (38 kDa and 35 kDa, respectively), a 1:1 weight ratio of the proteins would equate to an approximate 1:1 molar ratio of proteins. A kinase assay was carried out to establish whether the predicted optimum ratio of 1:1 *Leishmania* CRK3:CYC6 proteins would result in the most CRK3:CYC6 protein kinase activity. The assay was carried out with protein ratios ranging from CRK3his **2:1** CYC6his to CRK3his **1:2** CYC6his. The highest activity is seen in lanes 4 and 5, where the ratio of *Leishmania* CRK3his and CYC6his proteins is approximately 1:1 as predicted (Figure 3.7). A 1:1 ratio of CRK3his and CYC6his was used for all subsequent kinase assays.

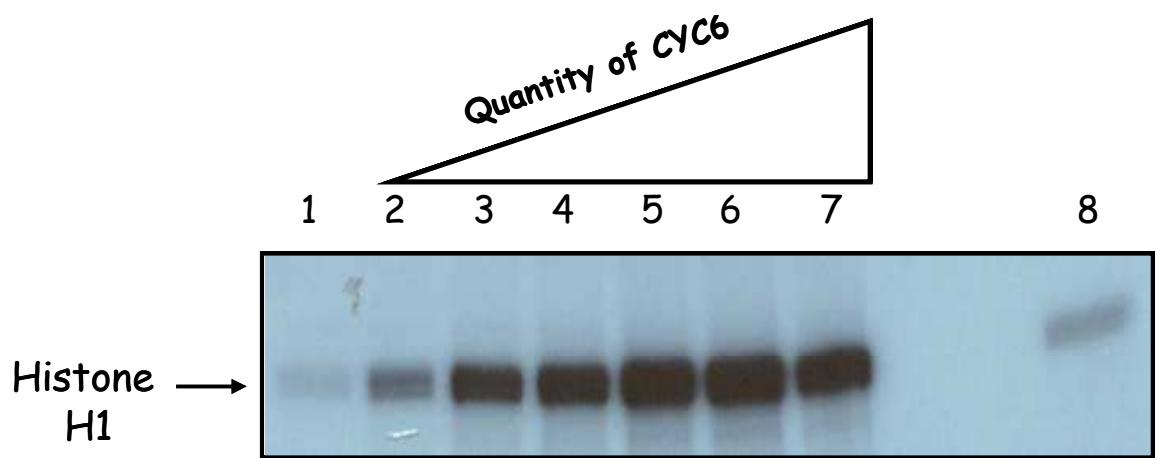


Figure 3.6 – Activation of the *Leishmania* CRK3:CYC6 protein kinase complex. Activity of *L. mexicana* CRK3 was assessed by its ability to phosphorylate a histone H1 substrate. 1.25µg of CRK3his was included in lanes 1-7. Increasing quantities of CYC6his were added from lanes 2-7: Lane 2, 0.025µg. Lane 3, 0.05µg. Lane 4, 0.075µg. Lane 5, 0.1µg. Lane 6, 0.125µg. Lane 7, 0.15µg. Lane 1 has 1.25µg of CRK3his only while lane 8 has 0.3µg of CYC6his only, as controls.

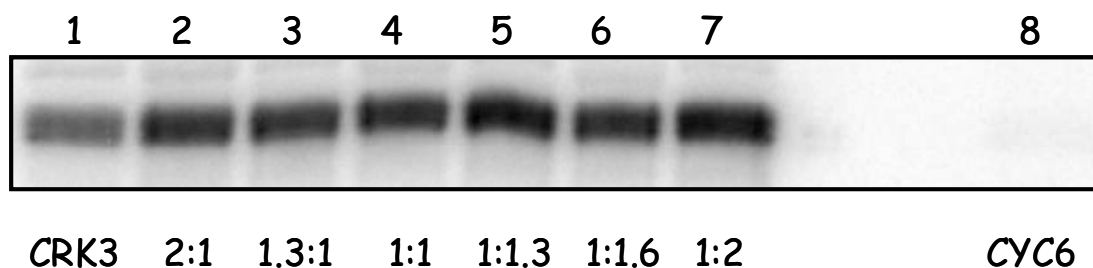


Figure 3.7 – Optimisation of the ratio of *Leishmania* CRK3 and CYC6 proteins. The optimum ratio of *Leishmania* CRK3 and CYC6 proteins was assessed by the ability of the complex to phosphorylate a histone H1 substrate. 4.4µg of CRK3his was included in lanes 1-7. Increasing quantities of CYC6his were added to lanes 2-7 corresponding to the ratios above. Lane 2, 2.2µg. Lane 3, 3.3µg. Lane 4, 4.4µg. Lane 5, 5.8µg Lane 6, 7.2µg. Lane 7, 8.8µg. This resulted in double the quantity of CRK3his as CYC6his in lane 2, progressing to a 1:1 ratio in lane 4, and to double the quantity of CYC6his as CRK3his in lane 7. Lane 8 contains 4µg of CYC6his as a negative control.

3.6 *Leishmania* CRK3:CYC6 protein kinase stability analysis.

The *Leishmania* CRK3 and CYC6 proteins were stored in the following buffer system provided by Cyclacel: 20mM HEPES, pH 7.4, 50mM NaCl, 2mM DTT, 1mM EGTA, 10% glycerol and 0.02% Brij-35. The proteins were stored separately and as a 1:1 complex at -80°C with Roche complete protease inhibitors. A kinase assay was carried out to determine whether the proteins remained active after four weeks of storage and whether they retain highest activity when stored separately or as a 1:1 complex (Figure 3.8). Assays with the *Leishmania* CRK3:CYC6 proteins stored as a complex (Lane 1) and proteins stored separately and mixed together on the day of the assay (Lane 2, mix) were carried out. CRK3his (Lane 3) and CYC6his (Lane 4) stored separately were included as controls. The proteins are still similarly active after four weeks when stored as a complex or when added together in a 1:1 ratio on the day of the assay (Figure 3.8). The controls show that there is no auto activity of CRK3his or CYC6his and the proteins are inactive when assayed after being stored separately. The activity levels of the complex and the mix of proteins is comparable; however, the stored complex is possibly more active. The buffer system is therefore successful in stabilizing and retaining the activity of the two proteins.

3.7 *Leishmania mexicana* CRK3^{T178E}his:CYC6his activity assay.

L. major CYC6his was used to try to activate a previously constructed mutant of *L. mexicana* CRK3, CRK3^{T178E} (Ali, 2002). The critical T-loop residue of CRK3, threonine 178 (T178), was mutated to a glutamic acid (E178) and the protein expressed. Mutation of this activation loop residue can mimic a phosphorylated protein (Nishiyama *et al.*, 2000). CRK3^{T178E}his (Lane 1), CYC6his (lane 8) and *Leishmania* CRK3:CYC6 protein kinase complex as a positive control (lane 9) were included. Lanes 2-7 have increasing quantities of CYC6his added to 3.5µg of CRK3his. However, there is no activity of CRK3^{T178E}his (Figure 3.9). This shows that CYC6his cannot activate CRK3^{T178E} and the mutation renders the CRK3 kinase dead, abolishing histone H1 kinase activity.

3.8 *S. cerevisiae* GST-Civ1

It was predicted that *S. cerevisiae* Civ1 may enhance the activity of the *Leishmania* CRK3:CYC6 protein kinase complex as was shown for *L. mexicana* CRK3:CYCA (F. Gomes and J.C. Mottram, unpublished). An activity assay with GST-Civ1 and histone H1 proteins was carried out to confirm that GST-Civ1 does not phosphorylate histone H1 independently (Figure 3.10). Histone H1 (Lane 1) and GST-Civ1 (lane 8) were included as controls. Increasing quantities of GST-Civ1 were added to histone H1 (Lanes 2-7). No increase in phosphorylation of the histone H1 substrate was observed by adding GST-Civ1 (Figure 3.10). This shows that GST-Civ1 independent of CRK3 does not phosphorylate histone H1. However, there is background activity of histone H1 seen in the assay. This is possibly due to the presence of a contaminant kinase in the GST-Civ1 preparation or histone H1 substrate.

To determine if GST-Civ1 would enhance the activity of the *Leishmania* CRK3:CYC6 protein kinase complex, a kinase assay was carried out (Figure 3.11). *Leishmania* CRK3:CYC6 protein kinase complex in a 1:1 ratio was included as a control (Lane 1). Lanes 2-7 had increasing quantities of GST-Civ1 added to the complex. Phosphorylation of CRK3his increases with increasing quantities of GST-Civ1 (Figure 3.11, upper arrow). However, no increase in activity of the CRK3:CYC6 protein kinase complex with increasing quantities of GST-Civ1 was observed (Figure 3.11, lower arrow). A further experiment was carried out with GST-Civ1 being added to *L. mexicana* CRK3his every five minutes for 20 minutes (data not shown). This was to maximise the phosphorylation of the threonine 178 residue of CRK3his. *L. major* CYC6 was then added to complete the complex. This again did not show any increase in activity of the complex, suggesting GST-Civ1 does not have a role in activating the *Leishmania* CRK3:CYC6 protein kinase complex, possibly because it is a yeast enzyme.

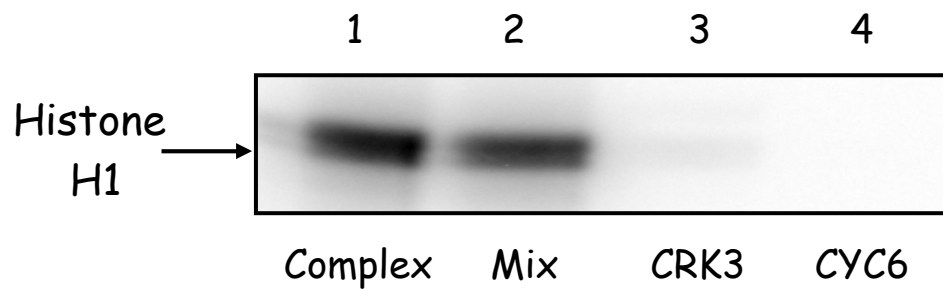


Figure 3.8 – Stability of the *Leishmania* CRK3 and CYC6 proteins. Proteins were stored at -80°C with Roche complete protease inhibitors in enzyme storage buffer. All proteins used were stored for four weeks. They were assessed for the ability to phosphorylate a histone H1 substrate. Lane 1, $4\mu\text{g}$ of *Leishmania* CRK3:CYC6 protein kinase complex stored in a 1:1 ratio. Lane 2, $2\mu\text{g}$ of CRK3his and $2\mu\text{g}$ of CYC6his stored separately and mixed for the assay. Lane 3, $2\mu\text{g}$ CRK3his only. Lane 4, $2\mu\text{g}$ CYC6his only.

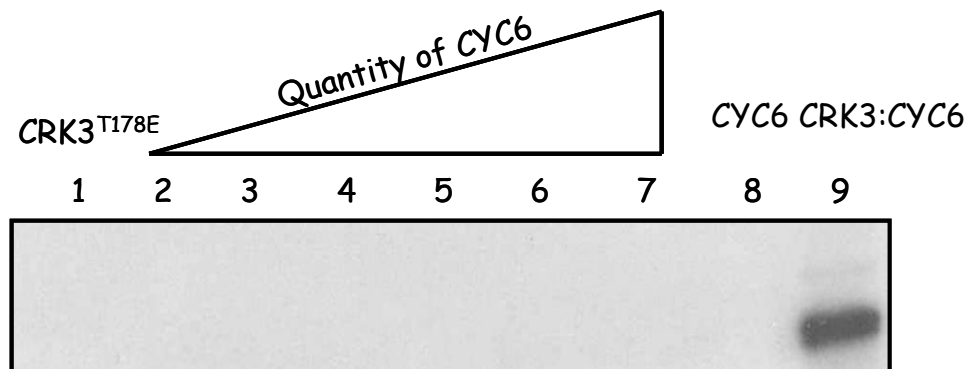


Figure 3.9 – Lack of activation of CRK3^{T178E} by *L. major* CYC6. The ability of *Leishmania major* CYC6_{his} to activate CRK3^{T178E}_{his} was assessed by the ability of the CRK3^{T178E}_{his}:CYC6_{his} protein kinase complex to phosphorylate a histone H1 substrate. Lanes 1-7 include 3.5µg of CRK3^{T178E}_{his}. Increasing quantities of CYC6_{his} were added to CRK3^{T178E}_{his} in lanes 2-7. Lane 2, 0.6µg. Lane 3, 1.2µg. Lane 4, 1.8µg. Lane 5, 2.4µg. Lane 6, 3µg. Lane 7, 3.5µg Lane 8 includes 3.5µg of CYC6_{his} only as a negative control. As a positive control, 3.5µg of active 1:1 *Leishmania* CRK3:CYC6 protein kinase complex was included in lane 9.

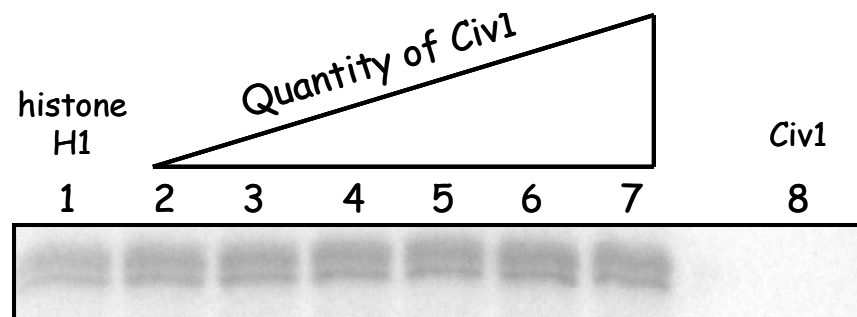


Figure 3.10 – *S. cerevisiae* Civ1:histone H1 activity assay. Activity of *S. cerevisiae* GST-Civ1 was assessed by its ability to phosphorylate a histone H1 substrate. Lanes 1-7 include 0.25µg of histone H1 substrate. Increasing quantities of GST-Civ1 were added to lanes 2-7. Lane 1, 0.3µg. Lane 2, 0.6µg. Lane 3, 0.9µg. Lane 5, 1.2µg. Lane 6, 1.5µg. Lane 7, 1.8µg. Lane 1 contains 0.25µg of histone H1 only and lane 8 has 3µg of GST-Civ1 only as controls.

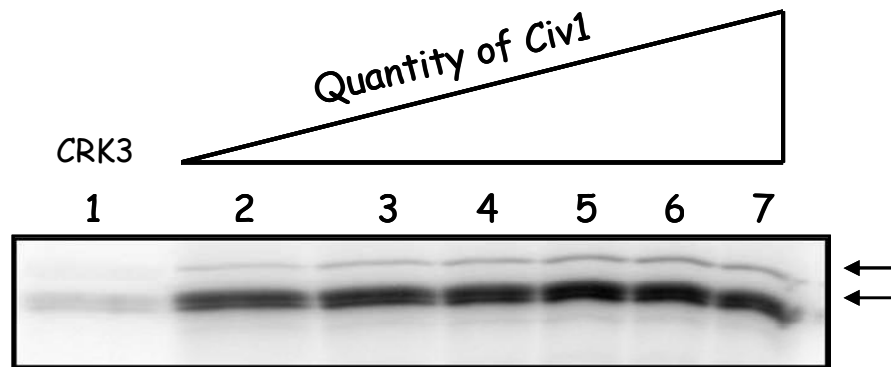


Figure 3.11 – Activation of the *Leishmania* CRK3:CYC6 protein kinase complex with *S. cerevisiae* Civ1. The ability of *S. cerevisiae* GST-Civ1 to activate the *Leishmania* CRK3:CYC6 protein kinase complex further was assessed by the phosphorylation of a histone H1 substrate (Lower arrow). Lane 1 includes CRK3 only as a control. Lanes 2-7 includes 5 μ g of *Leishmania* CRK3:CYC6 protein kinase complex in a 1:1 ratio. Increasing quantities of GST-Civ1 were added to lanes 2-7. Lane 2, 0.3 μ g. Lane 3, 0.6 μ g. Lane 4, 0.9 μ g. Lane 5, 1.2 μ g. Lane 6, 1.5 μ g. Lane 7, 1.8 μ g. The upper band (upper arrow) is CRK3his, which is being phosphorylated by GST-Civ1 on threonine 178.

3.9 Large scale *Leishmania* CRK3:CYC6 protein purification for radiometric assay development:

3.9.1 Co-expression and co-purification of *Leishmania* CRK3:CYC6.

E. coli BL21 (DE3) pLys-S cells were transformed with plasmid pGL1218 (CYC6his) and competent cells produced. The CYC6his competent cells were re-transformed with plasmid pGL751a (CRK3his) and the protein complex expressed. The protein complex was purified via nickel chelate and gel filtration columns. Following purification, the samples were loaded onto a 12% SDS-PAGE polyacrylamide gel. The *Leishmania* CRK3:CYC6 proteins were detected by Coomassie blue R250 gel staining (Figure 3.12). The CRK3his and CYC6his proteins were detected at their expected sizes of 38kDa and 35kDa, respectively (Lane 1) in an approximate 1:1 ratio. Some minor contaminant proteins were observed in the purification, likely to be additional bacterial proteins and proteins as a result of cleavage by bacterial peptidases. As there was protein kinase activity in the preparation, no further purification of the protein kinase complex was carried out. Individually purified CRK3his and CYC6his proteins are included in lanes 2 and 3, respectively. The identities of the proteins in lane 1 were confirmed by peptide mass fingerprinting and the yield of the complex determined at 4.5 mg litre⁻¹.

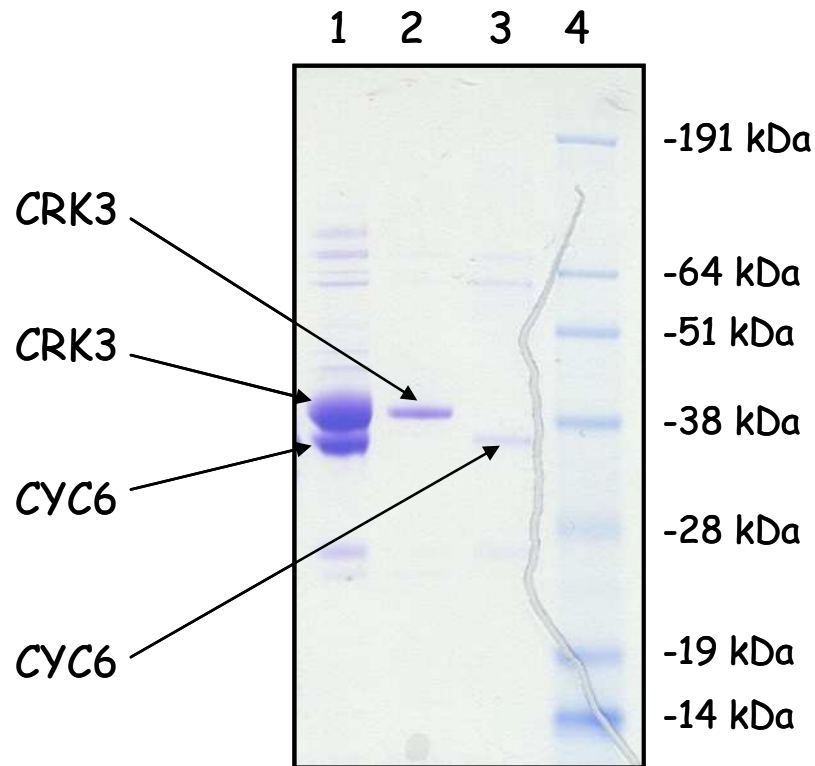


Figure 3.12 – Expression and purification of the *L. mexicana* CRK3 and *L. major* CYC6 cell cycle proteins. CRK3his and CYC6his were co-expressed in *E. coli* and purified via Ni-NTA and gel filtration columns. Lane 1, CRK3his, 38kDa and CYC6his, 35kDa. CRK3his and CYC6his were individually expressed in *E. coli* and purified via a Ni-NTA column. Lane 2, CRK3his, 38kDa. Lane 3, CYC6his, 35kDa. Lane 4, molecular weight protein standards.

3.10 Protein kinase assays: Radiometric protein kinase assays:

3.10.1 *Leishmania* CRK3:CYC6 protein kinase activity assay.

A plate based kinase assay was carried out to assess the activity of the *Leishmania* CRK3:CYC6 protein kinase complex. Such assays are adaptable to low to medium throughput screening, unlike the previous in-gel assay. This was performed with the co-purified *Leishmania* CRK3:CYC6 protein kinase complex with each assay point carried out in duplicate. A ten-point, two-fold enzyme titration of *Leishmania* CRK3:CYC6 was carried out with a top quantity of 1500ng. Activity increases in a linear fashion as increasing quantities of CRK3:CYC6 protein kinase complex is used in the assay until the assay plateaus due to enzyme saturation. The greatest activity observed is with neat complex with approximately 100,000 counts per minute, and although the assay is saturated at this point, it shows the proteins are active and the assay is functional (Figure 3.13). This identified 7.5ng of protein complex producing a signal of approximately 15,000 counts per minute, in the linear phase of the assay, with a signal to background ratio of approximately 15:1. This was an acceptable starting point for further assay development and 7.5ng of protein complex was used in all subsequent radiometric assays.

3.11 *Leishmania* CRK3:CYC6 time course assay.

A time course assay was carried out to establish the linearity period for the radiometric assay developed for the *Leishmania* CRK3:CYC6 protein kinase complex. The assay was carried out over 60 minutes at 30°C using 7.5ng per assay point and was stopped at 0, 5, 10, 20, 30, 45 and 60 minute time points. The assay was shown to be linear over the 60 min period examined (Figure 3.14). For subsequent assays, 30 minutes was chosen as the time point to carry out the assays owing to its good signal to background ratio and its linearity. The assay was validated with a Z' score of 0.67 which is considered excellent in terms of assay quality (Zhang *et al.*, 1999; Iversen *et al.*, 2006).

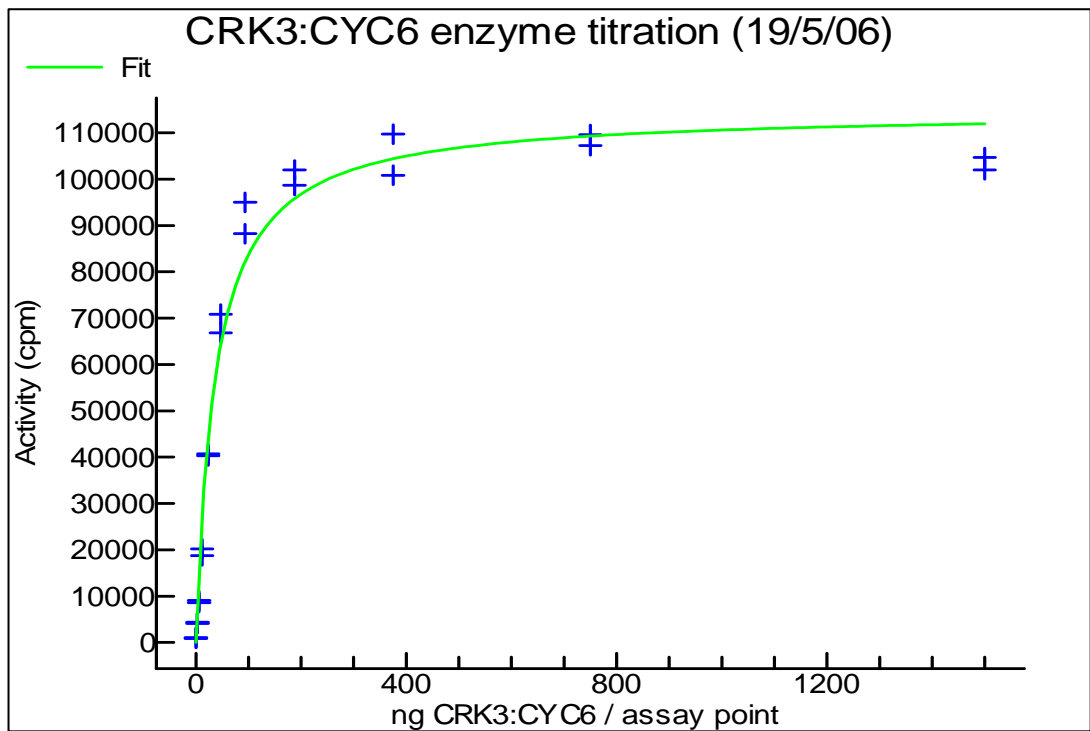


Figure 3.13 – Plate based activity assay of the *Leishmania* CRK3:CYC6 protein kinase complex. Activity of the *Leishmania* CRK3:CYC6 protein kinase complex was assayed in plate based form by its ability to phosphorylate a histone H1 substrate. A two-fold *Leishmania* CRK3:CYC6 enzyme titration was carried out. This identified that 7.5ng of enzyme complex could be used per assay point. Graphical analysis was carried out using XLfit 4.0 software from IDBS (www.idbs.com).

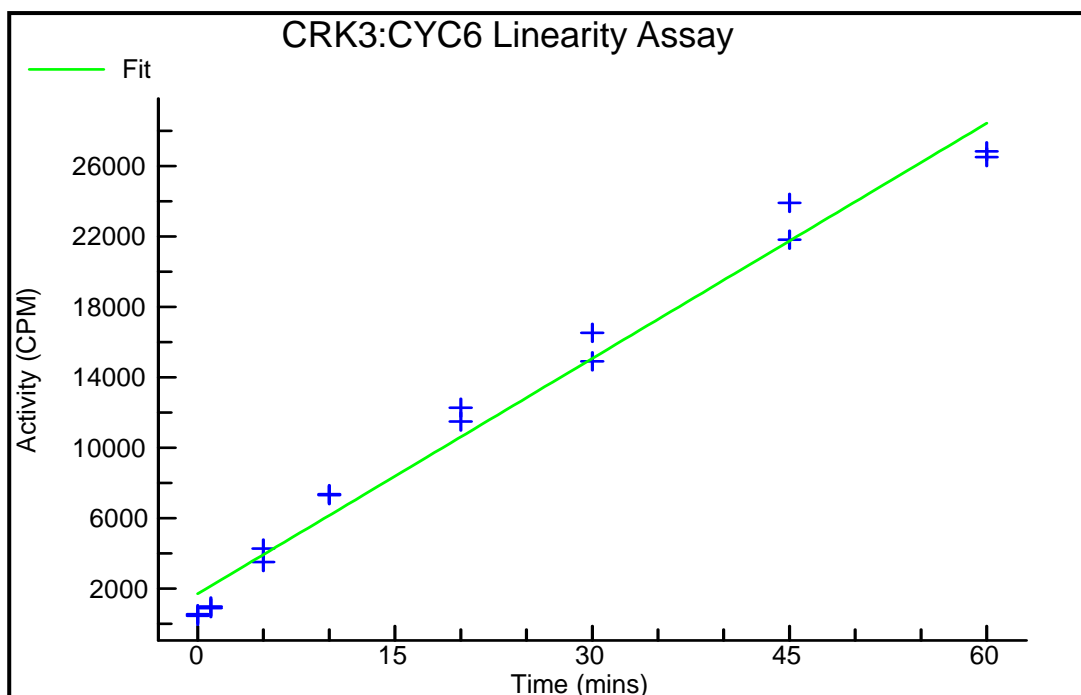


Figure 3.14 – Linearity of the *Leishmania* CRK3:CYC6 radiometric assay. The linearity of the assay developed for the *Leishmania* CRK3:CYC6 protein kinase complex was determined over 60 minutes. 7.5ng of *Leishmania* CRK3:CYC6, 0.4mg ml⁻¹ (3.6μM) histone H1 substrate and 100μM [γ -³²P]-Mg-ATP were incubated at 30°C. The assay was stopped at various time points by the addition of orthophosphoric acid. The reaction was spotted onto a P81 filter plate and following washing with orthophosphoric acid, was counted for the incorporation of radioactivity. Graphical analysis was carried out using XLfit 4.0 software from IDBS (www.idbs.com).

3.12 *Leishmania* CRK3:CYC6 ATP and histone H1 substrate K_m determinations.

Kinase assays were performed to establish the K_m values of ATP and the histone H1 substrate for the *Leishmania* CRK3:CYC6 protein kinase complex. A two-fold titration of ATP was set up resulting in concentrations of ATP ranging from 2 μ M to 1mM in the assay to determine whether the complex follows Michaelis-Menten kinetics. The K_m value of ATP was determined at 64 μ M \pm 26 μ M for CRK3:CYC6 (Figure 3.15, upper graph). Similarly, a two-fold titration of the histone H1 substrate was set up with concentrations ranging from 0.45 μ M to 232 μ M in the assay. The K_m for the histone H1 substrate was determined as 2.4 μ M \pm 0.48 μ M (Figure 3.15, lower graph).

3.13 Staurosporine and olomoucine IC_{50} determinations for the *Leishmania* CRK3:CYC6 protein kinase complex.

The IC_{50} values for staurosporine and olomoucine were determined for the *Leishmania* CRK3:CYC6 protein kinase complex. The IC_{50} value for staurosporine was determined at 37nM (Figure 3.16, upper graph) and 51 μ M for olomoucine (Figure 3.16, lower graph). The IC_{50} value for olomoucine is consistent with the IC_{50} value of 42 μ M determined for CRK3his purified from *L. mexicana* parasites (Grant *et al.*, 1998).

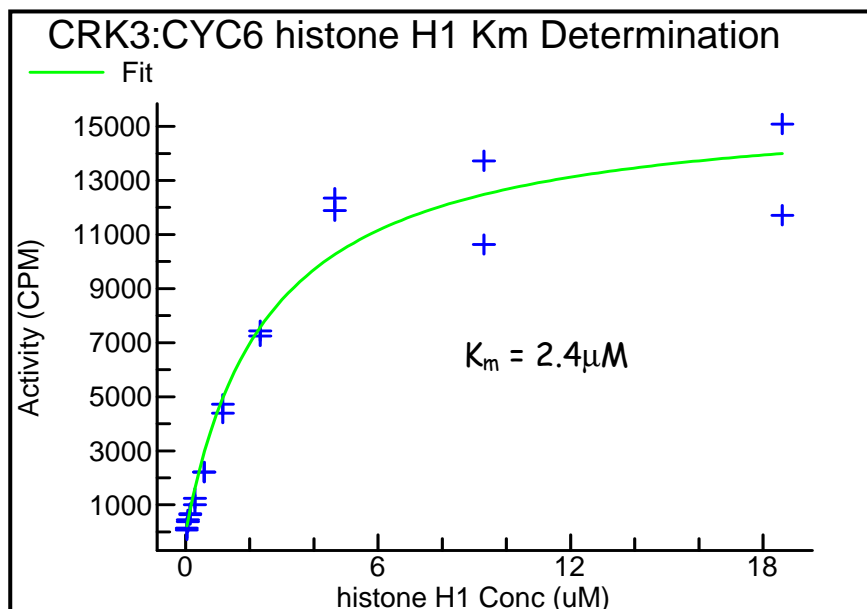
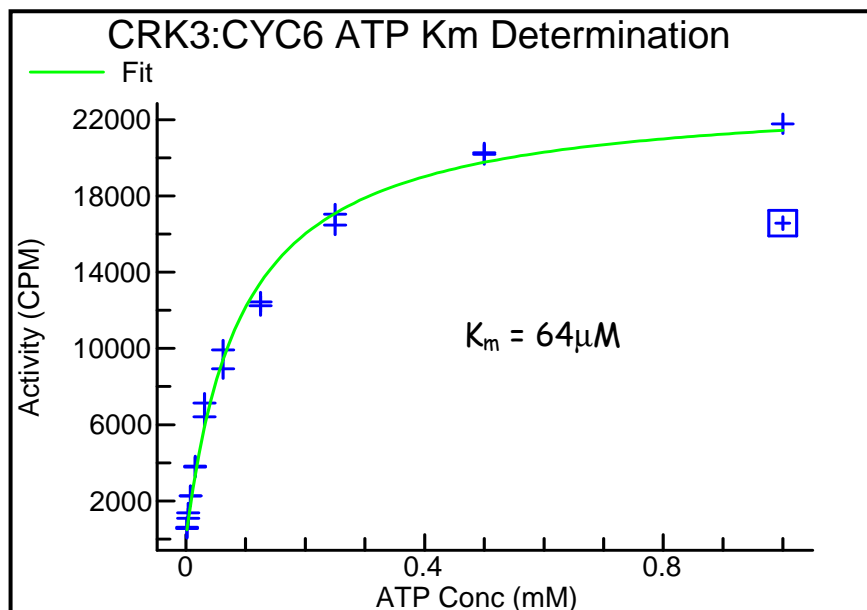


Figure 3.15 – ATP and substrate K_m determinations for the *Leishmania* CRK3:CYC6 protein kinase complex. K_m values for ATP (Upper graph) and a histone H1 substrate (Lower graph) determined for the *Leishmania* CRK3:CYC6 protein kinase complex. Graphical analysis was carried out using XLfit 4.0 software from IDBS (www.idbs.com) with a K_m determination model.

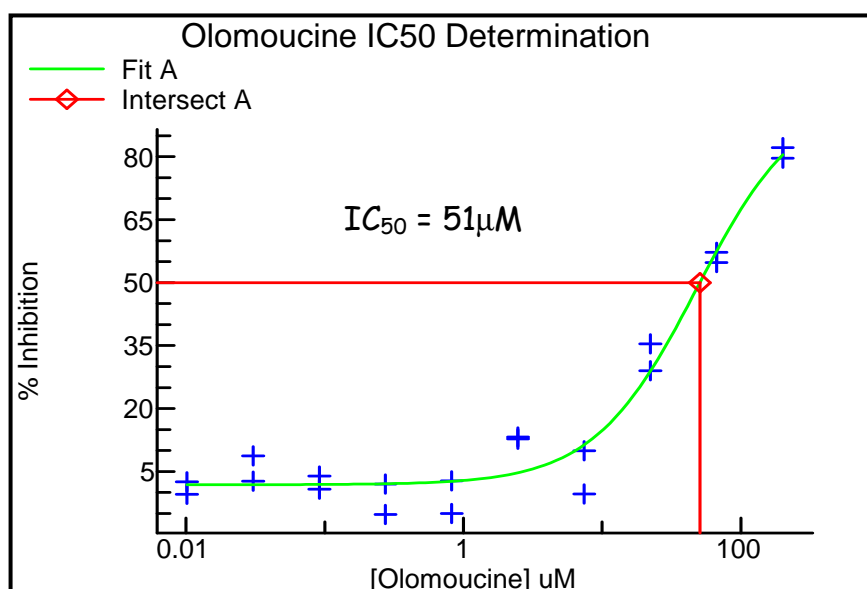
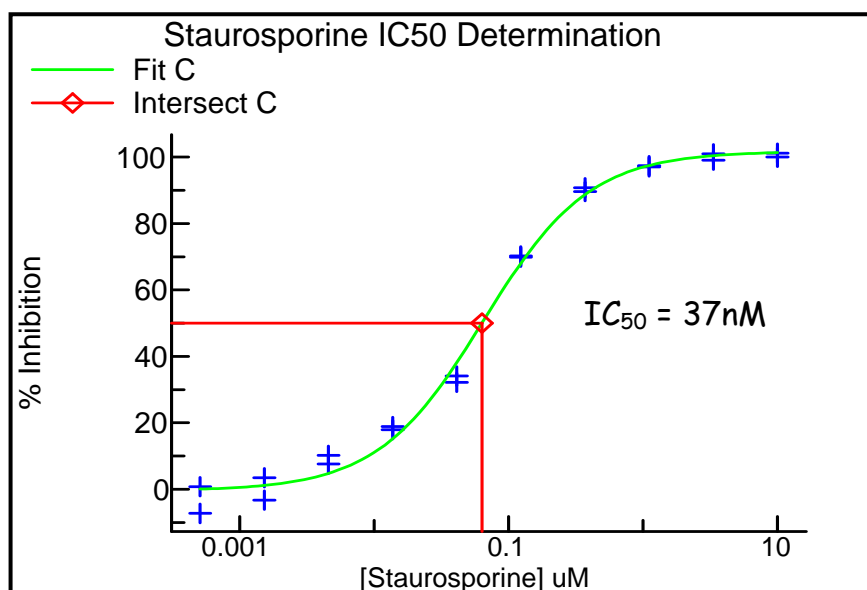
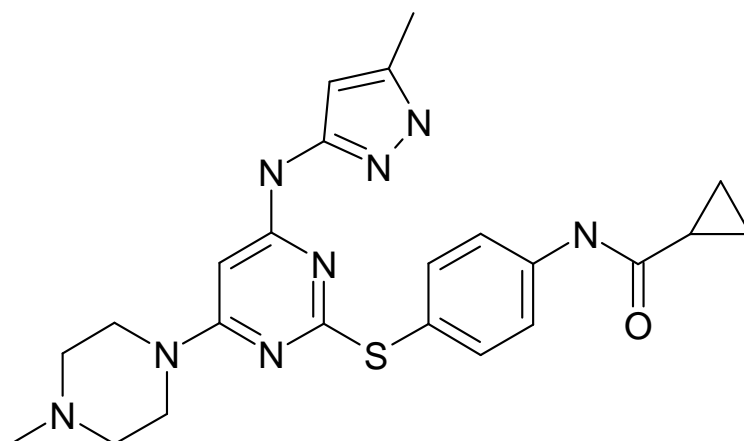


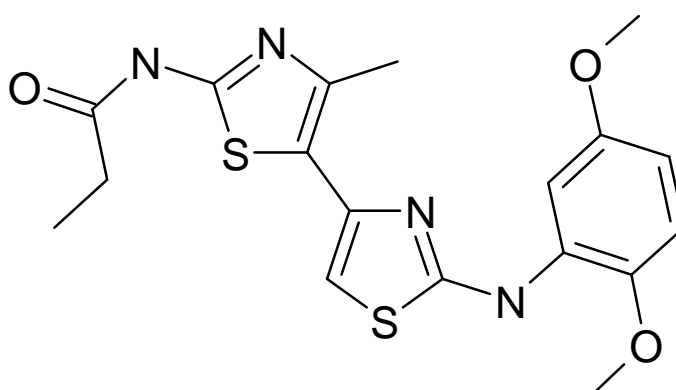
Figure 3.16 – Staurosporine and olomoucine IC₅₀ determinations for the *Leishmania* CRK3:CYC6 protein kinase complex. The IC₅₀ values for staurosporine (Upper graph) and olomoucine (Lower graph) protein kinase inhibitors determined for the *Leishmania* CRK3:CYC6 protein kinase complex. Graphical analysis was carried out using XLfit 4.0 software from IDBS (www.idbs.com).

3.14 Preliminary compound screen against *Leishmania* CRK3:CYC6.

A compound subset of 193 compounds from a number of Cyclacel in-house libraries was screened against the *Leishmania* CRK3:CYC6 protein kinase complex. Approximately 75% of the compounds were selected randomly from the Cyclacel library (Table 4.1). The remainder were selected for their known activities against one or more of the CDKs, Aurora kinases, Polo-like kinase 1 (PLK1) or Glycogen Synthase Kinase 3 (GSK-3) and included as positive controls. The compounds were screened at a fixed concentration of 10 μ M with 39/193 (20%) exhibiting >50% inhibition of *Leishmania* CRK3:CYC6 protein kinase activity. Thirty of these hits were known to be potent inhibitors of human CDK2:CycE and were not pursued for secondary screening against the *Leishmania* CRK3:CYC6 protein kinase complex. The remaining 9 compounds were secondary screened against the *Leishmania* CRK3:CYC6 protein kinase complex to determine their IC₅₀ values. This showed that 5/9 were false positives and did not inhibit *Leishmania* CRK3:CYC6 protein kinase activity, returning IC₅₀ values >50 μ M. This was possibly a result of carrying over more potent compounds from adjacent wells on the pipette tips when using the robotic technology, which has been seen at Cyclacel previously. The remaining 4/9 inhibited *Leishmania* CRK3:CYC6 protein kinase activity with IC₅₀ values ranging from 0.86 μ M to 13.4 μ M; however, two of these were screened and shown to be inhibitors of human CDK2:CycE with IC₅₀ values of 240nM and 1.2 μ M. The remaining 2/4, Vx-680 (Vertex) and compound A (ChemDiv) were inactive against human CDK2:CycE with IC₅₀ values of >50 μ M and their structures shown (Figure 3.17). The upper compound is Vx-680 from Vertex with an IC₅₀ of 6.2 μ M for the *Leishmania* CRK3:CYC6 protein kinase complex. The lower compound is from ChemDiv with an IC₅₀ of 13.4 μ M for the *Leishmania* CRK3:CYC6 protein kinase complex.



Vertex Vx-680



Compound A (ChemDiv)

Figure 3.17 – Structures of the compound hits from the *Leishmania* CRK3:CYC6 preliminary compound screen. The upper compound is Vx-680 from Vertex and the lower, compound A from ChemDiv.

3.15 Chapter discussion

A recombinant *L. major* CYC6 was cloned, sequenced and the protein shown to activate *L. mexicana* CRK3 *in vitro* to provide an active protein kinase complex. This complex was suitably active for radiometric assay development and compound screening. CRK3 homologues from three species of *Leishmania* have been cloned and are almost identical (Ali, 2002; Grant *et al.*, 1998; Wang *et al.*, 1998). There is a single amino acid change out of 311, in a non-conserved region in other CDKs, between *L. mexicana*, *L. major* and *L. donovani* CRK3. Therefore, the *Leishmania* CRK3:CYC6 protein kinase complex is essentially an *L. major* protein kinase complex with one amino acid difference.

CRK3, a *cdc2*-related protein kinase from *L. mexicana* (Grant *et al.*, 1998; Hassan *et al.*, 2001) was expressed and purified using the pET expression system (Figure 3.1, upper map). This provided a large quantity of CRK3his (~1mg litre⁻¹) as CRK3his is a relatively well expressed protein (Figure 3.2). CYC6his, a putative mitotic cyclin from *L. major*, was also cloned, sequenced and expressed using the pET expression system (Figure 3.1, lower map). *L. major* CYC6 is a homologue of *T. brucei* CYC6, which has been shown to associate with *T. brucei* CRK3 *in vivo* (Hammarton *et al.*, 2003a). Using this rationale, it was predicted that *L. major* CYC6 could associate with *L. mexicana* CRK3. When expressed in *E. coli*, it is notable that CYC6his is not present in as large a quantity (~0.5mg litre⁻¹) (Figure 3.3) as CRK3his (Figure 3.2), despite the expression conditions being optimised for CYC6his; an induction temperature of 19°C with 1mM IPTG in comparison with 19°C with 300µM IPTG for CRK3his. Using a higher concentration of IPTG to express CYC6his does not result in the level of protein expression seen with CRK3his. This is perhaps due to increased levels of CYC6his being toxic to the *E. coli* BL21 (DE3) pLys-S cells and interfering with bacterial growth. Therefore, the *E. coli* BL21 (DE3) pLys-S cells may control the expression levels of CYC6his by actively limiting it. The DE3 IPTG inducible systems are under control of the *lacUV5* promoter and it is known that this system leads to high mRNA and protein production. This can cause ribosome

destruction and *E. coli* cell death (Baneyx, 1999), another possible explanation accounting for the low level of CYC6 expression. Alternatively, expressing CYC6 in the absence of a kinase partner may lead to degradation of the protein.

L. major CYC6^{his} and *L. mexicana* CRK3^{his} were used in a gel-based kinase assay and protein kinase activity was observed when *L. major* CYC6^{his} was added, thereby validating it as a functional cyclin (Figure 3.6). The optimal ratio of *Leishmania* CRK3^{his} and CYC6^{his} proteins was established in order to obtain a fully active CRK3^{his}, where the greatest activity observed is present around the 1:1 ratio of *Leishmania* CRK3:CYC6 proteins (Figure 3.7). This is predicted to be the optimum ratio for full activation of CRK3^{his} as there is one PSTAIRE binding motif in CDKs capable of binding cyclins via the conserved cyclin box. As opposed to bacterial protein expression as used for *Leishmania* CRK3:CYC6, at Cyclacel, protein expression via baculovirus infected insect cells is carried out to produce active CDK:Cyclin complexes. Co-infection with a CDK and cyclin partner is a successful method of producing active CDK:Cyclin protein kinase complexes (Lawrie *et al.*, 2001) producing large quantities of protein in the process. This expression method allows for the optimal ratio of CDK to cyclin binding, predicted to be one CDK molecule to one cyclin, providing active protein kinase complexes.

The *S. cerevisiae* CDK activating kinase, Civ1, has been shown to phosphorylate and activate CDKs and is essential for cell viability in budding yeast (Thuret *et al.*, 1996). GST-Civ1 has been shown in the Mottram laboratory to phosphorylate CRK3^{his} on the T-loop T178 residue and that this further activates the *L. mexicana* CRK3:CYCA complex showing 3-5-fold higher activity (F.C. Gomes and J.C. Mottram, unpublished data). In order to determine whether a *Leishmania* CRK3:CYC6 protein kinase complex showing greater activity could be obtained through Civ1 activation, *S. cerevisiae* GST-Civ1 was purified (Figure 3.5). GST-Civ1 did not phosphorylate histone H1 itself (Figure 3.10) and was added to the *Leishmania* CRK3:CYC6 protein kinase complex and assayed for its

ability to activate the complex further. The increasing intensity of the upper band (Figure 3.11, upper arrow) highlights GST-Civ1 phosphorylating CRK3 on the T178 residue; however, no increase in the activity of the *Leishmania* CRK3:CYC6 protein kinase complex was seen (Figure 3.11, lower arrow). GST-Civ1 was therefore not used to activate the *Leishmania* CRK3:CYC6 protein kinase complex further in subsequent assays. This unexpected result highlights an interesting difference between the two *Leishmania* CRK3:CYC6 and CRK3:CYCA protein kinase complexes, and raises the question as to why GST-Civ1 activates the *L. mexicana* CRK3:CYCA protein kinase complex 3-5 fold but not the *Leishmania* CRK3:CYC6 protein kinase complex. Structural determination of these complexes may provide the answer.

A new expression and purification system for the histidine tagged *Leishmania* CRK3:CYC6 protein kinase complex was employed to obtain high quantities of active soluble protein for further assay development. The method previously used to purify CRK3his and CYC6his separately and mix the proteins together in a 1:1 ratio proved unacceptable for further assay development. The quantity of active soluble protein obtained was insufficient to screen the number of compounds required and so fresh protein would need to have been prepared on a weekly basis. Furthermore, there was a problem in expressing and purifying soluble *L. major* CYC6his from bacterial cells at Cyclacel. Different cell lines including *E. coli* BL21 (DE3) pLys-S, Rosetta (DE3) pLys-S, Origami (DE3) pLys-S and Rosetta-Gami (DE3) pLys-S were used in an attempt to obtain large quantities of *L. major* CYC6 but were unsuccessful (data not shown). In the event of no or low level protein expression using *E. coli*, infecting insect cells with baculovirus was considered as an alternative expression system. As mentioned, Cyclacel have experience with this expression system which has become one of the most widely used systems for the production of recombinant proteins (Kost *et al.*, 2005). Furthermore, an advantage that baculovirus has over bacterial expression is that proteins that undergo post-translational

modifications such as phosphorylation (in this instance, the conserved T-loop T178 residue in CRK3) may be obtained in their natural functional form (Fuchs *et al.*, 1995).

The new method, suggested by Professor Malcolm Walkinshaw at the Edinburgh Structural Biochemistry Group was co-expression and co-purification the *Leishmania* CRK3^{his} and CYC6^{his} proteins. Co-expression in *E. coli* has a number of advantages over reconstituting a complex from two separate proteins (Novy *et al.*, 2002), as was performed initially with CRK3 and CYC6 for in-gel kinase assays. These include enhanced solubility and proper folding of each protein, producing an enhanced yield of active protein complex. Co-expression has been performed previously in *E. coli* with human GST-CDK2 and *S. cerevisiae* GST-Civ1 to phosphorylate CDK2 on the T160 residue. This complex was subsequently co-purified with human cyclin A3, to provide a fully phosphorylated active CDK2:CycA protein kinase complex (Brown *et al.*, 1999b). However, the co-expression of two plasmids in the same cell line has historically had two prerequisites: that the plasmids have distinct resistance markers and distinct origins of replication (Yang *et al.*, 2001). It is widely believed that plasmids with the same replicon using the same replication machinery cannot coexist stably in *E. coli* and are thereby incompatible plasmids (Datta, 1979). This is because the plasmids will compete with each other during replication resulting in the cells containing one or the other, but not both plasmids after a few cell generations (Sambrook *et al.*, 1989). The generation of co-expression systems has been carried out to alleviate this problem, where two plasmids have distinct resistance markers and compatible origins of replication (Fribourg *et al.*, 2001) or one plasmid has two multiple cloning sites, allowing the expression of two genes (Novy *et al.*, 2002).

However, *Leishmania* CRK3:CYC6 was expressed via incompatible plasmids (section 2.4.2 and figure 3.1) (CRK3 in pET28a and CYC6 in pET15b) which according to the literature is likely to be unsuccessful. Although these pET vectors have two distinct antibiotic resistance markers (pET28a, kanamycin and pET15b, ampicillin), they have a

common origin of replication, pBR322, and therefore only one plasmid could remain as previously discussed. Co-expression of CRK3:CYC6 from *T. brucei* previously proved unsuccessful (E. Brown and J.C. Mottram, unpublished). In relation to the co-expression of *Leishmania* CRK3:CYC6, it has previously been described that two incompatible plasmids (pET21a and pET28a, Novagen) had been co-expressed in *E. coli* due to the selection pressure of the antibiotics for 14 hours (Yang et al., 2001). Co-purification has also been successfully carried out with His-tagged human cyclin B1 and HA-tagged human Cdc2 expressed in insect cells (Moore *et al.*, 1999). These examples show that co-expression and co-purification methods are successful in producing active protein kinase complexes. From 1 litre of bacterial culture, co-expression and co-purification produced 4.5mg of *Leishmania* CRK3:CYC6 protein kinase complex whose activity was suitable for further radiometric assay development. This quantity of *Leishmania* CRK3:CYC6 was sufficient and active enough, expressing the complex in a 1:1 ratio and therefore baculovirus expression was not required.

Leishmania CRK3:CYC6 protein kinase activation was established in a gel-based assay; however, it was vital this activity could be transferred to a plate based assay, as this is the method used at Cyclacel for low to medium throughput compound screening. In order to be useful for compound screening, assay criteria at Cyclacel require an assay to have a signal to background ratio of at least 10:1. An important aspect of assay development is to optimize the assay conditions in order to obtain a high signal to background ratio. This would enable compounds that are genuine inhibitors of the target to be identified with confidence from a background signal within the signal window. An initial activity assay carried out identified 7.5ng of protein complex producing counts of approximately 15,000 per minute compared to a background of approximately 1000 counts per minute, a signal to background ratio of approximately 15:1. *Leishmania* CRK3:CYC6 protein kinase activity was therefore suitably high to proceed with further assay development (Figure 3.13). The activity and signal to background ratio of the CRK3:CYC6 assay was comparable with a

number of other protein kinase assays developed at Cyclacel, which were used in the counter screening of the HTS hits against mammalian CDKs (section 4.12). By comparison, the plate-based assay was validated using 7.5ng of *Leishmania* CRK3:CYC6 protein kinase complex per assay point, which is significantly lower than that used in the in-gel assays, where micrograms (μg) of *Leishmania* CRK3:CYC6 proteins were being used to visualise protein kinase activity.

In initial experiments to establish whether to use recombinant *Leishmania* CRK3:CYC6 protein kinase complex or CRK3his purified from *L. mexicana* parasites for assay development; some biochemical analysis was carried out on the *Leishmania* CRK3:CYC6 protein kinase complex. The K_m values for ATP and a histone H1 substrate were determined (Figure 3.15). The K_m of ATP for the purified enzyme from the parasite is $35\mu\text{M}$ as determined by Karen Grant. The K_m of ATP for the *Leishmania* CRK3:CYC6 complex was $64\mu\text{M} \pm 26\mu\text{M}$, within two-fold of the parasite enzyme (Figure 3.15, upper graph), suggesting that the two CRK3 enzymes are biochemically similar. The K_m for the histone H1 substrate was determined at $2.4\mu\text{M} \pm 0.48\mu\text{M}$ (Figure 3.15, lower graph); however, this has not been determined for the purified enzyme from *L. mexicana* parasites. In the radiometric assay, $100\mu\text{M}$ ATP and $3.6\mu\text{M}$ of histone H1 substrate are used per assay point. These quantities are sufficiently above the K_m values, generating an acceptable signal window, without saturating the assay.

Further analysis of the *Leishmania* CRK3:CYC6 protein kinase complex was carried out to determine the IC_{50} values for staurosporine, a broad range kinase inhibitor, and olomoucine, a potent inhibitor of mammalian cdc2 with a narrow range of selectivity (Meijer, 1996). The IC_{50} value for staurosporine was 37nM (Figure 3.16, upper graph) and was potent towards *Leishmania* CRK3:CYC6 protein kinase activity as expected. However, the IC_{50} value for staurosporine against *L. mexicana* parasite CRK3 is currently

unknown and therefore could not be compared with the recombinant complex. The IC_{50} value for olomoucine against CRK3 purified from *L. mexicana* parasites is $42\mu\text{M}$ (Grant *et al.*, 1998) and was determined as $51\mu\text{M}$ against the *Leishmania* CRK3:CYC6 protein kinase complex (Figure 3.16, lower graph). These values are almost identical, further suggesting that the two enzymes are biochemically similar. Therefore it could be hypothesised that active CRK3 purified from *Leishmania* may be in complex with CYC6, and that CYC6 could be an *in vivo* partner of CRK3. On the other hand, parasite CRK3 may be in complex with another cyclin such as CYCA, whose complex may share similar biochemical characteristics to those of recombinant *Leishmania* CRK3:CYC6. Purifying CRK3 from *Leishmania* and analysing it via SDS-PAGE and Colloidal Blue staining may identify other proteins associated with CRK3. These could be analysed by peptide mass fingerprinting to help identify *in vivo* partners of CRK3, of which, CYC6 may be one. As the biochemical analysis suggested both the recombinant and parasite purified enzymes were similar, it was decided to use the recombinant *Leishmania* CRK3:CYC6 protein kinase complex for future assay development, as significant active quantities could be purified.

A preliminary screen of compounds from a number of in-house compound libraries was carried out to assess the developed radiometric assay and as a basis for the future high throughput screening of the *Leishmania* CRK3:CYC6 protein kinase complex. The screen returned four compounds which were active towards CRK3:CYC6 and were screened to determine their IC_{50} values. IC_{50} determinations showed two were potent inhibitors of human CDK2:CycE and were not pursued, with the remaining two inactive towards human CDK2:CycE. The structures of the two compounds active against the *Leishmania* CRK3:CYC6 protein kinase complex and inactive against human CDK2:CycE are shown in Figure 3.17. However, although Vx-680 is inactive towards human CDK2:CycE, it has been shown to be potent towards all three Aurora kinases. The apparent inhibition

constants ($K_{i \text{ (app)}}$) were 0.6, 18 and 4.6nM for Aurora-A, Aurora-B and Aurora-C, respectively (Harrington *et al.*, 2004). Intellectual properties notwithstanding, these two compounds could be possible starting pharmacophores for structural chemistry to make compounds more potent towards the *Leishmania* CRK3:CYC6 protein kinase complex. However, a wider library screen of approximately 25,000 compounds from the Cyclacel library was undertaken using a high throughput screening platform to identify more suitable candidates (Chapter 4).

Chapter 4

High throughput assay development and screening.

4.1 Chapter introduction and objectives.

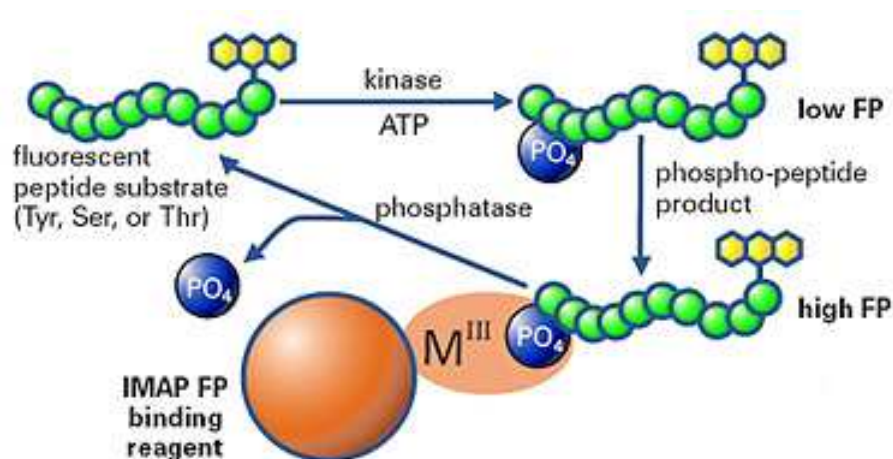
The radiometric ^{32}P assay developed for the *Leishmania* CRK3:CYC6 protein kinase complex described in chapter 3 is suitable for low to medium throughput compound screening; however, it is not a suitable platform for high throughput screening. This is due to the high quantities of radiation required for the assays and the time restraints imposed by the assay protocol, as it is carried out manually. As a result, the radiometric *Leishmania* CRK3:CYC6 assay was used as a reference assay to develop and validate a high throughput assay platform suitable for screening the 25,000 compound Cyclacel library. The high throughput screening approach utilised Cyclacel's experience in library screening by using the automated assay facilities capable of processing up to 10,000 assay points per day.

Three high throughput screening platforms were considered for the screen; ALPHA-screenTM luminescence from Perkin Elmer (www.perkinelmer.com), IQTM fluorescence quenching from Pierce Biotechnology (www.piercenet.com) and IMAPTM fluorescence polarization from Molecular Devices (www.moleculardevices.com). The ALPHA-screenTM (Amplified Luminescent Proximity Homogenous Assay) platform is a luminescence assay that uses a substrate bound to a donor bead and a phospho-specific antibody bound to an acceptor bead. Antibody binding to the phosphorylated substrate brings the acceptor bead into close proximity with the donor bead, resulting in light emission (www.perkinelmer.com). The IQTM (Intensity Quenching) platform is a fluorescence quenching assay that uses a proprietary iron-containing compound that reacts with phosphate groups on a fluorescently labelled peptide. Binding results in a change in relative fluorescence units which correlates directly to the number of peptides containing

phosphate groups (www.piercenet.com). The IMAPTM (Immobilized Metal Affinity-based fluorescence Polarization) technology is a fluorescence polarization assay that uses technology based on the specific, high-affinity interaction of trivalent metal containing nanoparticles with phosphogroups. Fluorescently-labelled peptides are phosphorylated in a kinase reaction. Addition of the IMAP binding system stops the kinase reaction and specifically binds the phosphorylated substrates. Phosphorylation and subsequent binding of the substrate to the beads can be detected by fluorescence polarization (Figure 4.1) (www.moleculardevices.com).

The IMAPTM platform (Figure 4.1) was chosen to carry out the high throughput screen. This was because the IMAPTM technology was the most up-to-date and because the other assay formats had prior requirements unlike the IMAPTM assay. The ALPHA-screenTM assay required an antibody and substrate pair and the IQTM assay required a specific peptide substrate which was unavailable commercially and required synthesizing at a large cost. As the IMAPTM platform did not have these prerequisites it was used for the high throughput screening of *Leishmania* CRK3:CYC6.

This chapter will focus on the IMAPTM assay that was developed, optimised and validated for *Leishmania* CRK3:CYC6. With this, the high throughput screening of *Leishmania* CRK3:CYC6 was carried out in order to identify inhibitors of *Leishmania* CRK3:CYC6 protein kinase activity within the Cyclacel library. Counter screening of the hits against mammalian kinases was carried out to determine the selectivity of the inhibitors towards *Leishmania* CRK3:CYC6. Follow up and related work on the identified hits will also be discussed in the chapter.

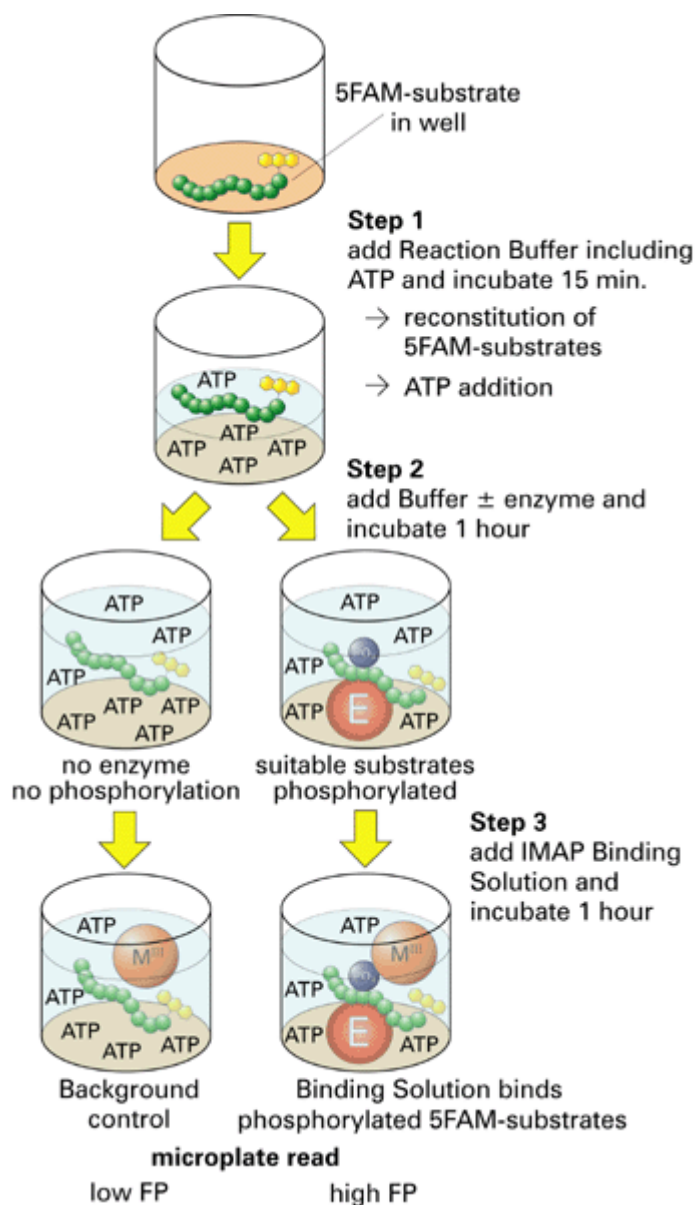


www.moleculardevices.com

Figure 4.1 – IMAPTM fluorescence polarisation assay schematic. The kinase reaction (enzyme, fluorescent substrate, ATP and plus or minus inhibitor) is set up in a volume of 20µl and incubated for 1 hour 20 minutes at room temperature. The kinase adds a phosphate (PO₄³⁻) group from the ATP onto the substrate. 50µl of the binding reagent (orange) is added to both stop the reaction and bind the fluorescently labelled phospho-peptide. This results in a reduction in rotational speed and an increase in fluorescence polarization which is detected in a microplate reader.

4.2 Optimum substrate identification for *Leishmania* CRK3:CYC6.

In order to identify the optimal substrate for CRK3:CYC6 for use in the IMAPTM HTS format, a substrate finder assay was carried out. The plate had 61 potential serine/threonine protein kinase substrates and the specific substrate finder assay protocol is shown in Figure 4.2. The raw data (Fluorescence polarization, mP) was pasted in to a data analysis programme provided by Molecular Devices, which generated a bar chart highlighting the background signal and specific signal for each peptide substrate and pre-phosphorylated calibrator peptides (Figure 4.3). The background signal was subtracted leaving the specific signal for each peptide substrate (Figure 4.4). Of the 61 peptide substrates on the plate, 6 showed a specific signal (Δ mP) of >100mP. The greatest Δ mP was with a generic serine/threonine kinase substrate peptide sequence GGGRSPGRRRRK (310mP), then a histone H1 derived peptide GGGPATPKKAKKL (295mP), then a short histone H1 derived peptide (amino acids 9-18) PKTPKKAKKL (280mP), then DYRKtide RRRFRPASPLRGPPK (190mP), then a CDK7 derived peptide FLAKSFGSPNRAYKK (180mP) and recombinant histone H1 protein (100mP) (Figure 4.4). Analysis of the 6 peptide substrates highlighted that they all contained a sequence pattern xS/TPxR/K, which is in accordance with the optimal recognition motif for CDKs, $x_{-1}(S/T)_0P_{+1}x_{+2}(K/R_{+3})$ (Stevenson-Lindert *et al.*, 2003) (Figure 4.5). The generic peptide substrate was chosen as the optimum substrate and used in all subsequent IMAPTM assays.



www.moleculardevices.com

Figure 4.2 – IMAP™ substrate finder assay schematic. The fluorescently labelled peptide substrates are reconstituted via the addition of ATP in the complete reaction buffer (CRB). CRB ± enzyme is added and incubated for 1 hour 20 minutes at room temperature. The IMAP™ binding solution is added, and the reaction incubated for a further 1 hour 20 minutes at room temperature before the plate was read in a microplate reader.

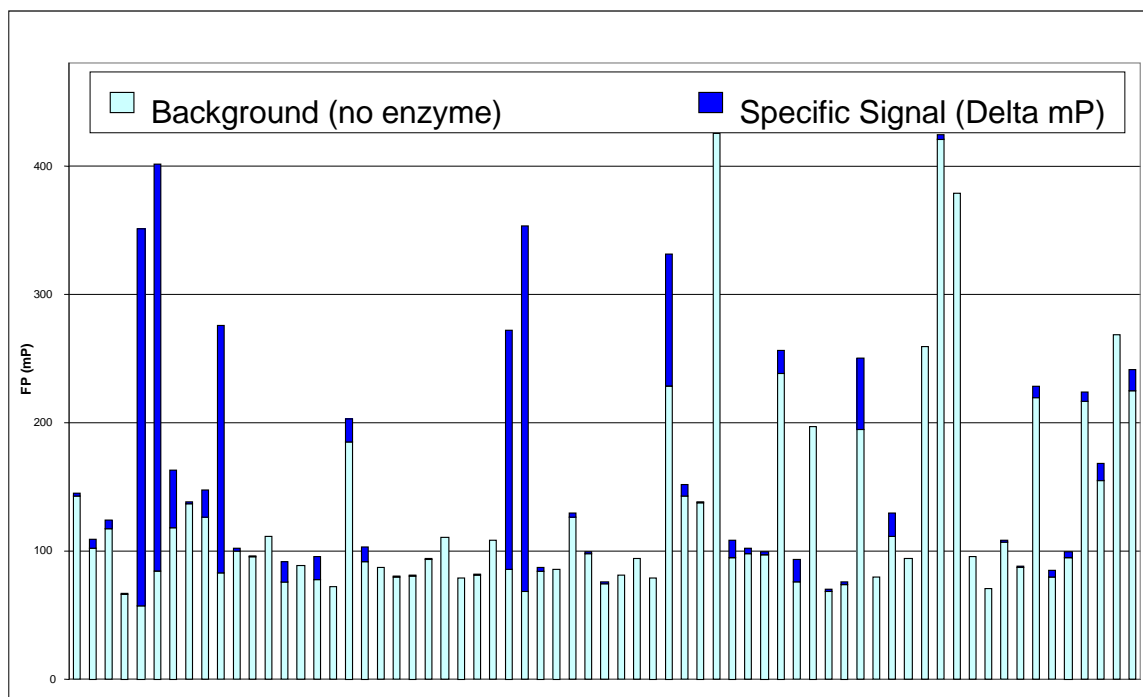


Figure 4.3 – IMAPTM substrate finder assay analysis using Molecular Devices data analysis software. Fluorescence polarization data was analysed using the data analysis macro provided by Molecular Devices. The bar chart shows the corresponding background and specific polarization signal (mP) generated by each of the 61 substrates and pre-phosphorylated control peptides.

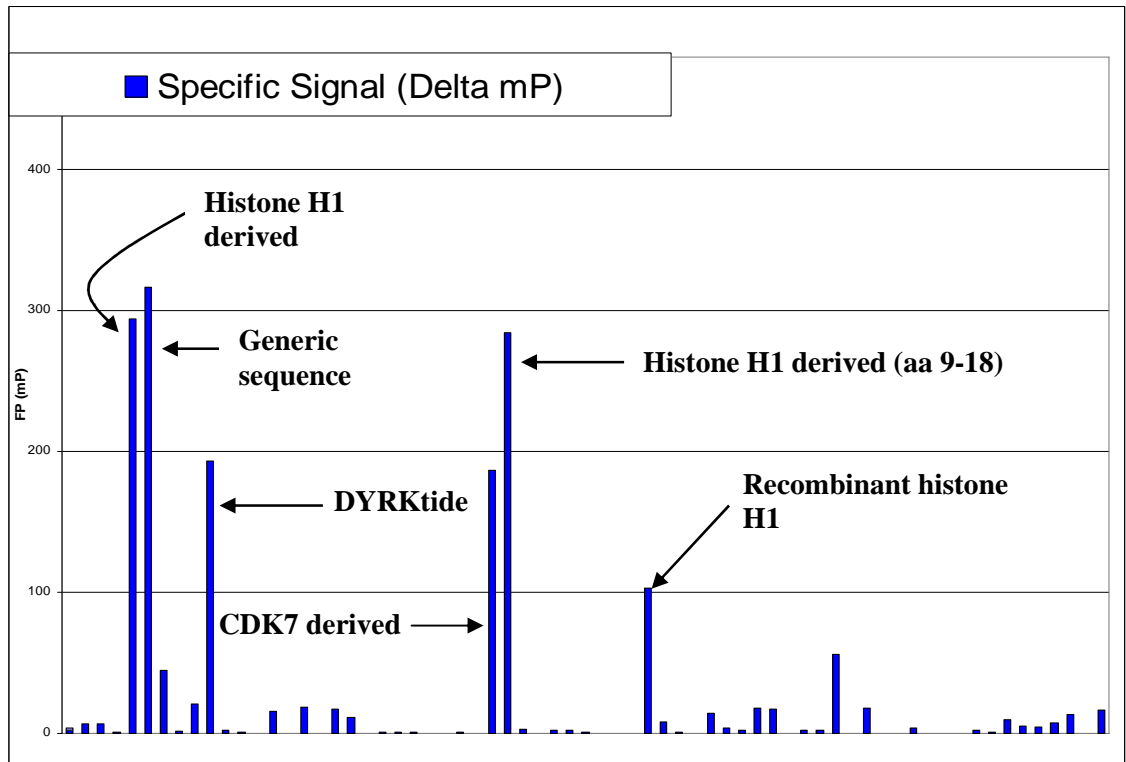


Figure 4.4 – IMAPTM substrate finder assay to identify the best substrates of CRK3:CYC6 for the HTS assay. A substrate plate containing 61 potential serine/threonine kinase substrates was assayed as described in Figure 4.2. Six substrates were identified showing a fluorescence polarization change >100mP. The generic sequence peptide was the optimum substrate for CRK3:CYC6 showing the greatest change in fluorescence polarization (Δ mP).

Amino acid position:

-1 0 +1 +2 +3

histone H1 derived:	G G G P A T P K K A K K L
Generic sequence:	G G G R S P G R R R R K
Short histone H1 derived:	P K T P K K A K K L
DYRKtide:	R R R F R P A S P L R G P P K
CDK7 derived:	F L A K S F G S P N R A Y K K

Sequence pattern: x S/T P x R/K

Optimal recognition motif for CDKs: $x_{-1} (S/T)_0 P_{+1} x_{+2} (K/R)_{+3}$

Figure 4.5 – IMAPTM substrate finder sequence analysis. The five peptides identified as substrates for CRK3:CYC6 were analysed by sequence alignment. The consensus sequence pattern follows the optimal recognition motif identified for mammalian CDKs. Highlighted in red are the serine/threonine amino acid residues (in the 0 position) which are phosphorylated by the CRK3:CYC6 protein kinase complex.

4.3 *Leishmania* CRK3:CYC6 two-fold enzyme titration.

In order to establish the quantity of CRK3:CYC6 to be used in the IMAPTM HTS assays, a two-fold enzyme titration was carried out (Figure 4.6). Carrying out the assay as described in 2.6.2, the titration identified that 1.25ng of kinase complex could be used per assay point. When running the assay for 1 hour 20 minutes, this produced a signal of approximately 280mP with a Δ mP of 180mP and was in the linear phase of the assay. The assay was validated under these conditions with a Z' score of 0.71 which is considered excellent in terms of assay quality (Zhang *et al.*, 1999; Iversen *et al.*, 2006) where the assay is reliable, robust and suitable for HTS (Yuhong *et al.*, 2007).

4.4 *Leishmania* CRK3:CYC6 ATP K_m determination.

A kinase assay was performed in order to establish the K_m value of ATP in the HTS format (Figure 4.7), to compare with the radiometric assay determination (Figure 3.15, Upper graph). A two-fold titration of ATP was set up resulting in concentrations of ATP ranging from 2 μ M to 1mM in the assay. The K_m value of ATP was determined to be 152 μ M \pm 13.4 μ M for CRK3:CYC6.

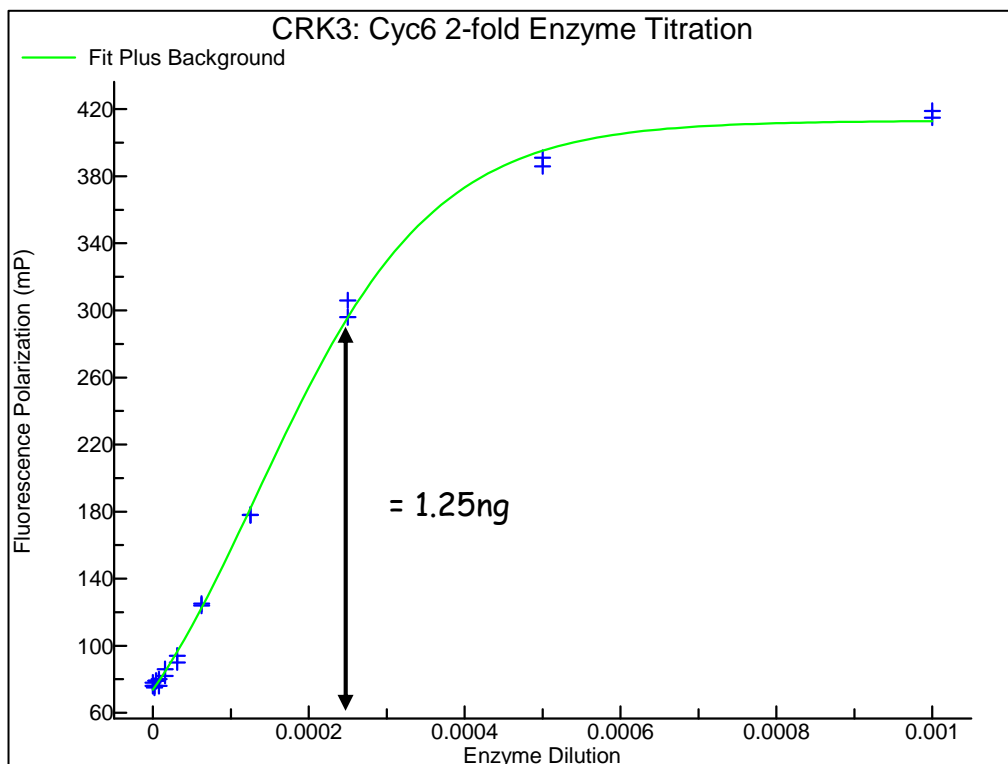


Figure 4.6 – CRK3:CYC6 IMAPTM assay development and validation – enzyme titration. Using the generic sequence peptide as the substrate, a two-fold enzyme titration was carried out. The kinase assay was carried out as described in 2.6.2. This identified that 1.25ng of CRK3:CYC6 could be used in the IMAP high throughput screen format. Graphical analysis was carried out using XLfit 4.0 software from IDBS (www.idbs.com).

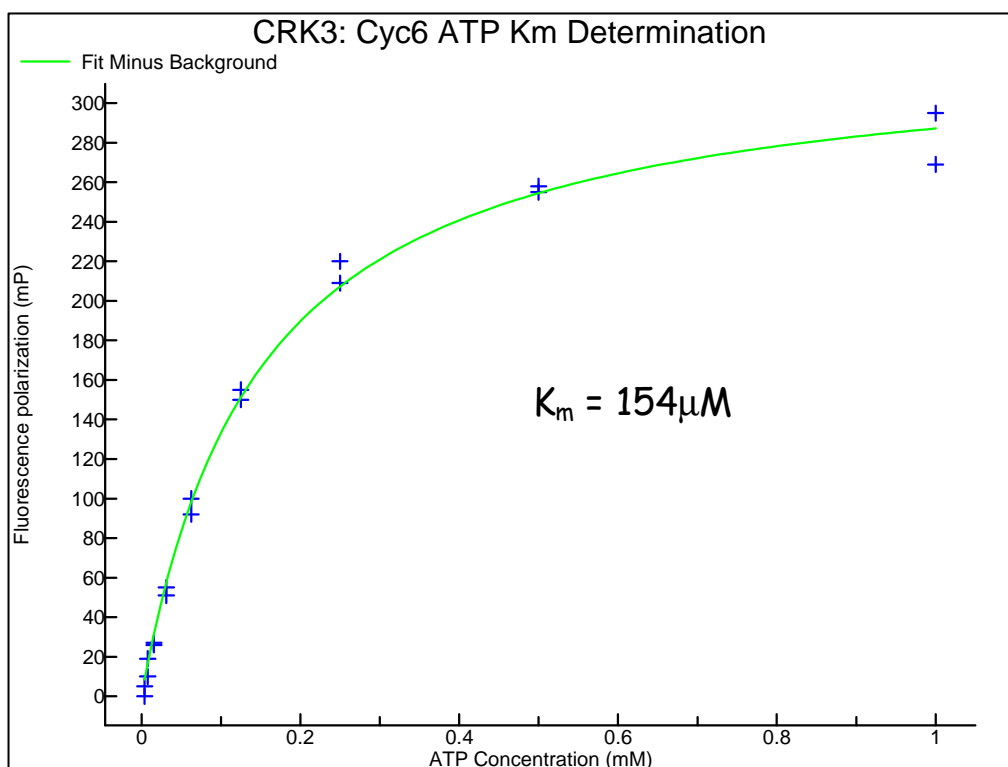


Figure 4.7 – ATP K_m determination for CRK3:CYC6 using the IMAPTM HTS assay.

The K_m value for ATP was determined for the CRK3:CYC6 complex. This was determined at $154\mu\text{M} \pm 13\mu\text{M}$. Graphical analysis was carried out using XLfit 4.0 software from IDBS (www.idbs.com) with a K_m determination model.

4.5 Staurosporine and olomoucine IC₅₀ determinations for *Leishmania* CRK3:CYC6.

The IC₅₀ values for staurosporine and olomoucine were determined for the CRK3:CYC6 complex in the HTS format (Figure 4.8), to compare with those determined in the radiometric assay (Figure 3.16). The IC₅₀ value for staurosporine was determined at 20nM (Figure 4.8, upper graph) and >10μM for olomoucine (Figure 4.8, lower graph).

4.6 Preliminary compound screen against *Leishmania* CRK3:CYC6.

The 193 compound preliminary screen in chapter 3 was repeated using the HTS format to determine if the newly developed assay would identify the same hits as found in the radiometric assay. 34 hits were expected, as 5/39 found were false positives in the radiometric assay. As expected, these 34 hits were all identified showing the developed assay was functional and valid (data not shown).

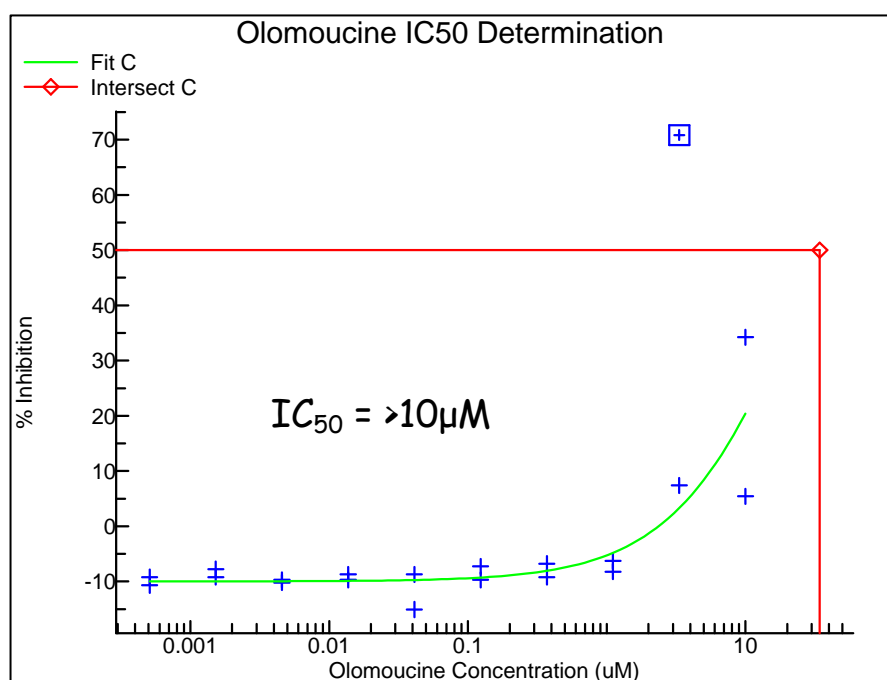
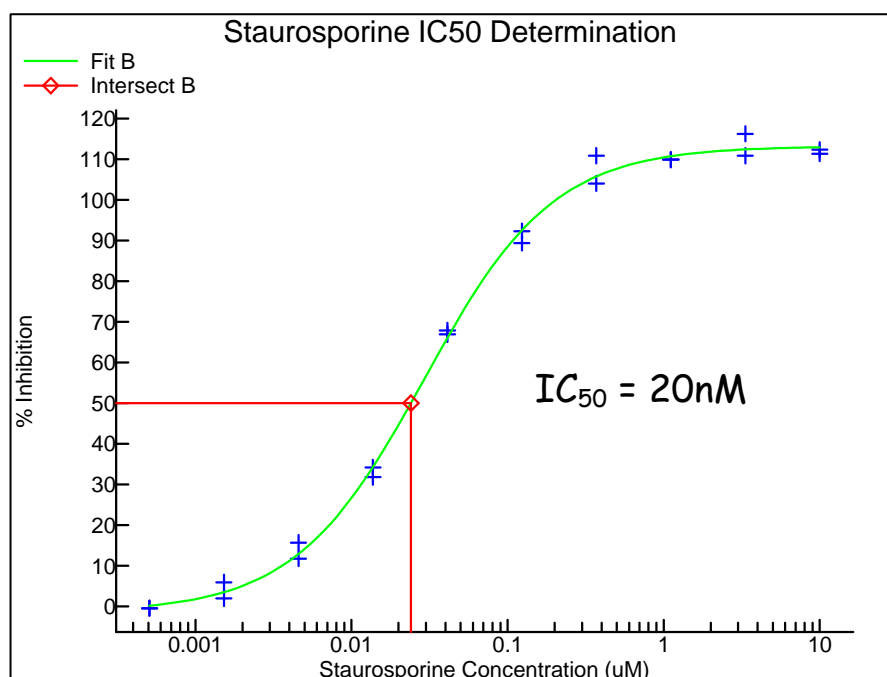


Figure 4.8 – Biochemical characteristics of CRK3:CYC6 using the IMAPTM HTS assay. The IC₅₀ values for staurosporine (upper graph) and olomoucine (lower graph) protein kinase inhibitors against CRK3:CYC6 were determined. Graphical analysis was carried out using XLfit 4.0 software from IDBS (www.idbs.com).

4.7 Development of an IMAPTM assay suitable for counter screening against human CDK2:CycA:

4.7.1 Human CDK2:CycA two-fold enzyme titration.

In order to establish the quantity of CDK2:CycA to be used in the IMAPTM HTS assays, a two-fold enzyme titration was carried out (Figure 4.9). The CDK2:CycA kinase complex was produced in-house at Cyclacel via baculovirus protein expression. Carrying out the assay as described in figure 4.1, the titration identified that 33ng of CDK2:CycA could be used per assay point. When running the assay for 1 hour 20 minutes, this produced a Δ mP signal of approximately 200mP and was in the linear phase of the assay. The assay was fully validated under these conditions with a Z' score of 0.67.

4.8 High throughput screening of the Cyclacel compound library:

4.8.1 *Leishmania* CRK3:CYC6 and human CDK2:CycA IMAPTM fluorescence polarization HTS assays.

The Cyclacel compound library screened against CRK3:CYC6 and CDK2:CycA contained approximately 25,000 compounds. This was comprised of two subset libraries which are described in Table 4.1. The Cyclacel library was screened against *Leishmania* CRK3:CYC6 and mammalian CDK2:CycA using IMAPTM fluorescence polarization technology (Figure 4.1). The assays were carried out as described in the methods section using the high throughput screening robotic technology at Cyclacel. The compound library was initially screened against *Leishmania* CRK3:CYC6 at a fixed concentration of 10 μ M and the data analysed using IDBS Activity Base software (www.idbs.com).

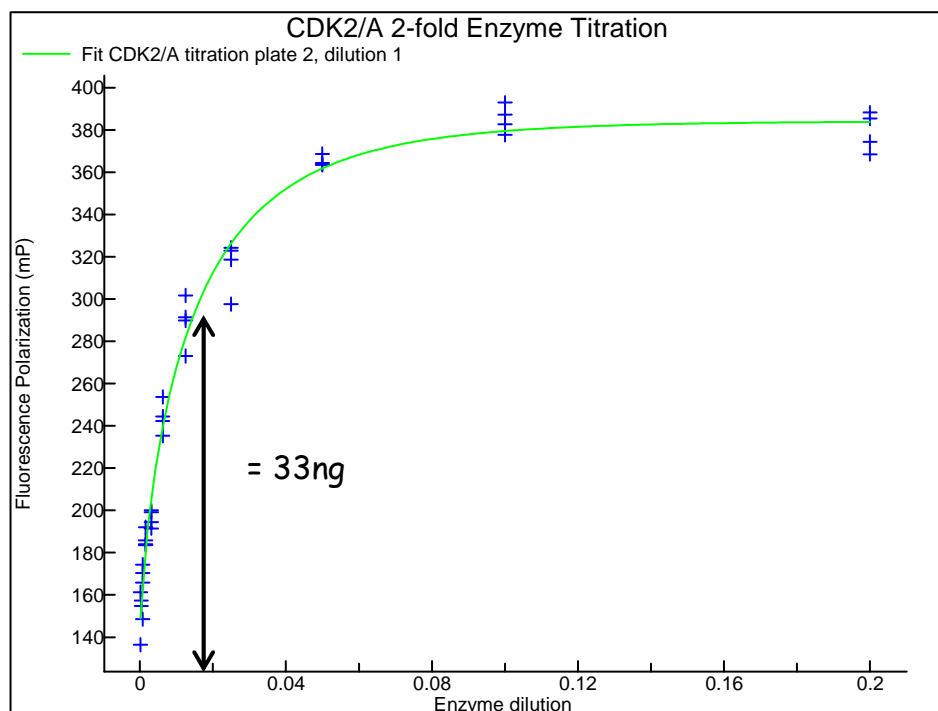


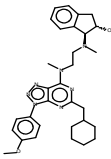
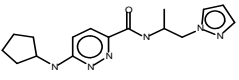
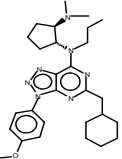
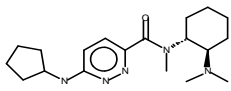
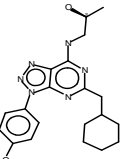
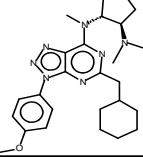
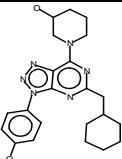
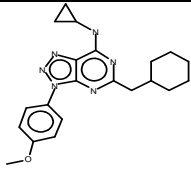
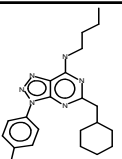
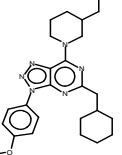
Figure 4.9 – Human CDK2:CycA IMAP™ assay development and validation. Using the generic sequence peptide identified, a two-fold enzyme titration was carried out. The kinase assay was carried out as described in figure 4.1. This identified that 33ng of human CDK2:CycA can be used in the IMAP™ high throughput screen format. Graphical analysis was carried out using XLfit 4.0 software from IDBS (www.idbs.com).

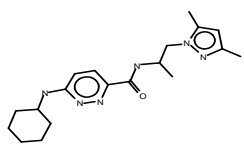
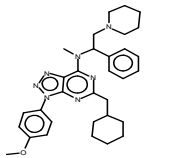
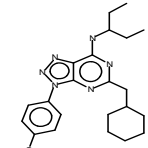
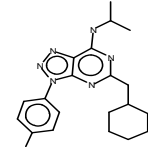
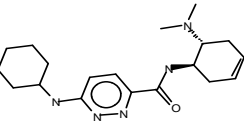
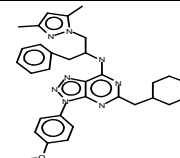
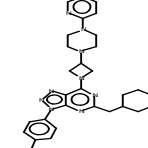
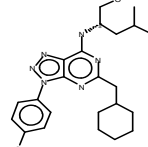
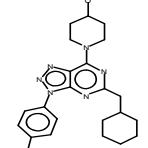
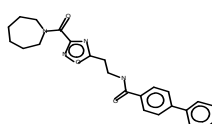
Heterocycle Library 2 (HL-2)	Kinase Inhibitor Theme library
~16,000 compounds	~8,000 compounds
6 synthetic themes	Heterocycle library 1 (HL-1)
10 heterocyclic themes	Published Adenine, Pyrimidine, Quinazoline and Quinoxaline CDK inhibitors.
Desirable pharmaceutical properties (Lipinski rules, ADME properties)	Natural product mimic library: kinase inhibitor themes, sugar nucleoside mimics, protease inhibitor themes, steroid mimics, aminoglycoside mimics and phosphatase inhibitor themes.

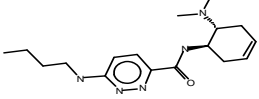
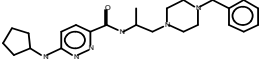
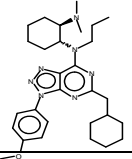
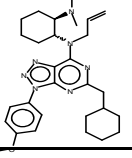
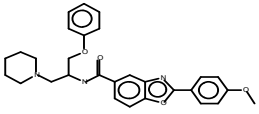
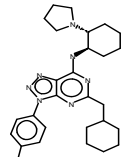
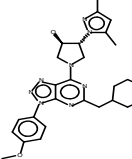
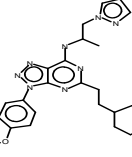
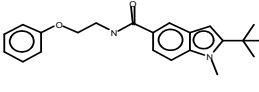
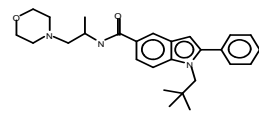
Table 4.1 – The Cyclacel compound library breakdown. The compound library is composed of two sub-libraries, the heterocycle 2 and kinase inhibitor theme libraries. They include known kinase inhibitors and natural product mimics as well as synthetic compounds. The heterocycle 2 compounds were designed with desirable pharmaceutical properties.

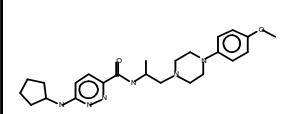
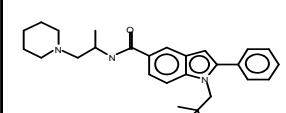
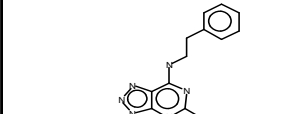
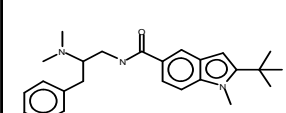
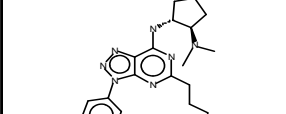
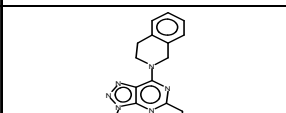
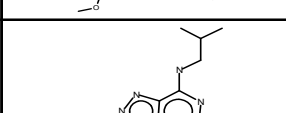
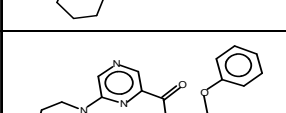
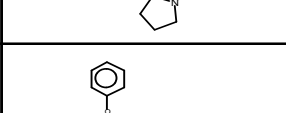
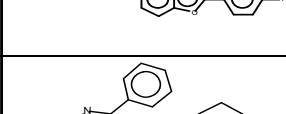
The screen identified 43 Cyclacel compounds that produced a $\geq 50\%$ inhibition of *Leishmania* CRK3:CYC6 protein kinase activity (Table 4.2, columns 1-4). The Cyclacel library was subsequently screened against human CDK2:CycA to both filter out any of the CRK3:CYC6 hits that target the human kinase, and to potentially provide more useful structure activity relationship (SAR) data as the library had not previously been screened against human CDK2:CycA. None of the 43 CRK3:CYC6 hits inhibited human CDK2:CycA significantly (Table 4.2, column 5) and therefore all were taken forward for secondary screening against CRK3:CYC6 to determine their IC_{50} values. The IC_{50} value determinations were carried out using the radiometric ^{32}P assay resulting in values ranging from 2.6 μ M to >50 μ M (Table 4.2, column 6).

In order to confirm the 43 hits did not significantly target mammalian CDK2:CycA, IC_{50} values were determined for this kinase complex. All 43 compounds returned IC_{50} values >50 μ M (Table 4.2, column 7) confirming the primary screen data for mammalian CDK2:CycA (Table 4.2, column 5). Based on the results, the compounds were divided into three groups; the top 18 which were taken forward for mammalian kinase counter screening (Table 4.2, Red); compounds not analysed further (Table 4.2, Blue) and compounds which were false positives and did not target CRK3:CYC6 (Table 4.2, Black).

Compound	Molecular Weight (g/mol)	Structure	% inhibition of CRK3:CYC6	% inhibition of CDK2:CycA	CRK3:CYC6 IC ₅₀ (μM)	CDK2:CycA IC ₅₀ (μM)
Compound 1	541.69		69.9	13.2	2.6	>50
Compound 2	314.39		59	3.7	2.67	>50
Compound 3	491.67		67.7	6	3.42	>50
Compound 4	345.48		57.5	9.4	3.62	>50
Compound 5	396.49		70.6	5.3	4.35	>50
Compound 6	465.59		72.3	5.3	4.38	>50
Compound 7	422.52		70.6	11.9	5.27	>50
Compound 8	378.47		65.7	9.1	5.79	>50
Compound 9	394.51		60	14	5.98	>50
Compound 10	436.55		73.1	12.3	6.9	>50

Compound	Molecular Weight (g/mol)	Structure	% inhibition of CRK3:CYC6	% inhibition of CDK2:CycA	CRK3:CYC6 IC ₅₀ (μM)	CDK2:CycA IC ₅₀ (μM)
Compound 11	356.47		57.4	14.1	7.14	>50
Compound 12	539.71		69.8	0.8	7.83	>50
Compound 13	408.54		55.2	7	8.12	>50
Compound 14	380.49		52.7	15.7	8.76	>50
Compound 15	427.54		53.2	-4.9	8.94	>50
Compound 16	550.69		67.9	1.4	10.12	>50
Compound 17	539.67		58.8	16.6	10.26	>50
Compound 18	438.57		60.9	4.3	10.69	>50
Compound 19	422.52		63.3	3.6	11.76	>50
Compound 20	418.49		60.8	-12.1	12.78	>50

Compound	Molecular Weight (g/mol)	Structure	% inhibition of CRK3:CYC6	% inhibition of CDK2:CycA	CRK3:CYC6 IC ₅₀ (μM)	CDK2:CycA IC ₅₀ (μM)
Compound 21	317.43		53.4	-20.8	15.4	>50
Compound 22	422.57		67.5	2.3	15.68	>50
Compound 23	505.69		63.8	11.2	15.78	>50
Compound 24	503.68		58.1	2.8	16.18	>50
Compound 25	485.57		53.1	4.3	16.96	>50
Compound 26	489.66		63.3	1.6	17.9	>50
Compound 27	502.61		60.7	3.9	18.1	>50
Compound 28	460.57		48	2.1	21.16	>50
Compound 29	350.45		64	2	21.98	>50
Compound 30	433.59		54.3	4.5	22.73	>50

Compound	Molecular Weight (g/mol)	Structure	% inhibition of CRK3:CYC6	% inhibition of CDK2:CycA	CRK3:CYC6 IC ₅₀ (μM)	CDK2:CycA IC ₅₀ (μM)
Compound 31	438.57		47.6	4.9	23.03	>50
Compound 32	431.61		47	9.9	27.71	>50
Compound 33	350.49		48	1.9	29.07	>50
Compound 34	391.55		52.6	2.5	29.32	>50
Compound 35	423.55		49.1	8.8	30.15	>50
Compound 36	428.53		48	10.1	41.07	>50
Compound 37	302.42		61.2	8.1	41.22	>50
Compound 38	423.55		56	14.7	>50	>50
Compound 39	473.54		52	1.1	>50	>50
Compound 40	360.45		50.2	23	>50	>50

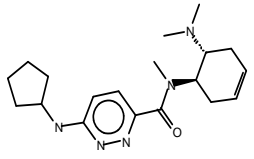
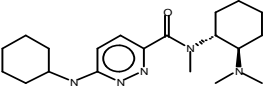
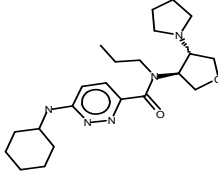
Compound	Molecular Weight (g/mol)	Structure	% inhibition of CRK3:CYC6	% inhibition of CDK2:CycA	CRK3:CYC6 IC ₅₀ (μM)	CDK2:CycA IC ₅₀ (μM)
Compound 41	343.47		50	3.7	>50	>50
Compound 42	359.51		47.6	4.3	>50	>50
Compound 43	401.55		45.3	15.9	>50	>50

Table 4.2 – CRK3:CYC6 and CDK2:CycA primary and secondary screening

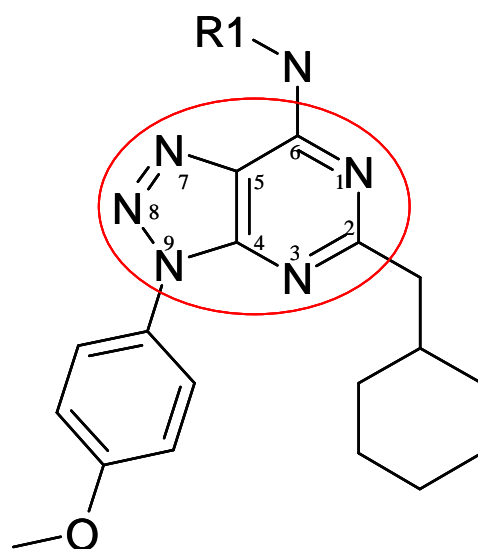
summary. The compound numbers and structures are shown for the 43 hits identified from the HTS and are ranked, top to bottom, in order of their IC₅₀ value towards CRK3:CYC6 (Column 6) . The primary screening data (% inhibition) and secondary screening data (IC₅₀ value) for the 43 hits identified from the HTS are shown for CRK3:CYC6 (Columns 4 and 6, respectively) and CDK2:CycA (columns 5 and 7, respectively). Compounds in red are those that were taken forward for screening against the mammalian kinase counter screening panel (Table 4.6). Those in blue are compounds that were not taken forward for further analysis. Those in black were determined to be false positives and not active towards CRK3:CYC6.

4.9 Structural analysis of the high throughput screen hits.

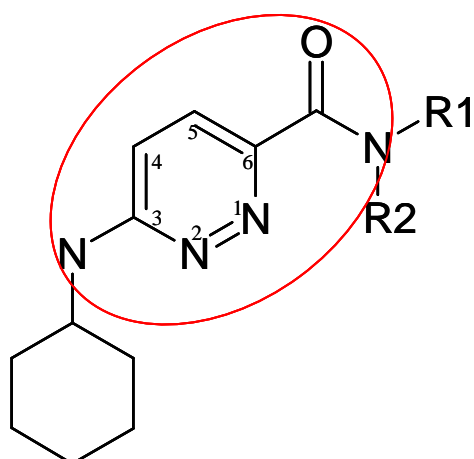
The secondary data confirmed there were 6 false positive hits from the CRK3:CYC6 high throughput screen. This resulted in 37 Cyclacel compounds that targeted CRK3:CYC6. The 18 compounds that had IC₅₀ values ranging from 2.6µM to approximately 10µM were chosen and taken forward for further mammalian kinase counter screening. The chemical structures of these 18 compounds were analysed and two distinct pharmacophores were identified, azapurine and aminopyridazine-3-carboxamide (Figure 4.10). Of the 18 structures, 14 were azapurines and 4 were aminopyridazine-3-carboxamides.

4.10 Structure activity relationship of the azapurines towards *Leishmania* CRK3:CYC6.

In order to determine some further SAR data for the azapurine class of compounds, the effect of modifications of the bulky groups on positions 2 and 9 of the azapurine ring was analysed. This focused on the methoxybenzene ring on the 9 position and the cyclohexylmethyl group on the 2 position (Figure 4.11).



Azapurine core structure



Aminopyridazine-3-carboxamide core structure

Figure 4.10 – Main compound core structures identified from the CRK3:CYC6 high throughput screen. The azapurine (upper structure circled in red) had a variable R1 group, a methoxybenzene ring on the 9 position and a cyclohexylmethyl group on the 2 position. The aminopyridazine-3-carboxamide (lower structure circled in red) had variable R1 and R2 groups and had a cyclohexylmethyl group attached to the nitrogen atom on the 3 position.

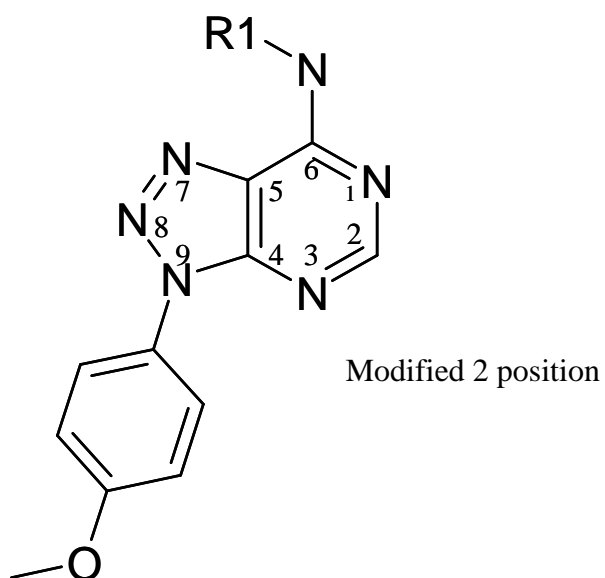
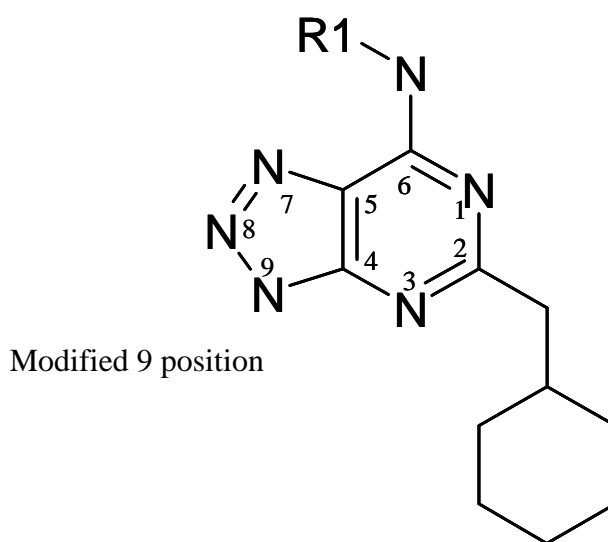


Figure 4.11 – Azapurine core structures minus the methoxybenzene ring (upper structure) and the cyclohexylmethyl groups (lower structure). Homologues of the azapurine structure with the modifications at the 2 and 9 positions shown above were chosen and screened. This was to highlight the importance of these particular groups in the molecules inhibiting CRK3:CYC6 protein kinase activity.

Initially, 4 hits from the *Leishmania* CRK3:CYC6 screen were chosen, compound 3, compound 6, compound 18 and compound 9 (Tables 4.3, 4.4 and 4.5 in red). With regard to the methoxybenzene ring group changes, one homologue of each hit was chosen which had identical R1 and cyclohexylmethyl groups but a modified methoxybenzene group at the 9 position of the azapurine ring (Figure 4.11, upper structure and Table 4.3, compounds in black). Replacement of the methoxybenzene ring at the 9 position resulted in at least a 5-fold loss of activity against *Leishmania* CRK3:CYC6.

This approach was also used to determine if modifications to the cyclohexylmethyl group contributed to any loss of activity. Two homologues of each hit were chosen with identical R1 groups and a methoxybenzene ring on the 9 position, with replacements in the 2 position (Figure 4.11, lower structure and tables 4.4 and 4.5, compounds in black). Deletion of the cyclohexylmethyl group and its replacement by a less bulky group also resulted in at least a 5-fold loss of activity against the target enzyme.

These compounds with modifications were inactive towards *Leishmania* CRK3:CYC6, all returning IC₅₀ values >50µM (Tables 4.3, 4.4 and 4.5). This highlights the importance of the methoxybenzene and cyclohexylmethyl groups at their appropriate positions within the azapurine ring structure for inhibiting *Leishmania* CRK3:CYC6 protein kinase activity.

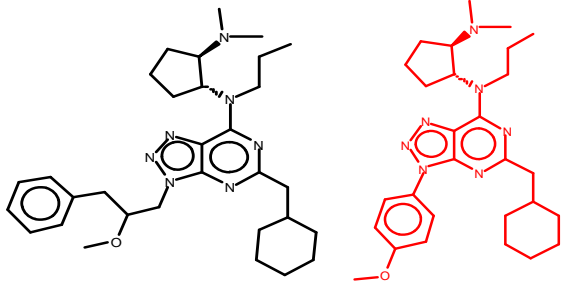
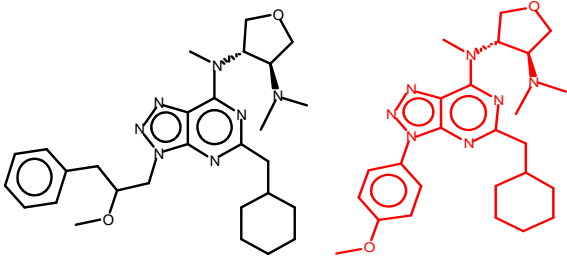
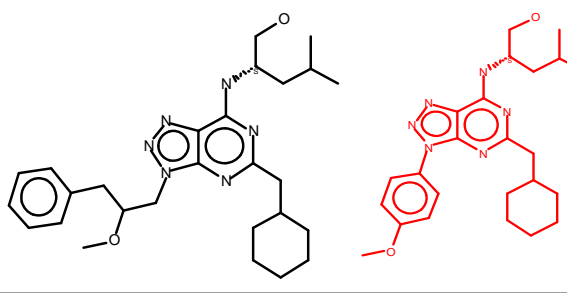
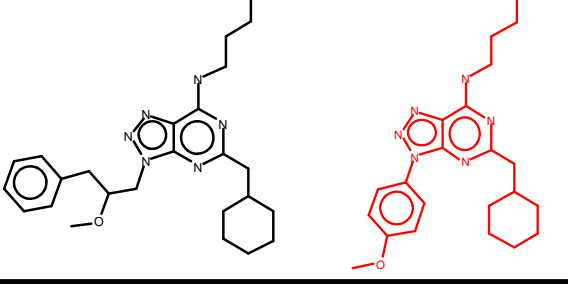
Compound	CRK3:CYC6 IC ₅₀ (μM)	Structures
Compound 44 Compound 3	>50 3.42	
Compound 45 Compound 6	>50 4.38	
Compound 46 Compound 18	>50 10.69	
Compound 47 Compound 9	>50 5.98	

Table 4.3 – Analysis of the azapurine methoxybenzene ring modifications at the 9 position. Four azapurine hits identified from the CRK3:CYC6 HTS were chosen (red). A homologue of each, with the same R1 and cyclohexylmethyl groups but with a modified group in place of the methoxybenzene ring was chosen (black). The IC₅₀ values of the hits and their homologues are shown highlighting the importance of the methoxybenzene ring in inhibiting CRK3:CYC6 protein kinase activity.

Compound	CRK3:CYC6 IC ₅₀ (μM)	Structures
Compound 48	>50	
Compound 49	>50	
Compound 3	3.42	
Compound 50	>50	
Compound 51	>50	
Compound 6	4.38	

Table 4.4 – Analysis of the azapurine cyclohexylmethyl group modifications at the 2 position (1). Two azapurine hits identified from the CRK3:CYC6 HTS were chosen (red). Two homologues of each, with the same R1 and methoxybenzene ring groups but with a modified group in place of the cyclohexylmethyl were chosen (black). The IC₅₀ values of the hits and their homologues are shown highlighting the importance of the cyclohexylmethyl group in inhibiting CRK3:CYC6 protein kinase activity.

Compound	CRK3:CYC6 IC ₅₀ (μM)	Structures
Compound 52	>50	
Compound 53	>50	
Compound 18	10.69	
Compound 54	>50	
Compound 55	>50	
Compound 9	5.98	

Table 4.5 – Analysis of the azapurine cyclohexylmethyl group modifications at the 2 position (2). Two additional azapurine hits identified from the CRK3:CYC6 HTS were chosen (red.) Two homologues of each, with the same R1 and methoxybenzene ring groups but with a modified group in place of the cyclohexylmethyl were chosen (black). The IC₅₀ values of the hits and their homologues are shown again highlighting the importance of the cyclohexylmethyl group in inhibiting CRK3:CYC6 protein kinase activity.

4.11 Mammalian kinase counter screening of the *Leishmania* CRK3:CYC6 hits.

The 18 compounds chosen were taken forward to screen against an expanded protein kinase panel to determine their selectivity. Ten mammalian protein kinases were selected from Cyclacel's in-house protein kinase panel and are shown in Table 4.6. The 18 compounds were screened against the 10 mammalian kinases to determine their IC₅₀ values for each. The 9 most potent compounds are shown ranked in order of their potency towards CRK3:CYC6 (Table 4.7, right hand column in red). Similarly, the remainder of the 18 hits screened are shown, again ranked in order of their potency against CRK3:CYC6 (Table 4.8, right hand column in red). The majority of the 18 compounds are inactive against all 10 kinases generating IC₅₀ values >50μM with the following exceptions. Compound 3 has an IC₅₀ value of 33.12μM against Plk1 while compound 13 and compound 18 have IC₅₀ values of 13.1μM and 9.68μM, respectively against Abl.

Of most interest with regard to the selectivity question is the CDK4:CycD1 data, where it is seen that all but four compounds show a degree of inhibition of CDK4:CycD1. The four compounds that do not show inhibition of the enzyme, compound 2, compound 4 (Table 4.7), compound 11 and compound 15 (Table 4.8) are all aminopyridazine-3-carboxamides. The remaining 14 compounds that do inhibit CDK4:CycD1, with IC₅₀ values <30μM, are all azapurines. This highlights a useful structure activity relationship (SAR) data for the two pharmacophores identified from the *Leishmania* CRK3:CYC6 HTS and will be discussed in more detail later in this chapter.

Kinase	Class	Group	Family
Akt/PKB	Ser/Thr	AGC	AKT
CDK1:CycB	Ser/Thr	CMGC	CDK
CDK4:CycD1	Ser/Thr	CMGC	CDK
CDK7:CycH	Ser/Thr	CMGC	CDK
CDK9:CycT1	Ser/Thr	CMGC	CDK
GSK3	Ser/Thr	CMGC	GSK
PIK1	Ser/Thr	Other	PLK
Aurora A	Ser/Thr	Other	AUR
Abl	TK	TK	Abl
Flt3	RTK	TK	PDGFR

Table 4.6 – Protein kinase counter screening panel. The table shows the 10 protein kinases chosen to counter screen with the CRK3:CYC6 HTS hits. These were chosen to include a number of kinases from the serine/threonine class and some from the tyrosine kinase class.

Kinase complex Compound	CDK2: CYCA	CDK1: CYCB	CDK4: CYCD1	CDK7: CYCH	CDK9: CYCT1	GSK3	Aur A	Plk1	Fit3	Abl	Akt/PKB	CRK3: CYC6
Compound 1	>50	>50	12.49	>50	>50	>50	>50	>50	>50	>50	>50	2.6
Compound 2	>50	>50	>50	>50	>50	>50	>50	>50	>50	>50	>50	2.67
Compound 3	>50	>50	5.61	>50	>50	>50	>50	33.12	>50	>50	>50	3.42
Compound 4	>50	>50	>50	>50	>50	>50	>50	>50	>50	>50	>50	3.62
Compound 5	>50	>50	21.94	>50	>50	>50	>50	>50	>50	>50	>50	4.35
Compound 6	>50	>50	10.27	>50	>50	>50	>50	>50	>50	>50	>50	4.38
Compound 7	>50	>50	9.71	>50	>50	>50	>50	>50	>50	>50	>50	5.27
Compound 8	>50	>50	26.75	>50	>50	>50	>50	>50	>50	>50	>50	5.29
Compound 9	>50	>50	17.27	>50	>50	>50	>50	>50	>50	>50	>50	5.98

Table 4.7 – Protein kinase counter screening panel summary 1. The table shows IC₅₀ values (μM) of the 9 most potent hits against CRK3:CYC6 and the protein kinases in the counter screen panel. Compounds are ranked in order of potency against CRK3:CYC6 (right hand column, red).

Kinase complex Compound	CDK2: CYCA	CDK1: CYCB	CDK4: CYCD1	CDK7: CYCH	CDK9: CYCT1	GSK3	Aur A	PIK1	Flt3	Abl	Akt/PKB	CRK3: CYC6
Compound 10	>50	>50	9.18	>50	>50	>50	>50	>50	>50	>50	>50	6.9
Compound 11	>50	>50	>50	>50	>50	>50	>50	>50	>50	>50	>50	7.14
Compound 12	>50	>50	19.54	>50	>50	>50	>50	>50	>50	>50	>50	7.83
Compound 13	>50	>50	26.86	>50	>50	>50	>50	>50	>50	13.10	>50	8.12
Compound 14	>50	>50	19.83	>50	>50	>50	>50	>50	>50	>50	>50	8.76
Compound 15	>50	>50	>50	>50	>50	>50	>50	>50	>50	>50	>50	8.94
Compound 16	>50	>50	7.31	>50	>50	>50	>50	>50	>50	>50	>50	10.12
Compound 17	>50	>50	6.73	>50	>50	>50	>50	>50	>50	>50	>50	10.26
Compound 18	>50	>50	4.64	>50	>50	>50	>50	>50	>50	9.68	>50	10.69

Table 4.8 – Protein kinase counter screening panel summary 2. The table shows the IC₅₀ values (μM) of the remainder of the 18 most potent hits against CRK3:CYC6 and the kinases in the protein kinase counter screen panel. Compounds are ranked in order of potency against CRK3:CYC6 (right hand column, red).

4.12. Alternative approaches to identify *Leishmania* CRK3:CYC6 inhibitors.

In addition to screening the Cyclacel library, alternative approaches were employed to identify inhibitors of *Leishmania* CRK3:CYC6 protein kinase activity. This involved molecular modelling and an *in silico* screen as well as testing additional compounds on the *Leishmania* CRK3:CYC6 protein kinase complex.

4.12.1 Screening of Naphthostyryl derivatives against *Leishmania* CRK3:CYC6.

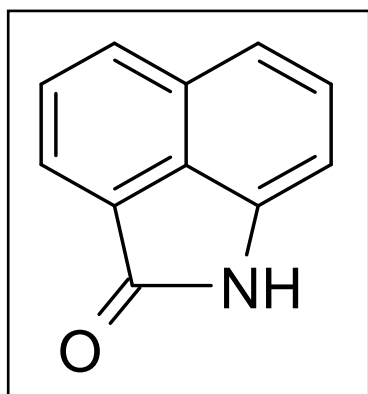
A *L. mexicana* CRK3 homology model based on mammalian CDK2 was generated by Kirk Malone at the Manchester Interdisciplinary Biocentre (MIB). The molecular modelling was carried out using Accelrys Discovery Studio software (www.accelrys.com/products/dstudio/). An *in silico* screen was carried out against the CRK3 homology model using the virtual compound library accompanying the software. Naphthostyryl was the top hit identified, which gave the best docking score against CRK3 and whose binding mode compared favourably to the binding of known inhibitors of CDK2. Subsequently, Naphthostyryl (Figure 4.12, top left structure) and 11 derivatives of the naphthostyryl structure were synthesised and screened against CRK3:CYC6 to determine their potency by IC₅₀ value determination. All 12 compounds tested, however, proved to be inactive against CRK3:CYC6, with IC₅₀ values >50µM (data not shown).

4.12.2 Screening of Indirubin derivatives against *Leishmania* CRK3:CYC6.

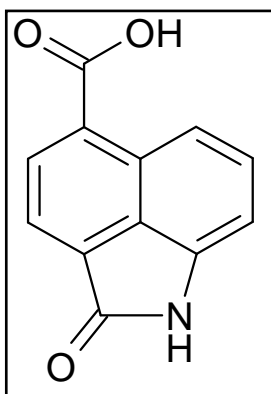
The Indirubin compounds are known inhibitors of CDKs (Hoessel *et al.*, 1999; Polychronopoulos *et al.*, 2004). Based on the structure in figure 4.13 (top left), a number of indirubin derivatives were obtained from Karen Grant at the University of Lancaster and Nick Westwood at the University of St. Andrews (Figure 4.13). Four of the compounds, TW3, TW21, TW23 and TW27 have been screened against transgenic CRK3 to determine their IC₅₀ values but had not been tested against promastigote *Leishmania* or macrophages (Table 4.9). Similarly, compounds whose activity is described as ND (not determined)

were not tested against *Leishmania* infected macrophages. The remainder of the compounds were tested against promastigote *Leishmania* and amastigote *Leishmania* in a macrophage infection at a single concentration of 10 μ M by Karen Grant. A brief description of the effect of each compound on the cell cycle of promastigote *Leishmania* and the activity against amastigotes in an infection assay (clearing amastigotes from macrophages and reducing the infection) is included in Table 4.9, columns 6 and 7, respectively.

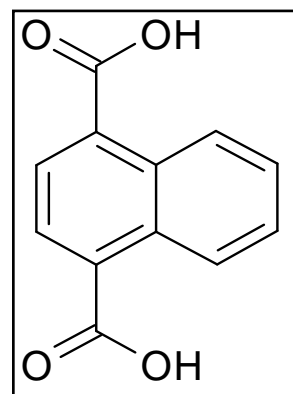
The indirubin derivatives were screened at 10 μ M against CRK3:CYC6 and human CDK2:CycA. IC₅₀ determinations for CRK3:CYC6 were performed and selected compounds were taken forward for screening against human CDK2:CycA and CDK1:CycB. Of the 55 Indirubins screened against CRK3:CYC6, 10 had IC₅₀ values <1 μ M, only one of which, DT-IND-83 showed good selectivity over the two human CDKs (Table 4.9). Of those others tested, a further three showed selectivity towards CRK3:CYC6 (Table 4.9, red asterisk) and two towards mammalian CDK2:CycA over CRK3:CYC6 (Table 4.9, blue asterisk).



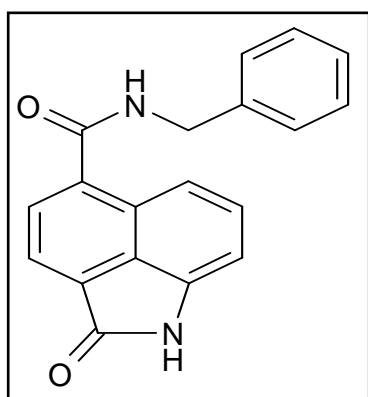
Naphthostyryl



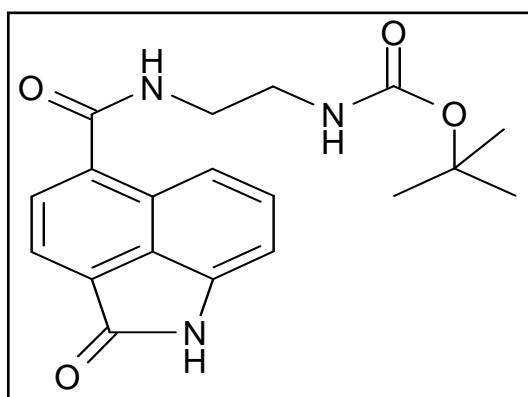
KM15



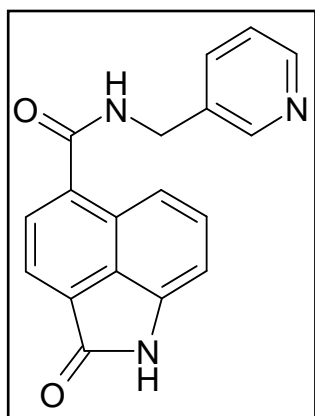
CAS 605-70-9



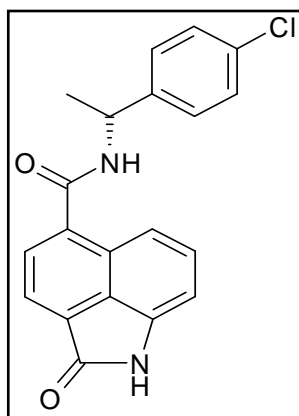
KM51



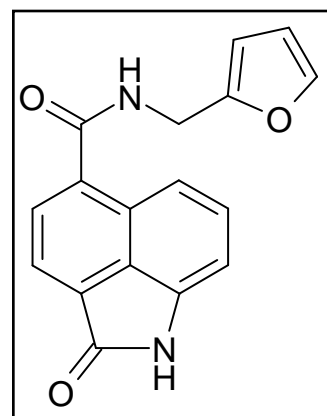
KM28



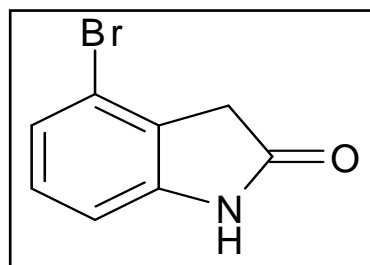
KM33



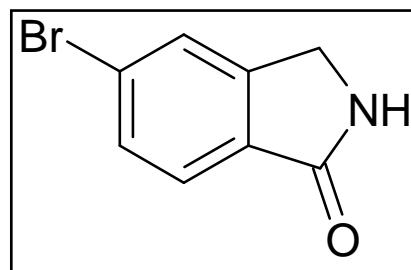
KM34_2



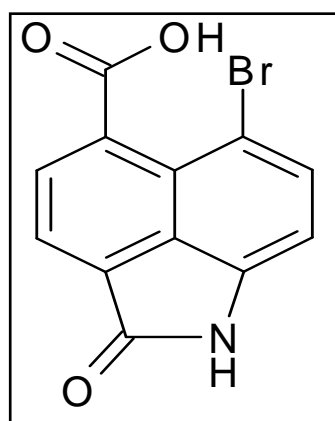
KM50



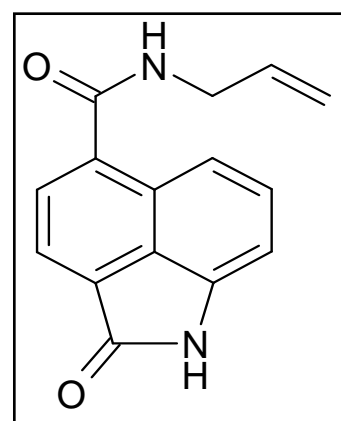
KM6



KM37

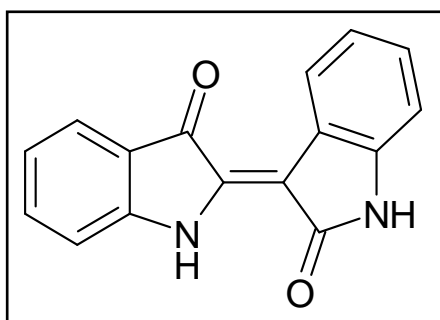


KM40

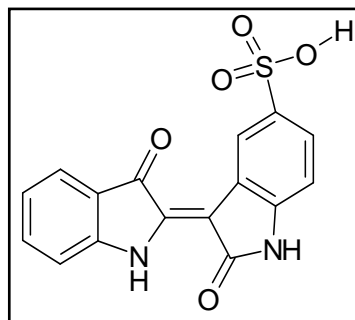


KM53

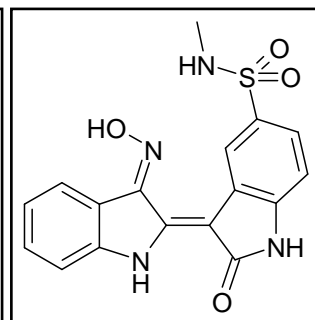
Figure 4.12 – The chemical structure of Naphthostyryl and derivatives. The top left structure (page 141), naphthostyryl, identified through an *in silico* screen as a potential compound to target CRK3:CYC6 was used as a scaffold to generate 11 derivatives which were screened against *Leishmania* CRK3:CYC6.



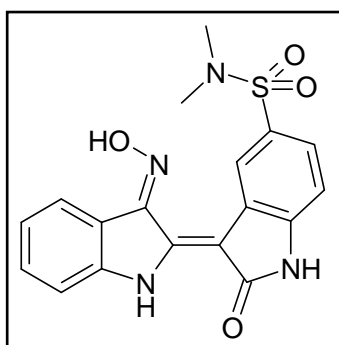
Indirubin



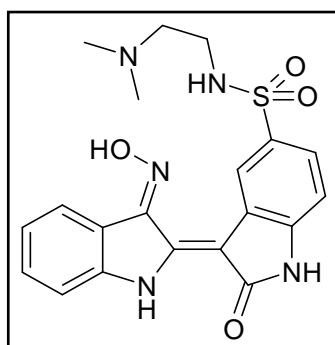
TW3



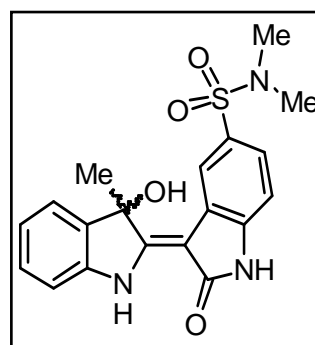
TW21



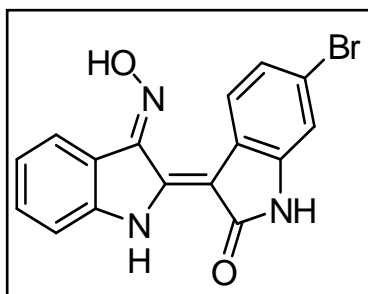
TW23



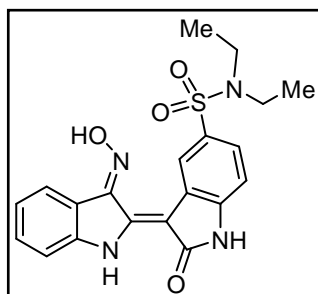
TW27



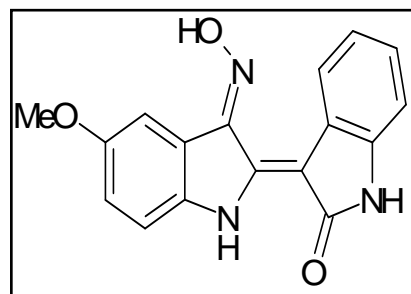
DT-IND-73



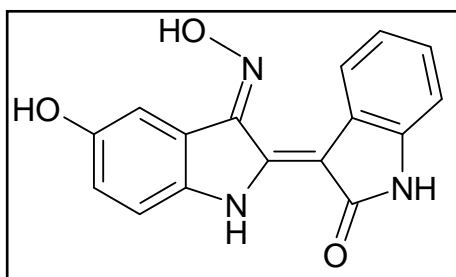
DT-IND-83



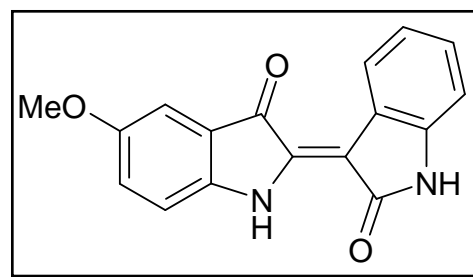
DT-IND-112-3



DT-IND-135



DT-IND-136



DT-IND-119

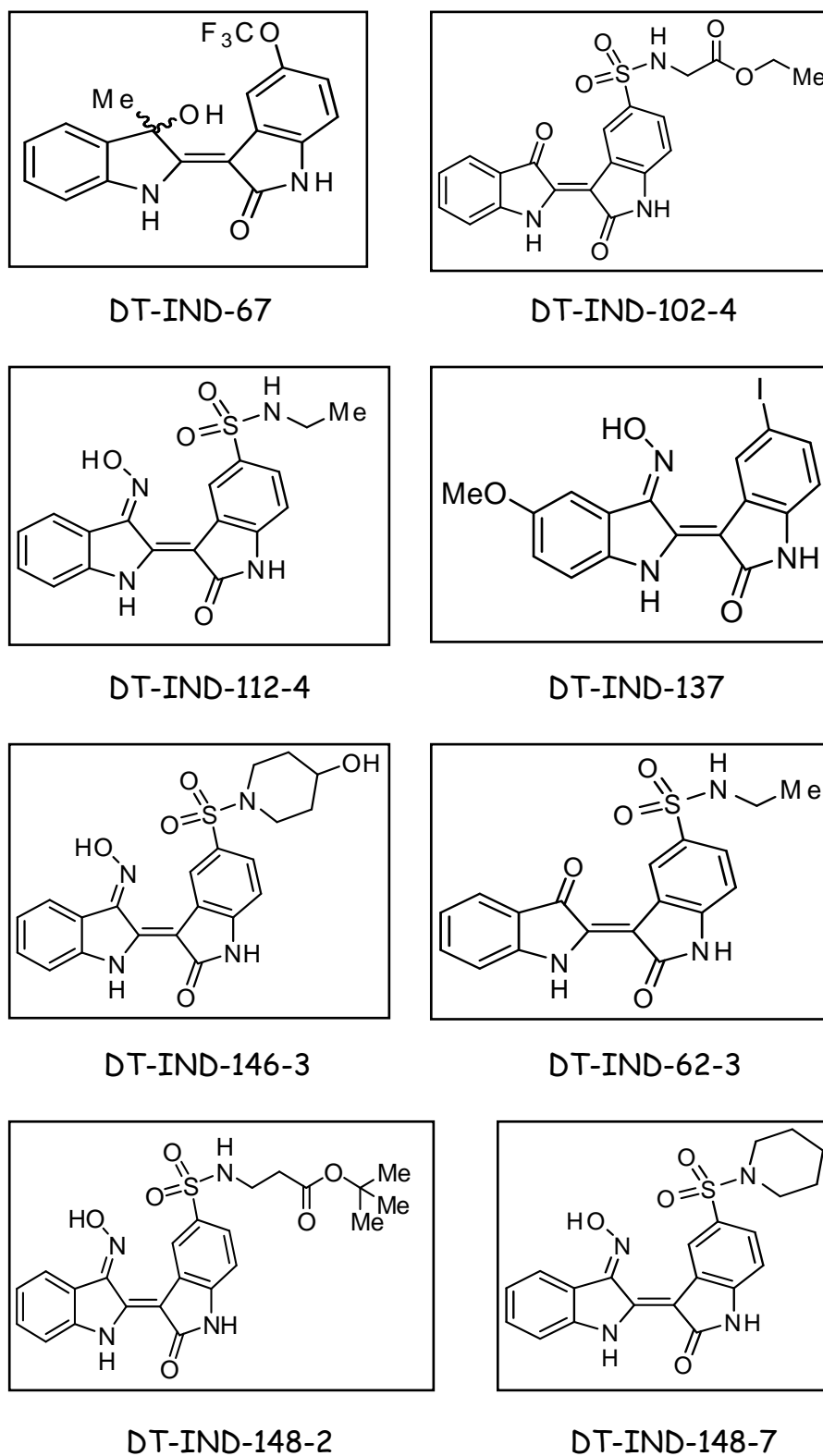


Figure 4.13 – The chemical structure of Indirubin and derivatives. The top left compound (page 143), Indirubin, a known inhibitor of GSK3 and CDKs, was used as a scaffold to generate several derivatives, which were screened against CRK3:CYC6.

Compound ID	Transgenic CRK3 IC ₅₀	CRK3:Cyc6 IC ₅₀	CDK2:CycA IC ₅₀	CDK1:CycB IC ₅₀	Promastigotes	Amastigotes
TW3	49nM	174nM	110nM	713nM		
TW21	440nM	32nM	26nM	116nM		
TW23	6nM	979nM	193nM	422nM		
TW27	450nM	182nM	87nM	1.1µM		
DT-IND-73		146nM	479nM	763nM	Growth arrest	Inactive
DT-IND-83	*	130nM	3µM	21.8µM	Growth arrest	Highly Active
DT-IND-112-3		2.3µM	908nM	3.6µM	Growth arrest	Active
DT-IND-135		2.0µM	5.6µM	>50µM	Growth arrest	ND
DT-IND-136		85nM	252nM	545nM	Growth arrest	Active
DT-IND-119	*	7.2µM	41.3µM	>50µM	Growth inhibition	Active
DT-IND-67	*	8.1µM	>45µM	>50µM	Growth inhibition	ND
DT-IND-102-4		987nM	551nM	5.4µM	Growth inhibition	ND
DT-IND-112-4		1.9µM	900nM	2.8µM	Growth inhibition	Inactive
DT-IND-137		700nM	198nM	2.1µM	Growth inhibition	ND
DT-IND-146-3	*	6.1µM	124nM	558nM	Growth inhibition	ND
DT-IND-62-3	*	>50µM	3.3µM	>50µM	Inactive	Inactive
DT-IND-148-2		735nM	466nM	1.9µM	Growth inhibition	ND
DT-IND-148-7	*	1.7µM	8.1µM	38.7µM	Growth inhibition	ND

Table 4.9 – Indirubins screened against *Leishmania CRK3:CYC6*, human CDK2:CycA and human CDK1:CycB.

IC₅₀ values (µM) for the 18 compounds screened against the three kinase complexes are shown. A description of the compound activity towards promastigote *L. mexicana* and *Leishmania* infected macrophages is included. Those highlighted with a red asterisk show initial selectivity towards CRK3:CYC6 and those with a blue asterisk show initial selectivity towards CDK2:CycA over CRK3:CYC6.

4.13 Chapter discussion

The optimum fluorescent peptide substrate for *Leishmania* CRK3:CYC6 was identified from a plate containing 61 potential serine/threonine kinase substrates identified from the literature. Of the 61 peptide substrates on the plate, 6 showed a specific signal (Δ mP) of >100 mP (Figures 4.3 and 4.4). The greatest Δ mP values were for a generic peptide sequence (GGGRSPGRRRRK), a histone H1 derived peptide (GGPATPKKAKKL), a short histone H1 derived peptide (amino acids 9-18) (PKTPKKAKKL), DYRKtide (RRRFRPASPLRGPPK), a CDK7 derived peptide (FLAKSFGSPNRAYKK) and recombinant histone H1 protein. Interestingly, the recombinant histone H1 as used in the radiometric assay is not the optimum substrate for *Leishmania* CRK3:CYC6 in the IMAPTM assay, producing a Δ mP approximately one third of the generic peptide i.e. 100mP versus 300mP (Figure 4.4). This is because fluorescence polarization works best with peptides rather than proteins in an IMAPTM format. Sequence alignment and analysis showed that the five peptide substrates identified exhibited a consensus sequence pattern: x S/T P x R/K (Figure 4.5). This consensus sequence pattern follows the minimal recognition motif identified for mammalian CDKs: x_{-1} (S/T)₀ P₊₁ x_{+2} (K/R)₊₃ (Stevenson-Lindert *et al.*, 2003). The generic peptide is a consensus phosphorylation site derived from several proteins (Srinivasan *et al.*, 1995) and was chosen as the optimum substrate and used in all IMAPTM assays.

In order to establish the quantity of CRK3:CYC6 needed per assay point for the HTS, a two-fold enzyme titration was carried out (Figure 4.6). A 1:250 dilution of the complex equating to 6ng of protein was the top concentration assayed and was diluted two-fold in a 10-point dilution curve. This highlighted that a 1:1200 dilution equating to 1.25ng of complex could be used per assay point. Using this quantity produced a mP signal of approximately 280mP and a Δ mP of 200mP using significantly less *Leishmania* CRK3:CYC6 than the radiometric assay. The radiometric assay required 7.5ng of protein

complex per assay point (Figure 3.13), whereas 1.25ng was used in the HTS assay (Figure 4.6), highlighting that the IMAPTM HTS format miniaturises the assay by requiring six times less *Leishmania* CRK3:CYC6 protein kinase complex per assay point.

HTS assay development was carried out by determining the K_m for ATP using the IMAPTM assay format (Figure 4.7) and comparing it with that determined using the radiometric assay platform. A two-fold dilution series of ATP was set up ranging from 1mM to 2 μ M ATP. The K_m determined was 154 μ M \pm 13 μ M approximately two-fold higher than determined in the radiometric assay (Figure 3.15, upper graph). This is possibly an artefact of the IMAPTM assay due to the tri-valent metal containing nanoparticles in the stop solution also binding to the phosphate groups of ATP at the higher ATP concentrations. This would possibly have the effect of shifting the curve to the right resulting in a slightly higher K_m for ATP than expected. It could also be due to variability between assays.

Further assay development was carried out to determine the IC_{50} values for staurosporine and olomoucine against the *Leishmania* CRK3:CYC6 protein kinase complex using the IMAPTM format. The IC_{50} value for staurosporine was 20nM (Figure 4.8, upper graph) in comparison with 37nM in the radiometric assay (Figure 3.16, upper graph). The values are within two-fold of one another and are therefore in close agreement. The IC_{50} determined for olomoucine was >10 μ M (Figure 4.8, lower graph), in comparison with 51 μ M in the radiometric assay (Figure 3.16, lower graph), again demonstrating it is not a potent inhibitor of CRK3:CYC6. The IMAPTM assay with olomoucine was carried out using a lower top concentration of inhibitor than in the radiometric assay, which explains the imprecise >10 μ M IC_{50} result. These results suggest the IMAPTM assay is performing similarly to the radiometric platform, and is suitable for continuing with compound screening.

The preliminary screen on 193 compounds was repeated using the IMAPTM format (data not shown). This was to confirm the developed assay was functional and comparable with the radiometric assay. The 193 compounds were screened at 10 μ M to establish if the hits identified in the radiometric assay, were also identified in the HTS assay. The 34 hits from the radiometric assay were identified in the HTS format showing the assay was functional. Interestingly, the five false positives picked up in the radiometric assay were not picked up in the HTS format showing the IMAPTM assay is perhaps more stringent.

In order to identify inhibitors of *Leishmania* CRK3:CYC6 a high throughput screen (HTS) of the Cyclacel compound library (Table 4.1) was carried out at Cyclacel using the IMAPTM fluorescent polarization assay. The IMAPTM HTS assays were carried out as described in sections 2.6.2 and 4.2.1. The primary screen carried out at 10 μ M yielded 43 hits that had approximately 50% or greater inhibition of *Leishmania* CRK3:CYC6 protein kinase activity (Table 4.2, column 4). The compound identification numbers (Table 4.2, column 1), molecular weights (Table 4.2, column 2) and structures (Table 4.2, column 3) for the hits are also included. Initial analysis of the compound hit rate (43/25,000) showed that 0.17% of the compounds in the Cyclacel library inhibited *Leishmania* CRK3:CYC6 protein kinase activity. This hit rate is in accordance with the two previous HTS carried out at Cyclacel with this compound library. The mammalian CDK7:CycH hit rate was 0.32% and mammalian Polo Like Kinase 1 (Plk1) was 0.7%. Subsequent screening of the hits against Plk1 showed a 40% rate of attrition, indicating the real hit rate was approximately 0.4%. However, both these HTS were performed using the ALPHA-screenTM format rather than IMAPTM.

The IMAPTM format was also chosen as the platform for carrying out a human CDK2:CycA counter screen. Molecular Devices had previously validated an IMAPTM peptide substrate for CDK2:CycA which was the same fluorescent peptide (generic peptide sequence, GGGRSPGRRRRK) used for *Leishmania* CRK3:CYC6 in these studies. In

preparation for the counter screen, assay development was carried out to establish the quantity of enzyme required for the assay. The CDK2:CycA enzyme used was expressed in baculovirus and purified at Cyclacel. A 1:5 dilution of the complex equating to 0.4µg of protein was diluted two-fold in a 10-point dilution curve (Figure 4.9). This highlighted that a 1:60 dilution equating to 33ng of complex could be used per assay point, approximately four times as much as *Leishmania* CRK3:CYC6. Using this quantity produced a mP signal of approximately 280mP with a ΔmP of 200mP. The CDK2:CycA HTS assay was developed and validated with this quantity of enzyme, and was functional for carrying out the counter screen.

The Cyclacel compound library was counter screened against human CDK2:CycA using the IMAPTM assay at a single compound concentration of 10µM. The counter screen was carried out to filter against the 43 compounds hits that targeted the *Leishmania* CRK3:CYC6 protein kinase complex, thereby identifying any that targeted a human kinase. None of the 43 compound hits from Table 4.2 targeted mammalian CDK2:CycA (Table 4.2, column 5) and as a result, all 43 compounds were taken forward for secondary screening against CRK3:CYC6 to determine their potency. Their IC₅₀ values were determined using the previously developed ³²P radiometric assay for *Leishmania* CRK3:CYC6 and are shown in Table 4.2, column 6 (ranked in order of potency towards *Leishmania* CRK3:CYC6 protein kinase activity). The most potent compound was compound 1 with an IC₅₀ value of 2.6µM towards the *Leishmania* CRK3:CYC6 protein kinase complex. This is not greatly potent towards the complex as it is a low µM inhibitor and not a nM inhibitor as desired. However, correspondence with Cyclacel suggested that identifying hits with IC₅₀ values lower than 1µM would be unlikely with this library, and identifying those with low micromolar potency, at best, was indeed a successful screen. These compounds can be used as a starting point for chemistry to improve potencies towards *Leishmania* CRK3:CYC6. The library is only 25,000 compounds strong and in

order to get nM potency, it has been proposed you need to screen at least 24,000,000 distinct compounds (Wintner and Moallemi, 2000). Alternatively, it is possible to screen a more focussed kinase selective library to attempt to achieve nM potency, a method adopted by the Drug Discovery Initiative at the University of Dundee (Brenk *et al.*, 2007) although such potent compounds may also prove to be pan-kinase inhibitors. The screen highlighted 6 compounds that were false positive hits and did not target *Leishmania* CRK3:CYC6 with a >50% IC₅₀ value (Table 4.2, compounds in black). Therefore, 6/43 giving a 14% rate of attrition for the HTS assay, better than that described for the Plk1 HTS assay above, where the rate of attrition was 40%, suggesting that IMAPTM may be a more stringent assay platform than ALPHA-screenTM. In order to confirm the 43 hits did not target mammalian CDK2:CycA, secondary screening against the kinase complex was carried out. All returned IC₅₀ values of >50µM (Table 4.2, column 7) confirming the primary screen data (Table 4.2, column 5) that human CDK2:CycA was not a target for any of the 43 hits. Taking into account the 6 false positive hits, there were 37 *Leishmania* CRK3:CYC6 hits in total. Those with an IC₅₀ value <10µM (18 in total) were taken forward for mammalian kinase counter screening (Table 4.2, compounds in red), the remaining 19 were not analysed further (Table 4.2, compounds in blue).

The structures of the 18 hits taken forward for mammalian kinase counter screening were analysed in detail and this identified two main pharmacophores, azapurine (Figure 4.10, upper structure) and aminopyridazine-3-carboxamide (Figure 4.10, lower structure), with the majority of the hits (14/18) being azapurines. The activity of the azapurine compounds towards *Leishmania* CRK3:CYC6 is in accordance with the literature where azapurines have recently been identified as new inhibitors of cyclin-dependent kinases (Havlicek *et al.*, 2005).

As the majority of the hits were azapurine compounds, these were studied further to develop structure activity relationship (SAR) data. This study focussed on examining modifications of the methoxybenzene ring and the cyclohexylmethyl group at the 9 and 2 positions, respectively of the azapurine structure (Figure 4.11). Initially four hits from the *Leishmania* CRK3:CYC6 HTS were chosen, compound 3, compound 6, compound 18 and compound 9 (Tables 4.3, 4.4 and 4.5 in red). Homologues of each hit were chosen which had the same R1 group and cyclohexylmethyl group at the 2 position but a modified 9 position in order to study the importance of the methoxybenzene ring (Figure 4.11, upper structure and Table 4.3). The homologues when screened against *Leishmania* CRK3:CYC6 all returned IC₅₀ values >50µM showing they had lost their activity towards the complex and highlighting the importance of the existing group at the 9 position (Table 4.3).

In addition, a similar study was carried out looking at modifying the 2 position whilst keeping the R1 group and the methoxybenzene ring at the 9 position constant to study the importance of the cyclohexylmethyl group (Figure 4.11, lower structure and Tables 4.4 and 4.5). When screened against CRK3:CYC6 these homologues also returned IC₅₀ values >50µM (Tables 4.4 and 4.5) demonstrating they had lost their activity towards the enzyme complex and thus highlighting the importance of the cyclohexylmethyl group at the 2 position.

These studies indicate the importance of the two hydrophobic groups in the interaction with and inhibition of *Leishmania* CRK3:CYC6 by the azapurine compounds. This highlights areas of the azapurine compounds where the structure possibly can and cannot be modified by iterative chemistry when developing a compound hit into a lead. Interestingly it seems the azapurines may tolerate a number of substitutions in the R1 position without losing their ability to inhibit *Leishmania* CRK3:CYC6. The groups in this position are generally large and it would be interesting to probe this position with some

smaller group substitutions in order to develop more potent *Leishmania* CRK3:CYC6 compounds.

In addition, many of the hits in Table 4.2 are of high molecular weight and this may also limit the number of modifications that can be made to develop the hits into leads. When considering Lipinski's rule of 5 for intestinal drug absorption, one of the criteria (for an orally administered compound) is that poor absorption is more likely when the molecular weight of a compound exceeds 500. Additionally, compounds should ideally have no more than 5 hydrogen bond donors, nor more than 10 hydrogen bond acceptors and a logP value under 5. However, analysis of drugs and their parent leads suggests there is a clear distinction. Drugs tend to have a higher molecular weight and logP values where the development from hit-to-lead to drug is accompanied by the addition of lipophilic moieties and therefore increases in molecular weight. Therefore, it has been proposed that screening compounds should be lead-like with molecular weights <350 and logP <3 (Teague *et al.*, 1999). Therefore, the hits from Table 4.2 with high molecular weight would have to be subject to subtle modifications in order to improve their potency whilst ideally not exceeding a molecular weight of 500 and being able to meet the additional criteria above.

The 18 most potent *Leishmania* CRK3:CYC6 HTS hits were taken forward and screened against an expanded kinase panel. The kinases were chosen from Cyclacel's in-house kinase panel. The 10 kinases chosen (Table 4.6) all had previously developed ³²P radiometric assays in place suitable for compound screening. The kinases were chosen largely to represent the serine/threonine class and family of cyclin-dependent kinases as *L. mexicana* CRK3 is a serine/threonine cyclin-dependent kinase. In addition, a tyrosine kinase (Abl) and a receptor tyrosine kinase (Flt3) were chosen to represent the other classes of kinases in the Cyclacel database. The 18 compounds were secondary screened against the 10 kinases to determine their potency by IC₅₀ determination (Tables 4.7 and

4.8). The IC₅₀ values of the 9 most potent hits against CRK3:CYC6 for the kinases in the mammalian kinase counter screen panel are shown in Table 4.7. The remainder of the 18 hits IC₅₀ values are shown in table 4.8. The majority of the compounds did not show activity towards any of the mammalian kinases with IC₅₀ values >50μM, showing selectivity towards *Leishmania* CRK3:CYC6. However, this is with the exception of mammalian CDK4:CycD1 where all of the azapurines, but not the aminopyridazine-3-carboxamides target the kinase with IC₅₀ values <30μM. This highlights structure activity relationship (SAR) data for the two pharmacophores which has been studied in collaboration with Malcolm Walkinshaw and Matt Nowicki at the University of Edinburgh. The binding mode of kinase inhibitors has been shown to be via a hydrogen bond donor-acceptor-donor (D-A-D) motif that interacts with the backbone residues of CDK2, Leu83 and Glu81, which is common to most, if not all, CDK2 inhibitors (Figure 4.14, upper structure). Interestingly, the azapurine compounds have no obvious H-bond donating atom and therefore binding to the ATP pocket must be driven by hydrophobic interactions and accepting H-bonding atoms from the protein. The azapurine compounds were modelled into the CRK3 ATP site by keeping the hydrophobic interactions of the cyclohexylmethyl moiety (an area of conservation between CDK2 and CRK3) and placing N⁷ and N⁸ of the triazole moiety within the limits of H-bond accepting to the backbone of Val102 (Leu83 in CDK2). The result showed that the O atom of the methoxybenzene group is situated in a position whereby it is able to H-bond with Tyr101. A third H-bonding interaction is evident between an aromatic H-atom and the backbone carbonyl of Val102. Three H-bonding interactions are evident between the protein and the azapurine inhibitors, but the motif is changed to A-D-A which is not possible in CDK2 as Tyr101 is replaced by Phe82 and is therefore unable to donate an H-bonding atom (Figure 4.14, lower structure). In CDK4, the tyrosine residue is replaced by histidine which would still be able to facilitate the A-D-A binding motif; therefore, the model also explains why the azapurine compounds exhibit a lesser selectivity for CRK3 over CDK4.

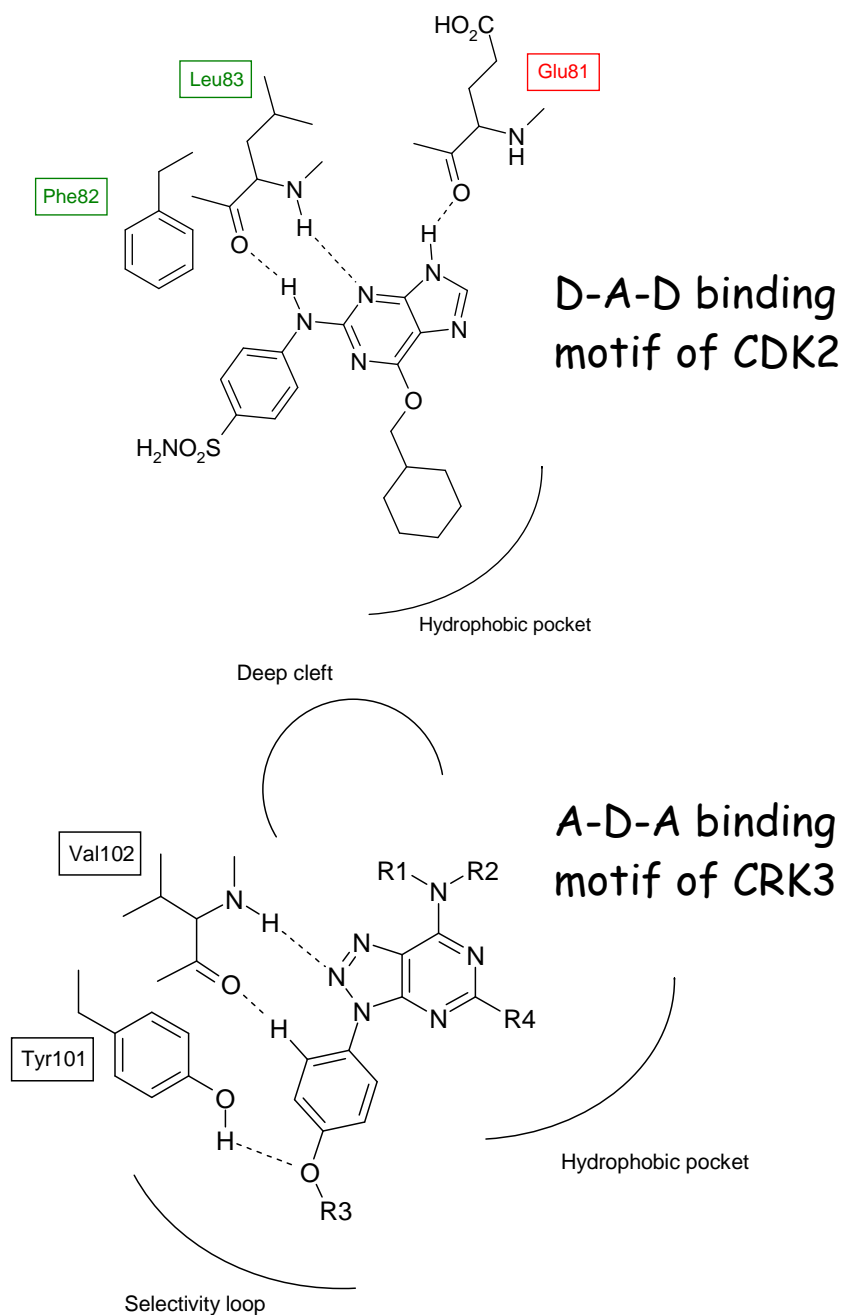


Figure 4.14 – Binding motifs of CDK2 and CRK3 with their respective inhibitors. The binding motif of CDK2 and the inhibitor NU6102 is via a hydrogen bonding D-A-D motif with CDK2 backbone residues (upper structure). The binding motif of CRK3 and an azapurine compound is via a hydrogen bonding A-D-A motif with CRK3 backbone residues (lower structure). Provided by Matt Nowicki, University of Edinburgh.

In collaboration with Nick Turner and Kirk Malone at the University of Manchester a number of additional compounds were generated and screened against the *Leishmania* CRK3:CYC6 protein kinase complex. Accelrys Discovery Studio software was used to carry out molecular modelling using a homology model of *L. mexicana* CRK3 based on human CDK2. The homology model was used as a base for an *in silico* screen using the Accelrys compound database accompanying the software. Naphthostyryl (Figure 4.12, top left structure) was the top hit, which gave the best docking score and whose binding mode made compared favourably to the binding of known inhibitors of CDK2 (Liu *et al.*, 2003). Attempts were made to achieve selectivity by comparing the CRK3 model to the crystal structure of human CDK2 and looking for differences. It appeared that there was 'more space' in the active site of CRK3 than CDK2. Based on this, the Naphthostyryl structure and 11 derivatives (Figure 4.12) were synthesised and all 12 were screened against the *Leishmania* CRK3:CYC6 protein kinase complex. However, none of the compounds inhibited CRK3:CYC6, all returning IC₅₀ values >50µM. This could be a result of limitations in the model itself and/or within the docking programme or due to the limited virtual library. Although unsuccessful, it is worth noting that the *in silico* screen was used to generate ideas using the Accelrys software with the compound database supplied, and that subsequent virtual libraries could be screened in the future.

In collaboration with Karen Grant at the University of Lancaster and Nicholas Westwood at the University of St. Andrews, 55 indirubin compounds were synthesised and screened against the *Leishmania* CRK3:CYC6 protein kinase complex. Indirubin (Figure 4.13, top left structure) is the active ingredient in the traditional Chinese medicine Dang Gui Long Hui Wan (Tang and Eisenbrand, 1992) which has been shown to be effective in the treatment of chronic myeloid leukaemia (Xiao *et al.*, 2002). In addition, indirubins may have a potential application against neurodegenerative diseases such as Alzheimer's disease as they are known cyclin-dependent kinase and GSK-3 inhibitors (Hoessel *et al.*,

1999; Polychronopoulos *et al.*, 2004). The 55 derivatives of Indirubin were grouped according to their activity against CRK3his from transgenic promastigote *L. mexicana* or by their relationship to the other indirubins. Initially 8 compounds which were previously screened against CRK3his from transgenic promastigote *L. mexicana* by Karen Grant were screened against the *Leishmania* CRK3:CYC6 protein kinase complex. This was to establish whether there was a correlation in IC₅₀ values between the native or recombinant CRK3 protein kinases. IC₅₀ values for 4 of the compounds (named TW in Table 4.9) show that there is a discrepancy between the two CRK3 protein kinases. This was also the case for the other 4 TW compounds (data not shown). This may be a result of two factors: the first is, the assays using transgenic CRK3his were carried out at an ATP concentration of 4μM whereas the recombinant *Leishmania* CRK3:CYC6 assays were carried out at 100μM, the ATP concentration at which the assay was validated. Depending on the enzyme's K_m for ATP, a higher ATP concentration can result in a higher IC₅₀ value due to there being more ATP for the compound to compete with. This is not the case, however, for compounds TW21 and TW27 in table 7 where they have a lower IC₅₀ when compared to the transgenic CRK3his. The second factor that may account for the IC₅₀ discrepancies is the cyclin partner of CRK3. The *in vivo* partner of CRK3 has been shown to be CYCA (F.C. Gomes and J.C. Mottram, unpublished). In addition, the homologue of CYCA in *L. donovani* has been identified, LdCYC1, (Banerjee *et al.*, 2003) and shown to form a complex with *L. donovani* CRK3 (Banerjee *et al.*, 2006). However, despite CYC6his activating CRK3his *in vitro*, it remains to be shown if it is a partner of CRK3 *in vivo*. A variety of cyclin partners which activate CRK3 *in vivo* could account for difference in transgenic CRK3 activity when compared to the CRK3his activity as a result of CYC6his binding. This in turn may affect the IC₅₀ values of the indirubin compounds tested. For example, it is known that the same compound can inhibit CDK2 with vastly different potencies depending on what cyclin partner (CycA or CycE) the enzyme is bound to (Cyclacel data, unpublished).

The 55 compounds were secondary screened against *Leishmania* CRK3:CYC6 to determine their IC₅₀ values. This resulted in 10 with IC₅₀ values <1μM and 3 with IC₅₀ values between 1μM and 2μM. Eighteen compounds were analysed further by secondary screening against mammalian CDK1:CycB and mammalian CDK2:CycA to determine any initial selectivity towards *Leishmania* CRK3:CYC6 (Table 4.9). Of those tested, 4 showed selectivity towards *Leishmania* CRK3:CYC6 (Table 4.9, red asterisk) and 2 towards mammalian CDK2:CycA (Table 4.9, blue asterisk). None of the compounds tested were selective towards mammalian CDK1:CycB over the other two enzymes. One of the most potent compounds against *Leishmania* CRK3:CYC6 (IC₅₀ 130nM) was DT-IND-83 which showed significant selectivity over CDKs 1 and 2 and also activity towards promastigote and amastigote *Leishmania* (Table 4.9, columns 6 and 7, respectively). As indirubins are known GSK-3 inhibitors, DT-IND-83 was screened against mammalian GSK-3 and returned an IC₅₀ value of 15nM (data not shown) highlighting that it is more potent against this enzyme over *Leishmania* CRK3:CYC6. Despite the known activity of indirubins against mammalian GSK-3, it would be interesting to establish their activity against parasite GSK-3 whose presence has been identified as a result of Tri-tryp kinome analysis (Parsons *et al.*, 2005).

Although the indirubin compounds may not be exclusively selective towards *Leishmania* CRK3:CYC6, they are, however, potent and may be an avenue to explore in developing leads against the *Leishmania* CRK3:CYC6 protein kinase complex. This is directly opposite to what was observed with the azapurine and aminopyridazin-3-carboxamide hits from the HTS where selectivity towards *Leishmania* CRK3:CYC6 is achieved, but the potency is not. Therefore, the hits require an iterative medicinal chemistry input in order to turn them into potent leads suitable for developing into drug candidates.

Chapter 5

***Leishmania* biology 2: The *Leishmania* CRK3:CYC6 protein kinase complex and *in vitro* compound analysis.**

5.1 Chapter introduction and objectives.

The IMAPTM HTS assay developed in chapter 4 was used to carry out a HTS against the *Leishmania* CRK3:CYC6 protein kinase complex. The two pharmacophores identified, azapurine and aminopyridazine-3-carboxamide, showed inhibition of and selectivity towards *Leishmania* CRK3:CYC6 protein kinase activity. Although the hits showed activity towards the complex *in vitro*, it is vital to test whether they show biological activity towards *Leishmania* and ultimately against the parasite *in vivo*. The *in vitro* model may not be mirrored *in vivo*. The focus of this chapter will be to report on testing the HTS hits against *Leishmania* promastigotes and in macrophage infection assays. In addition, work towards attempting to elucidate whether CYC6 is an *in vivo* partner of CRK3 will be discussed.

When targeting CRK3 in the promastigote life cycle stage of *Leishmania*, the compounds are required to cross the cell membrane and nuclear membrane to inhibit the enzyme. Therefore, the compounds need to be sufficiently “drug like” in order to cross the membranes required to get to the target enzyme. The situation is further complicated when targeting CRK3 in the amastigote life cycle stage of *Leishmania*. The compounds must first cross the macrophage cell membrane, followed by the parasitophorous vacuolar membrane, the amastigote cell membrane itself and the nuclear membrane (Figure 5.1). When considering Lipinski’s rule of 5 to evaluate the “drug like” criteria of a compound, compounds must possess certain characteristics in order to be likely candidates for orally active drugs in humans. Compounds being sufficiently lipophilic is vital so they can cross cellular membranes to get to their target (Lipinski *et al.*, 2001).

There are significant differences between promastigote and amastigote *Leishmania* in biochemistry and sensitivity to standard and experimental drugs (Croft *et al.*, 2006a). One example is with the first line drug Sodium stibogluconate (Pentostam, SSG), a pentavalent antimonial used to treat the visceral form of leishmaniasis. This was shown to have activity towards *Leishmania* amastigotes but not towards promastigote *Leishmania* (Neal and Croft, 1984). Therefore, it is possible to target the amastigote life cycle stage despite a number of membranes being required to be crossed by a compound.

5.2 Analysis of the biological activity of the Cyclacel library high throughput screen hits against cultured *L. major* parasites:

5.2.1 Against cultured *L. major* promastigote parasites.

The 10 compounds showing the greatest activity towards *Leishmania* CRK3:CYC6 protein kinase activity (Table 4.2, column 6) were tested against promastigote *L. major* cells *in vitro*. This was to analyse the biological activity of the compounds that were shown to be active against the *Leishmania* CRK3:CYC6 protein kinase complex (carried out in collaboration with Elaine Brown). A six-fold dilution series of each compound, with a top screening concentration of 10 μ M, with DMSO included as a control was set up and an Alamar blue absorption assay carried out as described in section 2.3.6. This highlighted one compound, compound 7, which had activity towards promastigote *L. major* with an IC₅₀ value of 8.57 μ M. The remainder of the 10 compounds returned IC₅₀ values >10 μ M suggesting they are essentially inactive towards promastigote *L. major* (Table 5.1). One compound, compound 5, reported an increase in cell growth (228.9%) at a concentration of 10 μ M, more than double that of the corresponding DMSO control, suggesting this compound may stimulate cell growth. Therefore, it is possible that compound 5 may induce host factors which can stimulate cell growth and proliferation. However, due to limited compound material, analysis of five of these compounds (compound 1, compound

2, compound 3, compound 4 and compound 6) was performed only once and therefore needs to be repeated to obtain more definitive data on their biological activity against *Leishmania*. The remaining five compounds plus another one from the HTS which were re-synthesised by Kirk Malone, University of Manchester (Figure 5.3) were tested against *Leishmania in vitro* to obtain more accurate data on their biological activity which is discussed in section 5.4.1.

5.2.2 Against amastigote *L. major* in a macrophage infection.

The 10 compounds showing the greatest activity towards *Leishmania* CRK3:CYC6 protein kinase activity were also tested against promastigote *L. major* infected macrophages *in vitro*. This was to analyse the biological activity of the compounds against *L. major* amastigotes. A five-fold dilution series of each compound, with a top screening concentration of 50 μ M was set up and a macrophage infection assay carried out as described in section 2.3.7. DMSO and Pentamidine were included as negative and positive controls, respectively. Infectivity of approximately 85% was observed with macrophages treated with DMSO only, an infection rate which has been observed previously in these assays. The IC₅₀ value for Pentamidine was 7.7 μ M, the concentration which cleared *L. major* amastigotes from 50% of the macrophage population. The assay highlighted one compound, compound 3, which returned an IC₅₀ value of 38.4 μ M. The remainder of the compounds returned IC₅₀ values >50 μ M (Table 5.2). This suggests that the compounds are essentially inactive towards *L. major* amastigotes. Due to limited compound material, analysis of five of these compounds (compound 1, compound 2, compound 3, compound 4 and compound 6) was performed only once and therefore requires repeating to obtain more definitive data on their biological activity against *Leishmania*. The remaining five compounds plus another one from the HTS which were re-synthesised (Figure 5.3) were tested against *Leishmania* amastigotes *in vitro* to obtain more accurate data on their biological activity which is discussed in section 5.4.2.

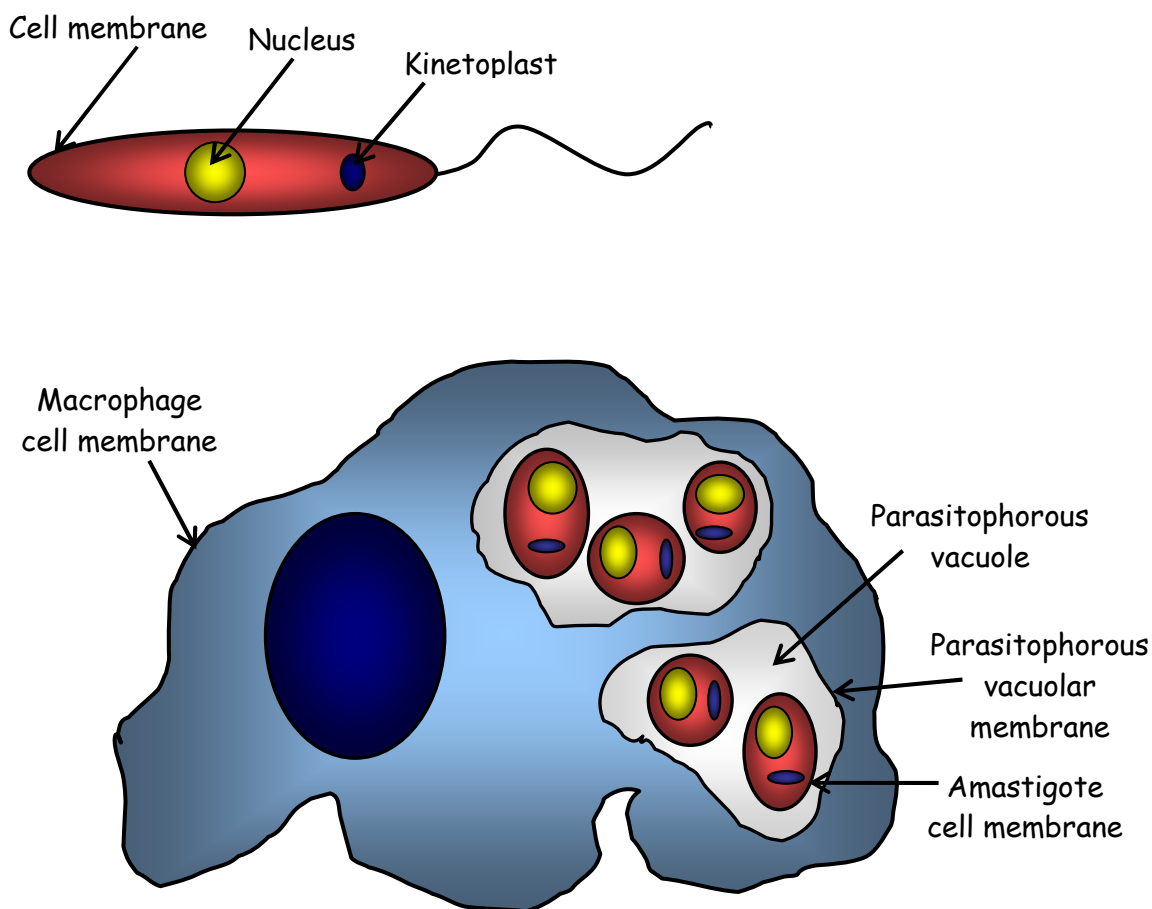


Figure 5.1 – Life cycle stages of *Leishmania* highlighting cellular membranes. The promastigote life cycle stage of *Leishmania* (Upper schematic) and amastigote life cycle stage within a macrophage cell (Lower schematic) are shown. Compounds are required to cross the cell membrane and the nuclear membrane to target CRK3 (Upper schematic). In the amastigote life cycle stage, the macrophage cell membrane, parasitophorous vacuolar membrane, amastigote cell membrane and the nuclear membrane must be crossed to target CRK3 (Lower schematic).

[Drug added] (μM)	Compound 1	Compound 2	Compound 3	Compound 4	Compound 5	Compound 6	Compound 7	Compound 8	Compound 9	Compound 10
10	93.6	133	89.4	92.2	228.9	167.7	43.3	105.7	116.5	145.2
1.56	129	159	139	149.4	146.8	149.6	141.1	91.2	84.9	96.3
0.244	115.3	120	155.9	177.4	117.2	99	101.4	101.3	98.7	95.4
0.038	106.5	104.6	108.9	113.8	135.4	104.1	101.1	106.7	105.4	104.3
0.006	107.1	103.9	91.2	105.7	100.1	105.1	109.2	105.7	102.9	102.3
0.0009	96	101.4	102	102.4	98.5	99	98.6	100.5	98.7	99.5
IC ₅₀	>10 μM	>10 μM	>10 μM	>10 μM	>10 μM	>10 μM	8.57 μM	>10 μM	>10 μM	>10 μM

Table 5.1 – Cyclacel HTS compound testing against promastigote *L. major*. The percentage growth of wild type promastigote *L. major* in relation to the corresponding DMSO control is shown for the top 10 HTS compounds at the concentrations examined against the parasites. The corresponding IC₅₀ value for each compound is also included.

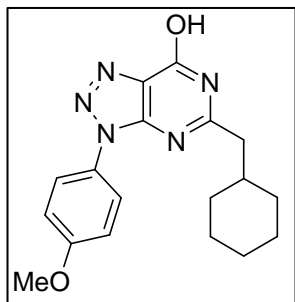
[Drug added] (μM)	Compound 1	Compound 2	Compound 3	Compound 4	Compound 5	Compound 6	Compound 7	Compound 8	Compound 9	Compound 10
50	89.8	51.2	4.93	59.2	85.2	60.4	92.9	82.1	78.1	94.3
10	95	87.4	96.2	83.7	83.3	81.8	89.7	95.2	88.6	85.8
2	94.3	90.8	85.2	96.1	82.2	89.2	92.1	93.1	91.9	93.4
0.4	95.2	87	90.6	98	85.5	90.6	93.4	92.5	90.8	94.1
0.08	91.9	94.7	92.6	95.1	88.6	88.8	86.8	91.1	88	93.1
IC ₅₀	>50 μM	50 μM	38.4 μM	>50 μM	>50 μM	>50 μM	>50 μM	>50 μM	>50 μM	>50 μM

Table 5.2 – Cyclacel HTS compound testing against promastigote *L. major* infected macrophages. The percentage of macrophages infected with wild type *L. major* amastigotes is shown for the top 10 HTS compounds at the concentrations examined. The corresponding IC₅₀ value for each compound is also shown.

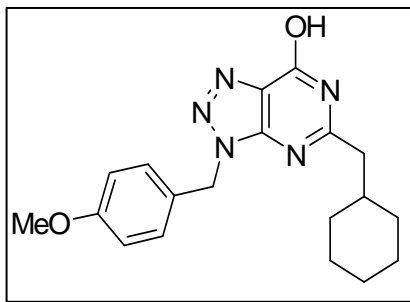
5.3 Analysis of the re-synthesised high throughput screen hits and azapurine derivatives against the *Leishmania* CRK3:CYC6 protein kinase complex.

It is standard practice in drug development to re-synthesise active HTS hits to fully evaluate their activity and potential as drug candidates. It is unwise to fully trust hits that are identified from master plates from a compound library, and they should only be treated as an indication of compounds or pharmacophores that should be investigated further. As a result six of the azapurine HTS hits were re-synthesised due to the ease of the chemical synthesis involved. In addition, iterative chemistry was performed on the azapurine pharmacophore identified from the *Leishmania* CRK3:CYC6 HTS. The re-synthesised azapurine HTS hits and azapurine derivatives were synthesised by Kirk Malone at the Manchester Interdisciplinary Biocentre (MIB), University of Manchester, and their activity towards *Leishmania* CRK3:CYC6 established by IC₅₀ determination. The structures of the 16 derivatives (Figure 5.2) and the six re-synthesised HTS hits (Figure 5.3) which were assayed are shown. The 16 derivatives and six re-synthesised HTS hit had their IC₅₀ values determined at Cyclacel, Dundee in collaboration with Graeme Thomson using the radiometric assay platform. This highlighted nine compounds KM59_2 (15.9µM), KM63_3 (39.1µM), KM114_C (4.2µM) (re-synthesised compound 7), KM114_D (30.3µM), KM117A (>50µM) (re-synthesised compound 8), KM117B (>50µM) (re-synthesised compound 9), KM117C (37.9µM) (re-synthesised compound 14), KM117D (4.4µM) (re-synthesised compound 10) and KM117E (24.2µM) (re-synthesised compound 5) which were active or were predicted to be active towards *Leishmania* CRK3:CYC6. Initial screening of compound 7 at Cyclacel returned an IC₅₀ value of 5.3µM (Table 4.2) which is almost identical to that of KM114_C. However, compound 8 returned 5.79µM versus 50µM for KM117_A, compound 9 returned 5.9µM versus >50µM for KM117_B, compound 14 returned 8.8µM versus 37.9µM for KM117_C, and compound 5 returned

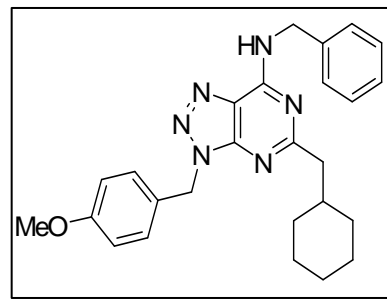
4.4 μ M versus 24.2 μ M for KM117_E. These values, surprisingly, are not in accordance with the IC₅₀ values determined for their corresponding re-synthesised compounds (KM compounds mentioned above). Only one other compound, compound 10 returned had an IC₅₀ value of 6.9 μ M which was in close agreement with the IC₅₀ value determined for its re-synthesised partner, KM117D (4.4 μ M). To clarify matters, the HTS hits from Cyclacel and the re-synthesised hits should be screened side-by-side; however, this was not possible due to limited HTS compound material available. The remainder of the 16 derivatives screened were inactive, returning IC₅₀ values of >50 μ M. As discussed, the re-synthesised HTS hits were tested against *Leishmania in vitro* (section 5.4).



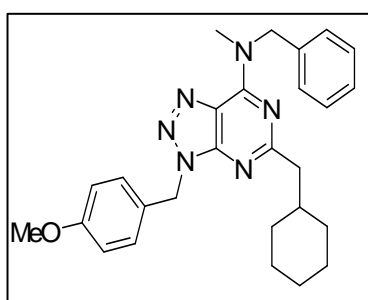
KM59_2 (15.9 μ M)



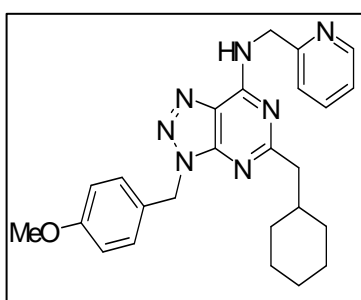
KM61 (>50 μ M)



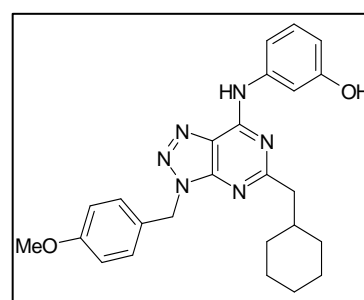
KM63_1 (>50 μ M)



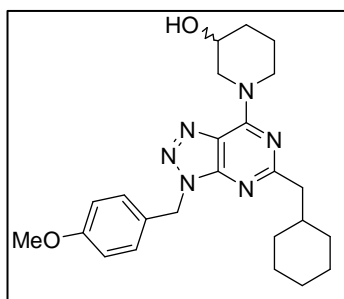
KM63_2 (>50 μ M)



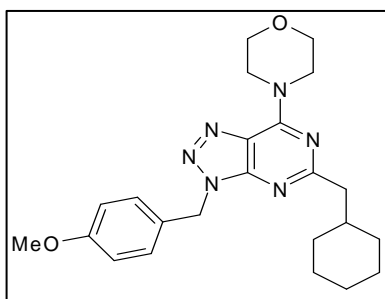
KM63_3 (39.1 μ M)



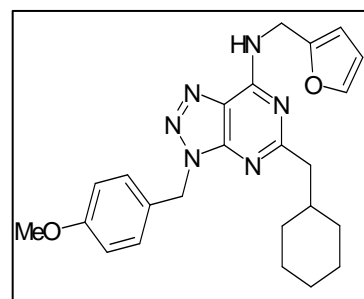
KM69 (>50 μ M)



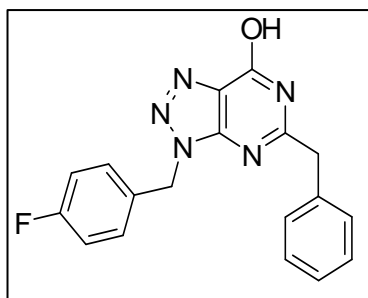
KM71 (>50 μ M)



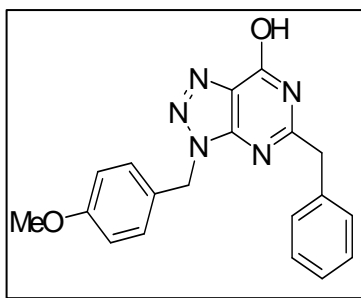
KM75_1 (>50 μ M)



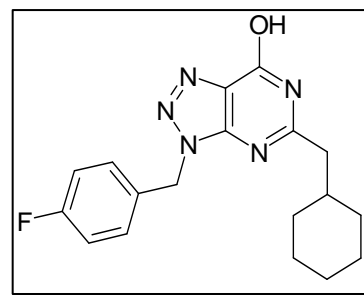
KM75_2 (>50 μ M)



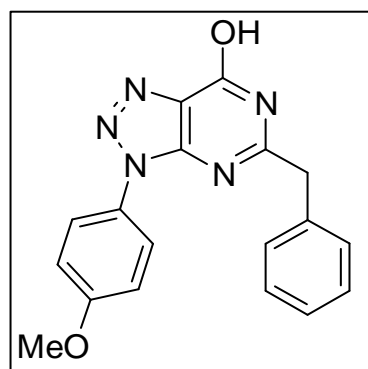
KM77 (>50 μ M)



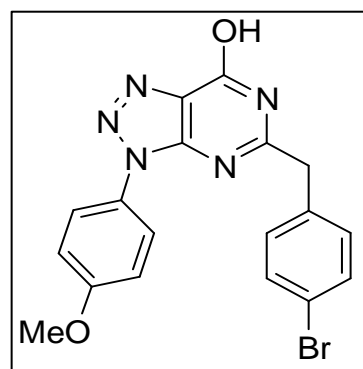
KM79 (>50 μ M)



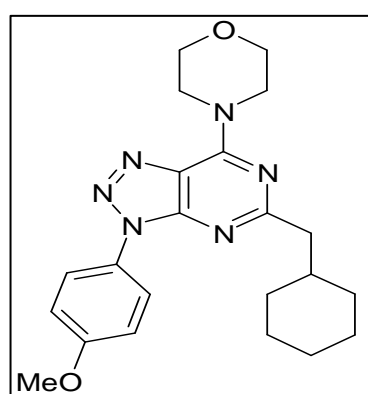
KM84 (>50 μ M)



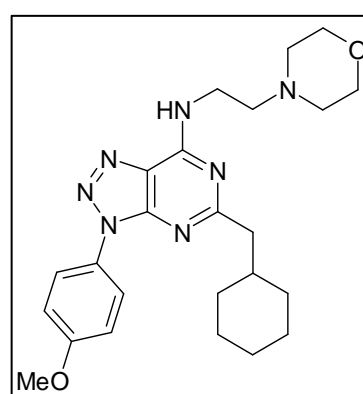
KM97 (>50 μ M)



KM98 (>50 μ M)



KM114_D (30.3 μ M)



KM114_E (>50 μ M)

Figure 5.2 – Azapurine derivatives tested against the *Leishmania* CRK3:CYC6 protein kinase complex. The azapurine structure (Figure 4.10, upper structure) identified from the CRK3:CYC6 HTS, was used as a scaffold to generate 16 derivatives. The IC₅₀ values were determined for the 16 derivatives screened against *Leishmania* CRK3:CYC6.

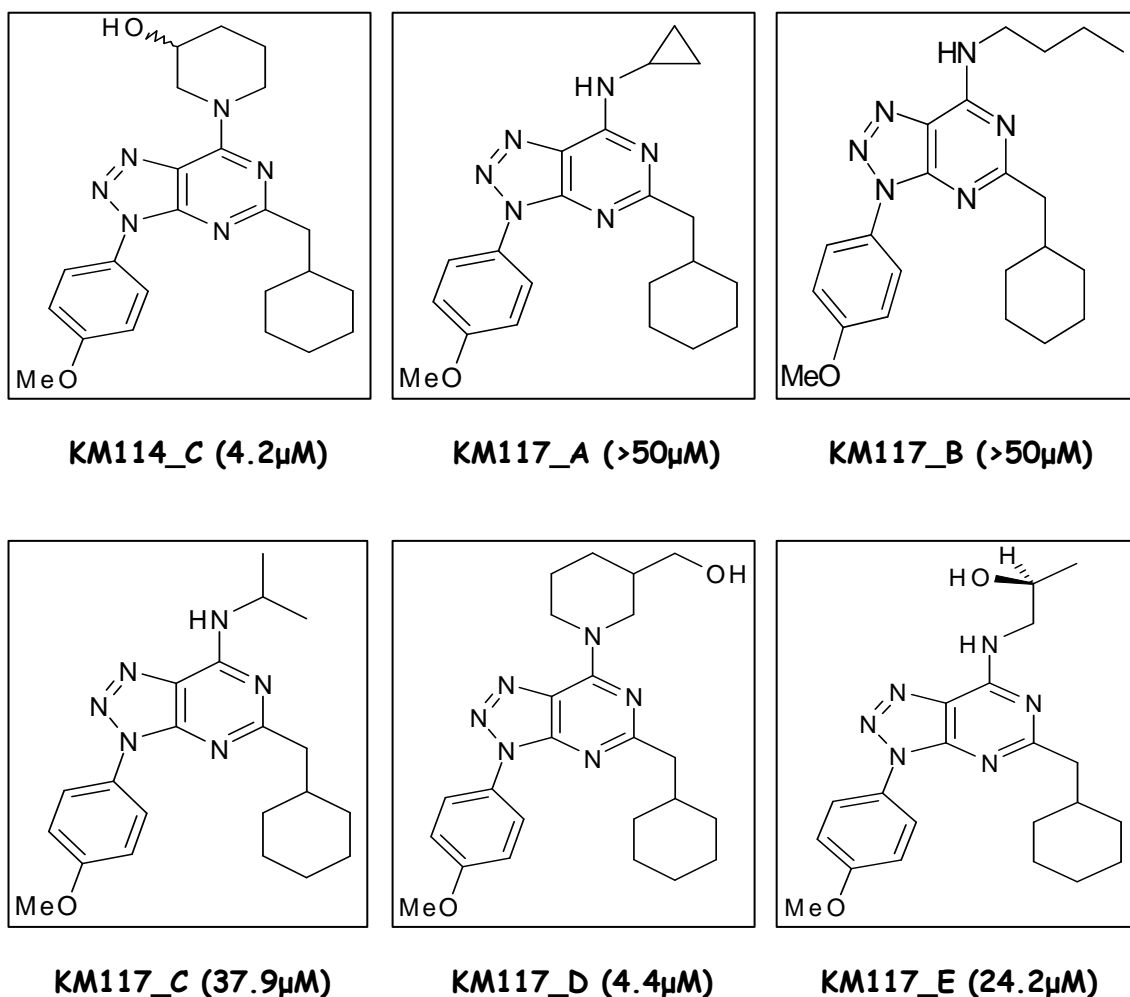


Figure 5.3 – Re-synthesised azapurine HTS hits tested against the *Leishmania* CRK3:CYC6 protein kinase complex and *Leishmania in vitro*. Six of the azapurine hits identified from the CRK3:CYC6 HTS were re-synthesised. Compound 7 was re-synthesised as KM114_C, Compound 8 re-synthesised as KM117_A, Compound 9 re-synthesised as KM117_B, Compound 14 re-synthesised as KM117_C, Compound 10 re-synthesised as KM117_D and Compound 5 re-synthesised as KM117_E.

5.4 Analysis of the biological activity of the azapurines against cultured *L.*

***major* parasites:**

5.4.1 Against cultured *L. major* promastigote parasites.

Nine compounds were assayed against promastigote *L. major* to analyse their biological activity. From the previous experiment against promastigote *L. major* (section 5.2.1), a top screening concentration of 10 μ M was not high enough to observe any biological effect against the parasites (Table 5.1). Therefore, a higher top screening concentration of 50 μ M was chosen for subsequent assays. The first assay highlighted seven of the nine compounds with activity towards *L. major* promastigotes with the most active being compound KM114_C with an IC₅₀ value of 3 μ M, with KM59_2 and KM117_B both inactive (Table 5.3). As a positive control, Pentamidine was included, returning an IC₅₀ value of 2.2 μ M, which is in accordance with that seen in previous assays. In order to confirm the activity of the compounds, the assay was repeated. However, in order to determine more accurate IC₅₀ values, the assay was carried out with an extensive range of concentrations for each compound (Table 5.4) Included in this assay was compound KM114_E, despite being inactive towards *Leishmania* CRK3:CYC6. This was due to the collaboration with Karen Grant, University of Lancaster, showing that KM114_E was active towards promastigote *L. major*, causing a growth arrest at 10 μ M (K.M. Grant, unpublished). This assay confirmed the activity of the compounds with the exception of compound KM117_A whose IC₅₀ was >40 μ M (Table 5.4) in comparison with 9 μ M (Table 5.3). The IC₅₀ value for Pentamidine in this assay was 1.7 μ M. The assay was repeated a final time with four compounds and to repeat the assay for compound KM114_E to confirm the IC₅₀ values from the previous determinations (Table 5.5). This confirmed the IC₅₀ values determined in the previous assays with the IC₅₀ for Pentamidine 2.4 μ M. The average IC₅₀ value for each compound was calculated and is shown in the summary table (Table 5.8, column 3). In summary, it was observed that against promastigote *L. major* compounds KM59_2, KM117_A, and KM117_B were inactive (>50 μ M) and compounds KM63_3, KM114_C,

KM114_D and KM114_E KM117_C, KM117_D and KM117_E were active (Table 5.8, column 3). These seven active compounds were taken forward for testing against amastigote *L. major* in a macrophage infection, to determine their biological activity.

[Drug added] (μM)	KM59_2	KM63_3	KM114_C (compound 7)	KM114_D	KM117_A (compound 8)	KM117_B (compound 9)	KM117_C (compound 14)	KM117_D (compound 10)	KM117_E (compound 5)
50	104	10.4	7.9	16.2	41	62.2	35.8	7.3	7.1
10	100.1	42.5	85.3	95.2	67.6	59.9	37	93.4	34.4
2	101.5	101	99.9	102.1	99.5	79	65.3	102.6	100.6
0.4	100	97.5	99.1	98.76	100	99.4	100.5	100.8	101.8
0.08	91.3	98.7	99.1	94.2	98.7	98.2	99.1	99.4	101
0.016	103.4	100.4	99.6	101.5	103.8	102.7	102.6	103.4	103.7
IC ₅₀	>50 μM	8.9 μM	27 μM	41 μM	9 μM	>50 μM	3 μM	28 μM	7.5 μM

Table 5.3 – Re-synthesised Cyclacel HTS and derivative compounds tested against promastigote *L. major* (1). The percentage growth of wild type promastigote *L. major* in relation to the corresponding DMSO control is shown for re-synthesised Cyclacel HTS compounds and the derivatives, at the concentrations examined against the parasites. The corresponding IC₅₀ value for each compound is also included.

[Drug added] (μM)	KM59_2	KM63_3	KM114_C	KM114_D	KM114_E	KM117_A	KM117_B	KM117_C	KM117_D	KM117_E
100	99.1	14.8	14.4	15.0	12.6	39.1	67.4	45.0	13.4	12.9
75	101.4	13.4	12.8	16.5	11.4	39.9	66.9	38.0	12.1	22.5
50	101.5	13.4	11.9	16.8	10.7	26.2	64.9	31.2	11.3	11.1
40	105.7	14.1	11.1	23.0	11.6	63.9	66.4	26.3	12.7	15.0
30	107.6	16.2	11.3	30.3	14.3	60.7	65.3	25.6	20.6	13.9
20	120.3	19.8	17.0	58.5	16.1	71.2	72.1	36.1	74.8	20.0
10	107.6	32.8	67.6	84.6	27.4	75.4	69.5	36.8	95.7	48.5
5	116.7	74.5	104.5	109.2	48.7	74.5	74.8	48.7	109.5	80.5
2.5	114.6	92.9	109.7	110.3	58.6	81.6	80.5	64.3	108.6	95.7
1	112.4	103.1	107.7	113.8	68.1	96.0	80.5	80.7	104.3	97.3
0.5	118.4	116.6	121.1	120.2	64.7	105.4	101.4	99.9	106.2	105.2
IC ₅₀	>100 μM	5.8 μM	10.4 μM	16.3 μM	6.8 μM	>40 μM	>100 μM	2.5 - 5 μM	22.1 μM	8.2 μM

Table 5.4 – Re-synthesised Cyclacel HTS and derivative compounds tested against promastigote *L. major* (2). The percentage growth of wild type promastigote *L. major* in relation to the corresponding DMSO control is shown for re-synthesised Cyclacel HTS compounds and the derivatives. A greater number of concentrations were examined here than was reported in table 5.3 to obtain a more accurate IC₅₀ value. The corresponding IC₅₀ value for each compound is also included.

[Drug added] (μM)	KM114_C	KM114_E	KM117_C	KM117_D	KM117_E
100	9.7	9.4	29.4	9.2	8.7
75	7.6	7.3	25.6	7.2	7.1
50	7.6	7.4	29.2	7.5	7.2
40	7.4	7.7	31.5	23.5	7.4
30	7.7	10.1	34.7	66.4	12.6
20	63.0	12.2	35.2	84.5	12.9
10	86.6	34.1	39.0	91.0	24.0
5	93.5	91.5	42.6	96.0	95.2
2.5	89.9	89.1	59.6	100.5	99.9
1	85.8	77.3	96.0	99.7	98.4
0.5	91.3	75.0	98.9	99.5	98.6
IC ₅₀	20.8μM	9.8μM	2.2μM	32μM	7.9μM

Table 5.5 – Re-synthesised Cyclacel HTS and derivative compounds tested against promastigote *L. major* (3). The percentage growth of wild type promastigote *L. major* in relation to the corresponding DMSO control is shown for re-synthesised Cyclacel HTS compounds and the derivatives. A greater number of concentrations were examined here than was reported in table 5.3 to obtain a more accurate IC₅₀ value. The corresponding IC₅₀ value for each compound is also included.

5.4.2 Against amastigote *L. major* in a macrophage infection.

The seven compounds showing activity towards promastigote *L. major* were tested against *L. major* infected macrophages *in vitro* with the experiment repeated to verify the percentage infections and IC₅₀ values determined. This was to analyse the biological activity of the compounds in an *L. major* infection. Five concentrations of each compound were analysed, with a top screening concentration of 50µM and a macrophage infection assay carried out as described in section 2.3.7. DMSO and Pentamidine were included as negative and positive controls, respectively. Infectivity of approximately 80% was observed with macrophages treated with DMSO only, a similar level of infection as seen previously (section 5.2.2). The IC₅₀ value for Pentamidine was 5µM, comparable to that observed previously (section 5.2.2), where the IC₅₀ value was 7.7µM. At 50µM, compound KM63_3 was toxic to the macrophages and therefore the percentage of infection could not be determined. At the lower concentrations, the percentage of infection was determined and the IC₅₀ value reported was between 5-15µM (Table 5.6 and 5.7). The software used to determine the IC₅₀ values was GraFit 5 which requires at least five data points in order to generate an IC₅₀ value. However, as only four data points were determined for KM63_3, the IC₅₀ value was loosely valued between 5-15µM, based on the percentage of infection for each concentration. This was also the case for compounds KM114_C and KM117_E, where the IC₅₀ value was determined between 5-15µM (Table 5.6 and 5.7). The IC₅₀ value for KM114_D was determined between 15-30µM (Table 5.6 and 5.7). The IC₅₀ value for KM114_E was 5.4µM and 6.7µM (Table 5.6 and 5.7, respectively). However, the IC₅₀ values for KM117_C and KM117_D could not be determined due to the compounds being toxic at the higher concentrations (Table 5.6 and 5.7). They do, however, appear to be inactive at the other concentrations examined up to the point of becoming toxic to the macrophages. In summary, five of the seven compounds were active in the macrophage infection assay; KM63_3, KM114_C, KM114_D, KM114_E and KM117_E. (Table 5.8,

column 4). Although the precise IC₅₀ values could not be determined for most of these compounds, they are active towards amastigote *L. major* in a macrophage infection.

[Drug added] (μM)	KM63_3	KM114C	KM114D	KM114E	KM117C	KM117D	KM117E
50	Toxic	Toxic	0	0	Toxic	Toxic	Toxic
30	37	Toxic	30	0	Toxic	Toxic	18
15	27	25	60	0	75	80	43
5	78	83	75	66	75	80	83
1	74	82	84	81	82	78	84
IC ₅₀	5-15 μM	5-15 μM	15-30 μM	5.4 μM	>15 μM	>15 μM	5-15 μM

Table 5.6 – Re-synthesised Cyclacel HTS and derivative compound testing against promastigote *L. major* infected macrophages (1). The percentage of macrophages infected with wild type *L. major* amastigotes is shown for the re-synthesised HTS compounds and their derivatives at the concentrations examined. The corresponding IC₅₀ value for each compound is also shown. Compounds reported as toxic, were toxic to the macrophages at the concentrations examined and the percentage of infection could not be determined.

[Drug added] (μM)	KM63_3	KM114C	KM114D	KM114E	KM117C	KM117D	KM117E
50	Toxic	Toxic	0	0	Toxic	Toxic	Toxic
30	40	Toxic	31	0	83	Toxic	14
15	44	24	58	1.5	78	82	39
5	78	87	79	64	79	82	80
1	79	78	79	80	79	80	80
IC ₅₀	5-15 μM	5-15 μM	15-30 μM	6.7 μM	>30 μM	>15 μM	5-15 μM

Table 5.7 – Re-synthesised Cyclacel HTS and derivative compound testing against promastigote *L. major* infected macrophages (2). The percentage of macrophages infected with wild type *L. major* amastigotes is shown for the re-synthesised HTS compounds and their derivatives at the concentrations examined. The corresponding IC₅₀ value for each compound is also shown. Compounds reported as toxic, were toxic to the macrophages at the concentrations examined and the percentage of infection could not be determined.

Compound	Structure	<i>Leishmania</i> CRK3:CYC6 IC ₅₀	Average Promastigote <i>L. major</i> IC ₅₀	Average Amastigote <i>L. major</i> IC ₅₀
KM59_2		15.9µM	>50µM	NA
KM63_3		39.1µM	7.4µM ± 2.2µM	5-15µM
KM114_C (Compound 7)		4.2µM	19.4µM ± 8.4µM	5-15µM
KM114_D		30.3µM	28.7µM ± 17.5µM	15-30µM
KM114_E		>50µM	8.3µM ± 2.1µM	6.1µM ± 0.9µM
KM117_A (compound 8)		>50µM	>40µM	NA
KM117_B (compound 9)		>50µM	>50µM	NA
KM117_C (compound 14)		37.9µM	2.6µM ± 0.6µM	>50µM
KM117_D (compound 10)		4.4µM	27.4µM ± 5µM	>50µM
KM117_E (compound 5)		24.2µM	7.9µM ± 0.35µM	5-15µM

Table 5.8 – Summary table of azapurine inhibition. Compounds displaying NA (not analysed) did not have their IC₅₀ values determined against *L. major* amastigotes due to being inactive against *L. major* promastigotes. The ± values represent the standard deviation for each of the average determinations.

5.5. *Leishmania* CRK3:CYC6 *in vivo* protein kinase complex.

The *Leishmania* CRK3:CYC6 protein kinase complex used in these studies is an *in vitro* complex. Therefore work was carried out in order to determine if *Leishmania* CRK3 and CYC6 are true binding partners that interact *in vivo* to form a functional *in vivo* protein kinase complex. This was carried out by adding N or C-terminal HA-tags to CYC6 and co-immunoprecipitating the protein via the HA-tags to attempt to identify CRK3 as a binding partner.

Both N and C-terminally tagged HA-CYC6 constructs were made in case a tag at either the N or C terminus would interfere with the CYC6 gene, and hence its expression and CYC6 activity.

5.5.1 *L. major* HA-tagged CYC6 episomal constructs:

Episomal expression of HA-tagged CYC6 was chosen as these constructs would not require chromosomal integration into the *Leishmania* genome and could express the protein in the cytoplasm. This expression system yields stable protein production at high levels.

5.5.1.1 N-terminal HA-tagged *L. major* CYC6.

The CYC6 gene with an N-terminal HA-tag was amplified by PCR. Amplification was carried out using Deep Vent DNA polymerase, pGL1169 (*L. major* CYC6 in PCR-script) as template DNA and oligonucleotides 1901 (5' CAGCGCCGGCAGCTCGTTACCTAGG 3') and 1902 (5' GCCCGGGATGT**TACCCCTACGACGTCCCGGACTATGCC**TTCGTGGAACGAGAGC 3') (to generate the N-terminal HA-tag (Underlined in bold)). The PCR product was purified and ligated into pGL102, a pXG episomal expression vector using *Xma*I and *Bam*HI. This plasmid was named pGL1391 (Figure 5.4, upper map).

5.5.1.2 C-terminal HA-tagged *L. major* CYC6.

The *CYC6* gene with a C-terminal HA-tag was amplified by PCR. Amplification was carried out using Deep Vent DNA polymerase, pGL1169 (*L. major* *CYC6* in PCR-script) as template DNA and oligonucleotides 1899 (5' CGCCCGGGATGTTTCGTGGAACGAG 3') and 1900 (5' TCAGGATCCCGGCATAGTCCGGGACGTCGTAGGGGTACAGCGCCGGCAGCTCGTTAGGCA 3') (to generate the C-terminal HA-tag (underlined in bold)). The PCR product was purified and ligated into pGL102 using *Xma*I and *Bam*HI. This plasmid was named pGL1390 (Figure 5.4, lower map).

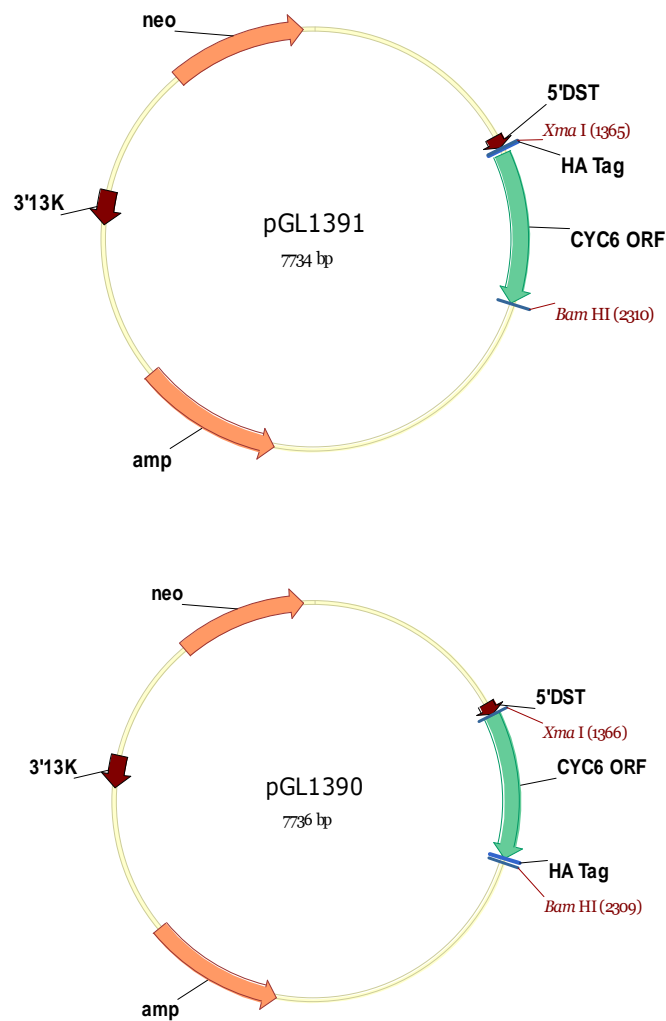


Figure 5.4 – Vector NTI maps of the *L. major* N and C-terminal HA-tagged *CYC6* episomal expression constructs pGL1391 and pGL1390. The N and C-terminal HA-tagged *CYC6* open reading frames, with *Xma*1 and *Bam*H1 restriction sites, were obtained via PCR amplification. These were sub-cloned into a similarly digested pXG vector with a neomycin (G418) resistance marker (NEO) and prokaryotic promoter (5'DST). The N-terminal HA-tagged *CYC6* construct, pGL1391 is shown in the upper panel, and the C-terminal HA-tagged *CYC6* construct, pGL1390, shown in the lower panel.

5.5.2 *L. major* HA-tagged *CYC6* ribosomal integration constructs:

Due to episomal expression of HA-tagged *CYC6* proving unsuccessful, an alternative method was employed. N and C-terminally HA-tagged *CYC6* open reading frames were sub-cloned into the pRIB ribosomal integration vector. This was to integrate HA-tagged *CYC6* into the ribosomal locus of *L. major* which is likely to provide constitutive and therefore high protein production (Mißlitz *et al.*, 2000).

5.5.2.1 N-terminal HA-tagged *L. major* *CYC6*.

The *CYC6* gene with an N-terminal HA-tag was amplified by PCR. Amplification was carried out using Deep Vent DNA polymerase, pGL1169 (*L. major* *CYC6* in PCR-script) as template DNA and oligonucleotides 2156 (5' CCTCGAGATG **TACCCCTACGACG** **TCCCGGACTATGCCATGTTCGTGGAACGAGAGC** 3') (to generate the N-terminal HA-tag (underlined in bold)) and 2157 (5' CGCGGCCGCTCACAGCGCCGGCAG 3') The PCR product was purified and ligated into pGL631, a pRIB ribosomal integration vector using *Xho1* and *Not1*. This plasmid was named pGL1484 (Figure 5.5, upper map).

5.5.2.2 C-terminal HA-tagged *L. major* *CYC6*.

The *CYC6* gene with a C-terminal HA-tag was amplified by PCR. Amplification was carried out using Deep Vent DNA polymerase, pGL1169 (*L. major* *CYC6* in PCR-script) as template DNA and oligonucleotides 2154 (5' CCTCGAGATGTTCG TGGAACGAGAG 3') and 2155 (5' CCGCGGCCGCTCA **GGCATAGTCCGGGACG** **TCGTAGGGGTAGGGGTACAGCGCCGGCAGCTCGTTAG** 3') (to generate the C-terminal HA-tag (underlined in bold)). The PCR product was purified and ligated into pGL631 using *Xho1* and *Not1*. This plasmid was named pGL1483 (Figure 5.5, lower map).

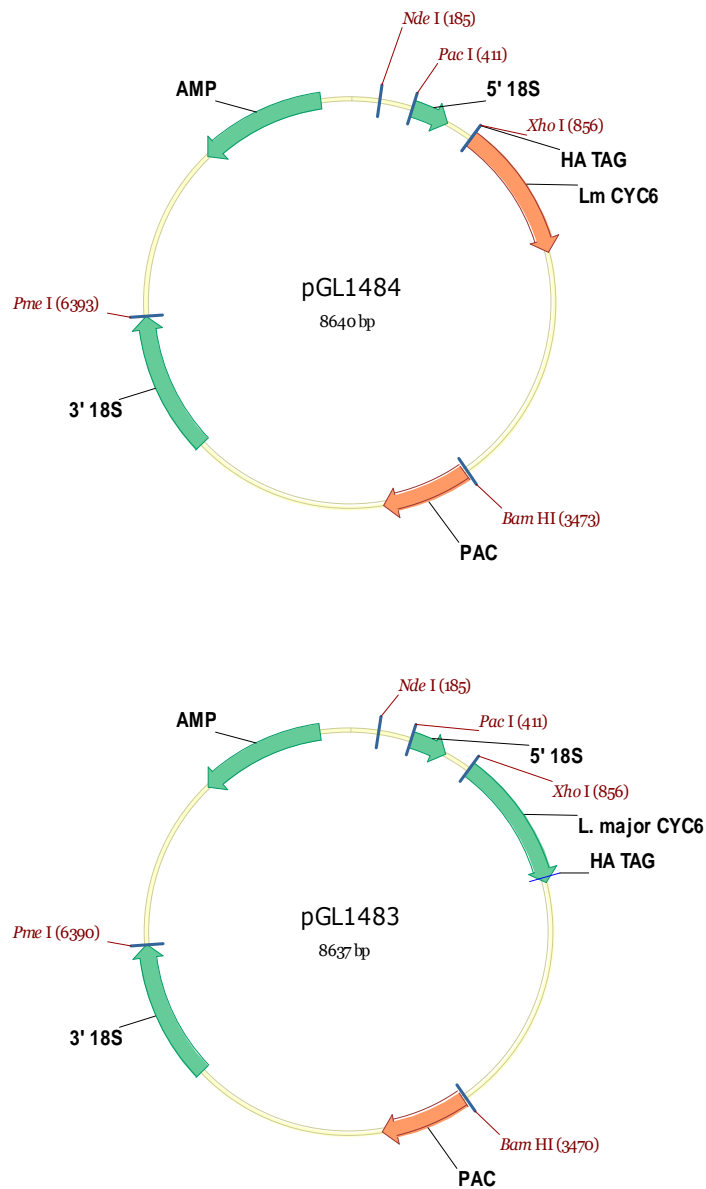


Figure 5.5 – Vector NTI maps of the *L. major* N and C-terminal HA-tagged CYC6 ribosomal integration constructs pGL1484 and pGL1483. The N and C-terminal HA-tagged *CYC6* open reading frames, with *Xho*1 and *Not*1 restriction sites, were obtained via PCR amplification. These were sub-cloned into a similarly digested pRIB vector with a puromycin resistance marker (PAC) between the 5' and 3' ribosomal flanking sequences (3' and 5' 18S). The N-terminal HA-tagged *CYC6* construct, pGL1484 is shown in the upper map, and the C-terminal HA-tagged *CYC6* construct, pGL1483, shown in the lower map.

5.6 Purification and detection of *L. major* HA-tagged CYC6.

5.6.1 CRK3:CYC6 co-immunoprecipitation and pull down assay.

Analysis was carried out to determine if CRK3 and CYC6 form an *in vivo* complex in *L. major*. The episomal HA-tagged CYC6 constructs pGL1390 and 1391 were transfected into wild type *L. major* as described in section 2.3.3.2. However, the episomal HA-tagged CYC6 transfectants failed to proliferate in the presence of the selecting drug (G418). As previously discussed, ribosomal integration of HA-tagged *CYC6* was then carried out. The HA-tagged *CYC6* ribosomal integration constructs pGL1483 and 1484 were successfully transfected into wild type *L. major* as described in section 2.3.3.3. Protein preparation from *L. major* was carried out as described in section 2.3.4 and Western blot analysis of the HA-tagged CYC6 S100 fractions carried out. Wild type *L. major* was included as a negative control. Included as a positive control, was an *E. coli* whole cell lysate containing a 41 kDa recombinant protein expressing 11 different epitope tags (Abcam), one of which was an HA-tag (amino acid sequence, YPYDVPDYA). No HA-tagged CYC6 was detected in lanes 2 and 3 with the positive control detected at the expected size of 41kDa (Figure 5.6). The S100 fractions were not used for further analysis of the CRK3 and CYC6 *in vivo* complex.

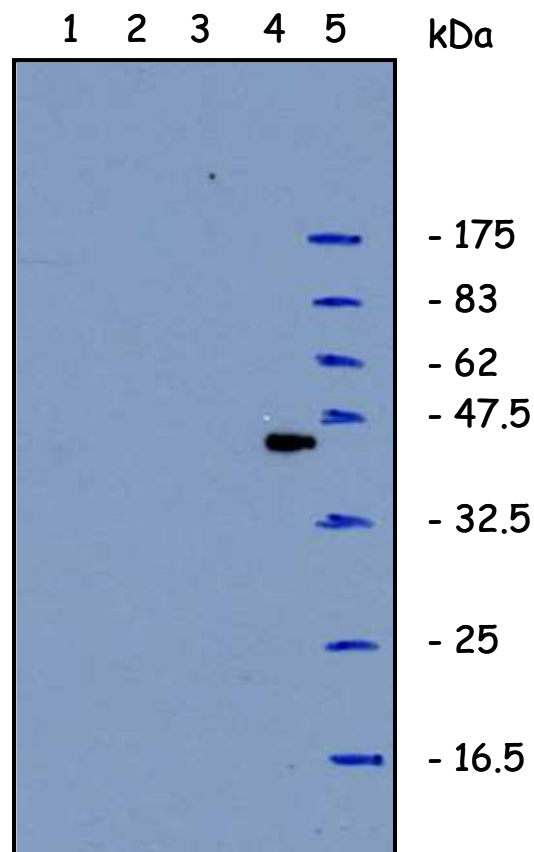


Figure 5.6 – Western blot analysis of N and C-terminal HA-tagged CYC6 purified from *L. major*. The S100 fractions from 200ml of 1×10^7 mid-log phase promastigote *L. major* cells expressing N and C-terminal HA-tagged CYC6 were analysed by Western blot. Lane 1 is the wild type *L. major* control. Lane 2 is the C-terminal HA-tagged CYC6. Lane 3 is the N-terminal HA-tagged CYC6. Lane 4 is the *E. coli* positive control and lane 5 the molecular weight protein standards.

5.7 Chapter discussion.

In order to determine the biological activity of the compound hits identified from the HTS, analysis against promastigote *L. major in vitro* was carried out. The 10 compounds showing the greatest activity towards *Leishmania* CRK3:CYC6 protein kinase activity (Table 4.2, column 6) were tested. Activity of the HTS compounds towards promastigote *L. major* was determined by an Alamar blue absorption assay carried out as described in section 2.3.6. In the assay, cells that are viable metabolise the reazurin salt, which turns pink in colour. If the cells are dead, the reazurin salt is not metabolised and remains blue in colour. This highlighted one compound, compound 7, which had activity towards promastigote *L. major* cells with an IC₅₀ value of 8.6µM. Conversely, compound 5 appeared to stimulate cell growth, an effect which has been seen previously with drugs tested against *Leishmania* (Kaur *et al.*, 1988b). *Leishmania* were genetically engineered to lack the folate-methotrexate transporter and were resistant to methotrexate (a potent dihydrofolate reductase inhibitor). Upon the addition of methotrexate, stimulated growth of wild type *Leishmania* and those lacking the transporter was observed in media deficient of folate. This suggested the antifolate analogs were serving as a pteridine source for the parasite and stimulated growth (Kaur *et al.*, 1988a). The remainder of the 10 compounds returned IC₅₀ values >10µM suggesting these are inactive towards promastigote *L. major* (Table 5.1) which could be due to a variety of reasons. As the HTS hits were active towards *Leishmania* CRK3:CYC6 protein kinase activity in the micromolar range (Table 4.2, column 6), it would be reasonable to assume that the compounds would be less active towards the parasites at the IC₅₀ values determined for CRK3:CYC6. Therefore a higher concentration of compound would be required to determine IC₅₀ values for the 10 HTS compounds towards promastigote *L. major* and observe a significant reduction in cell survival. Furthermore, in *Leishmania* CRK3:CYC6 protein kinase activity assays, compounds were assayed directly with the *Leishmania* CRK3:CYC6 protein kinase complex. When tested against promastigote *L. major*, the compounds must first cross the

parasite cell membrane and nuclear membrane in order to inhibit CRK3 activity, which the compounds may not have been able to do.

As CRK3 is the homologue of mammalian CDK1, we can predict that *Leishmania* CRK3 would also be located in the same cellular locations. CDK1, was shown to be a nuclear and centrosomal protein required for mitosis in mammals (Riabowol *et al.*, 1989). These subcellular locations of CDK1:CycB are vital to its function. The complex must locate to the nucleus in order to phosphorylate a variety of nuclear substrates which are necessary for the onset of mitosis (Porter and Donoghue, 2003). The location of CDK1 is in part, dependent on the isotype of its cyclin B partner, whose intracellular localization also varies. CDK1:CycB1 colocalize with cytoplasmic microtubules during interphase (Porter and Donoghue, 2003; Migone *et al.*, 2006), and translocates to the nucleus to initiate mitosis. CDK1:CycB2 colocalize with the golgi apparatus and CDK1:CycB3 is constantly located in the nucleus (Porter and Donoghue, 2003). As CRK3 would be predicted to be in both the nucleus and cytoplasm, the compounds would need to cross at least one membrane in order to target CRK3. Although the majority of the compounds in the Cyclacel library were designed with desirable pharmaceutical properties (Table 4.1), it may be the case that the top 10 HTS compounds found in this screen require further optimisation. Therefore, these compounds would likely require iterative chemistry in order to make them sufficiently “drug like” to cross the cell membrane and inhibit CRK3. Furthermore, the compounds may have gone off whilst being stored in the master plates. These reasons may explain why little or no inhibition of CRK3 was observed in promastigote *L. major* and why the cells were still viable.

The 10 compounds showing the greatest activity towards *Leishmania* CRK3:CYC6 protein kinase activity were also tested against promastigote *L. major* infected macrophages *in vitro*. As mentioned, there are significant differences between promastigote and amastigote *Leishmania* in biochemistry and sensitivity to standard and experimental drugs (Croft *et al.*,

2006a). This is highlighted with the first line drug Sodium stibogluconate (Pentostam, SSG), used to treat the visceral form of leishmaniasis, with activity towards amastigote *Leishmania* but not towards promastigote *Leishmania* (Neal and Croft, 1984). Within macrophages, Pentostam is metabolised and converted from the pentavalent form into a lethal trivalent form which kills amastigote *Leishmania*. It has recently been reported that Pentostam modifies the expression of eight genes in host cell lines, up-regulating six and down-regulating two (El Fadili *et al.*, 2008). These genes may therefore be implicated in the mode of action of Pentostam. However, the precise mode of action of Pentostam and whether it is macrophage or parasite factors which catalyse the conversion to a lethal trivalent form remains unknown. Therefore, it is possible the HTS compounds may have activity towards amastigote *L. major* despite the majority not showing activity towards the promastigote form. Using this knowledge as scientific rationale, the biological activities of the compounds in a *Leishmania* infection were carried out as described in section 2.3.7. This highlighted one compound, compound 3, which returned an IC₅₀ value of 38.4µM (Table 5.2). Interestingly, this compound did not show activity towards promastigote *L. major*, as seen with Pentostam. The remainder of the compounds returned IC₅₀ values >50µM, including compound 7, which had an IC₅₀ value of 8.57µM towards promastigote *L. major*. This suggests that these compounds are not active towards amastigote *L. major* infected macrophages. This could be for reasons previously discussed for the HTS compounds tested against promastigote *L. major*. The compounds must cross the parasite cell membrane and nuclear membrane in order to target CRK3; however, in amastigote infected macrophages, four membranes must be crossed. The compounds must first cross the macrophage cell membrane, followed by the parasitophorous vacuolar membrane surrounding the amastigotes, the amastigote cell membrane itself and finally the nuclear membrane. If, as mentioned previously, the compounds are insufficiently “drug like”, it is unlikely they will be able to cross four membranes in order to target CRK3. However, it is interesting that compound 3 shows activity towards amastigote *L. major* but not the

promastigote form. Despite the apparent lack of activity of the majority of the compounds against promastigote and amastigote *Leishmania*, it was vital that these compounds were re-synthesised and re-tested to confirm their biological activity, or lack thereof.

Due to time constraints and the complexity of chemical synthesis involved, only six of the HTS hits were re-synthesised. Others identified from the HTS screen will be synthesised and their biological activity evaluated in the future. These six compounds from the CRK3:CYC6 HTS were screened against *Leishmania* CRK3:CYC6, promastigote *L. major* and amastigote *L. major* in a macrophage infection; KM114_C, KM117_A, KM117_B, KM117_C, KM117_D and KM117_E (Figure 5.3). Only two of the re-synthesised HTS hits, KM114_C and KM117_D returned IC₅₀ values which were consistent with those of the original HTS hits. Furthermore, two of the hits, KM117_A and KM117_B, proved inactive towards CRK3:CYC6. This suggests there are discrepancies between the original HTS hits and the re-synthesised compounds. It could be that the original hits were not the compounds that they were thought to be or that there may be contaminating compounds mixed in, as a result of compound carry over from the HTS liquid handler causing a synergistic effect against *Leishmania* CRK3:CYC6. The identification of these compounds as inactive validates the re-synthesis process, highlighting that compounds taken directly from a master plate in a compound library should be treated with caution when identified as hits.

Although the first set of assays with compounds 1-10 showed the majority of the compounds were essentially inactive towards promastigote and amastigote *L. major* in a macrophage infection, activity was observed with a number of the re-synthesised compounds, which is promising for future drug development. However, this begs the question of what differences there are between the original HTS hits identified and the re-synthesised compounds when they should be identical. It is possible that partial

degradation of the compounds once made up in DMSO solvent and upon long-term storage may have occurred, accounting for the discrepancies observed.

The purine and aminopyridazine pharmacophores identified from the *Leishmania* CRK3:CYC6 HTS have previously been identified as biological inhibitors. For example roscovitine, a purine based CDK inhibitor is in Phase II clinical trials for treatment of cancer (Havlicek *et al.*, 2005). Furthermore, 2,6,9, trisubstituted purines, such as olomoucine, have been shown to inhibit CDKs (Vesely *et al.*, 1994) and it is known the 2,6,9, trisubstituted purines also inhibit CRK3 protein kinase activity (Grant *et al.*, 2004). It has also recently been reported that azapurine derivatives are shown to be inhibitors of CDKs (Havlicek *et al.*, 2005). Interestingly, to date, aminopyridazines have not been reported to be inhibitors of CDKs. They have, however, been shown to be inhibitors of acetylcholinesterase (Contreras *et al.*, 1999) and neuronal damage (Craft *et al.*, 2004), which may be important in the treatment of Alzheimer's disease. Therefore, the aminopyridazine compounds may prove to be novel drugs in the treatment of leishmaniasis by acting as CDK inhibitors, which further testing will confirm.

In order to obtain compounds which showed an increase in potency towards *Leishmania* CRK3:CYC6 protein kinase activity, iterative chemistry was performed on the azapurine pharmacophore identified from the *Leishmania* CRK3:CYC6 HTS (Figure 4.10, upper structure). 16 derivatives of the azapurine structure were synthesised and the structures are shown (Figure 5.2). Three of the compounds, KM-59_2, KM63_3 and KM114_D showed activity towards the *Leishmania* CRK3:CYC6 protein kinase complex, and as mentioned, the remainder were inactive, returning IC₅₀ values of >50µM. This is possibly due to certain chemical modifications on the R1, R2 and R3 groups, which might render the compounds inactive towards *Leishmania* CRK3:CYC6. Modifications to the R2 and R3 groups of the azapurine structure as determined in section 4.11 abolish activity towards *Leishmania* CRK3:CYC6 protein kinase activity. This may account for the derivatives that

have had R2 and R3 modifications showing no activity. Furthermore, the selectivity of the azapurines towards *Leishmania* CRK3:CYC6 protein kinase activity, vary because of the various groups in the R1 position (compare azapurine compounds, Table 4.2). For example, compound 1 has an IC₅₀ value towards *Leishmania* CRK3:CYC6 of 2.6µM and compound 26, 17.9µM. These compounds differ only in the R1 group highlighting that CRK3:CYC6 selectivity is partially determined by the chemical group on the R1 position. Therefore, certain modifications to the R1 group may again render these derivatives inactive towards *Leishmania* CRK3:CYC6.

Compound KM114_E is interesting as although it returned an IC₅₀ value of >50µM against CRK3:CYC6 it proved active towards promastigote *L. major*. As a result, the four active compounds (KM59_2, KM63_3, KM114_D and KM114_E) were tested against promastigote *L. major*, with the view to testing later against the amastigote form of the parasite. Compound KM59_2 was inactive against promastigote *L. major* possible due to the compound not crossing the membranes required to target CRK3. The remaining three compounds, however, were active including compound KM114_E. This suggests that although it is inactive towards CRK3:CYC6, it is likely active against another target in the cell, possibly another protein kinase. Although the azapurine compounds were counter-screened against a small panel of mammalian kinases, showing selectivity towards CRK3:CYC6, they were not counter screened against other *Leishmania* protein kinases. Therefore, it is conceivable that the HTS hits and any derivatives will be active against other *Leishmania* cellular protein kinases. The three compounds active against promastigote *L. major* (KM63_3, KM114_D and KM114_E) were tested against amastigote *L. major* in a macrophage infection. All three compounds were active with KM114_E the most active returning an average IC₅₀ value of 6.1µM, again suggesting that it is active against a target other than CRK3:CYC6.

As with some of the re-synthesised azapurine HTS hits showing activity towards promastigote and amastigote *L. major*, activity is also observed with the azapurine derivatives. This shows that the azapurine core structure is amenable to subtle chemical modifications resulting in some cases in an increased biological activity towards *Leishmania* (compare the re-synthesised compound KM114_C with the azapurine derivatives KM114_E and KM117_E). This is encouraging; highlighting that iterative chemistry performed on the azapurine pharmacophore is successful. Therefore, future derivatives may result in even more potent compounds which can be further developed to treat leishmaniasis.

N and C-terminal HA-tagged *CYC6* constructs were made using an *L. major* episomal expression vector, pXG (Figure 5.4). This was carried out in order to over express *L. major* *CYC6* and affinity purify *CYC6* to identify binding partners *in vivo* (predicted to be CRK3). These HA-tagged constructs were transfected into wild type promastigote *L. major* and selected with G418 antibiotic. However no cells survived after the addition of the antibiotic. This is possibly due to the over expression of *CYC6* when in complex with CRK3 causing an early cell cycle shift into mitosis as CRK3 is a G2-M kinase. Therefore the cells may not have fully replicated their genome before the onset of mitosis and cytokinesis, causing an irreversible cell cycle defect, resulting in cell death. An alternative explanation may be that the cells lost the episome and G418 antibiotic resistance and die upon the addition of G418, or that over expression of *CYC6* is toxic to the cells.

Due to the unsuccessful attempts to over express *CYC6* with an episomal vector, N and C terminal HA-tagged *CYC6* constructs were made using a ribosomal integration vector, pRIB (Figure 5.5). These HA-tagged constructs were transfected into wild type promastigote *L. major* and selected with puromycin antibiotic. The cells survived upon the addition of the antibiotic and were used to detect HA-*CYC6* by Western blot analysis with

an anti-HA antibody with the view to affinity purifying CYC6 via the HA-tags for further analysis.

The attempted purification of N and C terminal HA-tagged CYC6 from *L. major* promastigote cells was carried out as described in section 2.3.4. Detection of the HA-tagged CYC6 proteins was attempted by Western blot analysis using an anti-HA antibody. However no N or C terminal HA-tagged CYC6 was detected. The positive control was detected at the expected size of 41kDa (Figure 5.6). This suggests that the protein is either expressed at very low levels, below the detection capability of the Supersignal West Pico Chemiluminescent substrate reagents, or not expressed at all. However, as the cells survive upon the addition of puromycin, this suggests the puromycin resistance marker in the pRIB vector has been retained by the cells. Therefore it is possible that the gene has been rearranged by the cells and is no longer expressed due to over expression of CYC6 being detrimental to the progression of the cell cycle.

Chapter 6

Final discussion and conclusions

CDKs which govern the cell cycle are a class of enzymes that are potential targets for anti-parasite chemotherapy. Proteins, including enzymes specific to the parasite and absent or distinct from the host, which are essential in the pathogenic life cycle stage, are considered potential therapeutic drug targets. Gene knockout techniques to validate drug targets have proved successful tools; however, gene essentiality does not make it an automatic drug target. Knocking out a gene removes the gene product completely but *in vivo* the protein is present and it is this that needs to be down regulated. Many compounds do not provide 100% inhibition of their target and so the enzyme is able to still catalyse its reaction albeit at low levels in the cell (Barrett *et al.*, 1999). Despite genetic manipulation validating a gene as essential and therefore a potential drug target, chemical validation is also required to show a gene product can be targeted in the cell.

Protein kinases can be targeted with inhibitors and are druggable in the cell, with several compounds such as Gleevec® going to market to treat proliferative disorders. Other compounds such as Flavopiridol®, a CDK inhibitor, have progressed into clinical trials. However, no therapeutics, to date, have been developed against CDKs which have become commercially available anti-parasite drugs. None have successfully progressed through the drug discovery pipeline (Figure 1.10) fulfilling the criteria required to become a drug/clinical development candidate to treat parasitic diseases (Figure 1.11).

The aim of this work was to identify inhibitors of the *Leishmania* CDK, CRK3, which could ultimately pass through the drug development pipeline to become drug candidates to treat parasitic diseases. Initially, active *Leishmania* CRK3:CYC6 protein kinase complex was purified and an expression system suitable for large scale production of the complex developed. A HTS assay was developed with this material and the assay validated. Using

the HTS assay a chemical compound library was screened, identifying inhibitors of *Leishmania* CRK3:CYC6 protein kinase activity, which were subsequently screened against *Leishmania in vitro*, to evaluate their biological activity. In order to obtain compounds with higher potency towards *Leishmania* CRK3:CYC6 protein kinase activity, derivatives of the HTS hits were synthesised in collaboration with Nicholas Turner and Kirk Malone at the Manchester Interdisciplinary Biocentre (MIB). Active compounds were screened to determine their biological activity against *Leishmania in vitro*. This was with the view to screening the HTS hits and any active derivatives against *Leishmania in vivo*, and initiating pharmacokinetic studies on the active compounds. However due to time constraints, the *in vivo* and pharmacokinetic studies were not carried out.

Sufficient quantities of active *Leishmania* CRK3:CYC6 were obtained, which was active without phosphorylation on the conserved T178 residue. This is unusual as phosphorylation on the conserved T-loop residue is a prerequisite for an active protein kinase complex in many CDKs (Ducommun *et al.*, 1991; Solomon *et al.*, 1992). There are exceptions, however, as it has been reported that the activation of some CDK complexes such as CDK5-p35 and CDK7-cyclinH do not require phosphorylation (Nigg, 1996; Qi *et al.*, 1995) at the analogous site in the T-loop. The *Leishmania* CRK3:CYC6 protein kinase complex could therefore be a further example of this, where there is kinase activity without phosphorylation. However, *Leishmania* CRK3:CYC6 is a recombinant protein kinase complex and may not possess exactly the same activity and biochemical characteristics of active CRK3 in *Leishmania*. Therefore, is the *Leishmania* CRK3:CYC6 protein kinase complex biochemically similar to active CRK3 *in vivo* and as a result, a valid screening target? Some biochemical characterisation showed that the K_m values for ATP were within two-fold and the IC_{50} values for olomoucine were almost identical between the recombinant and parasite-purified enzymes. Therefore, this suggests the CRK3:CYC6 protein kinase complex and CRK3 in *Leishmania* are biochemically similar and it can be said with a degree of confidence that *Leishmania* CRK3:CYC6 is a valid screening target.

The azapurine and aminopyridazine hits identified from the HTS inhibited *Leishmania* CRK3:CYC6 protein kinase activity. However, little or no biological activity was observed against either *L. major* procyclic promastigotes or amastigotes with the compounds taken from the original master plates. This begs the question of whether these pharmacophores are of sufficient quality to be developed into leads and drug candidates (Figures 1.10 and 1.11). However, it is standard practice in drug development to re-synthesise active HTS hits to fully evaluate their activity and potential as drug candidates. This was carried out and some of the re-synthesised HTS hits, based on the azapurine pharmacophore, did show biological activity suggesting there are discrepancies between the two sets of compounds, thereby justifying the re-synthesis procedure. There may also have been complications when performing the assays with the original HTS hits, accounting for their lack of activity; however, the precise reason accounting for the differences in activity observed between the HTS hits and the re-synthesised hits remains unknown. Despite this, there is undoubtedly activity observed with some of the re-synthesised hits towards *L. major* promastigotes and amastigotes, which is encouraging for the progression of azapurine based compounds through the drug discovery pipeline. The re-synthesised HTS hits are currently at the “validated hits” stage in the drug development pipeline (Figure 1.10) where iterative chemistry is being performed to improve their potency. In terms of fulfilling drug candidate criteria (Figure 1.11), the re-synthesised HTS hits are showing the characteristics of a hit that can be developed into a lead compound, again something the iterative chemistry is attempting to achieve.

It is important to consider these HTS hits with respect to other current antileishmanials in similar stages of drug development. There are a number of synthetic compounds and those derived from natural products which are currently being evaluated for their antileishmanial properties. One such example is the Azaterphenyl diamidines. These were evaluated against axenic amastigote *Leishmania* where a number of the compounds tested reported IC₅₀ values of <1µM against axenic amastigotes (Hu *et al.*, 2008). This is an example of

compounds in a similar stage of drug development showing a high potency towards *Leishmania* amastigotes, although they were not tested against amastigotes in a macrophage infection. Another example of a class of compounds is the 2-(3-Aryloxopropen-1-yl)-9-*tert*-butyl-paullones. It is known that paullones are CDK inhibitors and have been shown to act on CRK3 as previously discussed. These paullones reduce the proliferation of axenic amastigotes and show activity against amastigotes at a concentration of 5 μ M in a macrophage infection (Reichwald et al., 2008). These are an example of a new chemotype that are active against *Leishmania*, possibly the situation that could be seen with aminopyridazine-3-carboxamide as a novel antileishmanial pharmacophore. Synthetic phospholipids also show potent antileishmanial activity, with many exhibiting IC₅₀ values <1 μ M against *Leishmania* amastigotes, similar to the Azaterphenyl diamidines. These were shown to be more active than that of the currently registered drug used to treat leishmaniasis, Miltefosine, which is also a phospholipid analogue (Seifert et al., 2007). These are potencies which we wish to achieve with the HTS hits in order to progress through the drug discovery pipeline. Further examples of compounds currently being tested against *Leishmania* are Amlodipine and Lacidipine, which are 1,4-Dihydropyridine derivatives. These were shown to inhibit *Leishmania* infection *in vitro* and in BALB/c mice when administered orally (Palit and Ali, 2008). One of the next steps for the CRK3 HTS hits once the potency is increased is to test them on mice infected with *Leishmania*.

Another question to ask is “was the Cyclacel library an appropriate and successful library to screen in terms of the hits identified?” Correspondence with Cyclacel suggested that this type of HTS with the Cyclacel library was successful by comparison with HTS they have carried out in the past. CDK inhibitors typically bond via a donor-acceptor-donor hydrogen bonding motif (D-A-D) as determined from CDK2 data described in chapter 4. Therefore, as a result of the HTS, identifying azapurine hits and elucidating the hydrogen bonding acceptor-donor-acceptor motif (A-D-A) of the azapurine pharmacophore with

CRK3:CYC6, may contribute to the future design of CDK inhibitors which are selective over other cellular kinases. Identifying two classes of compounds which were significantly selective towards *Leishmania* CRK3:CYC6 protein kinase activity is a promising starting point for further chemistry to increase the potency and biological effect of the hits. Therefore, the project was successful in terms of the HTS but it remains to be seen whether it will be successful in terms of being able to convert the hits into lead compounds in the future.

Because of limited compound, analysis of the biological activity of five of the ten most potent HTS hits on *L. major* parasites was only carried out once, thereby remaining preliminary data and inconclusive. It will be vital to remake these five HTS hits and re-screen them against the parasites *in vitro* to determine whether they do or do not have biological activity towards *Leishmania* as seen with some of the other re-synthesised HTS hits. In addition, it will be interesting to continue the synthesis of azapurines derivatives to identify compounds which may have increased potency towards *Leishmania* CRK3:CYC6 protein kinase activity and biological activity towards *Leishmania*. This will contribute to evaluating the azapurine pharmacophore as a potential for future drug development.

The chemical synthesis for reproducing the aminopyridazine-3-carboxamide compounds and further derivatives proved difficult and as a result, time restraints prohibited their synthesis. Therefore, it would be interesting to analyse the biological activity of this class of compound towards *Leishmania*, particularly because they proved more selective towards *Leishmania* CRK3:CYC6 protein kinase activity and did not inhibit mammalian CDK4:CycD1 protein kinase activity in comparison to the azapurine compounds. It therefore remains to be seen how successful this pharmacophore could be in terms of biological activity and further drug development against *Leishmania*.

An *in vivo* partner of *L. mexicana* CRK3 has been shown to be *L. mexicana* CYCA (F.C. Gomes and J.C. Mottram, unpublished). Furthermore, the homologue of CYCA in *L. donovani* has been identified, LdCYC1, (Banerjee *et al.*, 2003) and shown to form a complex with *L. donovani* CRK3 (Banerjee *et al.*, 2006), which as mentioned has 99% identity to *L. mexicana* CRK3. These complexes are implicated in the G1-S-phase of the cell cycle. However, CRK3 has been shown to have the properties of G2-M-phase protein kinase in *Leishmania* and continuing work with HA-tagged CYC6 could determine if CYC6 can bind and activate CRK3 *in vivo* in *Leishmania*. This may show that CRK3:CYC6 is the G2-M-phase protein kinase involved in this stage of cell cycle control as seen in *T. brucei*. Additional work with HA-tagged CYC6 constructs would include immunofluorescence assays to determine the cellular location of HA-CYC6. As discussed, CRK3 may reside in both the nucleus and cytoplasm as predicted from localization studies on CDK1. Therefore, CYC6 could be predicted to be in these same subcellular locations as CRK3. Furthermore, raising antibodies against recombinant CYC6 could confirm the cellular location of the native protein. Additional analysis of CYC6 could be to attempt to generate CYC6 null mutants in order to determine whether CYC6 is an essential gene. Hammarton *et al.*, showed that CYC6 formed a complex with CRK3 and that CYC6 was an essential cyclin in *T. brucei* (Hammarton *et al.*, 2003a). RNAi of CYC6 caused a mitotic block and a growth arrest in both bloodstream form and procyclic form trypanosomes, confirming CYC6 was required for mitosis. We have shown *L. mexicana* CRK3 forms a complex with *L. major* CYC6. Therefore, it could be predicted that CYC6 would be essential in *Leishmania*, due to a conserved function with *T. brucei* CYC6 at the G2-M-phase of the cell cycle.

Although the majority of HTS hits did not show significant biological activity towards *L. major* either against promastigote or amastigote life cycle stages, some of the re-synthesised hits did exhibit biological activity. Furthermore, a number of the azapurine derivatives synthesised also had biological activity towards both forms of the parasite. This

shows that the methodology of assay development and screening was successful, in terms of the azapurine pharmacophore. It remains to be seen how successful the aminopyridazine-3-carboxamide pharmacophore could be. The Cyclacel library was therefore a suitable compound library to screen in terms of the hits identified for this project. As a result, the azapurine and aminopyridazine-3-carboxamide pharmacophores may be useful starting points for further compound synthesis against *Leishmania*, which further biological testing will confirm. In addition it is possible that further compound screening of additional libraries using the methodology and protocols developed, may provide compounds with increased potent biological activity which can be developed as antileishmanials to treat leishmaniasis.

References

- Affranchino, J.L., González, S.A., and Pays, E. (1993). Isolation of a mitotic-like cyclin homologue from the protozoan *Trypanosoma brucei*. *Gene* 132, 75-82.
- Akoulitchev, S., Chuikov, S., and Reinberg, D. (2000). TFIID is negatively regulated by cdk8-containing mediator complexes. *Nature* 407, 106.
- Ali, N. O. M. An investigation of CRK protein kinases of *Leishmania* and the assessment of their potential as drug targets. 2002. University of Khartoum, Sudan.
Ref Type: Thesis/Dissertation
- Bajaj, N.P. (2000). Cyclin-dependent kinase-5 (CDK5) and amyotrophic lateral sclerosis. *Amyotrophic lateral sclerosis and other motor neuron disorders* 5, 319-327.
- Banerjee, S., Banerjee, R., Das, R., Duttagupta, S., and Saha, P. (2003). Isolation, characterization and expression of a cyclin from *Leishmania donovani*. *FEMS Microbiol. Lett.* 226, 285-289.
- Banerjee, S., Sen, A., Das, P., and Saha, P. (2006). *Leishmania donovani* cyclin 1 (LdCyc1) forms a complex with cell cycle kinase subunit CRK3 (LdCRK3) and is possibly involved in S-phase-related activities. *FEMS Microbiol. Lett.* 256, 75-82.
- Baneyx, F. (1999). Recombinant protein expression in *Escherichia coli*. *Curr. Opin. Biotechnol.* 10, 411-421.
- Barker, A.J., Gibson, K.H., Grundy, W., Godfrey, A.A., Barlow, J.J., Healy, M.P., Woodburn, J.R., Ashton, S.E., Curry, B.J., Scarlett, L., Henthorn, L., and Richards, L. (2001). Studies leading to the identification of ZD1839 (iressa(TM)): an orally active, selective epidermal growth factor receptor tyrosine kinase inhibitor targeted to the treatment of cancer. *Bioorg. Med. Chem. Lett.* 11, 1911-1914.
- Barrett, M.P., Burchmore, R.J.S., Stich, A., Lazzari, J.O., Frasch, A.C., Cazzulo, J.J., and Krishna, S. (2003). The trypanosomiasis. *Lancet* 362, 1469-1480.
- Barrett, M.P., Mottram, J.C., and Coombs, G.H. (1999). Recent advances in identifying and validating drug targets in trypanosomes and leishmanias. *Trends Microbiol.* 7, 82-88.

- Basco,R.D., Segal,M.D., and Reed,S.I. (1995). Negative regulation of G₁ and G₂ by S-phase cyclins of *Saccharomyces cerevisiae*. *Mol. Cell. Biol.* *15*, 5030-5042.
- Bates,P.A. (2007). Transmission of *Leishmania* metacyclic promastigotes by phlebotomine sand flies. *Int. J Parasitol.* *37*, 1097-1106.
- Berriman,M., Ghedin,E., Hertz-Fowler,C., Blandin,G., Renauld,H., Bartholomeu,D.C., Lennard,N.J., Caler,E., Hamlin,N.E., Haas,B., Bohme,U., Hannick,L., Aslett,M.A., Shallom,J., Marcello,L., Hou,L., Wickstead,B., Alsmark,U.C., Arrowsmith,C., Atkin,R.J., Barron,A.J., Bringaud,F., Brooks,K., Carrington,M., Cherevach,I., Chillingworth,T.J., Churcher,C., Clark,L.N., Corton,C.H., Cronin,A., Davies,R.M., Doggett,J., Djikeng,A., Feldblyum,T., Field,M.C., Fraser,A., Goodhead,I., Hance,Z., Harper,D., Harris,B.R., Hauser,H., Hostetler,J., Ivens,A., Jagels,K., Johnson,D., Johnson,J., Jones,K., Kerhornou,A.X., Koo,H., Larke,N., Landfear,S., Larkin,C., Leech,V., Line,A., Lord,A., MacLeod,A., Mooney,P.J., Moule,S., Martin,D.M.A., Morgan,G.W., Mungall,K., Norbertczak,H., Ormond,D., Pai,G., Peacock,C.S., Peterson,J., Quail,M.A., Rabbinowitsch,E., Rajandream,M.A., Reitter,C., Salzberg,S.L., Sanders,M., Schobel,S., Sharp,S., Simmonds,M., Simpson,A.J., Tallon,L., Turner,C.M., Tait,A., Tivey,A.R., Van Aken,S., Walker,D., Wanless,D., Wang,S., White,B., White,O., Whitehead,S., Woodward,J., Wortman,J., Adams,M.D., Embley,T.M., Gull,K., Ullu,E., Barry,J.D., Fairlamb,A.H., Opperdoes,F., Barrell,B.G., Donelson,J.E., Hall,N., Fraser,C.M., Melville,S.E., and El Sayed,N.M. (2005). The genome of the African trypanosome *Trypanosoma brucei*. *Science* *309*, 416-422.
- Berthet,C., Aleem,E., Coppola,V., Tessarollo,L., and Kaldis,P. (2003). Cdk2 knockout mice are viable. *Curr. Biol.* *13*, 1775-1785.
- Booher,R.N., Alfa,C.E., Hyams,J.S., and Beach,D.H. (1989). The fission yeast cdc2 cdc13 suc1 protein-kinase - regulation of catalytic activity and nuclear-localization. *Cell* *58*, 485-497.
- Borgne,A. and Meijer,L. (1996). Sequential dephosphorylation of p34^{cdc2} on Thr-14 and Tyr-15 at the prophase/metaphase transition. *J. Biol. Chem.* *271*, 27847-27854.
- Brenk,R., Schipani,A., James,D., Krasowski,A., Gilbert,I., Frearson,J.A., and Wyatt,P.G. (2007). Lessons learnt from assembling screening libraries for drug discovery for neglected diseases. *ChemMedChem* *3*, 435-444.

Brown,N.R., Noble,M.E., Lawrie,A.M., Morris,M.C., Tunnah,P., Divita,G., Johnson,L.N., and Endicott,J.A. (1999a). Effects of phosphorylation of threonine 160 on cyclin-dependent kinase 2 structure and activity. *J. Biol. Chem.* 274, 8746-8756.

Brown,N.R., Noble,M.E.M., Endicott,J.A., and Johnson,L.N. (1999b). The structural basis for specificity of substrate and recruitment peptides for cyclin-dependent kinases. *Nat. Cell Biol.* 1, 438-443.

Byrd,J.C., Lin,T.S., Dalton,J.T., Wu,D., Phelps,M.A., Fischer,B., Moran,M., Blum,K.A., Rovin,B., Brooker-McEldowney,M., Broering,S., Schaaf,L.J., Johnson,A.J., Lucas,D.M., Heerema,N.A., Lozanski,G., Young,D.C., Suarez,J.R., Colevas,A.D., and Grever,M.R. (2007). Flavopiridol administered using a pharmacologically derived schedule is associated with marked clinical efficacy in refractory, genetically high-risk chronic lymphocytic leukemia. *Blood* 109, 399-404.

Carnero,A. and Hannon,G.J. (1998). The INK4 family of CDK inhibitors. In *Cyclin-dependent kinase (CDK) inhibitors*, P.K.Vogt and S.I.Reed, eds. (Berlin: Springer), pp. 43-51.

Chen,H.H., Wang,Y.C., and Fann,M.J. (2006). Identification and characterisation of the CDK12/cyclin L1 complex involved in alternative splicing regulation. *Mol. Cell. Biol.* 26, 2736-2745.

Chen,H.H., Wong,Y.H., Genevière,A.M., and Fann,M.J. (2007). CDK13/CDC2L5 interacts with L-type cyclins and regulates alternative splicing. *Biochem. Biophys. Res. Commun.* 354, 735-740.

Cohen,M.H., Moses,M.L., and Pazdur,R. (2002a). Gleevec™ for the treatment of chronic myelogenous leukemia: U.S. food and drug administration regulatory mechanisms, accelerated approval, and orphan drug status. *Oncologist* 7, 390-392.

Cohen,M.H., Williams,G., Johnson,J.R., Duan,J., Gobburu,J., Rahman,A., Benson,K., Leighton,J., Kim,S.K., Wood,R., Rothmann,M., Chen,G., Khin,M., Staten,A.M., and Pazdur,R. (2002b). Approval summary for Imatinib mesylate capsules in the treatment of chronic myelogenous leukemia. *Clin. Cancer Res.* 8, 935-942.

Cohen,P. (2002). Protein kinases-the major drug targets of the twenty-first century? *Nat. Rev. Drug Discov.* 1, 309-315.

- Contreras,J.M., Rival,Y.M., Chayer,S., Bourguignon,J.J., and Wermuth,C.G. (1999). Aminopyridazines as acetylcholinesterase inhibitors. *J Med. Chem.* *42*, 730-741.
- Craft,J.M., Watterson,D.M., Frautschy,S.A., and Van Eldik,L.J. (2004). Aminopyridazines inhibit beta-amyloid-induced glial activation and neuronal damage in vivo. *Neurobiol. Aging* 1283-1292.
- Croft,S.L., Barrett,M.P., and Urbina,J.A. (2005). Chemotherapy of trypanosomiasis and leishmaniasis. *Trends Parasitol.* *21*, 508-512.
- Croft,S.L. and Coombs,G.H. (2003). Leishmaniasis--current chemotherapy and recent advances in the search for novel drugs. *Trends Parasitol.* *19*, 502-508.
- Croft,S.L., Seifert,K., and Yardley,V. (2006a). Current scenario of drug development for leishmaniasis. *Indian J. Med. Res.* 399-410.
- Croft,S.L., Sundar,S., and Fairlamb,A.H. (2006b). Drug resistance in leishmaniasis. *Clin. Microbiol. Rev.* *19*, 111-126.
- Cruz,A.K., Titus,R., and Beverley,S.M. (1993). Plasticity in chromosome number and testing of essential genes in *Leishmania* by targeting. *Proc. Natl. Acad. Sci. USA* *90*, 1599-1603.
- Cruz,J.C. and Tsai,L.H. (2004). A Jekyll and Hyde kinase: roles for cdk5 in brain development and disease. *Curr. Opin. Neurobiol.* *14*, 390-394.
- D'amico,G. (1987). The commonest glomerulonephritis in the world: IgA Nephropathy. *QJM* *64*, 709-727.
- da Cunha,J.P.C., Nakayasu,E.S., Elias,M.C., Pimenta,D.C., Tellez-Inon,M.T., Rojas,F., Manuel,M.o., Almeida,I.C., and Schenkman,S. (2005). *Trypanosoma cruzi* histone H1 is phosphorylated in a typical cyclin dependent kinase site accordingly to the cell cycle. *Mol. Biochem. Parasitol.* *140*, 75-86.
- Damiens,E., Baratte,B., Marie,D., Eisenbrand,G., and Meijer,L. (2001). Anti-mitotic properties of indirubin-3'-monoxime, a CDK/GSK-3 inhibitor: induction of endoreplication following prophase arrest. *Oncogene* *20*, 3786-3797.
- Dangas,G. and Kuepper,F. (2002). Restenosis: repeat narrowing of a coronary artery: prevention and treatment. *Circulation* *105*, 2586-2587.

Datta,N. (1979). Plasmid classification: Incompatibility grouping. In *Plasmids of Medical, Environmental and Commercial Importance*, K.N.Timmis and A.Puhler, eds. (Amsterdam: Elsevier), p. 3.

Desai,D., Wessling,H.C., Fisher,R.P., and Morgan,D.O. (1995). Effects of phosphorylation by CAK on cyclin binding by CDC2 and CDK2. *Mol. Cell. Biol.* *15*, 345-350.

Doerig,C., Meijer,L., and Mottram,J.C. (2002). Protein kinases as drug targets in parasitic protozoa. *Trends Parasitol.* *18*, 366-371.

Donadio,J.V. and Grande,J.P. (2002). IgA Nephropathy. *N. Engl. J. Med.* *347*, 738-748.

Draetta,G., Brizuela,L., Potashkin,J., and Beach,D. (1987). Identification of p34 and p13, human homologs of the cell-cycle regulators of fission yeast encoded by *cdc2+* and *suc1+*. *Cell* *50*, 319-325.

Ducommun,B., Brambilla,P., Felix,M.A., Franza,B.R., Karsenti,E., and Draetta,G. (1991). Cdc2 phosphorylation is required for its interaction with cyclin. *EMBO J.* *10*, 3311-3319.

Edamatsu,H., Gau,C.L., Nemoto,T., Guo,L., and Tamanoi,F. (2000). Cdk inhibitors, roscovitine and olomoucine, synergize with farnesyltransferase inhibitor (FTI) to induce efficient apoptosis of human cancer cell lines. *Oncogene* *19*, 3059-3068.

El Fadili,K., Imbeault,M., Messier,N., Roy,G., Gourbal,B., Bergeron,M., Tremblay,M.J., Legare,D., and Ouellette,M. (2008). Modulation of gene expression in human macrophages treated with the anti-*Leishmania* pentavalent antimonial drug sodium stibogluconate. *Antimicrob. Agents Chemother.* *52*, 526-533.

El Sayed,N.M., Myler,P.J., Bartholomeu,D.C., Nilsson,D., Aggarwal,G., Tran,A.N., Ghedin,E., Worthey,E.A., Delcher,A.L., Blandin,G., Westenberger,S.J., Caler,E., Cerqueira,G.C., Branche,C., Haas,B., Anupama,A., Arner,E., Aslund,L., Attipoe,P., Bontempi,E., Bringaud,F., Burton,P., Cadag,E., Campbell,D.A., Carrington,M., Crabtree,J., Darban,H., da Silveira,J.F., de Jong,P., Edwards,K., Englund,P.T., Fazelina,G., Feldblyum,T., Ferella,M., Frasch,A.C., Gull,K., Horn,D., Hou,L., Huang,Y., Kindlund,E., Klingbeil,M., Kluge,S., Koo,H., Lacerda,D., Levin,M.J., Lorenzi,H., Louie,T., Machado,C.R., McCulloch,R., McKenna,A., Mizuno,Y., Mottram,J.C., Nelson,S., Ochaya,S., Osoegawa,K., Pai,G., Parsons,M., Pentony,M., Pettersson,U., Pop,M., Ramirez,J.L., Rinta,J., Robertson,L., Salzberg,S.L., Sanchez,D.O., Seyler,A., Sharma,R., Shetty,J., Simpson,A.J., Sisk,E., Tammi,M.T., Tarleton,R., Teixeira,S., Van Aken,S., Vogt,C., Ward,P.N., Wickstead,B., Wortman,J., White,O., Fraser,C.M., Stuart,K.D., and

- Andersson,B. (2005). The genome sequence of *Trypanosoma cruzi*, etiologic agent of chagas disease. *Science* 309, 409-415.
- Elledge,S.J. and Spottswood,M.R. (1991). A new human p34 protein kinase, cdk2, identified by complementation of a CDC28 mutation in *Saccharomyces cerevisiae*, is a homolog of *Xenopus* Eg1. *EMBO J.* 10, 2653-2659.
- Engler,T.A., Henry,J.R., Malhotra,S., Cunningham,B., Furness,K., Brozinick,J., Burkholder,T.P., Clay,M.P., Clayton,J., Diefenbacher,C., Hawkins,E., Iversen,P.W., Li,Y., Lindstrom,T.D., Marquart,A.L., McLean,J., Mendel,D., Misener,E., Briere,D., O'Toole,J.C., Porter,W.J., Queener,S., Reel,J.K., Owens,R.A., Brier,R.A., Eessalu,T.E., Wagner,J.R., Campbell,R.M., and Vaughn,R. (2004). Substituted 3-Imidazo[1,2-a]pyridin-3-yl- 4-(1,2,3,4-tetrahydro-[1,4]diazepino- [6,7,1-hi]indol-7-yl)pyrrole-2,5-diones as highly selective and potent inhibitors of Glycogen Synthase Kinase-3. *J. Med. Chem.* 47, 3934-3937.
- Epstein,C.B. and Cross,F.R. (1992). CLB5 - a novel b-cyclin from budding yeast with a role in S-phase. *Genes & Dev.* 6, 1695-1706.
- Espinoza,F.H., Ogas,J., Herskowitz,I., and Morgan,D.O. (1994). Cell cycle control by a complex of the cyclin HCS26 (PCL1) and the kinase PHO85. *Science* 266, 1388-1391.
- Evans,T., Rosenthal,E.T., Youngbloom,J., Disterl,D., and Hunt,T. (1983). Cyclin: A protein specified by maternal mRNA in sea urchin eggs that is destroyed at each cleavage division. *Cell* 33, 389-396.
- Fairlamb,A.H. (2003). Chemotherapy of human African trypanosomiasis: current and future prospects. *Trends Parasitol.* 19, 488-494.
- Fesquet,D., Labbé,J.-C., Derancourt,J., Capony,J.-P., Galas,S., Girard,F., Lorca,T., Shuttleworth,J., Dorée,M., and Cavadore,J.-C. (1993). The *MO15* gene encodes the catalytic subunit of a protein kinase that activates cdc2 and other cyclin-dependent kinases (CDKs) through phosphorylation of Thr161 and its homologues. *EMBO J.* 12, 3111-3121.
- Fischer,P.M. (2003). Functions and Pharmacological inhibitors of Cyclin-Dependent Kinases (CDKs). *Cell transmissions* 19, 3-9.
- Fischer,P.M. (2004). The use of CDK inhibitors in oncology: a pharmaceutical perspective. *Cell Cycle* 3, 742-746.

- Fischer,P.M., Endicott,J., and Meijer,L. (2003). Cyclin-dependent kinase inhibitors. In Progress in cell cycle research, L.Meijer, A.Jezequel, and M.Roberge, eds. (Roscoff, France: Editions "Life in Progress"), pp. 235-248.
- Fischer,P.M. and Gianella-Borradori,A. (2005). Recent progress in the discovery and development of cyclin-dependent kinase inhibitors. *Expert Opin. Investig. Drugs* *14*, 457-477.
- Fisher,D.L. and Nurse,P. (1996). A single fission yeast mitotic cyclin B p34^{cdc2} kinase promotes both S-phase and mitosis in the absence of G₁ cyclins. *EMBO J.* *15*, 850-860.
- Fisher,R.P. and Morgan,D.O. (1994). A novel cyclin associates with MO15/CDK7 to form the CDK-Activating Kinase. *Cell* *78*, 713-724.
- Fitch,I., Dahman,C., Surana,U., Amon,A., Goetsch,L., Byers,B., and Futcher,B. (1992). Characterisation of four B-type cyclin genes of the budding yeast *S. cerevisiae*. *Mol Biol. Cell* *3*, 805-818.
- Frearson,J.A., Wyatt,P.G., Gilbert,I.H., and Fairlamb,A.H. (2007). Target assessment for antiparasitic drug discovery. *Trends Parasitol.* *23*, 589-595.
- Fribourg,S., Romier,C., Werten,S., Gangloff,Y.G., Poterszman,A., and Moras,D. (2001). Dissecting the interaction network of multiprotein complexes by pairwise coexpression of subunits in *E. coli*. *J. Mol. Biol.* *306*, 363-373.
- Fuchs,B., Hecker,D., and Scheidtmann,K.H (1995). Phosphorylation studies on rat p53 using the baculovirus expression system. Manipulation of the phosphorylation state with okadaic acid and influence on DNA binding. *Eur. J. Biochem.* *228*, 625-639.
- Glotzer,M., Murray,A.W., and Kirschner,M. (1991). Cyclin is degraded by the ubiquitin pathway. *Nature* *349*, 132-138.
- Gomez,E.B., Santori,M.I., Laria,S., Engel,J.C., Swindle,J., Eisen,H., Szankasi,P., and Tellez-Inon,M.T. (2001). Characterization of the *Trypanosoma cruzi* Cdc2p-related protein kinase 1 and identification of three novel associating cyclins. *Mol. Biochem. Parasitol.* *113*, 97-108.
- Gomez,M.L., Kornblihtt,A.R., and Tellez-Iñón,M.T. (1998). Cloning of a cdc2-related protein kinase from *Trypanosoma cruzi* that interacts with mammalian cyclins. *Mol. Biochem. Parasitol.* *91*, 337-351.

Gossage,S.M., Rogers,M.E., and Bates,P.A. (2003). Two separate growth phases during the development of *Leishmania* in sand flies: implications for understanding the life cycle. *Int. J Parasitol.* 33, 1027-1034.

Grana,X., Claudio,P.P., De Luca,A., Sang,N., and Giordano,A. (1994a). PISSLRE, a novel CDC2-related protein kinase. *Oncogene* 9, 2097-2103.

Grana,X., De Luca,A., Sang,N., Fu,Y., Claudio,P.P., Rosenblatt,J., Morgan,D.O., and Giordano,A. (1994b). PITALRE, a nuclear CDC2-related protein kinase that phosphorylates the retinoblastoma protein *in vitro*. *Proc. Natl. Acad. Sci. U. S. A* 91, 3834-3838.

Grant,K.M., Dunion,M.H., Yardley,V., Skaltsounis,A.-L., Marko,D., Eisenbrand,G., Croft,S.L., Meijer,L., and Mottram,J.C. (2004). Inhibitors of *Leishmania mexicana* CRK3 cyclin-dependent kinase: chemical library screen and antileishmanial activity. *Antimicrob. Agents Chem.* 48, 3033-3042.

Grant,K.M., Hassan,P., Anderson,J.S., and Mottram,J.C. (1998). The *crk3* gene of *Leishmania mexicana* encodes a stage-regulated cdc2-related histone H1 kinase that associates with p12^{cks1}. *J. Biol. Chem.* 273, 10153-10159.

Hammarton,T.C., Clark,J., Douglas,F., Boshart,M., and Mottram,J.C. (2003a). Stage-specific differences in cell cycle control in *Trypanosoma brucei* revealed by RNA interference of a mitotic cyclin. *J. Biol. Chem.* 278, 22877-22886.

Hammarton,T.C., Engstler,M., and Mottram,J.C. (2004). The *Trypanosoma brucei* cyclin, CYC2, is required for cell cycle progression through G1 phase and maintenance of procyclic form cell morphology. *J. Biol. Chem.* 279, 24757-24764.

Hammarton,T.C., Ford,J.R., and Mottram,J.C. (2000). *Trypanosoma brucei* CYC1 does not have characteristics of a mitotic cyclin. *Mol. Biochem. Parasitol.* 111, 229-233.

Hammarton,T.C., Mottram,J.C., and Doerig,C. (2003b). The cell cycle of parasitic protozoa: potential for chemotherapeutic exploitation. *Prog. Cell Cycle Res.* 5, 91-101.

Hanks,S.K. (1987). Homology probing: identification of cDNA clones encoding members of the protein-serine kinase family. *Proc. Natl. Acad. Sci. U. S. A.* 84, 388-392.

Harrington,E.A., Bebbington,D., Moore,J., Rasmussen,R.K., Ajose-Adeogun,A.O., Nakayama,T., Graham,J.A., Demur,C., Hercend,T., Diu-Hercend,A., Su,M., Golec,J.M.C.,

- and Miller, K.M. (2004). VX-680, a potent and selective small-molecule inhibitor of the Aurora kinases, suppresses tumor growth in vivo. *Nat. Med.* *10*, 262-267.
- Hartwell, L.H. (1974). *Saccharomyces cerevisiae* cell cycle. *Bacteriological reviews* *38*, 164-198.
- Hartwell, L.H. (1991). Twenty-five years of cell cycle genetics. *Genetics* *129*, 975-980.
- Hartwell, L.H., Culotti, J., Pringle, J.R., and Reid, B.J. (1974). Genetic control of the cell division cycle in yeast. *Science* *183*, 46-51.
- Hassan, P., Fergusson, D., Grant, K.M., and Mottram, J.C. (2001). The CRK3 protein kinase is essential for cell cycle progression of *Leishmania mexicana*. *Mol. Biochem. Parasitol.* *113*, 189-198.
- Havlicek, L., Fuksova, K., Krystof, V., Orsag, M., Vojtesek, B., and Strnad, M. (2005). 8-Azapurines as new inhibitors of cyclin-dependent kinases. *Bioorg. Med. Chem.* *13*, 5399-5407.
- Hayles, J., Fisher, D., Woollard, A., and Nurse, P. (1994). Temporal order of S phase and mitosis in fission yeast is determined by the state of the p34^{cdc2}-mitotic B cyclin complex. *Cell* *78*, 813-822.
- Hellmich, M.R., Pant, H.C., Wada, E., and Battey, J.F. (1992). Neuronal cdc2-like kinase - a cdc2-related protein kinase with predominantly neuronal expression. *Proc. Natl. Acad. Sci. USA* *89*, 10867-10871.
- Hereford, L.M. and Hartwell, L.H. (1974). Sequential gene function in the initiation of *Saccharomyces cerevisiae* DNA synthesis. *J. Mol. Biol.* *84*, 445-461.
- Herwaldt, B.L. (1999). Leishmaniasis. *Lancet* *354*, 1191-1199.
- Hindley, J. and Phear, G.A. (1984). Sequence of the cell-division gene cdc2 from *Schizosaccharomyces pombe*; patterns of splicing and homology to protein kinases. *Gene* *31*, 129-134.
- Hoessel, R., Leclerc, S., Endicott, J.A., Nobel, M.E.M., Lawrie, A., Tunnah, P., Leost, M., Damiens, E., Marie, D., Marko, D., Niederberger, E., Tang, W.C., Eisenbrand, G., and Meijer, L. (1999). Indirubin, the active constituent of a Chinese antileukaemia medicine, inhibits cyclin-dependent kinases. *Nat. Cell. Biol.* *1*, 60-67.

- Hu,L., Arafa,R.K., Ismail,M.A., Wenzler,T., Brun,R., Munde,M., Wilson,W.D., Nzimiro,S., Samyesudhas,S., Werbovetz,K.A., and Boykin,D.W. (2008). Azaterphenyl diamidines as antileishmanial agents. *Bioorg. Med. Chem. Lett.* *18*, 247-251.
- Ivens,A.C., Peacock,C.S., Worthey,E.A., Murphy,L., Aggarwal,G., Berriman,M., Sisk,E., Rajandream,M.A., Adlem,E., Aert,R., Anupama,A., Apostolou,Z., Attipoe,P., Bason,N., Bauser,C., Beck,A., Beverley,S.M., Bianchetti,G., Borzym,K., Bothe,G., Bruschi,C.V., Collins,M., Cadag,E., Ciarloni,L., Clayton,C., Coulson,R.M.R., Cronin,A., Cruz,A.K., Davies,R.M., De Gaudenzi,J., Dobson,D.E., Duesterhoeft,A., Fazelina,G., Fosker,N., Frasch,A.C., Fraser,A., Fuchs,M., Gabel,C., Goble,A., Goffeau,A., Harris,D., Hertz-Fowler,C., Hilbert,H., Horn,D., Huang,Y., Klages,S., Knights,A., Kube,M., Larke,N., Litvin,L., Lord,A., Louie,T., Marra,M., Masuy,D., Matthews,K., Michaeli,S., Mottram,J.C., Muller-Auer,S., Munden,H., Nelson,S., Norbertczak,H., Oliver,K., O'Neil,S., Pentony,M., Pohl,T.M., Price,C., Purnelle,B., Quail,M.A., Rabbinowitsch,E., Reinhardt,R., Rieger,M., Rinta,J., Robben,J., Robertson,L., Ruiz,J.C., Rutter,S., Saunders,D., Schafer,M., Schein,J., Schwartz,D.C., Seeger,K., Seyler,A., Sharp,S., Shin,H., Sivam,D., Squares,R., Squares,S., Tosato,V., Vogt,C., Volckaert,G., Wambutt,R., Warren,T., Wedler,H., Woodward,J., Zhou,S., Zimmermann,W., Smith,D.F., Blackwell,J.M., Stuart,K.D., Barrell,B., and Myler,P.J. (2005). The genome of the kinetoplastid parasite, *Leishmania major*. *Science* *309*, 436-442.
- Iversen,P.W., Eastwood,B.J., Sittampalam,G.S., and Cox,K.L. (2006). A comparison of assay performance measures in screening assays: signal window, Z' factor, and assay variability ratio. *J Biomol. Screen.* *11*, 247-252.
- Jeffrey,P.D., Russo,A.A., Polyak,K., Gibbs,E., Hurwitz,J., Massagué,J., and Pavletich,N.P. (1995). Mechanism of CDK activation revealed by the structure of a cyclinA-CDK2 complex. *Nature* *376*, 313-320.
- Johnson,D.G. and Walker,C.L. (1999). Cyclins and cell cycle checkpoints. *Annu. Rev. Pharmacol. Toxicol.* *39*, 295-312.
- Kasten,M. and Giordano,A. (2001). Cdk10, a Cdc2-related kinase, associates with the Ets2 transcription factor and modulates its transactivation activity. *Oncogene* *20*, 1832-1838.
- Kaur,K., Coons,T., Emmett,K., and Ullman,B. (1988a). Methotrexate-resistant *Leishmania donovani* genetically deficient in the folate-methotrexate transporter. *J. Biol. Chem.* *263*, 7020-7028.

- Kaur,K., Coons,T., Emmett,K., and Ullman,B. (1988b). Methotrexate-resistant *Leishmania donovani* genetically deficient in the folate-methotrexate transporter. *J. Biol. Chem.* *263*, 7020-7028.
- Kesavapany,S., Li,B.S., Amin,N., Zheng,Y.L., Grant,P., and Pant,H.C. (2004). Neuronal cyclin-dependent kinase 5:role in nervous system function and its specific inhibition by the cdk5 inhibitory peptide. *Biochim. Biophys. Acta* *1697*, 143-153.
- Kesavapany,S., Li,B.S., and Pant,H.C. (2003). Cyclin-dependent kinase 5 in neurofilament function and regulation. *Neurosignals* *12*, 252-264.
- Knight,Z.A. and Shokat,K.M. (2005). Features of selective kinase inhibitors. *Chem. Biol.* *12*, 621-637.
- Knockaert,M., Gray,N., Damiens,E., Chang,Y.-T., Grellier,P., Grant,K.M., Fergusson,D., Mottram,J.C., Soete,M., Le Roch,K., Doerig,C., Schultz,P.G., and Meijer,L. (2000). Intracellular targets of cyclin-dependent kinase inhibitors: identification by affinity chromatography using immobilised inhibitors. *Chem. Biol.* *7*, 411-422.
- Knockaert,M., Greengard,P., and Meijer,L. (2002). Pharmacological inhibitors of cyclin-dependent kinases. *Trends Pharmacol. Sci.* *23*, 417-425.
- Ko,J., Humbert,S., Bronson,R.T., Takahashi,S., Kulkarni,A.B., Li,E., and Tsai,L.H. (2001). p35 and p39 are essential for cyclin-dependent kinase 5 function during neurodevelopment. *J Neurosci.* *21*, 6758-6771.
- Kobayashi,H., Stewart,E., Poon,R., Adamczewski,J.P., Gannon,J., and Hunt,T. (1992). Identification of the domains in cyclin-a required for binding to, and activation of, p34(cdc2) and p32(cdk2) protein kinase subunits. *Mol. Biol. Cell* *3*, 1279-1294.
- Kost,T.A., Condeary,J.P., and Jarvis,D.L. (2005). Baculovirus as versatile vectors for protein expression in insect and mammalian cells. *Nat. Biotechnol.* *23*, 567-575.
- Kuhne,C. and Linder,P. (1993). A new pair of B-type cyclins from *Saccharomyces cerevisiae* that function early in the cell cycle. *EMBO J* *12*, 3437-3447.
- Laine,H., Doetzlhofer,A., Mantela,J., Ylikoski,J., Laiho,M., Roussel,M.F., Segil,N., and Pirvila,U. (2007). p19(Ink4d) and p21(Cip1) collaborate to maintain the postmitotic state of auditory hair cells, their codeletion leading to DNA damage and p53-mediated apoptosis. *J Neurosci.* *27*, 1434-1444.

- Lawrie,A.M., Tito,P., Hernandez,H., Brown,N.R., Robinson,C.V., Endicott,J.A., Noble,M.E.M., and Johnson,L.N. (2001). *Xenopus* phospho-CDK7/Cyclin H expressed in baculoviral-infected insect cells. *Protein Express. Purif.* 23, 252-260.
- Lee,J. and Greenleaf,A.L. (1991). CTD kinase large subunit is encoded by CTK1, a gene required for normal growth of *Saccharomyces cerevisiae*. *Gene Expression 1*, 149-167.
- Lee,M.G. and Nurse,P. (1987). Complementation used to clone a human homolog of the fission yeast cell cycle control gene *cdc2*. *Nature* 327, 31-35.
- Lees,E.M. and Harlow,E. (1993). Sequences within the conserved cyclin box of human cyclin A are sufficient for binding to and activation of *cdc2* kinase. *Mol. Cell. Biol.* 13, 1194-1201.
- Lenburg,M.E. and Oshea,E.K. (1996). Signaling phosphate starvation. *Trends Biochem. Sci.* 21, 383-387.
- Li,S., MacLachlan,T.K., De Luca,A., Claudio,P.P., Condorelli,G., and Giordano,A. (1995). The *cdc2*-related kinase, PISSLRE, is essential for cell growth and acts in G₂ phase of the cell cycle. *Cancer Res.* 55, 3992-3995.
- Li,T., Inoue,A., Lahti,J.M., and Kidd,V.J. (2004). Failure to proliferate and mitotic arrest of CDK11p110/p58-null mutant mice at the blastocyst stage of embryonic cell development. *Mol. Cell. Biol.* 24, 3188-3197.
- Li,Z. and Wang,C.C. (2003). A PHO80-like cyclin and a B-type cyclin control the cell cycle of the procyclic form of *Trypanosoma brucei*. *J. Biol. Chem.* 278, 20652-20658.
- Liao,S.-M., Zhang,J., Jeffery,D.A., Koleske,A.J., Thompson,C.M., Chao,D.M., Viljoen,M., Van Vuuren,H.J.J., and Young,R.A. (1995). A kinase-cyclin pair in the RNA polymerase II holoenzyme. *Nature* 374, 193-196.
- Lipinski,C.A., Lombardo,F., Dominy,B.W., and Feeney,P.J. (2001). Experimental and computational approaches to estimate solubility and permeability in drug discovery and development settings. *Adv. Drug. Delivery Rev.* 46, 3-26.
- Liu,J.J., Dermatakis,A., Lukacs,C., Konzelmann,F., Chen,Y., Kammlott,U., Depinto,W., Yang,H., Yin,X., Chen,Y., Schutt,A., Simcox,M.E., and Luk,K.C. (2003). 3,5,6-Trisubstituted naphthostyrils as CDK2 inhibitors. *Bioorg. Med. Chem. Lett.* 13, 2465-2468.

- Lolli,G. and Johnson,L.N. (2005). CAK - cyclin-dependent kinase activating kinase: a key kinase in cell cycle control and a target for drugs? *Cell Cycle* 4, 572-577.
- Loog,M. and Morgan,D.O. (2005). Cyclin specificity in the phosphorylation of cyclin-dependent kinases. *Nature* 434, 104-108.
- Loyer,P., Trembley,J.H., Katona,R., Kidd,V.J., and Lahti,J.M. (2005). Role of CDK/cyclin complexes in transcription and RNA splicing. *Cell. Signalling* 17, 1033-1051.
- Lusis,A.J. (2000). Atherosclerosis. *Nature* 407, 233-241.
- Mäkelä,T.P., Tassan,J.-P., Nigg,E.A., Frutiger,S., Hughes,G.J., and Weinberg,R.A. (1994). A cyclin associated with the CDK-activating kinase MO15. *Nature* 371, 254-257.
- Malumbres,M. and Barbacid,M. (2001). To cycle or not to cycle: a critical decision in cancer. *Nat. Rev. Cancer* 1, 222-231.
- Malumbres,M. and Barbacid,M. (2005). Mammalian cyclin-dependent kinases. *Trends Biochem. Sci.* 30, 630-641.
- Malumbres,M., Sotillo,R., Santamaria,D., Galan,J., Cerezo,A., Ortega,S., Dubus,P., and Barbacid,M. (2004). Mammalian cells cycle without the D-type cyclin-dependent kinases Cdk4 and Cdk6. *Cell* 118, 493-504.
- Manning,G., Whyte,D.B., Martinez,R., Hunter,T., and Sudarsanam,S. (2002). The protein kinase complement of the human genome. *Science* 298, 1912-1934.
- Marko,D., Schätzle,S., Friedel,A., Genzlinger,A., Zankl,H., Meijer,L., and Eisenbrand,G. (2001). Inhibition of cyclin-dependent kinase 1 (CDK1) by indirubin derivatives in human tumour cells. *Br. J. Cancer* 84, 283-289.
- Martin-Castellanos,C., Blanco,M.A., de Prada,J.M., and Moreno,S. (2000). The puc1 cyclin regulates the G1-phase of the fission yeast cell cycle in response to cell size. *Mol. Biol. Cell* 11, 543-554.
- Martin-Castellanos,C., Labib,K., and Moreno,S. (1996). B-type cyclins regulate G₁ progression in fission yeast in opposition to the p25^{rum1} cdk inhibitor. *EMBO J.* 15, 839-849.

- Matsushime,H., Quelle,D.E., Shurtleff,S.A., Shibuya,M., Sherr,C.J., and Kato,J.-Y. (1994). D-type cyclin-dependent kinase activity in mammalian cells. *Mol. Cell. Biol.* *14*, 2066-2076.
- Measday,V., Moore,L., Ogas,J., Tyers,M., and Andrews,B. (1994). The PCL2 (ORFD)-PHO85 cyclin-dependent kinase complex: A cell cycle regulator in yeast. *Science* *266*, 1391-1395.
- Meijer,L. (1995). Chemical inhibitors of cyclin-dependent kinases. In *Progress in Cell Cycle Research*, L.Meijer, S.Guidet, and H.Y.L.Tung, eds. (New York: Plenum Press), pp. 351-363.
- Meijer,L. (1996). Chemical inhibitors of cyclin-dependent kinases. *Trends Cell Biol.* *6*, 393-397.
- Meijer,L. and Raymond,E. (2003). Roscovitine and other purines as kinase inhibitors. From starfish oocytes to clinical trials. *Accounts Chem. Res.* *36*, 417-425.
- Meyerson,M., Enders,G.H., Wu,C.L., Su,L.K., Gorka,C., Nelson,C., Harlow,E., and Tsai,L.H. (1992). A family of human cdc2-related protein-kinases. *EMBO J.* *11*, 2909-2917.
- Meyerson,M. and Harlow,E. (1994). Identification of G₁ kinase activity for cdk6, a novel cyclin D partner. *Mol. Cell. Biol.* *14*, 2077-2086.
- Migone,F., Delnnocentes,P., Smith,B.F., and Bird,R.C. (2006). Alterations in CDK1 expression and nuclear/nucleolar localization following induction in a spontaneous canine mammary cancer model. *J. Cell. Biochem.* *98*, 504-518.
- Mißlitz,A., Mottram,J.C., Overath,P., and Aebischer,T. (2000). Targeted integration into a rRNA locus results in uniform and high level expression of transgenes in *Leishmania* amastigotes. *Mol. Biochem. Parasitol.* *107*, 251-261.
- Mondesert,O., McGowan,C.H., and Russell,P. (1996). Cig2, a B-type cyclin, promotes the onset of S in *Schizosaccharomyces pombe*. *Mol. Cell. Biol.* *16*, 1527-1533.
- Moore,J.D., Yang,J., Truant,R., and Kornbluth,S. (1999). Nuclear import of Cdk/cyclin complexes: Identification of distinct mechanisms for import of Cdk2/cyclin E and Cdc2/cyclin B1. *J. Cell Biol.* *144*, 213-224.

- Moreno,S., Hayles,J., and Nurse,P. (1989). Regulation of p34cdc2 protein kinase during mitosis. *Cell* 58, 361-372.
- Morgan,D.O. (1995). Principles of CDK regulation. *Nature* 374, 131-134.
- Morgan,D.O. (1997). Cyclin-dependent kinases: Engines, clocks, and microprocessors. *Annu. Rev. Cell Dev. Biol.* 13, 261-291.
- Mottram,J.C. (1994). cdc2-related protein kinases and cell cycle control in trypanosomatids. *Parasitol. Today* 10, 253-257.
- Mottram,J.C., Kinnaird,J., Shiels,B.R., Tait,A., and Barry,J.D. (1993). A novel CDC2-related protein kinase from *Leishmania mexicana*, LmmCRK1, is post-translationally regulated during the life-cycle. *J. Biol. Chem.* 268, 21044-21051.
- Mottram,J.C., McCready,B.P., Brown,K.P., and Grant,K.M. (1996). Gene disruptions indicate an essential function for the LmmCRK1 cdc2-related kinase of *Leishmania mexicana*. *Mol. Microbiol.* 22, 573-582.
- Mottram,J.C. and Smith,G. (1995). A family of trypanosome cdc2-related protein kinases. *Gene* 162, 147-152.
- Nasmyth,K. (1993). Control of the yeast cell cycle by the CDC28 protein kinase. *Curr. Opin. Cell Biol.* 5, 166-179.
- Naula,C., Parsons,M., and Mottram,J.C. (2005). Protein kinases as drug targets in trypanosomes and *Leishmania*. *Biochim. Biophys. Acta* 1754, 151-159.
- Neal,R.A. and Croft,S.L. (1984). An in-vitro system for determining the activity of compounds against the intracellular amastigote form of *Leishmania donovani*. *J. Antimicrob. Chemother.* 14, 463-475.
- Nelson,P.J., Gelman,I.H., and Klotman,P.E. (2001). Suppression of HIV-1 expression by inhibitors of cyclin-dependent kinases promotes differentiation of infected podocytes. *J. Am. Chem. Soc. Nephrol.* 12, 2827-2831.
- Nguyen,M.D., Lariviere,R.C., and Julien,J.P. (2001). Deregulation of Cdk5 in a mouse model of ALS: toxicity alleviated by perikaryal neurofilament inclusions. *Neuron* 1, 135-147.

- Nigg,E.A. (1996). Cyclin-dependent protein kinase 7: at the cross-roads of transcription, DNA repair and cell cycle control? *Curr. Opin. Cell Biol.* 8, 312-317.
- Nigg,E.A. (2001). Mitotic kinases as regulators of cell division and its checkpoints. *Nat. Rev. Mol. Cell Biol.* 2, 21-32.
- Ninomiya-Tsuji,J., Nomoto,S., Yasuda,H., Reed,S.I., and Matsumoto,K. (1991). Cloning of a human cDNA encoding a cdc2-related kinase by complementation of a budding yeast CDC28 mutation. *Proc. Natl. Acad. Sci. USA* 88, 9006-9010.
- Nishiyama,A., Tachibana,K., Igarashi,Y., Yasuda,H., Tanahashi,N., Tanaka,K., Ohsumi,K., and Kishimoto,T. (2000). A nonproteolytic function of the proteasome is required for the dissociation of Cdc2 and cyclin B at the end of M phase. *Genes Dev.* 14, 2344-2357.
- Novy,R., Yaeger,K., Held,D., and Mierendorf,R. (2002). Coexpression of multiple target proteins in *E. coli*. in *Novations* 15, 2-6.
- Nurse,P. (1990). Universal control mechanism regulating onset of M-phase. *Nature* 344, 503-508.
- Nurse,P. and Bissett,Y. (1981). Gene required for commitment to the cell cycle and in G2 for control of mitosis in fission yeast. *Nature* 292, 558-560.
- Nwaka,S. and Hudson,A. (2006). Innovative lead discovery strategies for tropical diseases. *Nat. Rev. Drug Discovery* 5, 941-955.
- Obara-Ishihara,T. and Okayama,H. (1994). A B-type cyclin negatively regulates conjugation via interacting with cell cycle 'start' genes in fission yeast. *EMBO J.* 13, 1863-1872.
- Ohshima,T., Ward,J.M., Huh,C.G., Longenecker,G., Veeranna, Pant,H.C., Brady,R.O., Martin,L.J., and Kulkarni,A.B. (1996). Targeted disruption of the cyclin-dependent kinase 5 gene results in abnormal corticogenesis, neuronal pathology and perinatal death. *Proc. Natl. Acad. Sci. USA* 93, 11173-11178.
- Palit,P. and Ali,N. (2008). Oral therapy with Amlodipine and Lacidipine, 1,4-dihydropyridine derivatives showing activity against experimental visceral leishmaniasis. *Antimicrob. Agents Chem.* 52, 374-377.

- Paris,J., Leguellec,R., Couturier,A., Leguellec,K., Omilli,F., Camonis,J., MacNeill,S.A., and Philippe,M. (1991). Cloning by differential screening of a *Xenopus* cDNA coding for a protein highly homologous to cdc2. Proc. Natl. Acad. Sci. USA 88, 1039-1043.
- Parsons,M., Worthey,E.A., Ward,P.N., and Mottram,J.C. (2005). Comparative analysis of the kinomes of three pathogenic trypanosomatids; *Leishmania major*, *Trypanosoma brucei* and *Trypanosoma cruzi*. BMC. Genomics 6, 127.
- Pevarello,P. and Villa,M. (2005). Cyclin-dependent kinase inhibitors: a survey of the recent patent literature. Expert Opin. Ther. Pat. 15, 675-703.
- Piggott,J.R., Rai,R., and Carter,B.L.A. (1982). A bifunctional gene product involved in two phases of the yeast cell cycle. Nature 298, 391-393.
- Pines,J. and Hunter,T. (1990). p34cdc2: The S and M kinase? New Biol. 2, 389-401.
- Pink,R., Hudson,A., Mouries,M., and Bendig,M. (2005). Opportunities and challenges in antiparasitic drug discovery. Nat. Rev. Drug. Discovery 4, 727-740.
- Polychronopoulos,P., Magiatis,P., Skaltsounis,A.L., Myrianthopoulos,V., Mikros,E., Tarricone,A., Musacchio,A., Roe,S.M., Pearl,L., Leost,M., Greengard,P., and Meijer,L. (2004). Structural basis for the synthesis of indirubins as potent and selective inhibitors of glycogen synthase kinase-3 and cyclin-dependent kinases. J. Med. Chem. 47, 935-946.
- Ponderato,N., Lagutina,I., Crotti,G., Turini,P., Galli,C., and Lazzari,G. (2001). Bovine oocytes treated prior to *in vitro* maturation with a combination of butyrolactone I and roscovitine at low doses maintain a normal developmental capacity. Mol. Reprod. Dev. 60, 579-585.
- Porter,L.A. and Donoghue,D.J. (2003). Cyclin B1 and CDK1: nuclear localization and upstream regulators. In Progress in Cell Cycle Research, L.Meijer, A.Jezequel, and M.Roberge, eds., pp. 335-347.
- Prelich,G. and Winston,F. (1993). Mutations that suppress the deletion of an upstream activating sequence in yeast: Involvement of a protein kinase and histone H3 in repressing transcription *in vivo*. Genetics 135, 665-676.
- Qi,Z., Huang,Q.-Q., Lee,K.-Y., Lew,J., and Wang,J.H. (1995). Reconstitution of neuronal Cdc2-like kinase from bacteria- expressed Cdk5 and an active fragment of the brain-specific activator. Kinase activation in the absence of Cdk5 phosphorylation. J. Biol. Chem. 270, 10847-10854.

Reed,S.I., Hadwiger,J.A., and Lorincz,A.T. (1985). Protein kinase activity associated with the product of the yeast cell division cycle gene *cdc28*. Proc. Natl. Acad. Sci. USA 82, 4055-4059.

Reichwald,C., Shimony,O., Dunkel,U., Sacerdoti-Sierra,N., Jaffe,C.L., and Kunick,C. (2008). 2-(3-Aryl-3-oxopropen-1-yl)-9-tert-butyl-paullones: a new antileishmanial chemotype. J. Med. Chem. 51, 659-665.

Reithinger,R., Dujardin,J.C., Louzir,H., Pirmez,C., Alexander,B., and Brooker,S. (2007). Cutaneous leishmaniasis. Lancet 7, 581-596.

Ren,S. and Rollins,B.J. (2004). CyclinC/Cdk3 promotes Rb-dependent G0 exit. Cell 117, 239-251.

Renslo,A.R. and McKerrow,J.H. (2006). Drug discovery and development for neglected parasitic diseases. Nat. Chem. Biol. 2, 701-710.

Riabowol,K., Draetta,G., Brizuela,L., Vandre,D., and Beach,D. (1989). The *cdc2* kinase is a nuclear-protein that is essential for mitosis in mammalian-cells. Cell 57, 393-401.

Richardson,H.E., Lew,D.J., Henze,M., Sugimoto,K., and Reed,S.I. (1992). Cyclin-B homologs in *Saccharomyces cerevisiae* function in S phase and in G₂. Genes & Dev. 6, 2021-2034.

Richardson,H.E., Wittenberg,C., Cross,R., and Reed,S.I. (1989). An essential G1 function for cyclin-like proteins in yeast. Cell 59, 1127-1133.

Rogers,M.E., Chance,M.L., and Bates,P.A. (2002). The role of promastigote secretory gel in the origin and transmission of the infective stage of *Leishmania mexicana* by the sandfly *Lutzomyia longipalpis*. Parasitology 124, 495-507.

Rosania,G.R. and Chang,Y.T. (2000). Targeting hyperproliferative disorders with cyclin dependent kinase inhibitors. Expert Opin. Ther. Pat. 10, 215-230.

Rossi,D.J., Londesborough,A., Korsisaari,N., Pihlak,A., Lehtonen,E., Henkemeyer,M., and Makela,T.P. (2001). Inability to enter S phase and defective RNA polymerase II CTD phosphorylation in mice lacking *Mat1*. EMBO J 20, 2844-2856.

Sambrook,J., Fritsch,E.F., and Maniatis,T. (1989). Molecular cloning: A laboratory manual., C.Nolan, ed. (Cold Spring Harbor, NY.: Cold Spring Laboratory Press).

- Santamaria,D., Barriere,C., Cerqueira,A., Hunt,S., Tardy,C., Newton,K., Caceres,J.F., Dubus,P., Malumbres,M., and Barbacid,M. (2007). Cdk1 is sufficient to drive the mammalian cell cycle. *Nature* 448, 811-816.
- Santori,M.I., Laria,S., Gomez,E.B., Espinosa,I., Galanti,N., and Tellez-Inon,M.T. (2002). Evidence for CRK3 participation in the cell division cycle of *Trypanosoma cruzi*. *Mol. Biochem. Parasitol.* 121, 225-232.
- Schang,L.M. (2001). Cellular proteins (cyclin dependent kinases) as potential targets for antiviral drugs. *Antiviral Chem. Chemother.* 12, 157-178.
- Schultz,C., Link,A., Leost,M., Zaharevitz,D.W., Gussio,R., Sausville,E.A., Meijer,L., and Kunick,C. (1999). Paullones, a series of cyclin-dependent kinase inhibitors: synthesis, evaluation of CDK1/Cyclin B inhibition, and *in vitro* antitumor activity. *J. Med. Chem.* 42, 2909-2919.
- Schwob,E. and Nasmyth,K. (1993). *CLB5* and *CLB6*, a new pair of B cyclins involved in DNA replication in *Saccharomyces cerevisiae*. *Genes & Dev.* 7, 1160-1175.
- Seifert,K., Lemke,A., Croft,S.L., and Kayser,O. (2007). Antileishmanial structure-activity relationships of synthetic phospholipids: *in vitro* and *in vivo* activities of selected derivatives. *Antimicrob. Agents Chem.* 51, 4525-4528.
- Sekine,C., Sugihara,T., Miyake,S., Hirai,H., Yoshida,M., Miyasaka,N., and Kohsaka,H. (2008). Successful treatment of animal models of rheumatoid arthritis with small-molecule cyclin-dependent kinase inhibitors. *J Immunol* 180, 1954-1961.
- Senderowicz,A.M. (1999). Flavopiridol: the first cyclin-dependent kinase inhibitor in human clinical trials. *Invest. New Drugs* 17, 313-320.
- Shapiro,G.I. (2004). Preclinical and clinical development of the cyclin-dependent kinase inhibitor Flavopiridol. *Clin. Cancer Res.* 10, 4270S-44275.
- Sielecki,T.M., Boylan,J.F., Benfield,P.A., and Trainor,G.L. (2000). Cyclin-dependent kinase inhibitors: Useful targets in cell cycle regulation. *J. Med. Chem.* 43, 1-18.
- Simanis,V. and Nurse,P. (1986). The cell-cycle control gene *cdc2+* of fission yeast encodes a protein-kinase potentially regulated by phosphorylation. *Cell* 45, 261-268.
- Solomon,M.J., Glotzer,M., Lee,T.H., Philippe,M., and Kirschner,M. (1990). Cyclin activation of p34cdc2. *Cell* 63, 1013-1024.

- Solomon, M.J., Lee, T., and Kirschner, M.W. (1992). Role of phosphorylation on p34cdc2 activation: identification of an activating kinase. *Mol. Cell. Biol.* *3*, 13-27.
- Soni, R., O'Reilly, T., Furet, P., Muller, L., Stephan, C., Zumstein-Mecker, S., Fretz, H., Fabbro, D., and Chaudhuri, B. (2001). Selective *in vivo* and *in vitro* effects of a small molecule inhibitor of cyclin-dependent kinase 4. *J. Natl. Cancer Inst.* *21*, 446.
- Srinivasan, J., Koszelak, M., Mendelow, M., Kwon, Y.-G., and Lawrence, D.S. (1995). The design of peptide-based substrates for the cdc2 protein kinase. *Biochem. J.* *309*, 927-931.
- Sriram, V. and Patterson, C. (2001). Cell cycle in vasculoproliferative diseases: potential interventions and routes of delivery. *Circulation* *103*, 2414-2419.
- Stern, B. and Nurse, P. (1996). A quantitative model for the cdc2 control of S phase and mitosis in fission yeast. *Trends Genet.* *12*, 345-350.
- Sterner, D.E., Lee, J.M., Hardin, S.E., and Greenleaf, A.L. (1995). The yeast carboxyl-terminal repeat domain kinase CTDK-I is a divergent cyclin-cyclin-dependent kinase complex. *Mol. Cell. Biol.* *15*, 5716-5724.
- Stevenson-Lindert, L.M., Fowler, P., and Lew, J. (2003). Substrate specificity of CDK2-cyclin A - What is optimal? *J. Biol. Chem.* *278*, 50956-50960.
- Surana, U., Robitsch, H., Price, C., Schuster, T., Fitch, I., Futcher, A.B., and Nasmyth, K. (1991). The role of CDC28 and cyclins during mitosis in the budding yeast *Saccharomyces cerevisiae*. *Cell* *65*, 145-161.
- Tassan, J.P., Jaquenoud, M., Fry, A.M., Frutiger, S., Hughes, G.J., and Nigg, E.A. (1995a). *In vitro* assembly of a functional human CDK7-cyclin H complex requires MAT1, a novel 36 kDa RING finger protein. *EMBO J.* *14*, 5608-5617.
- Tassan, J.P., Jaquenoud, M., Léopold, P., Schultz, S.J., and Nigg, E.A. (1995b). Identification of human cyclin-dependent kinase 8, a putative protein kinase partner for cyclin C. *Proc. Natl. Acad. Sci. USA* *92*, 8871-8875.
- Teague, S.J., Davis, A.M., Leeson, P.D., and Oprea, T. (1999). The Design of Leadlike Combinatorial Libraries. *Angew. Chem. Int. Ed Engl.* *38*, 3743-3748.
- Thuret, J.Y., Valay, J.G., Faye, G., and Mann, C. (1996). Civ1 (CAK *in vivo*), a novel Cdk-activating kinase. *Cell* *86*, 565-576.

- Tsai,L.H., Harlow,E., and Meyerson,M. (1991). Isolation of the human cdk2 gene that encodes the cyclin A- and adenovirus E1A-associated p33 kinase. *Nature* 353, 174-177.
- Tsai,L.H., Lees,E., Faha,B., Harlow,E., and Riabowol,K. (1993). The cdk2 kinase is required for the G1-to-S transition in mammalian cells. *Oncogene* 6, 1593-1602.
- Tsai,L.H., Lee,M.S., and Cruz,J. (2004). Cdk5, a therapeutic target for Alzheimer's disease? *Biochim. Biophys. Acta* 1697, 137-142.
- Tsutsui,T., Hesabi,B., Moons,D.S., Pandolfi,P.P., Hansel,K.S., Koff,A., and Kiyokawa,H. (1999). Targeted disruption of CDK4 delays cell cycle entry with enhanced p27Kip1 activity. *Mol. Cell. Biol.* 19, 7011-7019.
- Tu,X. and Wang,C.C. (2004). The involvement of two cdc2-related kinases (CRKs) in *Trypanosoma brucei* cell-cycle regulation and the distinctive stage-specific phenotypes caused by CRK3 depletion. *J. Biol. Chem.* 279, 20519-20528.
- Tu,X. and Wang,C.C. (2005). Pairwise knockdowns of cdc2-related kinases (CRKs) in *Trypanosoma brucei* identified the CRKs for G1/S and G2/M transitions and demonstrated distinctive cytokinetic regulations between two developmental stages of the organism. *Eukaryotic Cell* 4, 755-764.
- Valay,J.G., Simon,M., and Faye,G. (1993). The Kin28 protein kinase is associated with a cyclin in *Saccharomyces cerevisiae*. *J. Mol. Biol.* 234, 307-310.
- Van Hellemond,J.J., Neuville,P., Schwartz,R.J., Matthews,K.R., and Mottram,J.C. (2000). Isolation of *Trypanosoma brucei* CYC2 and CYC3 cyclin genes by rescue of a yeast G₁ cyclin mutant. Functional characterisation of CYC2. *J. Biol. Chem.* 275, 8315-8323.
- Vesely,J., Havlicek,L., Strnad,M., Blow,J.J., Donella-Deana,A., Pinna,L., Letham,D.S., Kato,J., Detivaud,L., Leclerc,S., and Meijer,L. (1994). Inhibition of cyclin-dependent kinases by purine analogues. *Eur. J. Biochem.* 224, 771-786.
- Wang,Y.X., Dimitrov,K., Garrity,L.K., Sazer,S., and Beverley,S.M. (1998). Stage-specific activity of the *Leishmania major* CRK3 kinase and functional rescue of a *Schizosaccharomyces pombe* cdc2 mutant. *Mol. Biochem. Parasitol.* 96, 139-150.
- Ward,P., Equinet,L., Packer,J., and Doerig,C. (2004). Protein kinases of the human malaria parasite *Plasmodium falciparum*: the kinome of a divergent eukaryote. *BMC. Genomics* 5, 79.

- Westerling,T., Kuuluvainen,E., and Makela,T.P. (2007). Cdk8 is essential for preimplantation mouse development. *Mol. Cell. Biol.* 27, 6177-6182.
- Wintner,E.A. and Moallemi,C.C. (2000). Quantized Surface Complementarity Diversity (QSCD): A model based on small molecule-target complementarity. *J. Med. Chem.* 43, 1993-2006.
- Xiang,J., Lahti,J.M., Grenet,J., Easton,J., and Kidd,V.J. (1994). Molecular cloning and expression of alternatively spliced PITSLRE protein kinase isoforms. *J. Biol. Chem.* 269, 15786-15794.
- Yang,W., Zhang,L., Lu,Z., Tao,W., and Zhai,Z. (2001). A new method for protein coexpression in *Escherichia coli* using two incompatible plasmids. *Protein Express. Purif.* 22, 472-478.
- Ye,X., Zhu,C., and Harper,J.W. (2001). A premature-termination mutation in the *Mus musculus* cyclin-dependent kinase 3 gene. *Proc. Natl. Acad. Sci. U. S. A* 98, 1682-1686.
- Yuhong,D., Moulick,K., Rodina,A., Aguirre,J., Felts,S., Dingleline,R., Haiian,F., and Chiosis,G. (2007). High throughput screening fluorescence polarization assay for tumor-specific Hsp90. *J Biomol. Screen.* 12, 915-924.
- Zhang,J.H., Chung,T.D.Y., and Oldenburg,K.R. (1999). A simple statistical parameter for use in evaluation and validation of high throughput screening assays. *J Biomol. Screen.* 4, 67-73.
- Zijlstra,E.E., Musa,A.M., Khalil,E.A.G., El-Hassan,I.M., and El-Hassan,A.M. (2003). Post-kala-azar dermal leishmaniasis. *Lancet Infect. Dis.* 3, 87-98.